THE UNIVERSITY OF QUEENSLAND

AUSTRALIA

INVESTIGATIONS INTO THE ROLE OF THE ErbB4 RECEPTOR IN CARDIOMYOCYTE HYPERTROPHY AND ADULT CARDIAC FUNCTION

Zhen Wang

BAgrSc, MAgrSc

A thesis submitted for the degree of Doctor of Philosophy at

The University of Queensland in 2014

School of Biomedical Science

Abstract

ErbB receptors (ErbB1 - ErbB4) are a subfamily of tyrosine kinase receptors that regulate cell proliferation and differentiation. It has been proposed that the ErbB1 subtype is transactivated by Ang II to mediate cardiac hypertrophy. However, whether other ErbB receptors, in particular the abundant subtype ErbB4, are involved in this process is not known. ErbB4 has four isoforms due to alternative splicing, each of which might play a distinct role in regulating cell activity. However, the role of individual ErbB4 isoforms in hypertrophic signalling has not been investigated. In addition, ErbB4 activation is critical for cardiac development, cardiomyocyte survival in various rodent models of cardiovascular pathologies. However, the physiological role of ErbB4 in the adult heart remains poorly understood. The overall aim of my PhD project is to examine the role of the ErbB4 receptor in mediating hypertrophic growth of cardiomyocytes *in vitro*, and maintenance of the adult heart *in vivo*.

To investigate the role of ErbB1, ErbB2 and ErbB4 in mediating hypertrophy, I inhibited individual ErbB receptors in primary neonatal rat ventricular cardiomyocytes using RNA interference or a pharmacological inhibitor (AG1478). Hypertrophy induced with Ang II (100 nM) or NRG1 (10 nM) was assessed by measuring the promoter activity of hypertrophic genes, ERK1/2 activation, and hypertrophic growth. The NRG1-induced hypertrophy was reduced by down-regulation of ErbB4 receptor but not other ErbB receptors. The down-regulation of individual ErbB receptor (ErbB1, ErbB2 and ErbB4) did not affect Ang II-induced hypertrophy. Similar results were observed with the receptor tyrosine kinase inhibitor, AG1478. This suggested that whilst ErbB4 is required for NRG1-induced hypertrophy, none of the individual ErbB receptor subtypes are required for Ang II-induced hypertrophy.

Following the studies above, I investigated whether the different ErbB4 isoforms had any functional differences in the cardiomyocytes. Irrespective of any changes in total ErbB4 mRNA levels, expression of the non-cleavable JM-b isoform was always predominant in adult heart in both physiological and pathological conditions. Although the cleavable isoform JM-a was detectable, it is not cleaved in cardiomyocytes. I replaced the endogenous ErbB4 with exogenous individual isoform in cardiomyocytes and found that all four isoforms of ErbB4 could mediate the NRG1-induced hypertrophic signalling. This suggests that the hypertrophy is triggered by a common feature of the four isoforms (ostensibly the kinase activity), and appears independent of isoform-specific features, such as the cleavable domain.

To investigate the physiological function of ErbB4 in adult heart, we adopted the tamoxifen-

inducible αMHC-MerCreMer/loxP system to induce ErbB4 deletion from cardiomyocytes in the adult mouse. The expression of ErbB4 was reduced by ~ 90% at 10 days after tamoxifen treatment. Echocardiography revealed no differences in cardiac function (fractional shortening) between ErbB4-conditional knockout (ErbB4-cKO) and control groups at 3-4 months after deletion of ErbB4. However, the heart weight was increased in ErbB4-cKO animals. Interestingly, there is no change in cardiac structure (cardiomyocyte size and cardiac fibrosis) or the expression of genes associated with pathological hypertrophy. This suggests that the cardiac hypertrophy observed following ErbB4 deletion may be physiological, and raises the question as to how these animals developed cardiac hypertrophy without alteration in cardiomyocyte size or development of fibrosis. One possibility is more cardiac cells generated to cause the cardiac hypertrophy. Indeed, I found that the number of pH3 (phosphorylated histone 3, a marker of proliferation) positive cells was significantly increased in ErbB4-cKO animals. Consistent with this, the expression of NRG1, the ErbB4 selective agonist, was selectively up-regulated following ErbB4 receptor deletion. NRG1 has been suggested to induce cardiomyocyte proliferation and protect the heart under pathological conditions. Thus I proposed that this up-regulation in NRG1 may explain both the cardiac cell proliferation and the lack of cardiac dysfunction in the ErbB4-cKO animals, despite the loss of the ErbB4 receptor. Finally, we examined the long-term effects of cardiac ErbB4 deletion in mice at 7-8 months after tamoxifen treatment. These ErbB4-cKO animals developed milder physiological cardiac hypertrophy than that seen in 3-4 months cohort. Surprisingly, the cardiac ErbB4 expression in the ErbB4-cKO mice was no longer different to the controls, whereas it was reduced by ~67% at 3-4 months and ~90% at 10 days after tamoxifen treatment. The potential reasons for this reversal are not clear, but may explain the unexpected maintenance of cardiac physiology in this model.

In conclusion, the data presented in this thesis demonstrates that activation of the ErbB4 receptor is required for NRG1-induced cardiomyocyte hypertrophy. All of the four isoforms of ErbB4 can mediate this hypertrophic response. Deletion of ErbB4 from cardiomyocytes in adult mice leads to physiological cardiac hypertrophy as well as an up-regulation of NRG1. We speculate that NRG1 might protect the heart from the dysfunction caused by the loss of ErbB4, and promote cell proliferation to cause cardiac hypertrophy.

Declaration by author

This thesis is composed of my original work, and contains no material previously published or written by another person except where due reference has been made in the text. I have clearly stated the contribution by others to jointly-authored works that I have included in my thesis.

I have clearly stated the contribution of others to my thesis as a whole, including statistical assistance, survey design, data analysis, significant technical procedures, professional editorial advice, and any other original research work used or reported in my thesis. The content of my thesis is the result of work I have carried out since the commencement of my research higher degree candidature and does not include a substantial part of work that has been submitted to qualify for the award of any other degree or diploma in any university or other tertiary institution. I have clearly stated which parts of my thesis, if any, have been submitted to qualify for another award.

I acknowledge that an electronic copy of my thesis must be lodged with the University Library and, subject to the policy and procedures of The University of Queensland, the thesis be made available for research and study in accordance with the Copyright Act 1968 unless a period of embargo has been approved by the Dean of the Graduate School.

I acknowledge that copyright of all material contained in my thesis resides with the copyright holder(s) of that material. Where appropriate I have obtained copyright permission from the copyright holder to reproduce material in this thesis.

Publications during candidature

Conference abstracts during candidature

Wang Z, Chen C, Paravicini TM, Thomas WG. Angiotensin II-induced activation of hypertrophic signalling in cardiomyocytes: involvement of epidermal growth factor receptors. ASCEPT/AuPS/HBPRCA Joint Meeting, Perth, 2011. *(Student travel award)*

Wang Z, Chen C, Paravicini TM, Thomas WG. Transactivation of ErbB4 by Ang II: does it mediate cardiomyocyte hypertrophy? SBMS Pharmacology Retreat, Brisbane, 2012.

Wang Z, Chan HC, Chen C, Thomas WG, Paravicini TM. Investigating the Role of Epidermal Growth Factor Receptors in Angiotensin II-induced Hypertrophic Signalling in Cardiomyocytes. HBPR conference, USA, 2013.

Wang Z, Chan HC, Thomas WG, Paravicini TM. The function of ErbB4 receptor in the postnatal mouse heart. HBPRCA Meeting, Melbourne, 2013.

Wang Z, Chan HC, Thomas WG, Paravicini TM. Investigating the role of epidermal growth factor receptors in Ang II-induced hypertrophic signalling in cardiomyocytes. ASCEPT Meeting, Melbourne, 2013. *(Student travel award)*

Wang Z, Thomas WG, Paravicini TM. The function of ErbB4 receptor in adult mouse heart. HBPR conference, USA, 2014.

Publications included in this thesis

No publications included.

Contributions by others to the thesis

The vast majority of the work presented in this thesis was performed by Zhen Wang. The conception and design of the experiments as well as critical revision of work was provided by Prof. Walter Thomas and Dr. Tamara Paravicini. Contribution of other researchers is listed as following:

Figure 3.1 was contributed by Dr. Hsiu-wen Chan (University of Queensland, Australia). The shErbB4 vector and kdrErbB4 isoform vectors used in the study in Chapter 3 and Chapter 4 were also constructed by Dr. Hsiu-wen Chan.

The RNA samples from embryonic mice hearts (Chapter 4) were provided by Dr. David Pennisi (University of Queensland, Australia).

The RNA samples from postnatal mice hearts (Chapter 4) were provided by Dr. Enzo Porrello (University of Queensland, Australia).

The RNA samples from I/R model and calcineurin transgenic mice (Chapter 4) were provided by Prof. Eric Olson (UT Southwestern Medical Center, Dallas, USA).

Echocardiography (Chapter 5) was performed with training and assistance from Dr. Fiona Campbell (School of Veterinary Science, University of Queensland, Australia).

Statement of parts of the thesis submitted to qualify for the award of another degree

None.

Acknowledgements

I have been very fortunate to study my PhD under the principal supervision of Prof. Walter (Wally) Thomas (Receptor Biology Group, School of Biomedical Sciences, The University of Queensland). To Wally, thank you very much for giving me the opportunity to work in your lab and for helping me to develop skills in experimental design, academic writing and critical thinking. As an international student, I particularly thank you for your patience, given the limitation of my language and communication and for your support and backing at each step during my PhD candidature. I appreciate your effort in helping me achieve this thesis. I sincerely appreciate all your efforts to build me into a considered and informed scientist.

To my other supervisors, Dr. Tamara Paravicini (School of Biomedical Sciences, The University of Queensland), I would thank you for your valuable suggestions on these projects throughout my PhD. I am appreciative for your help with experimental design, bench technique and your diligent and critical comments on my writing. To Prof. Chen Chen (School of Biomedical Sciences, The University of Queensland), thank you for assisting my location to Australia and your encouragement during my PhD candidature.

I would like to acknowledge the following researchers for their scientific contributions to this work: Dr. Hsiu-Wen Chan for her previous study on the EGFR transactivation, construction of the shErbB4 vector and kdrErbB4 isoform vectors and her contribution to the Figure 3.1 in Chapter 3 of my thesis; Dr. Brooke Purdue (Receptor Biology Group, School of Biomedical Sciences, The University of Queensland) for training me in molecular biology; Dr. Enzo Porrello (Heart Regeneration Group, School of Biomedical Sciences, The University of Queensland) for providing the protocol for pH3 staining, providing RNA samples of postnatal mice and valuable advice on my project; Dr. David Pennisi (The University of Queensland) for embryonic mice heart isolation and RNA extraction; Prof. Eric Olson (UT Southwestern Medical Center, Dallas, USA) for provision of

mice hearts from I/R model and calcineurin transgenic mice; and Dr. Fiona Campbell (School of Veterinary Science, The University of Queensland) for help with the echocardiography.

This project would have been impossible without financial support. I would take this opportunity to thank the University of Queensland and the China Scholarship Council, who provided a joint scholarship to support my tuition and living stipend in Australia, the Australian Society of Clinical and Experimental Pharmacologists and Toxicologists (ASCEPT) and High Blood Pressure Research Council of Australia (HBPRCA) who provided travel awards to fund my travel and attendance at their conferences.

To all the members in Wally's lab, thank you for your scientific input, support and friendship during my PhD study. Without you guys around, the PhD journey would have been less enjoyable. Similarly, to friends and colleagues within the SBMS, and across UQ, whom I have interacted with, thank you.

Last but not least, a big thank you to my family, Mum and Dad for all your understanding and support; and to my husband, Yan Yun, for his constant encouragement and support, which kept me always positive.

Keywords

ErbB4, Ang II, NRG1, transactivation, cardiomyocyte hypertrophy, conditional knockout

Australian and New Zealand Standard Research Classifications (ANZSRC)

ANZSRC code: 060110, Receptor and Membrane Biology, 80%

ANZSRC code: 110201, cardiology 20%

Fields of Research (FoR) Classification

FoR code: 0601, Biochemistry and Cell Biology, 80%

FoR code: 1102, Cardiovascular medicine and haematology, 20%

Table of contents

List of Figures & Tables

Figures

Tables

Abbreviations

Abbreviations	Full name
ACE	angiotensin-converting-enzyme
ADAM	A disintegrin and metalloprotease
Ang II	Angiotensin II
ANOVA	Analysis of variance
ANP	Atrial natriuretic peptide
AP-2	Activator protein 2
AREG	amphiregulin
AT_1R	Angiotensin II type 1receptor
ATP	Adenosine triphosphate
BNP	Brain natriuretic peptide
BrdU	bromodeoxyuridine
BSA	Bovine serum albumin
BTC	betacellulin
COL1A1	alpha-1 type I collagen
COL3A1	alpha-1 type III collagen
DMEM	Dulbecco's modified Eagle's medium
DTT	dithiothreitol
EGF	Epidermal growth factor
EGFR	Epidermal growth factor receptor
ER	estrogen receptor
ErbB4-cKO	ErbB4 conditional knockout
EREG	epiregulin

ERK	extracellular signal-regulated kinase
ET-1	endothelin-1
FBS	foetal bovine serum
FS	fractional shortening
Gab1	Grb2-associated binder 1
GFP	green fluorescent protein
GPCR	G protein-coupled receptor
Grb2	growth factor receptor-bound protein 2
HB-EGF	heparin-binding epidermal growth factor
HW	Heart weight
ICD	Intracellular domain
IGF	insulin-like growth factor
IP_3	inositol trisphosphate
IVS	intraventricular septum thickness
Kap1	Krab-associated protein 1
KW	Kidney weight
LB	Luria broth
LPA	lysophosphatic acid
LVID	left ventricular internal dimension
LVPW	left ventricle posterior wall thickness
MEM	modified Eagle’s media
MLC-2V	myosin light chain 2v
MMP	Matrix metalloproteases
NRG	neuregulin
PBS	phosphate-buffered saline

PDGFR	Platelet-derived growth factor receptor
pH3	phosphorylated histone H3
PI3K	phosphoinositide 3-kinase
PKC	protein kinase C
PLC	phospholipase C
RAS	renin-angiotensin system
SERCA	reticulum calcium ATPase
SH2	Src homology 2 domain
shRNA	short hairpin ribonucleic acid
siRNA	small interfering ribonucleic acid
STAT5A	signal transducer and activator of transcription 5A
TGFα	transforming growth factor α
TL	Tibial length
VSMC	vascular smooth muscle cell
WGA	Wheat germ agglutinin
YAP	Yes-associated protein
α-MHC	α myosin heavy chain
β-MHC	β myosin heavy chain

CHAPTER 1

GENERAL INTRODUCTION

1. General introduction

1.1 Cardiac hypertrophy

1.1.1 Epidemiology and definition of cardiac hypertrophy

Cardiovascular diseases (CVD) such as heart failure, stroke, heart attack, cardiomyopathy and peripheral arterial disease killed 17.3 million people in 2008, representing 30% of all global deaths. It is estimated that by 2030 CVD and its complications will still be the leading cause of death in the world, with 24 million people affected (WHO, 2010). Considerable numbers of CVD patients have cardiac hypertrophy, which is an increase in cardiac mass primarily occurring through the enlargement of individual cardiomyocytes. It is initially a compensatory growth response to increased demand for cardiac function caused by various physiological or pathological stimuli. At some point, this compensation fails to meet demand and the heart transitions to failure, accompanied by stiffening of the cardiac tissue (fibrosis). Heart failure is irreversible and continues despite best available therapies, and is a primary risk factor for early death.

1.1.2 Cardiomyocyte hypertrophy

The heart is mainly composed of cardiomyocytes and fibroblasts. Cardiomyocytes occupy approximately 75% of the normal myocardial tissue volume and comprise between 30-40% of the total cell numbers (Adler *et al.*, 1981; Vliegen *et al.*, 1991). During embryogenesis, cardiomyocytes can both proliferate and enlarge to cause cardiac growth. Shortly after birth in mammals, the cardiomyocytes exit the cell cycle and lose the ability to proliferate (Markwald *et al.*, 2010). Thus, postnatal heart growth is mainly dependent on the enlargement (i.e., hypertrophy) of differentiated cardiomyocytes. Cardiomyocyte hypertrophy represents an increase in the mass of the cardiac muscle cells without proliferation (Dorn, 2007). It is a compensatory growth response to increased demand for cardiac function.

1.1.3 Types of cardiac hypertrophy

Cardiac hypertrophy can be categorised as *physiological* or *pathological* according to the nature of the stimuli and whether the hypertrophy is reversible or not (Frey *et al.*, 2003; Heineke *et al.*, 2006; McMullen *et al.*, 2007). Physiological cardiac hypertrophy is observed during pregnancy and as a consequence of exercise. Physiological cardiac hypertrophy is usually reversible - thus, the cardiac hypertrophy observed in athletes (Ellison *et al.*, 2011) or pregnancy (Mone *et al.*,

1996; Eghbali *et al.*, 2005) (due a demand for increased cardiac output) often regresses after the cessation of training or delivery of the newborn. In contrast, pathological hypertrophy is usually caused by chronic hypertension, an overactive neurohormonal system (such as the renin-angiotensin system or increased sympathetic drive), or other diseases associated with cardiovascular disease, such as diabetes. Pathological hypertrophy initially resembles physiological hypertrophy as an adaptive mechanism to preserve cardiac function in the short-term (Iemitsu *et al.*, 2001). However, in the longer term, the persistent cardiac hypertrophy will cause the death of cardiomyocytes, which are replaced by proliferating fibroblasts (Grossman, 1980; Shiojima *et al.*, 2005). The cardiac function declines due to the loss of cardiomyocytes and the ensuing fibrosis. This process is termed cardiac remodelling and eventually leads to heart failure. Pathological cardiac hypertrophy has been recognized as an important predictor for cardiovascular morbidity and mortality as well as an independent risk factor for heart failure, myocardial infarction, arrhythmias and sudden death (Wachtell *et al.*, 2007; Artham *et al.*, 2009; Bombelli *et al.*, 2009; Søraas *et al.*, 2010).

Morphologically, cardiac hypertrophy can be categorised as *concentric* hypertrophy or *eccentric* hypertrophy (Grossman *et al.*, 1975). Concentric hypertrophy is characterised by an increase in ventricular wall thickness, and at the cellular level the cardiomyocytes grow in a transverse direction without changes in cell length (Carabello, 2002). Eccentric hypertrophy is exemplified by ventricle cavity dilatation that can lead to dilated cardiomyopathy. At a cellular level, it is characterised by hypertrophic growth of cardiomyocyte hypertrophy in both the longitudinal and transverse directions (Grossman *et al.*, 2013). The stimuli that cause pressure overload (e.g. hypertension) result in concentric hypertrophy, whilst stimuli that cause volume overload (e.g. aortic regurgitation) lead to eccentric hypertrophy (McMullen *et al.*, 2007).

At a molecular level, pathological cardiac hypertrophy is usually characterized by sarcomere reorganisation and induction of the fetal gene program in cardiomyocytes (Drazner, 2005). The sarcomere is the basic unit of muscle cells. Sarcomere reorganisation resulting in the remodelling of the cardiomyocytes, affecting the ability of the cardiomyocytes to contract (Telley *et al.*, 2007). The activation of the "fetal gene program" involves the re-expression (in the adult) of genes normally only expressed during fetal development including of α-skeletal actin, β-myosin heavy chain (β-MHC), atrial natriuretic peptide (ANP) and myosin light chain-2v (MLC-2V) (Parker *et al.*, 1990; Taegtmeyer *et al.*, 2010). Some of the induced fetal genes code for contractile proteins. The re-induction of fetal gene expression is coupled with the down-regulation of genes which are normally

expressed at high levels in the adult ventricle, such as α-MHC and sarco/endoplasmic reticulum calcium ATPase (SERCA2) (Barry *et al.*, 2008). The dysregulation of these contractile and Ca^{2+} handling proteins potentially contributes to alterations in the contractile ability of cardiomyocytes (Razeghi *et al.*, 2001; Taegtmeyer *et al.*, 2010).

1.1.4 Therapy for cardiac hypertrophy

The presence of cardiac hypertrophy is usually an adverse characteristic of various cardiovascular disorders, and regression or prevention of cardiac hypertrophy has benefits in reducing the risk of CV events and sudden cardiac death in the hypertensive population (Wachtell *et al.*, 2007; Artham *et al.*, 2009; Bombelli *et al.*, 2009; Søraas *et al.*, 2010). As hypertension is commonly associated with the development of pathological left ventricle hypertrophy (LVH), most anti-hypertensive drugs can attenuate LVH, such as angiotensin converting enzyme (ACE) inhibitors and Ang II type 1 receptor (AT_1R) blockers (ARB) (Solomon *et al.*, 2011; Müller *et al.*, 2012), calcium channel blockers (Devereux *et al.*, 2001), and β-blockers (Cabrera-Bueno *et al.*, 2007). Each treatment may reduce the LVH to a different extent, which correlates with the degree of blood pressure reduced (Kjeldsen *et al.*, 2002; Ruilope *et al.*, 2008). However, meta-analysis of clinical trials has proposed that ACE inhibitors and ARBs have a better efficacy for LVH regression compared to other drugs (Devereux *et al.*, 2001; Dahlöf *et al.*, 2002; Klingbeil *et al.*, 2003; Okin *et al.*, 2003; Pitt *et al.*, 2003; Dahlöf *et al.*, 2005), suggesting the importance of activation of RAS in cardiac hypertrophy.

1.1.5 Factors and mechanisms that can induce cardiac hypertrophy

Factors causing pathological cardiac hypertrophy can be categorized as mechanical or chemical. Pressure overload (due to increased systolic pressure) or volume overload (due to increased diastolic pressure) are forms of mechanical stress that can arise from hypertension (Roman *et al.*, 2010; Katholi *et al.*, 2011), exercise, pregnancy, or cardiac dysfunction (Dorn, 2007). This causes an increase in cardiac wall tension and adaptive growth of the myocardium to normalize this tension, resulting in cardiac hypertrophy (Frey *et al.*, 2003; Frey *et al.*, 2004). The molecular mechanisms linking mechanical stress and cardiac hypertrophy have yet to be fully identified (Heineke *et al.*, 2006). However, many hormonal factors such as endothelin-1 and Ang II are released in an autocrine or paracrine way during this process, which can contribute to the cardiac hypertrophy (Yamazaki *et al.*, 1996). Cardiac homeostasis is maintained by a complex network of hormonal factors that regulate cardiac structure, growth, survival and function. Disorders in the production and regulation of these hormones can thus be a stimulus for pathological cardiac

hypertrophy. For instance, endothelin-1 has been found to be up-regulated in human and rat right ventricular hypertrophy (Nagendran *et al.*, 2013), and cardiac specific deletion or inhibition of the endothelin-1 receptor attenuates aging-associated or pressure overload induced cardiac hypertrophy in rodents (Ceylan-Isik *et al.*, 2013; Visnagri *et al.*, 2013). The molecular mechanism by which hormonal stimuli such as endothelin-1 and Ang II cause cardiac hypertrophy is via binding and activating their receptors, which primarily are GPCRs (Sugden *et al.*, 1998).

G protein-coupled receptors (GPCRs) are seven-transmembrane spanning proteins that couple to GTP-binding proteins (heterotrimeric G proteins) and use the latter to transduce signals to activate effector enzymes and to open cell surface ion channels (Hanson *et al.*, 2009). G proteins have three subunits: Gα, Gβ, and Gγ. Gα can be further divided into four classes according to the downstream effectors: Gαs, Gαi, Gαq and G12/13 (Wall *et al.*, 1995). Gαs and Gαi have opposite effects in that Gαs activates adenylyl cyclase (AC), whereas Gαi inhibits AC. Gαq can activate the phospholipase C (PLC) pathway. The Gβ and Gγ subunits form a tight bond and in the inactive state they are associated with the Gα subunit. When GPCRs are activated, this catalyses the GTP-GDP exchange on the Gα subunit and causes the dissociation of Gα from the Gβ/γ subunits, which can then activate downstream effectors (Casey *et al.*, 1988). The Gαq-coupled GPCRs are the predominant GPCRs that mediate cardiac hypertrophy (Esposito *et al.*, 2002). Expression of a constitutively activate Gαq mutant in cardiomyocytes resulted in hypertrophic growth, which then rapidly progressed to apoptotic cardiomyocyte death (Adams *et al.*, 1998). Consistent with this, genetic overexpression of Gq to autonomously activate Gq signalling in cardiomyocytes induced stable cardiac hypertrophy in heterozygous transgenic mice, whereas the persistent high level of the Gαq activation in double heterozygous transgenic mice resulted in heart failure (Adams *et al.*, 1998). Amongst the agonists for Gαq-coupled GPCRs, Ang II is one of the prime agents that can induce cardiac hypertrophy both *in vitro* and *in vivo*.

1.1.6 Ang II induces cardiomyocyte hypertrophy

Ang II is a octapeptide produced by the renin-angiotensin system (Ferrario, 2011). Ang II is known to increase blood pressure by causing blood vessel constriction and increasing salt and water retention (Cassis *et al.*, 2009), however Ang II can also induce cardiomyocyte growth directly. In isolated neonatal rat cardiomyocytes, stimulation with Ang II for 48 h induced a significant increase in cardiomyocyte protein synthesis without changing the DNA synthesis rate (Sadoshima *et al.*, 1993). The expression of "fetal gene program" genes (including myosin light chain 2v (MLC-2V), skeletal α actin, CyclinD, and atrial natriuretic factor (ANP)) was elevated at 6 hours of Ang II

stimulation (Sadoshima *et al.*, 1993). In mice, chronic subpressor doses of Ang II significantly induced left ventricular hypertrophy and increased in cardiomyocyte cross section area without changes in blood pressure (Schultz *et al.*, 2002). ACE inhibitor treatment to reduce the systemic production of Ang II in hypertensive rats (abdominal aorta banding model) inhibited cardiac hypertrophy, whereas normalisation of blood pressure with an arterial vasodilator or calcium antagonist did not (Linz *et al.*, 1989), suggesting that Ang II is an independent factor for cardiac hypertrophy. However, whether Ang II can induce cardiac hypertrophy independently of its effects on blood pressure remains controversial. Coffman *et al*. showed that the increase in blood pressure, but not the direct effect of Ang II on cardiac cells, was responsible for cardiac hypertrophy in a model of Ang II-induced hypertension. The deletion of the major Ang II receptor subtype in the kidney inhibited Ang II-induced hypertension and cardiac hypertrophy, whereas extrarenal deletion of the receptor did not (Crowley *et al.*, 2006). Although these experiments are well performed with proper controls, it is hard to refute the observations of other studies suggesting that Ang II directly targets cardiomyocytes to induce hypertrophic growth.

Ang II induces cardiomyocyte hypertrophy by binding to and activating the AT_1R receptor. The AT_1R is the major receptor for Ang II in cardiomyocytes and is a member of the GPCR family with a molecular mass of approximately 41 kDa (Mukoyama *et al.*, 1993; Yasuda *et al.*, 2008). Upon binding Ang II, AT_1R is activated and predominantly trigger Gq signalling pathways (Mehta *et al.*, 2007; Harris *et al.*, 2009). The classical Gαq signalling pathway activated by AT_1R is shown in Figure 1.1 (Dr. Hsiu-Wei Chan, PhD thesis): AT_1R interacts with the Gq protein leading to the activation of protein kinase C (PKC) and mobilization of Ca^{2+} from intracellular stores. The activated PKC and mobilized Ca^{2+} trigger individual downstream signalling pathways (Ohtsu *et al.*, 2008). PKC is a critical kinase that regulates multiple cellular activities such as cell proliferation, survival and apoptosis. In cardiomyocytes, it is involved in the regulation of cardiomyocyte contraction and hypertrophic growth (Mackay *et al.*, 2001; Braz *et al.*, 2002). PKC has multiple subtypes, and by now at least 12 isoforms have been identified (Steinberg, 2012). In cardiomyocytes, the most abundant isoform is PKCα (Pucéat *et al.*, 1994). The activation of PKCα promotes the hypertrophic growth of cardiomyocytes (Sabri *et al.*, 2003) and PKC inhibition attenuates agonist-induced hypertrophy (Zou *et al.*, 1996). Although some of these signalling pathways have been discovered, the detailed molecular mechanisms of how AT_1R activation leads to hypertrophic growth have yet to be fully identified. There is evidence showing that activation of epidermal growth factor receptor (EGFR), a member of the ErbB family, is involved in, and critical for, the cardiomyocyte hypertrophy caused by Ang II.

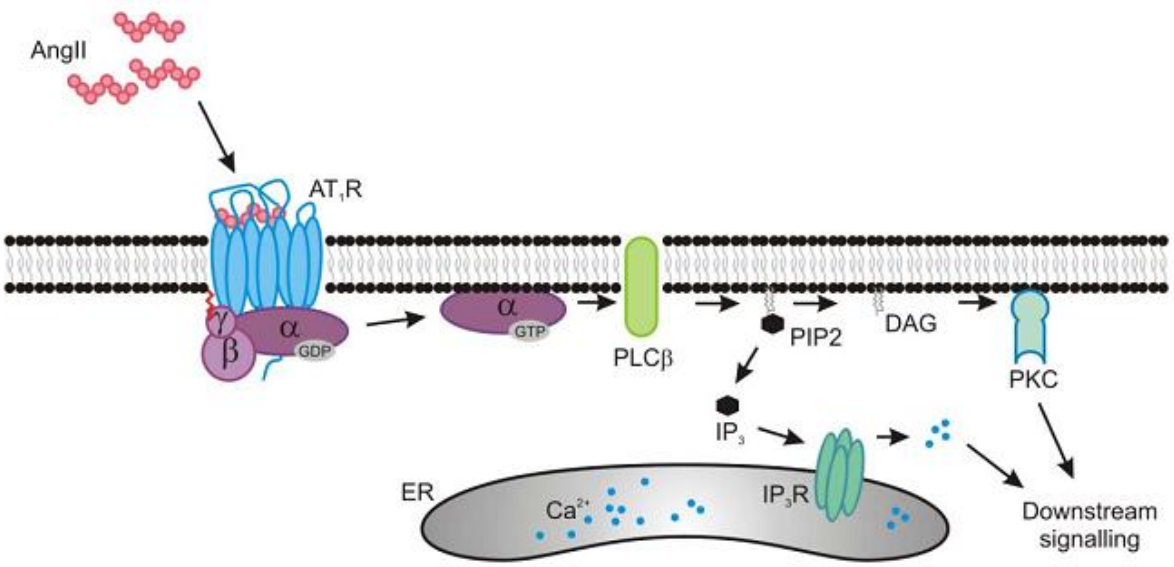

Figure 1.1 Classic Gq signaling pathway mediated by AT_1R with Ang II stimulation. In the inactive state, the GDP-bound α subunit is associated with the Gβγ subunits. Upon activation, GPCRs catalyse the GTP-GDP exchange on the Gα subunit and subsequently results in the dissociation of the Gα from the βγ subunits, each unit triggering different intracellular signalling cascades (Lee *et al.*, 1992). The classical Gq signalling pathway activated by AT_1R involves hydrolysis of phosphoinositides by active PLC, leading to the generation of diacylglycerol (DAG) and inositol trisphosphate (IP_3) (Hepler *et al.*, 1993; Smrcka *et al.*, 1993). IP_3 mobilises Ca^{2+} from its intracellular stores while DAG activates PKC. Figure from Dr. Hsiu-wen Chan (PhD thesis).

1.2 The ErbB receptors

1.2.1 Overview of ErbB receptors

ErbB receptors are a subfamily of receptor tyrosine kinases that regulate cell proliferation, survival and differentiation (Burgess, 2008). There are currently four known ErbB receptor subtypes encoded by distinct genes - ErbB1, ErbB2, ErbB3 and ErbB4 (Scaltriti *et al.*, 2006). The sequence identity of ErbB receptors ranges from 37% - 49% with a molecular mass of approximately 180 kDa (Jorissen *et al.*, 2003). The typical ErbB receptor comprises a large extracellular ligand-binding domain (ECD), a single transmembrane domain, an intracellular tyrosine kinase domain and a carboxyl-tail (Figure 1.2). Most ErbB receptors are in an inactive conformation in the absence of ligands. Ligand binding results in a conformational change in the ECD and tyrosine kinase domain, exposing previously embedded surfaces. The surface exposure in the ECD promotes dimer formation between ErbB receptors (Weiss *et al.*, 1998) and the critical sites exposed in the tyrosine kinase domain results in the activation of the kinase (Zhang *et al.*, 2006). The receptor dimerisation brings the intracellular kinase domains in each receptor into proximity to cross-phosphorylate the tyrosine residues in the cytoplasmic tail of its neighbour receptor in the dimeric complex (Hubbard *et al.*, 1998) (Figure 1.2). The phosphotyrosine residues in the cytoplasmic tail provide binding sites for multiple factors containing Src-homology 2 (SH2) domain or phosphotyrosine binding (PTB) domains (Sweeney *et al.*, 2000), which recruit downstream effectors to trigger signalling (Olayioye *et al.*, 2000; Yarden *et al.*, 2001; Mendelsohn *et al.*, 2003). The recruitment specificity is determined by the amino acids surrounding the phosphotyrosine residues of the receptor. Thus, each ErbB receptor can trigger a unique complex of intracellular signalling pathways based on this specificity (Figure 1.3). ErbB receptors can form both homodimers and heterodimers (Figure 1.2). The diversity of the heterodimerisation formed by different ErbB receptors adds more variety to the ErbB signalling pathways (Burgess, 2008). ErbB2 differs from other subtypes as its extracellular region is unable to bind any identified ligand, and thus it mainly functions as the preferred ErbB dimerisation partner (Timolati *et al.*, 2006). ErbB2 adopts an active conformation and can enhance the dimerisation and the downstream signalling. ErbB3 can bind ligands and provides multiple docking sites for downstream effectors in its cytoplasmic tail, however, due to an abrogated kinase activity, it has to trigger downstream signalling with the assistance of dimerising partners (Rohrbach *et al.*, 2005). All ErbB receptors are detectable in the embryonic heart across different species. In postnatal cardiomyocytes, the expression level of ErbB receptors declines and the expressed subtypes include ErbB1, ErbB2 and ErbB4 (Zhao *et al.*, 1998; Rohrbach *et al.*, 1999),

with ErbB2 and ErbB4 being the most abundant subtypes. ErbB3 is not expressed at high levels in postnatal cardiomyocytes (Zhao *et al.*, 1998; Rohrbach *et al.*, 1999).

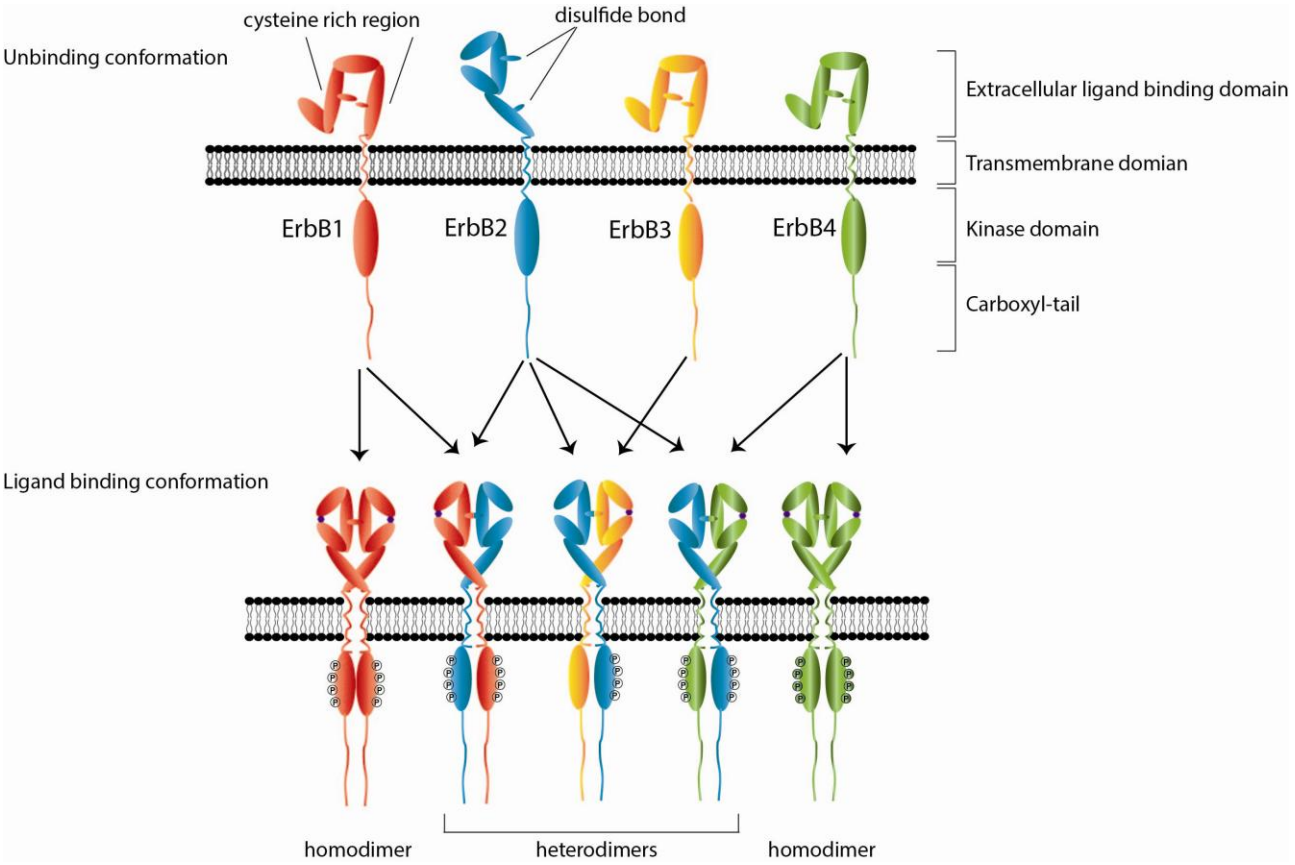

Figure 1.2 Structure of ErbB receptors in active and inactive conformation. The ectodomain of ErbB receptor is heavily N-glycosylated and characterised by two cysteine-rich regions which produce 25 disulfide bonds, forming a ligand binding site. The cytoplasmic region includes a tyrosine kinase domain and C-terminal domain containing binding sites for multiple factors. The majority of ErbB receptors stay in an inactive conformation without the ligand binding. The exception is ErbB2, which adopts the ligand binding conformation in the absence of ligand. Upon activation, the ErbB receptors can form homo- and hetero-dimers with each other. The typical dimers formed are shown in the bottom panel.

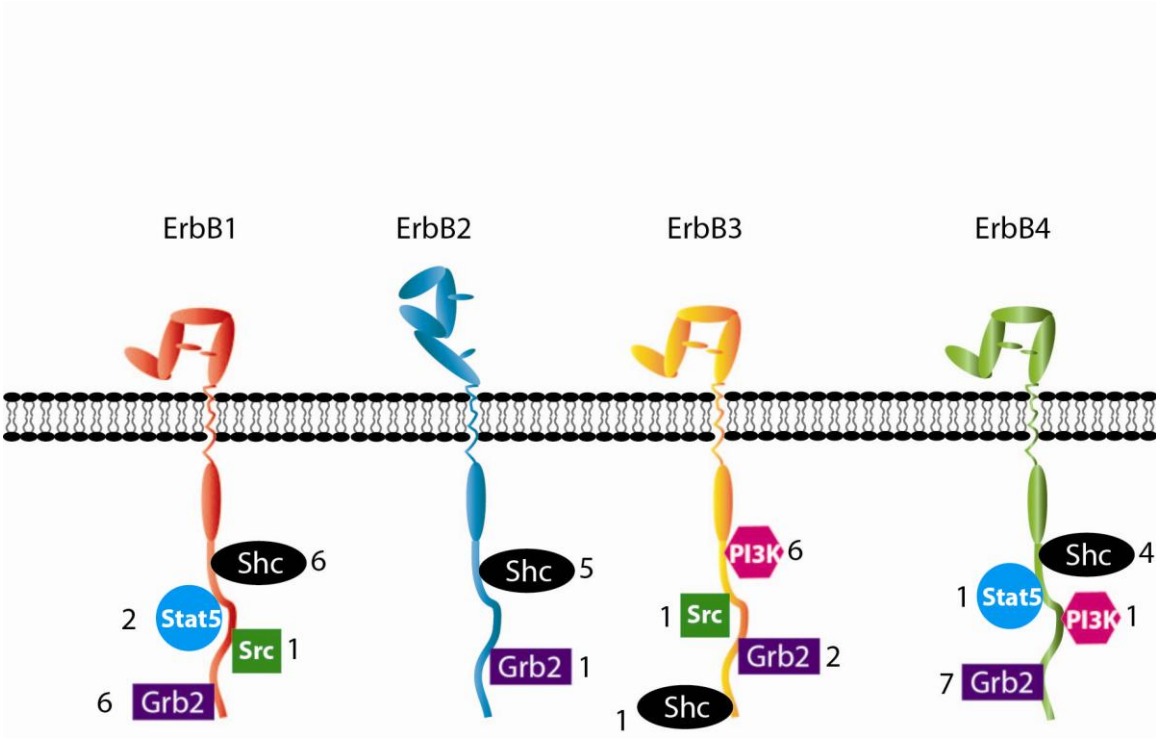

Figure 1.3 Downstream effectors potentially recruited to individual ErbB receptors. Each ErbB receptor can recruit multiple downstream effectors upon activation. The recruitment specificity is determined by the amino acids surrounding the phosphotyrosine residues in the carboxyl-tail of the receptor. The Shc and Grb2 proteins are commonly recruited by ErbB receptors and can lead to activation of MAPK signalling pathways. The numbers shown represents the amount of binding sites provided by each receptor for a particular protein. Together, each ErbB receptor induces a unique combination of downstream signalling patterns in addition to the fundamental Shc and Grb2 pathways.

1.2.2 The function of ErbB receptors in heart

The importance of ErbB signalling in the heart is highlighted by observations from transgenic mice. Mutations in ErbB2 and ErbB4 lead to a lethal phenotype at embryonic day (E) 10.5 due to defects in ventricular trabeculae formation (Gassmann *et al.*, 1995; Lee *et al.*, 1995; Sibilia *et al.*, 1995). ErbB3 null mice have normal heart trabeculation but have disrupted endocardial cushion formation and die at E13.5 (Erickson *et al.*, 1997; Riethmacher *et al.*, 1997). ErbB1 null mice have severe defects, and die before birth or within 2-3 weeks postnatally depending on the genetic background (Miettinen *et al.*, 1995; Threadgill *et al.*, 1995). Besides their essential function in heart development, ErbB receptors also play important roles in regulating cardiac growth, survival and function in the postnatal heart. Cardiomyocyte-specific expression of a dominant-negative ErbB1 in adult mice blocked both ErbB1 and ErbB2 phosphorylation, resulting in cardiac dilation and decreased cardiac contraction (fractional shortening) (Rajagopalan *et al.*, 2008). The phenotype caused by cardiac specific deletion of ErbB2 in adult heart has not yet been reported. However, administration of an ErbB2 blocking antibody in humans increases the risk of heart failure (Seidman *et al.*, 2002). Consistent with this, inhibition of ErbB2 activity causes myofibrillilary structural damage and associated inhibition of excitation-contraction coupling (Pentassuglia *et al.*, 2009b), suggesting that ErbB2 receptors are required for adult heart homeostasis. Currently, the phenotype of ErbB4 deletion in adult heart has not been reported, although accumulating evidence indicates that ErbB4 signalling may be important in regulating adult cardiomyocyte function (refer to section 1.6.7).

In addition to its critical function in regulating cardiac homeostasis, activation of ErbB receptors mediates cardiac hypertrophy both *in vivo* and *in vitro*. Activation of ErbB1 has been reported to mediate cardiomyocyte hypertrophy to Ang II (Asakura *et al.*, 2002). In cell culture, ErbB4 agonists induced potent cardiomyocyte hypertrophy (Zhao *et al.*, 1998). More detail on the cardiomyocyte hypertrophy induced by direct administration of ErbB agonists is discussed in section 1.2.4.

1.2.3 Signalling pathways of ErbB receptors

As mentioned above, there are highly diversified pathways activated by ErbB receptors due to heterodimerisation of these receptors. Among them are two fundamental and critical pathways mediating cardiac hypertrophy, the MAPK and PI3K-Akt pathways. Upon activation, ErbB receptors activate Ras GTPases (Yarden *et al.*, 2001). Ras GTPases are a family of mostly membrane resident proteins that shuttle between an inactive GDP-bound and active GTP bound

conformation (Scheffzek *et al.*, 1997; Coleman *et al.*, 2004). In its activation conformation, Ras·GTP binds to a number of effector molecules, including the serine/threonine kinase Raf and phosphoinositide 3-kinase and recruits them to the membrane compartment for activation and signalling (Kumar *et al.*, 2005).

The Ras-Raf-MEK-ERK (MAPK) pathway

The MAPK pathway is a primary mechanism by which extracellular mediators, such as growth factors, can regulate cellular activities such as cell growth, survival, apoptosis and metabolism. After recruitment to the cell membrane by Ras·GTP, Raf activates upstream kinases to stimulate the extracellular signal-regulated kinases1/2 (ERK1/2). There are at least 5 members of the ERK family (ERK1 to 5), which are activated and regulated by different upstream kinases (Nishimoto *et al.*, 2006). ERK1/2 proteins are phosphorylated on threonine and adjacent tyrosine residues in the Thr-Glu-Tyr motif. ERK1/2 are the most intensively studied and abundantly expressed ERK family members (Nishimoto *et al.*, 2006). In cardiomyocytes, ERK1/2 activation plays an important role in mediating cardiomyocyte hypertrophy. Cardiac-specific activation of ERK1/2 by overexpression of activated MEK1 (the immediate upstream activator of ERK1/2) in 9 independent MEK1 transgenic mouse lines led to stable concentric hypertrophy in the majority of these mice lines. Most activated MEK1 transgenic lines demonstrated a 25-30% increase in heart to body weight ratio with increased cardiac function and no signs of cardiomyopathy until 12 months of age (Bueno *et al.*, 2000). The mechanism by which ERK1/2 activation causes cardiomyocyte hypertrophy is complicated. It has been proposed that ERK1/2 regulates protein synthesis during cardiomyocyte hypertrophy via an association with p70 S6 kinase (Wang *et al.*, 2001). ERK1/2 is also associated with phosphorylation of transcriptional factors such as GATA4 that regulate ribosomal RNA transcription in cardiomyocytes (Morimoto *et al.*, 2000; Liang *et al.*, 2001). GATA4 is a cardiac-enriched transcriptional factor critical in the regulation of most cardiac-expressed structural genes such as α-myosin heavy chain, myosin light chain 1/3, and cardiac troponin C and I (Molkentin, 2000);(Liang *et al.*, 2002; Akazawa *et al.*, 2003), as well as hypertrophy responsive genes such as BNP (Hasegawa *et al.*, 1997).

PI3K-Akt pathway

Another important downstream pathway activated by ErbBs in cardiac hypertrophy is the phosphoinositide 3-kinase (PI3K) pathway. PI3Ks belong to a family of lipid kinases which convert phosphatidylinositol (4, 5)-bisphosphate (PIP2) into phosphatidylinositol (3, 4, 5)-trisphosphate (PIP3). PIP3, in turn, causes the phosphorylation of the kinase Akt. Akt can activate multiple

transcriptional factors such as GATA4, β-catenin, c-Myc and NFAT to promote cardiac hypertrophy (Heineke *et al.*, 2006). Akt also promotes cardiac hypertrophy by enhancing protein synthesis via activation of mTOR pathways (Proud, 2004). PI3K consists of two subunits. One is the regulatory subunit that contains p85, p55α, p50α, p85β and p55γ, and is responsible for anchorage to the docking site of other proteins, such as ErbB receptors. The other is the p110 subunit, containing p110α, p110β and p110δ, which are associated with recruitment of Akt to the cellular membrane and activation of downstream signalling (Vanhaesebroeck *et al.*, 2010). The p85 and p110α subunits are the most studied. Expression of the constitutively active p110α in the heart leads to physiological cardiac hypertrophy with preserved cardiac function (Shioi *et al.*, 2000). Myocardial expression of a dominant negative form of p110α inhibits the physiological hypertrophy during postnatal cardiac developmental growth or in response to exercise (McMullen *et al.*, 2003). Similarly, genetic mutations in the p85 subunit decrease heart size at baseline as well as physiological hypertrophy after exercise training (Luo *et al.*, 2005). These studies suggested an important role of PI3K in mediating physiological cardiac hypertrophy.

1.2.4 EGF-like factors

EGF-like factors are the agonists for ErbB receptors (Harris *et al.*, 2009). All EGF-like ligands are made as type I transmembrane proteins that are inserted into the plasma membrane and are cleaved by cell surface proteases to release mature growth factors (Schneider *et al.*, 2009). The selectivity of EGF-like factors in binding the ErbB receptors is shown in Table 1.1 (Linggi *et al.*, 2006; Edwards *et al.*, 2008).

Matrix metalloproteases (MMPs) and a disintegrin and metalloproteases (ADAMs) are part of the metalloprotease family (Page-McCaw *et al.*, 2007; Reiss *et al.*, 2009). They are anchored in the membrane and are responsible for the ectodomain shedding of EGF-like ligand precursors to produce the mature soluble EGF-like ligands (Nagase *et al.*, 2006; Klein *et al.*, 2011). Among 38 identified subtypes, ADAM 17 and ADAM 10 seem to be the principal sheddases for EGF-like ligands, and the current understanding of ADAM-mediated shedding is largely based on studies of ADAM17 and ADAM10 (Mochizuki *et al.*, 2007). Among the many EGF-like ligands, only HB-EGF is known to be a substrate for MMPs (Yu *et al.*, 2002; Hao *et al.*, 2004).

The EGF-like factors that have been identified in the cardiovascular system include EGF, TGF-α, HB-EGF, amphiregulin (AREG), betacellulin (BTC), epigen, epiregulin (EREG), and neuregulin (NRG)-1. Accumulated evidence from transgenic mice suggests a requirement of these factors in

regulating cardiac development and homeostasis, consistent with the observations for the ErbB receptors. In addition, administration of growth factor peptides or over-expression of growth factors induces cardiomyocyte hypertrophy both *in vitro* and *in vivo* (Zhao *et al.*, 1998; Schneider *et al.*, 2005; Yoshioka *et al.*, 2005). In our laboratory (Dr Hsiu-wen Chan, PhD thesis), the ability of various EGF ligands to mediate hypertrophic growth (measured as protein:DNA ratio) in primary isolated cardiomyocytes was compared. These EGF-like factors were categorized into three classes according to their ability to promote cardiomyocyte hypertrophy. The most potent hypertrophic agonists include BTC, NRG1β1 and NRG2β, which are primarily agonists for ErbB4. These agonists increased the mass of cardiomyocytes (total protein content) by 33%-49% in absence of changes in DNA content. Amphiregulin, TGFα, epiregulin and NRG2α caused a 16%-24% increase in cell mass, and these ligands (except NRG2α) selectively activate ErbB1. EGF, HB-EGF, epigen and NRG1α weakly induced hypertrophic growth (~10% increase), and are a mixture of ErbB1 agonists and ErbB4 agonists. Together, these studies suggested that the ErbB4 might have a stronger ability to mediate cardiomyocyte hypertrophy than ErbB1.

Table 1.1 The specificity of ligand binding to ErbB receptor subtypes and activation by specific ADAMs.

Ligand	Receptor				ADAM
	ErbB1	ErbB2	ErbB3	ErbB4	
EGF	+	-	-	-	ADAM-8, -10, -12, -17
TGF- α	+	-	-	-	ADAM-17
HB-EGF	+	-	-	+	ADAM-8, -9, -12, -17, -19
Amphiregulin	+	-	-	-	ADAM-17, -19
Betacellulin	+	-	-	+	ADAM-8, -10, -17
Epigen	+	-	-	-	ADAM-17
Epiregulin	+	-	-	+	ADAM-17
Neuregulin-1	-	-	+	+	ADAM-17, -19
Neuregulin-2	-	-	+	+	Unknown
Neuregulin-3	-	-	-	+	Unknown
Neuregulin-4	-	-	-	+	Unknown

This table was modified from table 1 in Edward *et.al*. (Linggi *et al.*, 2006; Edwards *et al.*, 2008) and the table 2 in Linggi *et.al*. (Linggi *et al.*, 2006; Edwards *et al.*, 2008).

1.3 Transactivation of ErbB receptors

1.3.1 Transactivation of ErbB by GPCRs

As discussed above, growth factors can cause cell growth via activating their receptors to trigger downstream growth signalling pathways, such as the MAPK pathway. The growth induced by activation of various GPCRs can also be mediated by activation of the MAPK pathway. However, the mechanisms by which GPCRs activate growth signalling pathway is less clear compared to the growth factor receptors. In 1996, for the first time, Daub *et al*. found that GPCRs could transactivate the EGFR to trigger downstream growth signalling. They demonstrated that endothelin-1, lysophosphatic acid (LPA) and thrombin treatment rapidly phosphorylated the EGFR followed by activation of MAPK pathway in Rat-1 fibroblasts (an immortalized cell line). All of these agonists activated GPCR receptors: endothelin-1 activated the endothelin receptor isoform ET_A, lysophosphatic acid activated the LPA receptor and thrombin activated proteinase-activated receptors. Inhibition of EGFR (ErbB1) with tyrophostin AG1478 or a dominant-negative EGFR inhibited the GPCR-activated MAPK signalling, confirming that the GPCR mitogenic signalling is mediated by the transactivation of EGFRs (Daub *et al.*, 1996).

The transactivation of ErbB1 by Ang II was first reported by Eguchi *et al*. in primary vascular smooth muscle cells (Eguchi *et al.*, 1998). Since then, increasing evidence demonstrates that the transactivation of EGFR by Ang II occurs in various cells, including renal epithelial cells, hepatic C9, cos-7, MCF-7 and importantly, cardiomyocytes (Asakura *et al.*, 2002; Thomas *et al.*, 2002; Muscella *et al.*, 2003; Shah *et al.*, 2004; Chen *et al.*, 2006). Infusion of antisense oligodeoxynucleotides to ErbB1 in adult rats significantly attenuated the cardiac hypertrophy induced by Ang II (Kagiyama *et al.*, 2002). Transgenic mice expressing dominant negative ErbB1 are resistant to the Ang II induced cardiac hypertrophy (Zhai *et al.*, 2006). Taken together, these studies indicate that ErbB1 is required for Ang II induced cardiac hypertrophy *in vivo*.

1.3.2 Potential mechanisms for ErbB1 transactivation by Ang II: the TMPS pathway

How does Ang II transactivate ErbB1? One proposed mechanism is the triple membrane-passing signalling (TMPS) pathway. In this process, activation of the AT_1R by Ang II leads to the activation of metalloproteases that release ErbB1 ligands from the membrane. These ligands subsequently bind to ErbB1 and trigger downstream signalling (Figure 1.4). The TMPS mechanism describes the inside-outside-inside route of transactivation in three steps.

In the first step of this process, Ang II binding to the AT_1R triggers Gq signalling (Ohtsu *et al.*, 2008), which in turn activates PKC and Ca^{2+} signalling. Both PKC and Ca^{2+} can potentially contribute to triggering the next step in the TMPS pathway. In hepatic or breast cancer cell lines, PKC mediates the release of EGF-like factors, contributing to transactivation (Shah *et al.*, 2002; Muscella *et al.*, 2003). In cardiomyocytes and vascular smooth muscle cells, it has been shown that Ca^{2+} but not PKC is essential for ErbB1 transactivation (Eguchi *et al.*, 1998; Thomas *et al.*, 2002; Smith *et al.*, 2011).

The second step involves cleavage of EGF-like factors. There is evidence to indicate that EGF-like factor shedding (particularly of HB-EGF) might be required for the transactivation of ErbB1 by Ang II. Inhibition of HB-EGF with a small molecule inhibitor or a blocking antibody reduces the transactivation of EGFR by Ang II in various cell types, including Cos-7 cells, cardiomyocytes, renal epithelial cells and hepatocytes (Asakura *et al.*, 2002; Saito *et al.*, 2002; Mifune *et al.*, 2005; Ohtsu *et al.*, 2006b). HB-EGF shedding can be mediated by ADAM12, ADAM17 or MMP2/9 (Saito *et al.*, 2002; Shah *et al.*, 2004; Asakura *et al.*, 2002). Dominant negative expression or pharmacological inhibition of ADAM12, ADAM17 or MMP2/9 blocked HB-EGF shedding and subsequent transactivation of EGFR by Ang II (Asakura *et al.*, 2002; Saito *et al.*, 2002; Ohtsu *et al.*, 2006b). Thus, ADAM 12, ADAM17 and MMP2/9 and HB-EGF are essential for the transactivation of ErbB1, and ADAM/MMP activity may mediate transactivation by shedding HB-EGF.

The transactivation of ErbB1 by Ang II leads to dimerisation of ErbB receptors and the phosphorylation of intracellular tyrosine residues (Scaltriti *et al.*, 2006). The phosphorylated ErbB1 eventually recruits proteins and leads to phosphorylation of ERK1/2 (Shah *et al.*, 2002). Phosphorylated ERK1/2 proteins are imported into the nucleus where they phosphorylate specific transcription factors involved in cell growth (Hill *et al.*, 1995; Gaestel, 2006). To date, ErbB1 is the only member of the ErbB family identified to be transactivated by Ang II to induce hypertrophy (Asakura *et al.*, 2002; Thomas *et al.*, 2002; Muscella *et al.*, 2003; Shah *et al.*, 2004; Chen *et al.*, 2006).

The TMPS paradigm provides a potential scheme for transactivation mechanisms, however the details of transactivation signalling pathways are more complicated and involve more kinases than just those mentioned above. There is evidence showing that Src kinase links the activation of EGFR and GPCRs (Dikic *et al.*, 1996; Fischer *et al.*, 2003). Pharmacological inhibition or RNAi-silencing of Src abrogated the Ang II induced phosphorylation of EGFR (Bokemeyer *et al.*, 2000; Yano *et al.*,

2007). The non-receptor tyrosine kinase Pyk2 has also been proposed to mediate the transactivation of EGFR by GPCRs (Soltoff, 1998; Keely *et al.*, 2000). In vascular smooth muscle cells, Pyk2 binds Src and this was associated with activation of EGFR by Ang II (Eguchi *et al.*, 1999). However, the roles of these factors are controversial. For instance, some studies have proposed pathways for GPCR-mediated EGFR transactivation that are independent of Src activation: expression of a kinase-mutant Pyk2 did not affect the EGFR activation induced by bradykinin (which activates the bradykinin 2 GPCR) in PC-12 cells (Zwick *et al.*, 1999). In addition, inhibition of Pyk2 in cardiomyocytes did not affect the endothelin-1 induced activation of EGFR, suggesting that there is no requirement for Pyk2 in the transactivation of EGFR by endothelin-1 (Kodama *et al.*, 2002). Despite this controversy, these studies suggested that it is highly possible that there are more factors involved in transactivation that are yet to be discovered. Recently, a siRNA screen identified multiple new candidates such as TRIO, BMX and CHKA that may mediate the transactivation of EGFR by Ang II in a human mammary epithelial cell line (George *et al.*, 2013). Individual down regulation of TRIO, BMX or CHKA attenuated the activation of EGFR by Ang II, but not by the EGFR agonist EGF, suggesting that these factors are located upstream of EGFR and required for EGFR transactivation (George *et al.*, 2013). These studies suggested that the pathway for GPCR to transactivate EGFR is much more complicated than that previously proposed.

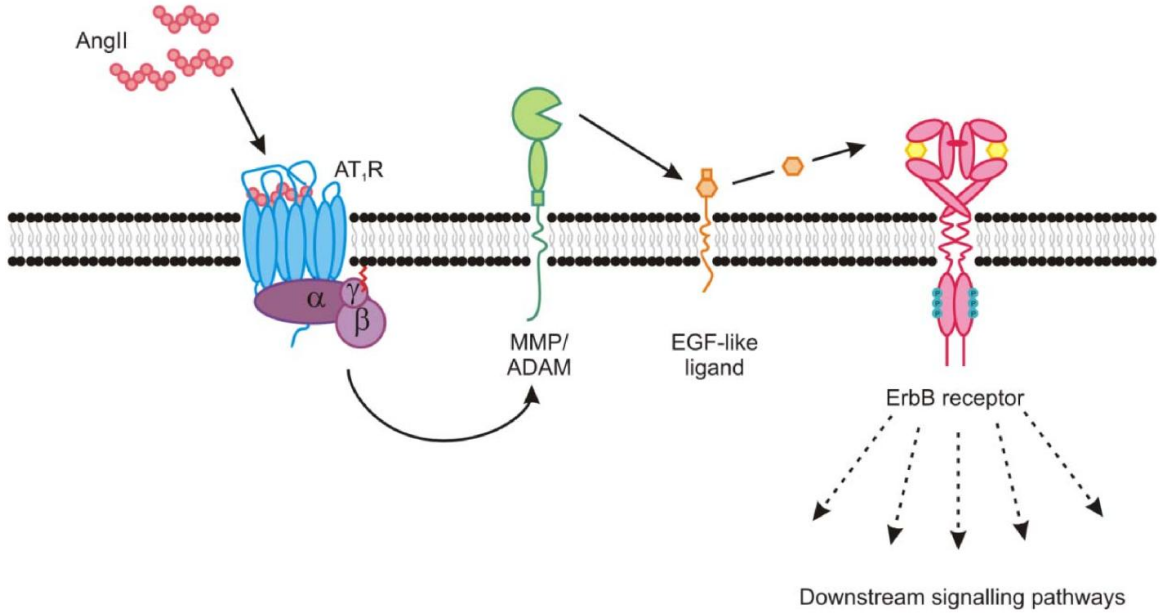

Figure 1.4 Triple membrane-passing signaling (TMPS) pathway. Activation of the AT_1R by Ang II leads to the activation of metalloproteases that release ErbB1 ligands from the membrane. These ligands subsequently bind to ErbB1 and trigger downstream signaling.

1.4 Characteristics of the ErbB4 isoforms

1.4.1 Introduction to the ErbB4 isoforms

Among the ErbB family, ErbB4 is unique in having distinct isoforms as a result of alternative splicing. The four isoforms of ErbB4 structurally differ in two domains: the extracellular juxtamembrane (JM) domain (JM-a and JM-b) and intracellular CYT domain (CYT-1 and CYT-2) (Figure 1.5). The four combinations of the JM and CYT domains form the four primary isoforms of ErbB4. The JM-a isoform contains 23 amino acids in the JM domain that allow for ectodomain shedding by ADAMs (Junttila *et al.*, 2000). JM-b contains an alternative 13 amino acids that makes it resistant to shedding (Junttila *et al.*, 2000). Cleavage of the JM-a isoform occurs in 2 steps, and produces an 80-kDa soluble fragment. First, the JM-a isoform can be subjected to ectodomain cleavage by the metalloprotease ADAM17 to produce a 120-kDa ectodomain fragment and an 80-kDa fragment (Vecchi *et al.*, 1997; Rio *et al.*, 2000; Zhou *et al.*, 2000). The 120-kDa ectodomain fragment is released into the extracellular medium and the 80-kDa fragment remains in the membrane, containing the cytoplasmic and transmembrane domains and several ectodomain residues. The 80-kDa fragment can be subsequently cleaved by γ-secretase within the lipid bilayer to release the intracellular domain (Chang-Yuan *et al.*, 2001).

The CYT-1 isoform has 16 amino acids inserted in the cytoplasmic tail when compared to the CYT-2 isoform. It has been identified that the 16 amino acids of CYT-1 provide a docking site for PI3K, WWOX containing proteins and other proteins, allowing the activation of specific signalling pathways (Veikkolainen *et al.*, 2011). The structural differences of the four ErbB4 isoforms could lead to the functional differences between these isoforms.

The expression of each isoform is tissue specific. In human and mouse adult heart, the most abundant isoform is the JM-b CYT-1, in kidney it is JM-a CYT-2, and in cerebellum it is JM-a CYT-2 and JM-b CYT-2 (Elenius *et al.*, 1997; Elenius *et al.*, 1999). The tissue-specific expression proposes a potentially distinct biological function of each isoform. In some tissues (e.g. mammary cells, neurons) differences in biological function between isoforms has been shown (Naresh *et al.*, 2006; Feng *et al.*, 2007; Law *et al.*, 2007; Muraoka-Cook *et al.*, 2009). For instance, during the brain development only the cleavable JM-a isoform can regulate the time of astrogenesis in the mouse (Sardi *et al.*, 2006). However, whether there are functional differences between isoforms in cardiomyocytes is unknown.

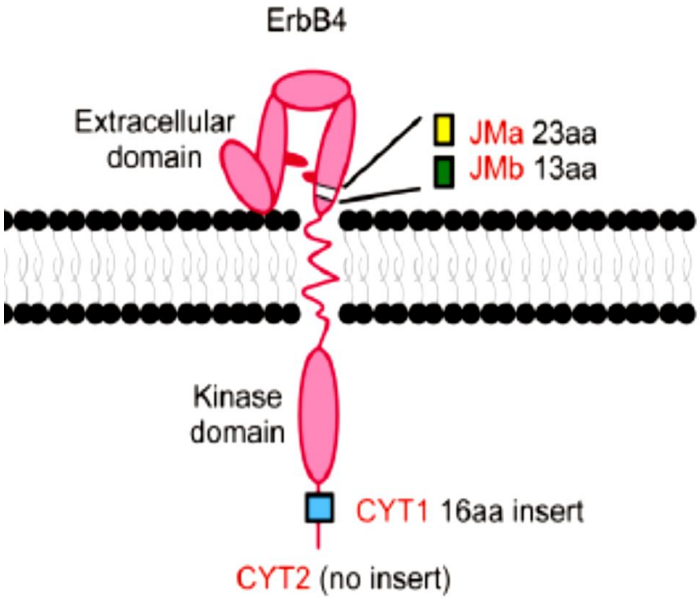

Figure 1.5 Structural differences of ErbB4 isoforms. The four isoforms of ErbB4 structurally differ in two domains: the extracellular juxtamembrane (Jm) domain (JM-a and JM-b) and intracellular CYT domain (CYT-1 and CYT-2). The four combinations of the Jm and CYT domains form the four isoforms of EbB4. The JM-a isoform contains 23 amino acids in the Jm domain that allow for ectodomain shedding. JM-b contains an alternative 13 amino acids that resistant to shedding. The whole receptor containing 1292 -1318 amino acids depends on which isoform it is.

1.4.2 Cleavage in the JM-a domain

As mentioned above, the defining feature of JM-a-containing ErbB4 isoforms is the potential to be cleaved. ADAM 17 is involved in the cleavage of ErbB4 (Rio *et al.*, 2000). Thus, stimuli that activate ADAM 17 such as PKC activators (e.g. the phorbol ester PMA), ErbB4 agonists (e.g. NRG) and ligands that activate certain GPCRs (e.g. gonadotropin-releasing hormone) potentially possess the ability to trigger the cleavage process. PMA was the first agonist found to trigger the cleavage of the ErbB4, and can release the ICD of ErbB4 from the membrane in a wide range of cell types, including breast cancer cells, ovarian cancer cells, lung cancer cells, and a glioma cell line (Vecchi *et al.*, 1996; Zhou *et al.*, 2000; Määttä *et al.*, 2006; Zeng *et al.*, 2009). Cleavage of the ErbB4 induced by NRG is also observed in multiple cell types such as T47D (breast cancer cell line), OVCAR3, and OVCA432 (ovarian cell lines) (Vecchi *et al.*, 1996; Zhou *et al.*, 2000). It has been shown recently that gonadotropin-releasing hormone (a GPCR agonist) caused ADAM 17-dependent cleavage of the ErbB4 and production of 80 kDa fragment in immortalized neurons that endogenously express the JM-a isoform (Higa‐Nakamine *et al.*, 2012).

After being released from the membrane, the 80 kDa ICD can enter the nucleus. The residues 676-684 of the ICD domain are essential for nuclear accumulation of the ICD. Mutation of these residues destroyed the ICD localization to the nucleus without affecting production of the ICD (Williams, Allison *et al*. 2004). Furthermore, it has been shown that the tyrosine kinase activity of ErbB4 is essential for the nuclear localiztion of the ICD (Sundvall *et al.*, 2007). The regulatory mechanism for ICD nuclear localization is not clear. However, the CYT-2 ICD has been shown to accumulate in the nucleus more than CYT-1 ICD due to enhanced tyrosine kinase activity in the intracellular domain of the CYT-2 ICD (Sundvall *et al.*, 2007). Both CYT-2 ICD and CYT-1 ICD possess phosphorylation sites in the intracellular domain, but none of these are specifically located in the extra 16 amino acid sequence possessed by CYT-1. The reason why CYT-2 ICD possesses stronger tyrosine kinase activity than CYT-1 is still unknown.

1.4.3 Biological function of the ICD

By homing to the nucleus and interacting with transcriptional regulatory proteins, the 80 kDa ICD may regulate cell proliferation, apoptosis, differentiation, and DNA damage responses. The transcriptional regulatory proteins identified as interacting with the ErbB4 ICD include AP-2, Yes-associated protein (YAP), signal transducer and activator of transcription 5A (STAT5A), estrogen receptor α (ER α) and Krab-associated protein 1 (Kap1) (Omerovic *et al.*, 2004; Williams *et al.*,

2004; Zhu *et al.*, 2006a; Gilmore-Hebert *et al.*, 2010; Gough, 2010). In a mouse fibroblast cell line, AP-2 was found to interact with the ICD of JM-a CYT-2 to positively regulate the platelet-derived growth factor receptor-alpha (PDGFA) promoter leading to cell proliferation under normal conditions and survival during serum starvation (Gough, 2010). The interaction between YAP and ICD interferes with p73-stimulated proapoptotic signalling (Komuro, Nagai *et al.* 2003; Omerovic, Puggioni *et al.* 2004), whereas interaction of STAT5A with the ICD leads to nuclear localization of STAT5A and activation of the milk genes, such as β-casein and whey acidic protein, thus contributing to the differentiation of the mammary cells (Long *et al.*, 2003; Williams *et al.*, 2004). In addition, interaction of ICD with ERα promotes cell proliferation in the T47D breast cancer cell line (Zhu *et al.*, 2006b); and the ErbB4 ICD interaction with Kap1 mediates the response to DNA damage (Gilmore-Hebert *et al.*, 2010). Clearly, the release and trafficking of the ICD into the nucleus provide a new paradigm for ErbB4 signalling.

In the above section, I described how the ICD interacts with regulatory proteins to regulate cell activity. However, it should be noted that there are two types of ICD. The CYT-1 ICD is different from the CYT-2 ICD in possessing 16 extra amino acids. Compared to the CYT-2 ICD, the 16 amino acid insertion in CYT-1 ICD contains a unique PI3K binding site ("YTPM") and extra PPXY domain that binds WW-containing proteins, such as WWOX and YAP (Junttila *et al.*, 2000; Aqeilan *et al.*, 2005). It has been proposed that this difference in structure may lead to differences in regulatory ability.

Both *in vitro* and *in vivo* experiments have shown that CYT-1 ICD and CYT-2 ICD may have different functions in promoting the growth, death and differentiation of cells. Mammary cell lines expressing exogenous CYT-2 ICD grow more rapidly than the same cell line expressing the CYT-1 ICD (Muraoka-Cook *et al.*, 2009). The CYT-1 ICD probably decreases mammary epithelial cell proliferation by reducing of the rate of cell cycle progression, whereas CYT-2 ICD promotes cell proliferation by increasing cyclinD via the wnt-β-catenin signalling pathway (Sartor *et al.*, 2001; Muraoka-Cook *et al.*, 2006b; Strunk *et al.*, 2007). CYT-1 ICD expression promotes cell apoptosis during serum starvation, whereas the CYT-2 ICD prevented this effect (Naresh *et al.*, 2006; Feng *et al.*, 2007; Muraoka-Cook *et al.*, 2009). A mammary cell line exogenously expressing CYT1-ICD formed more acinar structures in 3D culture when compared with the cells expressing CYT2-ICD (Muraoka-Cook *et al.*, 2006a), indicating that CY1-ICD promotes differentiation of these cells. *In vivo*, transgenic mice expressing CYT-1 ICD have distended mammary ducts filled with secretory material and ductal epithelium that consists of multiple cell layers. Furthermore, fewer terminal end

buds were observed in the mammary glands of mice expressing CYT-1 ICD compared to those of mice expressing CYT-2 ICD (Muraoka-Cook, Sandahl *et al*. 2009). These studies suggest that CYT-1 ICD and CYT-2 ICD have different roles in the regulation of mammary development. Taken together, this work shows that the CYT-1 ICD and CYT-2 ICD can exert divergent functions in cells.

In addition to studies where the CYT-1 ICD and/or CYT-2 ICD are expressed in cells, others have noted profound differences in the function of full length ErbB4 receptors *in vivo*. One seminal study directly compared the functions of the intact JM isoforms by overexpressing full-length JM-a and JM-b in mouse embryonic astrocytes in an ErbB4-null background. The findings demonstrated that only the cleavable JM-a isoform is capable of suppressing astrocyte differentiation (Sardi *et al.*, 2006). This supports the idea that the intact isoforms of ErbB4 may also have distinct functions *in vivo*. In the heart, there have been no studies examining the distinct function of each ErbB4 isoform.

1.5 Cardiomyocyte proliferation

Amphibia and fish can repair their injured hearts by cardiac regeneration. Initially, this regeneration was attributed to stem cells inherent in the heart (Lepilina *et al.*, 2006), but the contemporary view challenges this idea. Recently, with the assistance of genetic fate mapping technology, researchers have been able to follow the fate of newly generated cells and this has been applied to trace the source of newly generated cardiomyocytes (Jopling *et al.*, 2010; Kikuchi *et al.*, 2010). In a genetic fate mapping model, zebrafish with the cardiac-specific *cmlc2a* (cardiac myosin light chain 2a) promoter driving the expression of tamoxifen-inducible Cre recombinase were crossed with animals possessing a GFP gene with its stop codon flanked by loxP sites. In the offspring, the pre-existing cardiomyocytes can be induced to express GFP by tamoxifen treatment. If the newly generated cardiomyocytes also expressed GFP, this suggests that the new cells are generated from pre-existing cardiomyocytes; if not, it is potentially from other source, such as stem cells. With this method, two groups independently demonstrated that heart regeneration in zebrafish occurs principally from the proliferation of pre-existing cardiomyocytes (Jopling *et al.*, 2010; Kikuchi *et al.*, 2010).

In mammals, it is believed that cardiomyocyte proliferation only occurs during the embryonic stage, and that shortly after birth the majority of cardiomyocytes exit the cell cycle and lose the ability to proliferate. A study showed that in neonatal mice retain the capacity to regenerate the intact heart after the left ventricle apex is resected (Porrello *et al.*, 2011). However, this regenerative capacity is only observed in the mice up to seven days. Older mice completely lose the ability for cardiac regeneration, suggesting the proliferative potential in neonatal cardiomyocytes is reduced 1-2 weeks after birth (Porrello *et al.*, 2011). Genetic fate mapping in this study indicated that the majority of new cardiomyocytes originated from preexisting cardiomyocytes (Porrello *et al.*, 2011). This suggested that the capacity to regenerate the heart is similar between fish and mammals at or around birth. It is generally believed that the adult mammalian heart is not capable of fully regenerating the heart following damage (e.g. a myocardial infarction), however the degree to which adult mammalian cardiomyocytes can proliferate remains highly controversial.

Cardiomyocyte proliferation can be measured by immunofluorescence staining for Ki67 or phosphorylated histone H3 (pH3), or BrdU incorporation. Ki67 and pH3 are proliferation markers that label the cardiomyocytes in the transient mitosis stage. Due to the transient nature of the mitosis stage and low proliferation levels of adult cardiomyocytes, pH3 and Ki67 will usually stain only the small number of cells that are currently in mitosis. BrdU is a synthetic analog of thymidine.

It can be incorporated in the genomic DNA when cells undergo DNA synthesis, and is subsequently detected via immunofluorescence. Thus, BrdU incorporation can reflect the total number of proliferating cardiomyocytes over a longer time period. However, this method can induce a false positive stain in the presence of DNA repair and thus potentially exaggerate the results. Despite the limitations of these methods, there is an accumulation of evidence to propose that cardiomyocytes can proliferate in postnatal mice in response to injury or various stimuli. Beltrami *et al*. showed that in the infarcted heart, the fraction of myocytes undergoing mitosis (labeled by Ki67) is 4 percent in the region adjacent to the infarct and 1 percent in those in regions distant from the infarct (Beltrami *et al.*, 2001). Treatment with periostin to induce the reentry of differentiated cardiomyocytes into the cell cycle contributed to a reduction in infarct size and improvement of cardiac function in a rodent infarction model (Kühn *et al.*, 2007). Similarly, infusion of the ErbB4 ligand (NRG1) in adult mice significantly increased the proliferation of mononucleated cardiomyocytes (measured by BrdU incorporation) (Bersell *et al.*, 2009). Interestingly, both the NRG1 and periostin-induced cardiomyocyte proliferation is PI3K-dependent. Inhibition of ERK1/2 with compound PD985059 (1μM) did not inhibit the periostin-induced cell-cycle reentry, whereas inhibition of the PI3K pathway by LY294002 (10 μM) or its downstream signalling Akt pathway by SH-6 (10 μM) fully inhibited periostin-induced cardiomyocyte cell-cycle reentry (Kühn *et al.*, 2007). Using functional inhibition with PTEN (a PI3K inhibitor), Bersell *et al*. demonstrate that the NRG1-induced proliferation of adult cardiomyocytes also required the PI3K pathway (Bersell *et al.*, 2009).

Although these observations strongly suggest that cardiomyocytes in the adult mouse can proliferate in response to various stimuli, there is a study that argues against this. With genetic fate mapping in mice, Hsieh *et al*. showed that the percentage of GFP positive cardiomyocytes was significantly reduced after infarction, indicating dilution of the pre-existing cardiomyocytes by the proliferation of stem or progenitor cells and their subsequent differentiation into new cardiomyocytes. This suggested that in the adult mouse heart, injury-induced cardiac repair depends more on the proliferation of cardiomyocyte progenitor cells or stem cells rather than fully differentiated cardiomyocytes (Hsieh *et al.*, 2007). Irrespective of the source of the regenerated cardiomyocytes, these studies describe above demonstrated that adult mammalian cardiomyocytes can be regenerated to at least some degree.

The proliferation of cardiac cells discussed above has all been investigated in animal models. Measuring the degree of cardiomyocyte regeneration in humans is more challenging. Two recent studies have directly measured cardiomyocyte proliferation rates in the human heart. Bergmann *et*

al. established the age of cardiomyocytes in human heart by taking advantage of the integration into DNA of carbon-14 generated by nuclear bomb testing during the cold war (Bergmann *et al.*, 2009). With mathematical modelling, they revealed that the cardiomyocyte turnover rate gradually decreased from 1% per year at the age of 25 to 0.45% at the age of 75. In contrast, the non-cardiomyocyte turnover rate is up to 18% per year depending on the cell type. All together, less than half the cardiomyocytes are refreshed during a normal life span, and 55% of cardiomyocytes persist from birth. In another study, cardiomyocyte proliferation in human heart was examined by analysing the incorporation of iododeoxyuridine (Idu, a thymidine analog) in postmortem samples obtained from cancer patients who were treated with this drug (Kajstura *et al.*, 2010). The portion of cardiomyocytes labeled with Idu was 2.5-46%. The large variation in the Idu incorporation rate is attributed to the great differences in frequency, period and interval of Idu treatment given to patients. Mathematical modelling of this data suggested that the rate of cardiomyocyte renewal is around 22%. There is a large variation in the cardiomyocyte renewal rate reported in these two studies, from 1% to nearly 22% per year in humans. It is hard to determine which is more accurate by direct comparison of the studies given the totally different methods employed. Compared with other observations, the annual 22% turnover rate of adult cardiomyocytes seems to be the highest report, and thus needs to be carefully considered. Although these studies confirm that there is the potential for cardiomyocytes to renew during human lifespan, the functional regeneration of a damaged heart appears not to occur. While the innate rate of cardiomyocyte replacement seems insufficient to permit complete repair of a damaged heart, the mere existence of a demonstrable regenerative response (and its potential to be augmented by various stimuli) is encouraging in moving towards directed therapies aimed at improving cardiac repair and function.

1.6 Importance of the NRG1-ErbB4 signalling axis

1.6.1 An introduction to NRG1

NRG1 (Neuregulin1) is encoded by a large gene (around 1400kb), less than 0.3% of which encodes protein (Stefansson *et al.*, 2002). Due to splicing, at least 15 different NRG1 isoforms are generated (Buonanno *et al.*, 2001; Falls, 2003). The motif common to all NRG isoforms is an epidermal growth factor-like (EGF) domain that is responsible for binding and activation of receptors. NRG1 can be synthesized as either a secreted protein or membrane precursor. Based on differences in the N-terminal sequence, the membrane-inserted NRG1 can be further divided into 3 types, I - III. Both type I and type II isoforms are single-transmembrane spanning proteins. Cleavage of these isoforms by ADAMs releases bioactive fragments into the circulation, where they then participate in paracrine regulation. Type III isoforms are two-transmembrane spanning and will generate a membrane anchor fragment containing the EGF-like receptor binding domain after cleavage by ADAMs, and thus participate in juxtacrine regulation (Buonanno *et al.*, 2001). Alternative splicing at the C-terminus of the EGF-like domain leads to the generation of NRG1α and NRG1β variants. NRG1α and NRG1β isoforms have different affinities for the ErbB receptors. The NRG1β isoform possess 10-100 times greater bioactivity and a higher affinity for ErbB3 and ErbB4, whereas the predominant isoform expressed in cardiovascular system is NRG1α (Cote *et al.*, 2005). Thus, although NRG1α is the predominant isoform in heart, the NRG1β isoforms may be equally important. Combined with the structural differences in other domains, at least 3 different NRG1α isoforms and 8 NRG1β isoforms are expressed in the adult heart (Pentassuglia *et al.*, 2009a).

NRG1 is mainly distributed in the endocardial endothelium and the cardiac microvascular endothelium (Kuramochi *et al.*, 2004; Lemmens *et al.*, 2006), which share a common embryonic lineage (Misfeldt, 2008). Whether it is expressed in larger veins is controversial - some studies have reported NRG1 expression in human coronary artery endothelial cells (Hedhli *et al.*, 2011), whereas others have failed to detect it in coronary arteries or aortic endothelium (Lemmens *et al.*, 2006). The released NRG1 can target cardiomyocytes and regulate their growth (Zhao *et al.*, 1998; Giraud *et al.*, 2005), survival (Liu *et al.*, 2006), contraction (Brero *et al.*, 2010) and proliferation (Bersell *et al.*, 2009).

1.6.2 NRG1 signalling and cardiomyocyte hypertrophy

NRG1 potently induces cardiomyocyte hypertrophy *in vitro*. Treatment of neonatal cardiomyocytes with 20-30 ng/ml NRG1 increased L-leucine uptake (a marker of protein synthesis), expression of

the hypertrophic genes ANP and α-skeletal actin, and promoted sarcomeric reorganization (Zhao *et al.*, 1998; Giraud *et al.*, 2005). Similar results were observed in primary isolated adult cardiomyocytes (Zhao *et al.*, 1998; Giraud *et al.*, 2005). NRG1-induced cardiomyocyte hypertrophy is thought to be mediated by ErbB2/ErbB4-ERK1/2 signalling. Treatment with 20 ng/ml NRG1for 5 min induced phosphorylation of ErbB4 and its preferential dimerisation partner ErbB2 in both neonatal and adult cardiomyocytes (Zhao *et al.*, 1998). Intravenous administration of 10μg/kg recombinant human NRG1 (rhNRG1) in mice for 10 min induced phosphorylation of ERK in the heart, which reached a 7-fold increase after 90 min treatment (Liu *et al.*, 2006). The rhNRG1-enhanced sarcomeric organization was blocked by the ERK pathway inhibitor PD98059, but not the PI3K kinase inhibitor Wortmannin, suggesting that the rhNRG1-enhanced sarcomere organization is via ERK, but not PI3K, signalling pathways (Liu *et al.*, 2006). Activation of ERK1/2 promotes protein synthesis and sarcomere reorganization during NRG1 induced cardiomyocyte hypertrophy. Activation of ErbB2 by treating cardiomyocytes with an ErbB2 activating antibody induced phosphorylation of ERK1/2, demonstrating that ErbB2 phosphorylation is sufficient for activation of ERK1/2. In contrast, ErbB2 inhibition reduces basal phosphorylation of ERK1/2 (Fukazawa *et al.*, 2003).

1.6.3 NRG1 signalling in cardiac protection

NRG1 can be released from cardiac microvascular endothelial cells (CMEC) under conditions of oxidative stress. H_2O_2 increased the NRG1 level in culture medium of CMECs (Kuramochi *et al.*, 2004) *in vitro,* whilst *in vivo* ischaemia-reperfusion injury increased the NRG1 level in the perfused coronary effluent (Kuramochi *et al.*, 2004). The released NRG1 appears to have a cardioprotective effect. Liu *et al*. showed that NRG1 improved both cardiac performance and survival in various models of LV failure, including the LAD ligation infarct model, doxorubicin-induced cardiomyopathy model, Coxsackie virus B3-induced myocarditis model, and a chronic rapid pacing model (Liu *et al.*, 2006). The cardioprotective effect of NRG1 is attributed, at least in part, to its ability to promote cardiomyocyte survival and enhance myofibril organization.

Primary neonatal cardiomyocytes deprived of serum in culture exhibit a gradual loss in cell viability (Zhao *et al.*, 1998). Addition of NRG1 into the culture medium increases cell viability by 30% compared to the control (as measured by the activity of NAD(P)H-dependent cellular oxidoreductase enzymes using the colorimetric assay MTT) (Zhao *et al.*, 1998). In addition, NRG1 treatment also significantly decreases apoptosis (measured by TUNEL) of primary cardiomyocytes in serum-free medium (Zhao *et al.*, 1998). A microarray study showed that NRG1 increased the

expression of oxidative stress defense related factors (e.g. thioredoxin) and reduced expression of the apoptosis factors, harakiri (HRK) and programmed cell death 2 (PDCD2) in cardiomyocytes, which may also contribute to cardiomyocyte survival (Giraud *et al.*, 2005).

During cardiomyocyte damage, myofibrillar disarray and myofibril loss are often observed. NRG1 treatment significantly attenuates the myofibrillar disarray and myofibril loss induced by doxorubicin. This attenuation contributes to the preservation of cardiac function in these animals (Bian *et al.*, 2009). Troponin is a complex of three regulatory proteins (troponin C, troponin I, and troponin T) that is integral to cardiac muscle contraction. The degradation of myofibrils releases the troponin subunits into the blood, where they are important markers for detection of myocardial injury (Katus *et al.*, 1991; Adams *et al.*, 1993). Doxorubicin treatment significantly decreases levels of cardiac troponin in mice, an effect that is attenuated by administration of NRG1 (Bian *et al.*, 2009). In agreement with this, another study showed that NRG1 reduces both troponin I release into serum (which occurs during cardiomyocyte damage) and histological alterations associated with myocarditis (Muraoka-Cook *et al.*, 2006a).

The ErbB-PI3K-Akt pathway was proposed to be the central downstream signalling pathway that mediates the ability of NRG to modulate the survival and function of cardiomyocytes (Brero *et al.*, 2010; Fang *et al.*, 2010; Jie *et al.*, 2012; An *et al.*, 2013). For instance, treatment of cardiomyocytes with the PI3-kinase inhibitor wortmannin or overexpression of a dominant-negative Akt abolished the protective effect of NRG1 on daunorubicin-induced caspase-3 activation and apoptosis (Fukazawa *et al.*, 2003). Pretreating cardiomyocytes with anti-ErbB2 antibodies abolished the protective actions of cardiac microvascular endothelium (a source for NRG1) against cardiomyocyte apoptosis (Lemmens *et al.*, 2006). AG879 (an ErbB2 inhibitor) treatment abolished the ability of NRG1 to attenuate the doxorubicin- induced decrease in cardiac troponin I and troponin T (Bian *et al.*, 2009), suggesting that the NRG1 induced cardioprotective effect is ErbB2-dependent.

1.6.4 NRG1 signalling in cardiomyocyte contraction/relaxation

Calcium is a critical factor for regulating cardiomyocyte contraction and relaxation. Disorders of Ca^{2+} homeostasis contribute to the development of heart failure. Myocyte contraction is regulated by Ca^{2+} release from the sarcoplasmic reticulum (SR) into the cytoplasm, and relaxation by uptake of Ca^{2+} into the SR. This Ca^{2+} uptake is mediated by SR Ca^{2+} ATPase (SERCA2a). NRG1 can enhance cardiomyocyte relaxation by regulating the Ca^{2+} uptake. NRG1 induced activation of

PI3K/Akt promotes the activation of PKG (Mery *et al.*, 1991; Brero *et al.*, 2010), which enhances the relaxation of cardiomyocytes by regulating major components of excitation-contraction coupling, such as L-type Ca^{2+} channel (LTCC) , phospholamban (PLB) and troponin I (Blumenthal *et al.*, 1978). PLB activation promoted the SERCA2a activation (Macdougall *et al.*, 1991; Verboomen *et al.*, 1992) and caused Ca^{2+} uptake into the SR (Brero *et al.*, 2010) to enhance cardiomyocyte relaxation.

1.6.5 NRG1 signalling in cardiomyocyte proliferation

In addition to the functions mentioned above, a role for NRG1 in promoting cardiomyocyte proliferation has also been proposed. Zhao et al. demonstrated that treatment with NRG1 for 30h caused an approximately 2 fold increase in DNA synthesis in embryonic cardiomyocytes as measured by [^{3}H]-thymidine uptake. NRG1 also significantly increased the [^{3}H]-thymidine uptake in neonatal cardiomyocytes cultured in serum-free medium (Zhao *et al.*, 1998). In addition to promoting DNA synthesis, NRG1can also stimulate cell division, including both karyokinesis and cytokinesis. Bersell *et al*. detected cytokinesis in cardiomyocytes by using immunofluorescence to stain the marker protein aurora B kinase, which is required for contractile ring formation in cytokinesis. They found the number of positively stained cells was significantly increased by NRG1 treatment. A similar result was observed for karyokinesis measured with video microscopy (Bersell *et al.*, 2009). Interestingly, the effect of NRG1 on cardiomyocyte proliferation may be dictated by the degree of stimulation. Zhou *et al*. showed that the maximum proliferative effect of NRG1 occurs at 0.1 nM (Zhou et al., patent application published as WO00/37095). Similar to this, Bersell *et al.* also showed an increased DNA synthesis in response to NRG1, which was maximal between 0.1-1nM (Bersell *et al.*, 2009). At higher concentrations, NRG1 may inhibit DNA synthesis due to the persistent activation of the MAPK signalling pathway, which inhibits CyclinD to arrest the cell at G1 phase (Zhou *et al*., patent application published as WO00/37095). Direct evidence that NRG-induced cardiomyocyte proliferation is mediated by ErbB4 is also provided by Bersell *et.al*. (2009). Administration of NRG1 induced 14.3% of mononucleated cardiomyocytes to proliferate (as indicated by BrdU incorporation) in the adult mice heart, and this proliferation was attenuated in transgenic mice with cardiac-specific deletion of ErbB4. In cultured adult cardiomyocytes, blocking ErbB4's preferential dimerisation partner ErbB2 with an inhibitory antibody also decreased DNA synthesis (Bersell *et al.*, 2009), suggesting an critical role of the ErbB2/ErbB4 dimer in mediating NRG1-induced proliferation.

1.6.6 Interactions between NRG1 signalling and the endocrine system

As a critical paracrine factor that is potentially beneficial to the heart, it is important that the synthesis and release of NRG1 is adaptive to cardiac activity. Indeed, the expression and release of NRG1 is controlled, at least partially, by endocrine factors or stimuli such as pressure overload. As mentioned earlier, NRG1 (detected in perfused coronary effluent) can be released from the microvascular endothelium in response to ischaemia-reperfusion (Kuramochi *et al.*, 2004). In addition to that, stretch induces the expression of NRG1 in cardiac microvascular endothelium. Correspondingly, transverse aortic constriction (TAC) induces the up-regulation of NRG1 in the heart (Lemmens *et al.*, 2006). A study showed that NRG1, in primary isolated microvascular endothelial cells, is increased by endothelin-1 treatment (Zhao *et al.*, 1998). In contrast, Ang II and phenylephrine decreased the expression of NRG1 in cardiac microvascular endothelium (Lemmens *et al.*, 2006). Due to the beneficial effects of NRG1 on cardiac tissues (as discussed above), the up-regulated NRG1 might serve as a mechanism to counterbalance the effect of pathological stimuli and thus protect the cardiomyocytes to some degree in these pathological conditions. In contrast, in other conditions, such as activation of RAS system, the NRG1 down-regulation might facilitate the progression of the cardiac disease. NRG1 also provides a negative feedback on these stimuli. Treatment with NRG1 in LAD ligation mice significantly reduced the increased concentrations of renin, AngI, Ang II and aldosterone in the circulation, suggesting that the rhNRG1 attenuated activation of the renin-angiotensin-aldosterone axis (Muraoka-Cook *et al.*, 2006a). Besides, NRG1 can interact with adrenergic signalling to regulate cardiomyocyte contractility, where it has been demonstrated that NRG1 reduces the contractile response of cardiomyocytes to α-adrenergic stimulation (Lemmens *et al.*, 2004). Cardiomyocytes lacking effective neuregulin signalling (NRG-gene mutant animals) are unable to counterbalance the adrenergic effect (Okoshi *et al.*, 2004).

1.6.7 Function of ErbB2 and ErbB4 in the heart

The importance of NRG1 signalling highlights the potential role of its receptor, ErbB4 and its preferred dimerisation partner (ErbB2) in adult heart function. ErbB3 can also bind with NRG1, however, ErbB3 expression is not detectable in the adult heart (Campreciós *et al.*, 2011). ErbB2 is overexpressed in breast cancer (Houston *et al.*, 1999; Sørlie *et al.*, 2001), and monoclonal antibodies targeting ErbB2 have been used in treatment of this disease. The monoclonal antibody for ErbB2, trastuzumab, has been trialled for breast cancer therapy, but its administration increases the risk for cardiac dysfunction: the incident rate was 27% in patients receiving trastuzumab and anthracycline-containing chemotherapy, compared with 8% incidence among patients who received chemotherapy alone (Seidman *et al.*, 2002). Despite the fact that anthracycline is also cardiac toxic

and trastuzumab-induced cardiac dysfunction is reversible (79% patients improved after receiving standard treatment for congestive heart failure), this clinical observation led to the idea that ErbB2 signalling is critical in the adaptive response of adult heart to stress (Seidman *et al.*, 2002). A further study using ErbB2 conditional knockout animal models confirmed the importance of ErbB2 in cardiac function and structural maintenance (Özcelik *et al.*, 2002). In this study, the MLC-2V promoter was used to drive expression of Cre recombinase to specifically induce deletion of ErbB2 from 50-60% cardiomyocytes in heterozygous ErbB2$^{flox/+}$ animals. There were no functional or morphological differences between the wild type and mutant animals at birth, but the mice with ErbB2 deletion developed severe cardiomyopathy in adulthood. This cardiomyopathy was characterised by cardiac dysfunction (i.e., a decreased fractional shortening measured by echocardiography), dilatation of both ventricles (i.e., increased chamber size with thinned walls) and cardiac hypertrophy (Özcelik *et al.*, 2002). In support of this, cultured adult myocytes treated with a non-activating ErbB2 specific antibody display myofilament disarray (Pentassuglia *et al.*, 2009b), which was significantly increased following co-treatment with chemotherapeutic agents like doxorubicin.

Given ErbB2 does not bind EGF ligands and is instead activated by forming dimers with other ligand-stimulated ErbB receptors (particularly ErbB4 in heart), the above observations lead to the hypothesis that the NRG1-ErbB4 interaction likely plays an important role in adult heart. Accordingly, global deletion of ErbB4 leads to death during mid-embryogenesis due to the defective development of myocardial trabeculae in the ventricles (Gassmann *et al.*, 1995). The heart defects in ErbB4 mutant mice could be rescued by cardiac-specific expression of ErbB4 (driven by a myosin promoter). These rescued mice reached adulthood and were fertile, suggesting that ErbB4 is critical for heart development (Tidcombe *et al.*, 2003). In contrast to global deletion, cardiac-specific deletion of ErB4 using Cre (under the MLC-2V promoter) did not cause embryonic lethality, nor did it alter cardiac morphology or function in neonatal mice. It is important to note that the MLC-2v promoter becomes active during the differentiation of ventricular cardiomyocytes, which might be later than the initiation of the heart generation (Klug *et al.*, 1996; Franco *et al.*, 1999). However, when mice with cardiomyocyte-specific deletion of ErbB4 reached adulthood, they developed dilated cardiomyopathy that was characterised by thinning of the ventricular walls, eccentric hypertrophy, reduced contractility and conduction delays (Garcia-Rivello *et al.*, 2005). Interestingly, conditional knockout of ErbB4 also caused alterations in the morphology of intercalated disks and an abnormal distribution of ErbB2 on the plasma membrane, indicating that

ErbB4 may play an important role in maintaining cell-cell contact and ErbB2 localisation (Garcia-Rivello *et al.*, 2005).

1.7 The rationale and aims for this project

In the past 10 years, the transactivation of ErbB1 by Ang II has been shown in various cell types, including cardiomyocytes, renal epithelial cells, and cell lines such as hepatic C9, cos-7 and MCF-7 cells (Eguchi *et al.*, 1998; Thomas *et al.*, 2002; Muscella *et al.*, 2003; Shah *et al.*, 2004; Chen *et al.*, 2006). However, previous experiments in our laboratory (Hsiu-wen Chan, PhD thesis) showed that ErbB4 agonists selectively induce cardiomyocyte hypertrophy (as measured by the increase in protein/DNA ratio and reorganisation of the actin cytoskeleton), whereas the ErbB1 selective agonist, EGF, did not. Thus, it seems that in cardiomyocytes, ErbB4 receptor activation might be a stronger stimulus for hypertrophy than ErbB1 activation, and opens up the untested possibility that Ang II/AT_1R may transactivate ErbB4 in this setting. **As a consequence, based on the studies above, the first aim of my PhD project is to investigate the role of ErbB4 receptors in Ang II-mediated cardiomyocyte hypertrophy.**

As discussed above, ErbB4 is spliced into four isoforms (JM-a CYT-1, JM-a CYT-2, JM-b CYT-1 and JM-b CYT-2) that have unique characteristics. Whilst preliminary observations indicate that these four ErbB4 isoforms are present in rat cardiomyocytes (Hsiu-wen Chan, PhD thesis), this finding needs to be confirmed and quantified. There is also no information as to whether the processing of the ErbB4 receptor (to cleave and release the extracellular and intracellular domains) occurs in cardiomyocytes and if this can be stimulated by GPCRs like the AT_1R. Furthermore, whether ErbB4 isoforms and/or their processing contribute equally to cardiomyocyte hypertrophy has not been examined. **Thus, the second major aim of my study will be to investigate the role of ErbB4 isoforms in mediating cardiomyocyte hypertrophy**.

Finally, NRG1-ErbB4 signalling is critical for heart development, anti-apoptosis and hypertrophy (refer to section 1.6). Despite the power of the elegant transgenic approaches (detailed above) to reveal potential functions for ErbB4 in heart, it is critical to appreciate that these models all modulate deletion of ErbB2 or ErbB4 in the embryo. Thus, the likelihood that the phenotypes observed in adulthood are caused by defects in cardiac development cannot be completely excluded. In order to unambiguously link the ErbB4 receptor to cardiac function in the adult, **my final aim is to develop a cardiomyocyte-specific conditional deletion of ErbB4 in mice and investigate the cardiac phenotype of these mice**.

CHAPTER 2
GENERAL METHODS

2. General Methods

2.1 Animal Ethics statement

1-2 day old neonatal rats (Sprague Dawley) were used for cardiomyocyte isolation and handled in accordance with the Australian code of practice for care and use of animals for scientific purposes under ethics approval number SBMS/237/09/NHMRC/NHF "Regulation of cardiac hypertrophy" from the University of Queensland Ethics Committee.

All experiments in Chapter 5 were done under the ethics approval number SNMS/253/12/NHMRC "Growth factor receptors in cardiac hypertrophy". The animals were bred under the ethics approval numbers SBMS/295/11/NHMRC/BREED "Cardiac-specific gene deletion-floxed ErbB4 mice" and SBMS/294/11/NHMRC/BREED "Cardiac-specific gene deletion-creER mice".

2.2 Chemicals and reagents

All chemicals and reagents were analytical or cell culture grade and purchased from Sigma-Aldrich (New South Wales, Australia), Invitrogen (Victoria, Australia), Applied Biosystem (Victoria, Australia), Thermo Fisher Scientific (Victoria, Australia), Qiagen (Victoria, Australia), Gibco (Victoria, Australia) and New England Biolabs (Massachusetts, USA). Plasticware such as Falcon tube, Eppendorf tube, pipette tips, cell culture flasks/plates were purchased from Corning Life Science (New South Wales, Australia), Biopointe Scientific (California, USA) and Eppendorf South Pacific (New South Wales, Australia). Suppliers for each chemical or reagent will be listed in each research chapter where they were used.

2.3 Vector constructs

The ErbB1 shRNA and ErbB2 shRNA expressing vectors (shErbB1 and shErbB2) were constructed by James Goonan and the ErbB4 shRNA expressing vector (shErbB4) by Dr Hsiu-wen Chan. The shRNA knockdown-resistant isoform of ErbB4 (kdr-JM-a CYT1; kdr-JM-a CYT2; kdr-JM-b CYT1; kdr-JM-b CYT2) were constructed and tested by Dr Hsiu-wen Chan. The luciferase reporter plasmids driven by hypertrophic gene promoters (MLC-2V, ANP-328, and CyclinD) were gifts from Dr Mona Nemer (Canada). The GFP tagged isoforms of ErbB4 (pEGFP-N1-JM-a CYT-

1, pEGFP-N1-JM-a CYT-2, pEGFP-N1-JM-b CYT-1 or pEGFP-N1-JM-b CYT-2) were constructed by myself as described in Chapter 4 method 4.2.5.

2.4 Cell culture

2.4.1 Cardiomyocyte culture

Neonatal ventricular cardiomyocytes preparations were performed by myself, Dr. Brooke Purdue, Dr. Simon Foster, Dr. Tamara Paravicini and Mr. Gregory Quaife-Ryan. 1-2 day old Sprague Dawley rat pups were sacrificed by decapitation. Hearts were harvested and atria were carefully removed. The ventricles were cut into multiple pieces and subject to 7 enzyme digestions (0.03% collagenase and 0.08% pancreatin). Each digestion was processed at 37°C for 20 min using a water jacketed spinner flask. The first collection rich in blood cells was discarded. The other collections were kept on ice and combined with newborn calf serum to neutralize the enzymes. The cells were centrifuged at 1000×g for 6 min at 4°C and then resuspended with ADS buffer (refer to the Appendix A). The cardiomyocytes were isolated from non-myocardial cells using discontinuous percoll gradient centrifugation. The percoll gradient was prepared by adding 4 ml 40% percoll (diluted in ADS) on top of 3 ml 59 % percoll in 15 ml sterile falcon tube. Around 2 ml of cell suspension was overlaid on top of the percoll gradient before centrifugation (3000 rpm for 30 min). After centrifugation, there were two cell layers: the upper layer is rich in fibroblasts, whilst the lower layer is rich is cardiomyocytes. The purified cardiomyocytes were collected and washed in ADS buffer twice before being seeded in 0.1% gelatin-coated cell culture plates with MEM culture medium (supplemented with 10% newborn calf serum, 5- bromo-2'-deoxyuridine (BrdU) and antibiotics). The next day, cardiomyocytes were washed twice with PBS and maintained in DMEM CCT SS2 (refer to Appendix A). DMEM CCT SS2 is the serum free media (using vitamins, amino acids, insulin etc. to replace FBS) used for ongoing cardiomyocyte culture, with BrdU to prevent fibroblast proliferation and 50 mM KCl to stop spontaneous contraction.

2.4.2 Maintenance of CHO and HEK293-T cell lines

HEK293-T cell and CHO cells were maintained in DMEM supplemented with 10% FBS and antibiotics. All cells were incubated at 37°C in a humidified 5% CO_2 incubator. When confluent, cells were passaged by washing once with PBS and then incubating with 0.25% Trypsin-EDTA (Invitrogen Australia) at 37°C for 1-3 min. Culture media was added to stop the digestion followed by centrifugation (3000 rpm for 3min). The supernatant was removed and the cells were resuspended in culture medium before plating.

2.4.3 Drug treatment

Cells were incubated in serum free media for a day prior to drug treatment. Cells were treated with various agonists (Ang II and NRG1β1) and inhibitors (AG1478) at certain concentrations for the indicated time at 37°C. Treatment was terminated by washing cells with ice-cold PBS and incubating cells on ice.

2.5 DNA/siRNA Transfection

2.5.1 DNA Transfection

DNA were transfected into cells using lipofectamine 2000^{TM} (Invitrogen) according to the manufacturer's instruction. The protocols used for transfection of cardiomyocytes and cell lines are slightly different and will be briefly described here.

For luciferase assay, cardiomyocytes in 12 well plates were transfected in 360µl Opti-MEM (Invitrogen) containing 0.8 µl lipofectamine 2000^{TM} and total of 500ng DNA for luciferase assays. The lipofectamine 2000^{TM} and DNA were individually diluted in 45µl Opti-MEM and incubated separately for 5 min at room temperature before mixed together for another 30 min incubation. Then the DNA and lipofectamine 2000^{TM} mixture was added to individual cell culture wells containing 270 µl Opti-MEM. After 6 hours or overnight, the transfection medium was changed into the normal culture medium for cardiomyocytes (DMEM CCT SS2).

HEK293-T cells or CHO cells were seeded onto 6 well plates and transfected in 2ml Opti-MEM containing 500-600 ng DNA and three times the amount lipofectamine 2000^{TM} relative to the DNA amount (1.5-1.8 µl). The lipofectamine 2000^{TM} and DNA were individually diluted in 100 µl Opti-MEM and incubated separately for 5 min at room temperature before mixed together for another 30 min incubation. The DNA and lipofectamine 2000^{TM} mixture was then added to individual cell culture wells containing 1.8 ml Opti-MEM. The cells were incubated with the transfection reagents for 6 hour before the Opti-MEM was replaced with normal culture media (DMEM supplemented with 10% FBS). At 24-48 hours after transfection, cells were harvested and subjected to Western blot analysis.

2.5.2 siRNA transfection

The cardiomyocytes can be transfected with siRNA via forward or reverse methods. Both methods can induce efficient knockdown and were developed separately by myself (reverse method) and Ms. Choon Boon Sim (forward). For forward transfection, 5 µl Lipofectamine® RNAiMAX (Invitrogen) and 2 µl siRNA (20 µM) was individually suspended in 250 µl DMEM CCTSS2 (antibiotic free) and incubated at room temperature for 5-10 min. siRNA and lipid were mixed together and subject to 30 min incubation before being applied to one well of a 6 well-plate, which already contained 1.5 ml DMEM CCTSS2. For reverse transfection, the same amount of Lipofectamine® RNAiMAX and siRNA was suspended in 250 µl DMEM (antibiotic and serum free). After incubation, the DNA and lipid mixture was mixed with 1.5 ml cell suspension (1.8×10^6 cells in antibiotic free DMEM supplied with 13% serum) and then added to one well of a 6 well-plate. For both reverse and forward methods, the transfection medium was changed into normal cardiomyocyte culture medium (DMEM CCTSS2) 24 h later. For detection of phosphorylated ERK1/2 in cardiomyocytes (Figure 3.6), the reverse transfection method was used. For the hypertrophy assay, the forward transfection (Figure 3.7) was used. The forward transfection efficiency is shown in Figure 3.5, and the reverse transfection had a similar efficiency with the same siRNA (data not shown). The reason I switched from reverse transfection to forward transfection is because the latter is easier to handle. The forward transfection method was developed by Ms. Choon Boon Sim in our lab after I finished the experiments shown in Figure 3.6.

2.6 Luciferase assays

To detect the activation of the hypertrophic genes (ANP, CyclinD and MLC-2V), hypertrophic gene promoter driven luciferase reporters were constructed by fusing the core sequence of each promoter to the firefly luciferase reporter. The reporter constructs for ANP, CyclinD and MLC-2V have been described previously (Henderson *et al.*, 1989; Knowlton *et al.*, 1991; Suzuki-Yagawa *et al.*, 1997). Cardiomyocytes seeded in 12 well plates were transfected with 300 ng of luciferase reporters along with other DNA constructs (100 ng AT_1R and 100 ng shRNA). 24-48 h after transfection, cardiomyocytes were stimulated with agonists for 48 h. Then cells were washed with ice-cold PBS twice and lysed with 150 µl of Luciferase Cell Culture Lysis Reagent (Promega). To ensure sufficient lysis, cells were subjected to a cycle of freezing and thawing at -80°C and room temperature and scraped off from the plates. Cell lysates were collected into 1.5 ml Eppendorf tube before centrifuged at 12,000 x g for 2 min at 4°C. 20 µl aliquots of supernatant were transferred to a 96-well white flat-bottomed assay plates. Luminometry was performed with an Optima microplate

Reader (BMG LABTECH Company) and 100 µl Luciferase Assay Mix (Promega) was injected into each well containing cell lysate.

2.7 Protein extraction and Western analysis

2.7.1 Protein extraction and BCA assay

To detect ErbB receptors, total and phosphorylated ERK1/2 proteins were extracted from cardiomyocytes or cell lines (HEK-293 or CHO). Cells were washed with PBS and harvested with RIPA lysis buffer (a strong denaturing buffer). For cell lines cultured on 6 well plates, 200 µl RIPA lysis buffer was applied per well. For cardiomyocytes, 70-80 µl RIPA lysis buffer was applied to each well. Cells were scraped off on ice and the lysate collected into 1.5 ml Eppendorf tube and vortexed before centrifugation at 12000 x g for 15 min at 4°C. The supernatant was transferred into new Eppendorf tubes (pre-chilled). The concentration of total protein was estimated with the BCA assay according to the manufacturing instruction (Thermo Scientific Pierce BCA Assay Kit). Briefly, 25 µl cell lysates were added into 96 well plates (in triplicate) and mixed with 200 µl BCA working reagent (Thermo Scientific Pierce BCA Assay Kit). Standard samples were prepared using Bovine Serum Albumin (Sigma) dissolved in the same lysis buffer. After 30 min of incubation at 37°C (with plates covered by membrane), samples were analysed for absorbance at 560nm with an Optima microplate reader (BMG Labtech).

2.7.2 SDS-PAGE and Western blot analysis

To separate proteins according to their size, total proteins were resolved by sodium dodecyl sulphate polyacrylamide gel electrophoresis (SDS-PAGE) using the Mini-PROTEAN gel system (Bio-Rad) (for samples ≤ 50 µl) or SE600 gel system (Hoefer) (for samples ≥ 50 µl). Protein samples were mixed with SDS loading buffer and boiled for 5 minutes at 95°C. Protein samples and a molecular weight standard (Precision Plus Protein™ Dual Color standards, BIO-RAD) were electrophoresed at 100V for approximately 2 h (Mini-PROTEAN gel) or at 25 mA for 5 h (SE600 gel) using PowerPac^{TM} Basic Power Supply (Bio-Rad). Then proteins were transferred onto polyvinylidene fluoride (PVDF) membrane using Mini Trans-Blot Cell system (for small gels) at 60 volts for 1.5 h (for small size proteins such as ERK1/2) or Trans-Blot Cell system (for large gels) (Bio-Rad) at 400 mA for 5-6 h (for larger proteins such as ErbB receptors). The membrane was incubated with blocking buffer (Odyssey) at RT for 1h and then with primary antibody (1:1000 dilution in blocking buffer) at 4°C overnight. The membrane was washed with washing buffer (PBS with 0.1% Tween20) for 4 times for 5 min each and incubated with the secondary antibody for 1 h

at RT (1:10000 dilution in blocking buffer). After further washing, membranes were scanned using an Odyssey Licor Scanner (LI-COR Biosciences).

2.8 RT-qPCR

2.8.1 RNA extraction

To analyse mRNA for gene expression, RNA was extracted from animal tissues or cultured cells using TRIzol reagent (Invitrogen) according to the company's instruction. Briefly, for cells cultured in 6 well plates, media was removed and cells washed with PBS before adding 1 mL of TRIzol per well. For animal tissues (heart and skeletal muscle), ~20 mg of tissue was homogenised in a 2 ml Eppendorf tube containing 500 µl TRIzol reagent using a Polytron tissue homogeniser (Kinematica). To remove the fat and extracellular connective tissues, tissue samples were centrifuged at 12000×g for 10 min at 4°C following homogenization, The supernatant containing RNA was collected into a new tube and the pellet containing fat and extracellular connective tissues were discarded. Then chloroform (1/5 volume relative to the amount of TRIzol) was added to the cell lysate or homogenised tissue sample. After vigorously mixing by hand, the samples were incubated at room temperature for 2-3 min and then centrifuged at 12000×g for 15 min at 4°C. Three separate layers were observed after centrifugation. The top aqueous phase was carefully transferred into a new tube without drawing any of the interphase or organic layer in the bottom. Then ½ volume isopropanol (relative to the TRIzol reagent amount) was added to the aqueous phase followed by 10 min incubation at RT. Samples were centrifuged at 12000×g for 10 min at 4°C and the supernatant removed. The pellet was washed with 1 volume of 75% ethanol (relative to the TRIzol reagent amount). The wash was discarded after centrifuge at 7500 g for 5 min at 4°C. The pellet was air dried for 5-10 min and resuspended in nuclease-free water at 55°C for 10 min.

2.8.2 DNase treatment

DNase I is a nuclease which causes the degradation of almost all forms of DNA (single-strand or double strand DNA, DNA-RNA hybrids and chromatin). DNase I treatment is a routine method to remove the potentially contaminating genomic DNA from RNA preparation. For this, the isolated RNA was treated with using TURBO DNA free kit (Applied Biosystem) according to company's instructions. Briefly, the RNA was treated with DNase I in a 25 µl reaction volume (containing 2 µg RNA, 1 µl TURBO DNase, and 1×TURBO DNase buffer) at 37°C for 30 min. The reaction was stopped by adding 5 µl DNase inactivation reagent (supplied in TURBO DNA free kit). After 5 min

incubation at room temperature, the mixture was centrifuged at 10000 g for 90s. The supernatant was carefully collected using a 20 µl pipette without touching the bottom pellet.

2.8.3 cDNA synthesis

The mRNA was reverse transcribed into cDNA using the SuperScript™ III Reverse Transcriptase Kit (Invitrogen). Briefly, 250 ng of random primers, 500 ng RNA and 10 nM dNTPs were mixed and topped up to 13 µl reaction volume with nuclease-free water. After incubation at 65°C for 5 min, the samples were left on ice for 1 min and supplemented with 200 units SuperScript™ III RT, 40 units RNaseOUT™ Recombinant RNase Inhibitor, 100 nM DTT, and 1× First-Strand Buffer (final concentration). The mixture was collected to the bottom of the PCR tube by brief centrifugation and then mixed thoroughly by pipetting. The reverse transcription was performed using a PCR machine with the following conditions: 25°C for 5 min (incubation), 50°C for 60 min (reverse transcription) and then 70°C for 15 min (inactivation).

2.8.4 Real-time PCR

Real-time PCR is a technology that detects the amount of PCR product formed following each cycle of the reaction. It uses fluorescent chemicals to detect the generated DNA and combines the amplification and detection into one step. Currently, two common types of fluorescent systems are used: the SYBR Green reagent and TaqMan probe. SYBR Green dye binds with double-stranded DNA formed during PCR and emits much stronger fluorescence signal when bound than when free in solution. Thus, the fluorescence signal is in proportion to the amount of total DNA product formed. Because the SYBR Green dye binds to all double-stranded DNA, the strength of the fluorescence signal does not always reflect the amount of PCR product from the target gene, especially if there is non-specific amplification. It is important that the primers are designed to specifically amplify the targeted sequence. For some genes, this is very hard due to the shortness and/or homology of gene sequences. Thus, a more specific method is often used, such as TaqMan. The TaqMan method employs a TaqMan probe and a pair of normal PCR primers. A TaqMan probe consists of 18-30 oligonucleotide annealed to the target gene. The primer pair is designed to amplify the region the probe anneals to. TaqMan probe is labelled with a reporter dye on the 5’ end and a quencher dye on the 3’ end. The quencher reduces the reporter fluorescence by FRET when the probe is intact. During the extension step of the PCR, the probe annealed to the DNA template will be degraded by the 5’ exonuclease activity of Taq polymerase. The reporter dye then emits the fluorescence signal. As the fluorescence signal is only generated if the probe is annealed to complementary template, the TaqMan method has higher specificity than SYBR green PCR. The

primers or probes and detection method for the targeted genes are listed in Appendix B. The SYBR Green PCR assay contained 3 µM of primers, 1× Advanced FAST SYBR Green PCR reagent (Applied Biosystems) and 5-10 ng cDNA or DNA template in a 10 µl reaction volume. Thermal cycling was performed with StepOnePlus Real-Time PCR system (Applied Biosystem) as: 95°C for 20 s, followed by 40 cycles of 3s at 95°C and 30s at 60°C. The TaqMan PCR was performed in a 10 µl reaction volume containing 300 nM of primers (Sigma), 200 nM of probe, 1×Taqman advanced fast master mix (Applied Biosystems) and 5-10 ng cDNA templates. Cycling was initiated 20s at 95°C, followed by 40 cycles of 1s at 95°C and 20s at 60°C.

2.8.5 Relative quantification of the real-time PCR

Data from real-time PCR can be analysed using absolute quantification or relative quantification. Absolute quantification requires a standard curve, which is used to determine the initial copy number of the transcript interest (refer to section 4.2.3). Relative quantification describes the expression of target gene in treated group(s) relative to a control. To perform relative quantification, the expression of the gene of interest needs to be normalized to an internal control. The internal control is usually a house-keeping gene and expressed abundant in majority cell types. In my studies, 18S was consistently used as an internal control. Except for the ErbB4 isoforms in Chapter 4 (described in section 4.2.3), the gene expression data presented in this thesis were all analysed by relative quantification using $2^{(-\Delta\Delta CT)}$ method as described (Livak *et al.*, 2001).

2.9 Data presentation and statistical analysis

Results are presented as mean ± standard error of the mean (SEM) throughout. Statistical analysis was performed using Graphpad Prism 6 for Windows. For comparison between two groups, Student's t-tests were utilised for data analysis. For multiple comparisons, One-way or Two-way ANOVA with Bonferroni or Dunnett's post-hoc comparisons were used. The adopted statistical analysis method is indicated in the figures or the method section in each chapter

.

CHAPTER 3

THE ROLE OF ErbB RECEPTORS IN Ang II-INDUCED CARDIOMYOCYTE HYPERTROPHY

3. The role of ErbB receptors in Ang II-induced cardiomyocyte hypertrophy

3.1 Background

Cardiac hypertrophy is characterised by cardiomyocyte growth and extracellular matrix accumulation. It is an independent risk factor for heart failure, myocardial infarction, arrhythmias and other cardiac morbidity and mortality (Frey *et al.*, 2003; Adabag *et al.*, 2010). Cardiac hypertrophy can be induced by physiological stimuli (e.g. pregnancy or exercise training) or pathological stimuli (e.g. the pressure/volume overload associated with hypertension, or increased production of circulating or paracrine pro-hypertrophic factors) (Solomon *et al.*, 2009; Iwata *et al.*, 2011). Angiotensin II (Ang II) is a key component of the renin-angiotensin system that is a major regulator of blood pressure and cellular growth. Whilst Ang II can cause cardiac hypertrophy subsequent to hypertension, it can also directly induce cardiomyocyte hypertrophy (Paradis *et al.*, 2000; Schultz *et al.*, 2002). We have previously shown that Ang II can directly promote cardiomyocyte hypertrophy via activation of the $AT_{1A}R$ and Gq protein coupling (Thomas *et al.*, 2002; Smith *et al.*, 2011). At the molecular level, Ang II-induced cardiomyocyte hypertrophy is characterized by the re-induction of the 'fetal gene program' (increased expression of ANP, CyclinD and MLC-2V), along with reorganization of the cardiomyocyte sarcomere (Sadoshima *et al.*, 1993; Aoki *et al.*, 1998). However, the exact molecular mechanisms responsible for the hypertrophic growth of cardiomyocytes are yet to be fully elucidated.

One paradigm for Ang II-induced cardiomyocyte hypertrophy is the transactivation of receptor tyrosine kinases, such as the epidermal growth factor receptors (ErbBs) (Asakura *et al.*, 2002; Thomas *et al.*, 2002). ErbB receptors are a subfamily of receptor tyrosine kinases that regulate cell proliferation, survival and differentiation (Burgess, 2008). There are four known ErbB receptor subtypes (ErbB1-4), three of which (ErbB1, ErbB2 and ErbB4) (Scaltriti *et al.*, 2006) are expressed in postnatal rat cardiomyocytes (Zhao *et al.*, 1998). The ErbB receptors can be selectively activated by EGF family ligands, such as EGF (an agonist for ErbB1) and NRG1β1 (the agonist for ErbB4). ErbB2 is not directly activated by ligand binding, but is the preferred dimerisation partner for the other isoforms. Upon activation by agonists, the receptors form hetero- or homodimers (Burgess *et al.*, 2003), phosphorylate intracellular tyrosine residues and thus activate downstream signalling pathways (Olayioye *et al.*, 2000; Yarden *et al.*, 2001; Mendelsohn *et al.*, 2003). There is evidence

for a role of ErbB1, 2 and 4 in cardiac development and function (Gassmann *et al.*, 1995; Wadugu *et al.*, 2012). Mutations in any of ErbB1, ErbB2 and ErbB4 lead to embryonic death or postnatal death due to defects in cardiac development (Gassmann *et al.*, 1995; Lee *et al.*, 1995; Miettinen *et al.*, 1995; Sibilia *et al.*, 1995; Threadgill *et al.*, 1995). Cardiomyocyte-specific expression of the dominant-negative ErbB1 in adult mice results in dilated cardiomyopathy (Rajagopalan *et al.*, 2008), and administration of an ErbB2 blocking antibody in humans increased the risk of heart failure (Seidman *et al.*, 2002).

We and others have shown that one mechanism for Ang II-induced hypertrophy is via the 'hijacking' or transactivation of EGFR (ErbB1) (Thomas *et al.*, 2002; Ohtsu *et al.*, 2006b; Smith *et al.*, 2011). Given previous studies showing important roles for ErbB2 and ErbB4 in cardiac physiology (Zhao *et al.*, 1998; Özcelik *et al.*, 2002) we speculated that these receptors may also be involved in AT_1R-ErbB transactivation and cardiomyocyte hypertrophy. Thus, in this study we have compared and contrasted the contribution of different ErbB receptor isoforms in AT_1R transactivation using both pharmacological and RNAi-based approaches.

3.2 Methods

3.2.1 Animal ethics

All experiments were conducted in accordance with the Australian Code of Practice for Care and Use of Animals for Scientific Purposes and approved by the institutional ethics committees of The University of Queensland.

3.2.2 Vector constructs

The ErbB1 shRNA and ErbB2 shRNA expressing vectors were constructed by James Goonan and the ErbB4 shRNA expressing vector by Dr Hsiu-wen Chan. The shRNA knockdown-resistant ErbB4 constructs were constructed and tested by Dr Hsiu-wen Chan. The luciferase reporter plasmids driven by hypertrophic gene promoter (MLC-2V, ANP-328, and CyclinD) were gifts from Dr Mona Nemer (Canada).

3.2.3 Cardiomyocyte culture

Cardiomyocytes were isolated from ventricles of 1-2 day old Sprague Dawley rats and purified via gradient centrifugation as previously described (Thomas *et al.*, 2002). To mimic the up regulation of AT_1R during hypertrophy, a modest level of AT_1R was delivered into cardiomyocytes using DNA transfection or adenoviral vectors as required and indicated in the figures (Thomas *et al.*, 2002).

3.2.4 Drug treatment

Cardiomyocytes were stimulated with the following hypertrophic agents: Ang II (100 nM), NRG1β1 (10 nM), EGF (10 nM). Drugs to inhibit ErbB receptors (AG1478, 500 nM or 5 μM) or Gq (YM254890, 100nM) were added to cells 30 min before stimulation. AG1478 was purchased from Sigma-Aldrich Corporation (New South Wales, Australia). Human recombinant EGF and NRG1β1 were purchased from R&D Systems (Minnesota, USA). Human Angiotensin II was sourced from Auspep Pty Ltd (Victoria, Australia). YM254890 was a gift from Astellas Incorporation, Japan.

3.2.5 DNA transfection and luciferase reporter assay

Reporter assays were used to measure the re-activation of the prototypic 'hypertrophic genes' ANP, cyclin D and MLC2v. Cardiomyocytes were transiently transfected with equal amounts (total 500 ng) of DNA constructs (promoter driven luciferase reporters, AT_1R and shRNAs targeting specific ErbBs) using Lipofectamine™ 2000 (Life Technologies). Twenty four hours after transfection, hypertrophic signalling was induced by treatment with Ang II, NRG1β1 or EGF, and another forty-eight hours later, the cells were harvested and assayed with a luciferase assay kit (Promega).

3.2.6 siRNA transfection

The siRNAs specific for ErbB1, ErbB2 and ErbB4 (ON-TARGETplus, Dharmacon) were transfected (Lipofectamine® RNAiMAX, Life Technologies) into cells 24 hours after isolation. Non-targeting siRNA was used as a control.

3.2.7 Real-time PCR

RNA was isolated from cardiomyocytes using TRIzol® reagent (Life Technologies) and DNase-treated before reverse transcription. The cDNA was amplified with Taq polymerase (FAST SYBR Green PCR Master Mix, Life Technologies). The primer sequence used were: for ErbB1 forward 5'-TCCCTTTGGAGAACCTGCAG-3' Reverse 5'-TCGCACAGCACCGATCAGAA-3'(Mizobuchi *et al.,* 2013); for 18S forward 5'-TCGAGGCCCTGTAATTGGAA-3' Reverse 5'-CCCTCCAATGGATCCTCGTT-3' (Advani *et al.,* 2009).

3.2.8 Western blot

Western Blotting was performed as described in detail previously (Carabatsos *et al.,* 2000). Western blots of cellular protein lysates were probed with primary antibodies to ErbB4 (sc-283, Santa Cruz), ErbB2 (Ab-3, Calbiochem), ErbB1 (1005, Santa Cruz), p-Erk1/2 (#9106, Cell Signalling), Erk1/2 (#4695, Cell Signalling) and β-actin (AC-15, Sigma). IRDye-conjugated secondary antibodies and the LI-COR odyssey infrared imaging system (Millennium Science) were used to quantify protein expression.

3.2.9 Hypertrophy assay

Cells were lysed in TE buffer containing 0.06% SDS for 4 hours at room temperature. Lysates were then assayed for both protein (BCA assay, Thermo Scientific) and DNA content (Picogreen dsDNA

assay kit, Life Technologies). Before the DNA assay, cell lysates were treated with 0.2g/L proteinase K (Life Technologies) overnight. Hypertrophy was defined by the increase in the total protein in the absence of change of DNA levels.

3.2.10 Phalloidin stain

Cardiomyocytes were fixed with 4% PFA followed by staining with Alexa594-labelled phalloidin as per the manufacturer's protocol (Invitrogen). The cardiomyocytes were then subjected to confocal microscopy to examine the F-actin reorganization into the sarcomere. For each treatment, images of cardiomyocytes were taken randomly under 400 × magnification.

3.2.11 Statistical analysis

Data are shown as mean ± SEM. Data were analysed by Student's t-test, or One-way or Two-way ANOVA with Bonferroni post-hoc comparisons, as indicated in the figures. $P < 0.05$ was considered statistically significant.

3.3 Results

3.3.1 Different ErbB ligands produce different effects on hypertrophy and remodelling

Ang II produces cardiomyocyte hypertrophy (Thomas *et al.*, 2002) and cytoskeletal remodelling (Figure 3.1) as has been previously described. EGF (an ErbB1 selective agonist) does not increase protein:DNA ratio or induce sacromeric reorganization in cardiomyocytes across a range of concentrations, suggesting that ErbB1 receptor activation is not tightly coupled to the hypertrophic response (Figure 3.1). In contrast, NRG1β1 (an ErbB4 selective agonist) produces robust cardiomyocyte hypertrophy, increasing protein:DNA ratio by up to 35% with a corresponding alteration in cell morphology and F-actin reorganization (Figure 3.1).

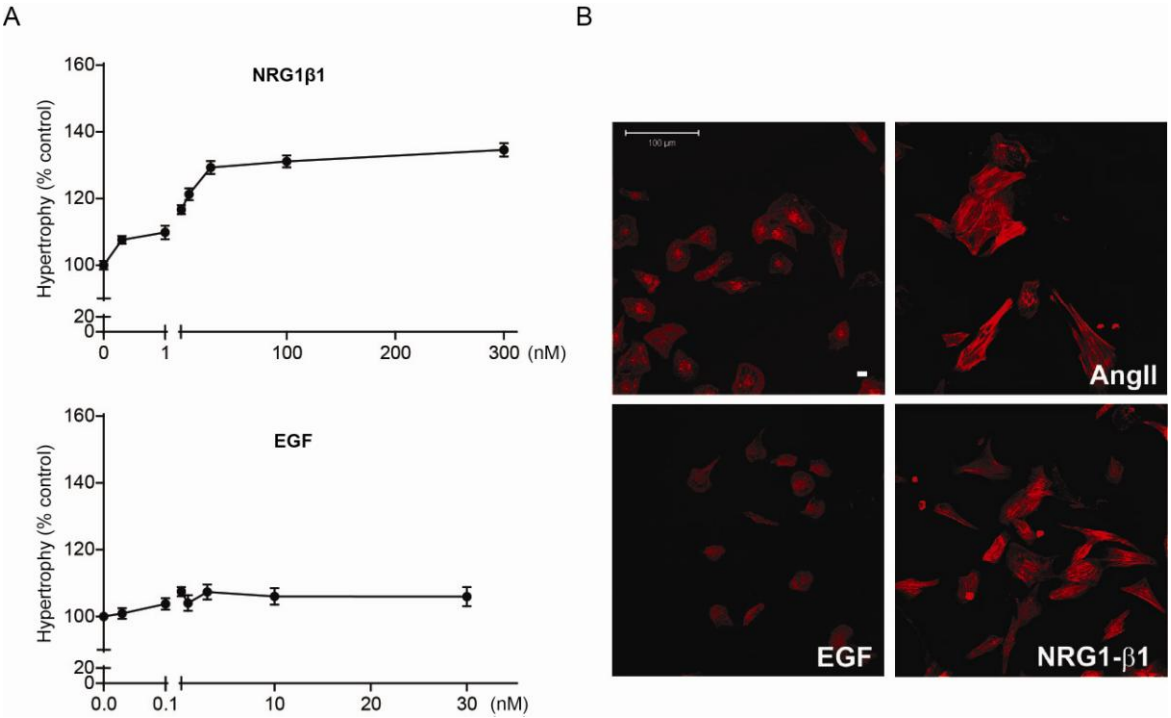

Figure 3.1 Different ErbB ligands produce different effects on hypertrophy and remodeling A. CM were subjected to hypertrophic assay following treatment with increasing concentrations of NRG1β1 or EGF for 60-72h. B.CM were fixed and stained with phalloidin after treated with 100 nM Ang, 10 nM NRG1β1 or 10nM EGF for 72h. The white bar in the first panel is a 100 μm indicator. These images are representative images of three independent experiments. Data shown as mean ± SEM (n=3).

3.3.2 Ang II-induced activation of hypertrophic gene promoter activity does not require ErbB receptors

We designed shRNA plasmid constructs specifically targeting ErbB1, ErbB2 and ErbB4 receptors, and confirmed that these constructs could down-regulate receptor expression (Figure 3.2). These shRNA constructs were then used to selectively silence individual ErbB receptors in cardiomyocytes, and subsequently examine the role of these receptors in hypertrophic signalling responses to Ang II and NRG1β1. Ang II and NRG1β1 both increased promoter activity for MLC-2v (Figure 3.3 A), ANP (Figure 3.3 B) and cyclin D (Figure 3.3 C), indicating re-activation of the hypertrophic gene program. Knockdown of ErbB4, but not ErbB1 or ErbB2, significantly reduced NRG1β1-induced activation of MLC-2v promoter activity by 62 % (Figure 3.3 A). NRG1β1-induced activation of ANP and cyclin D were also inhibited by ErbB4 shRNA (Figure 3.3 B and C). In contrast, knockdown of ErbB1, 2 or 4 did not reduce Ang II-induced activation of MLC-2v (Figure 3.3 A), nor did knockdown of ErbB4 affect Ang II-induced activation of ANP or cyclin D (Figure 3.3 B and C).

To complement our observation that ErbB receptors are not essential for Ang II-induced activation of the hypertrophic gene program, we also used AG1478 to pharmacologically inhibit ErbB activity, and used phosphorylation of ERK1/2 as a measure of ErbB1 or ErbB4 activation in cardiomyocytes (Figure 3.4 A and B). At higher concentrations of AG1478 (5 μM), the ERK1/2 phosphorylation induced by both EGF (an ErbB1 agonist) and NRG1β1 (an ErbB4 agonist) was blocked. However, at lower concentrations of AG1478 (0.5 μM) only the EGF-induced ERK1/2 phosphorylation was abolished (Figure 3.4 A). This suggests that at 0.5 μM AG1478 selectively inhibits ErbB1 receptors, whereas at 5 μM AG1478 inhibits both ErbB1 and ErbB4 receptors.

Similarly, NRG1β1-induced ANP promoter activity was inhibited by 5 μM of AG1478 but not by 0.5 μM AG1478 (Figure 3.4 C), confirming that at higher concentrations, AG1478 has inhibitory effects on hypertrophic signalling via ErbB4 receptors. In contrast, neither concentration of AG1478 inhibited Ang II-stimulated ANP promoter activity (Figure 3.4 C), suggesting that neither ErbB4 nor ErbB1 is involved in Ang II-induced activation of hypertrophic signalling. These results are consistent with those obtained from the shRNA experiments described above. The Gq inhibitor YM254890 (0.1 μM) significantly inhibited Ang II-stimulated activation of ANP, confirming that the Gq signalling pathway is essential for this process. NRG1β1-induced activation of ANP promoter activity was unaffected by YM254890 (Figure 3.4 C). Taken together, these data suggest that in isolated cardiomyocytes the activation of hypertrophic signalling pathways by Ang II is

independent of ErbB receptor activation, whereas ErbB4 receptors are important for NRG1β1-induced hypertrophic signalling.

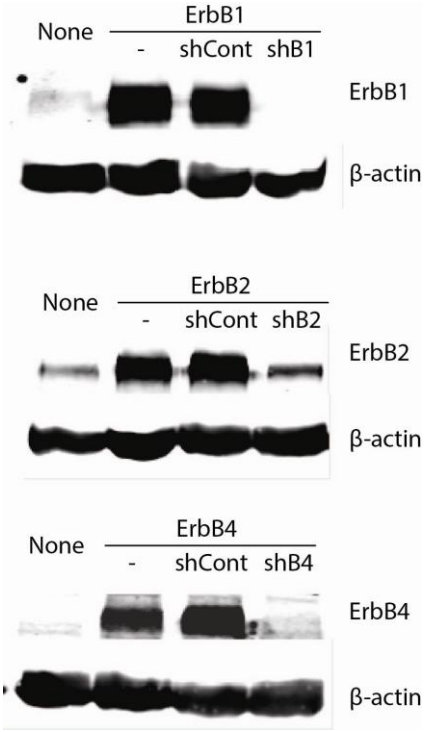

Figure 3.2 ErbB silencing by shRNA in a cell line. CHO cells were transfected with 500 ng of plasmids expressing either ErbB1, ErbB2 or ErbB4, and with 500 ng of shControl (shCont) or shErbB1, shErbB2 or shErbB4 (shB1, shB2 and shB4). Controls were left untransfected. Expression of ErbB receptors was measured by Western blot with β-actin as control.

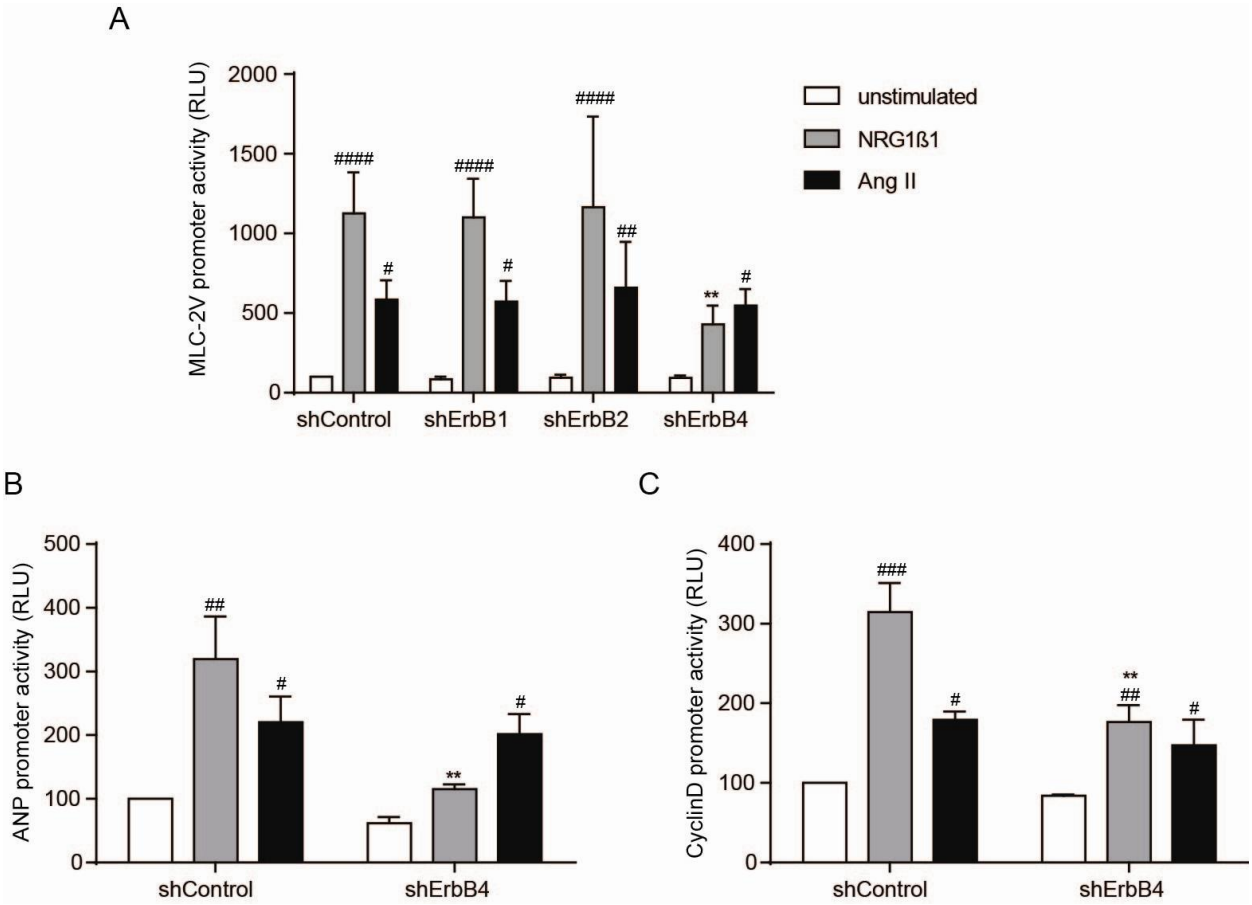

Figure 3.3 A role for ErbB receptors in hypertrophic gene promoter activity. CMs were transfected with 100 ng AT_1R, 100 ng ErbB shRNA or non-silencing shRNA (shControl), and 300 ng of either MLC-2V (A), ANP (B) or CyclinD (C) promoter-driven luciferase reporter constructs. 24 h after transfection cells were stimulated with NRG1β1 (10 nM) or Ang II (100 nM) for 48 h. Data are presented as mean ± SEM (A, n=5; B, n=4; C, n=3) of relative light units (RLU) expressed as a percentage of the shControl. Data were analysed by Two-way ANOVA with Bonferroni post-test (***P*<0.01 vs shControl with NRG1β1 stimulated; ####*P*<0.0001, ###*P<0.001*, ##*P*<0.01, #*P*<0.05 vs unstimulated in each shRNA treated group).

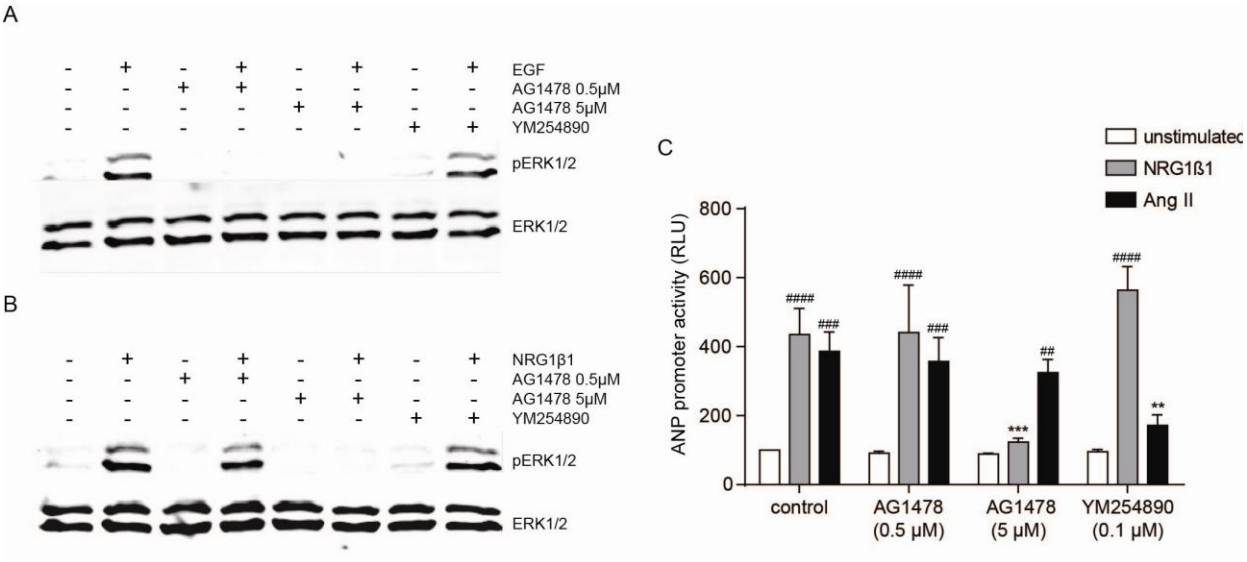

Figure 3.4 Divergent effects of the ErbB inhibitor AG1478 and Gq inhibitor YM254890 on ERK1/2 phosphorylation and ANP promoter activity in response to NRG1β1 and Ang II stimulation. CMs were infected with AT_1R adenovirus for 48h. Cells were then treated with AG1478 (0.5 or 5 μM) or YM254890 (0.1 μM) for 30 min before stimulating with (A) EGF (10 nM) or (B) NRG1β1 (10 nM) for 5 min. Levels of total and phosphorylated ERK1/2 were measured by Western blot; images are representative of two independent experiments. In (C) CMs were transfected with 100 ng AT_1R, 100 ng shControl and 300 ng ANP promoter-driven luciferase reporter constructs. 24 h after transfection cells were treated with either AG1478 or YM254890 and stimulated with NRG1β1 or Ang II, as described above. Data are presented as mean ± SEM (n=3) of RLU expressed as a percentage of the unstimulated control and were analysed by Two-way ANOVA with Bonferroni post-test (****P*<0.001 vs control treated with Ang II, ***P*<0.01 vs control treated with NRG1β1; ; ####*P*<0.0001, ###*P<0.001*, ##*P*<0.01 vs unstimulated in each shRNA treated group).

3.3.3 Ang II-induced MAPK signalling does not require ErbB receptors

Given the potential controversy of the above findings, we were concerned that the reporter constructs used above are limited by only being transfected into a very small proportion (1-2%) of cardiomyocytes. Thus, we wanted to expand our studies to measure indices of hypertrophic signalling in the wider, more representative population of cardiomyocytes. To do so, we used siRNA oligonucleotides that can be transfected into cells at much higher efficiencies than plasmid constructs to silence individual ErbB receptors. Western blots confirmed successful siRNA-mediated knockdown of ErbB1, ErbB2 and ErbB4 for up to 96 hours after transfection (Figure 3.5 A-C). This knockdown was selective for the targeted isoform, as knockdown of one ErbB subtype did not affect expression of other ErbB receptors (Figure 3.5).

Both NRG1β1 and Ang II increase ERK1/2 phosphorylation (Figure 3.6 A). Stimulation with NRG1β1 increased the activation of ERK1/2 by 21-fold relative to the unstimulated group. siRNA-mediated knockdown of ErbB4 reduced this activation by approximately 40% relative to the siControl (Figure 3.6 B), confirming that ErbB4 is required for the NRG1β1-induced ERK1/2 signalling. However, similar to the results for hypertrophic gene promoter activity, Ang II-stimulated ERK1/2 activation was unaffected by knockdown of ErbB receptors (Figure 3.6 C). Together, these data further indicate that whilst ErbB4 is required for NRG1β1-induced activation of hypertrophic signalling pathways, ErbB receptors are not involved in Ang II-induced hypertrophic signalling in cardiomyocytes.

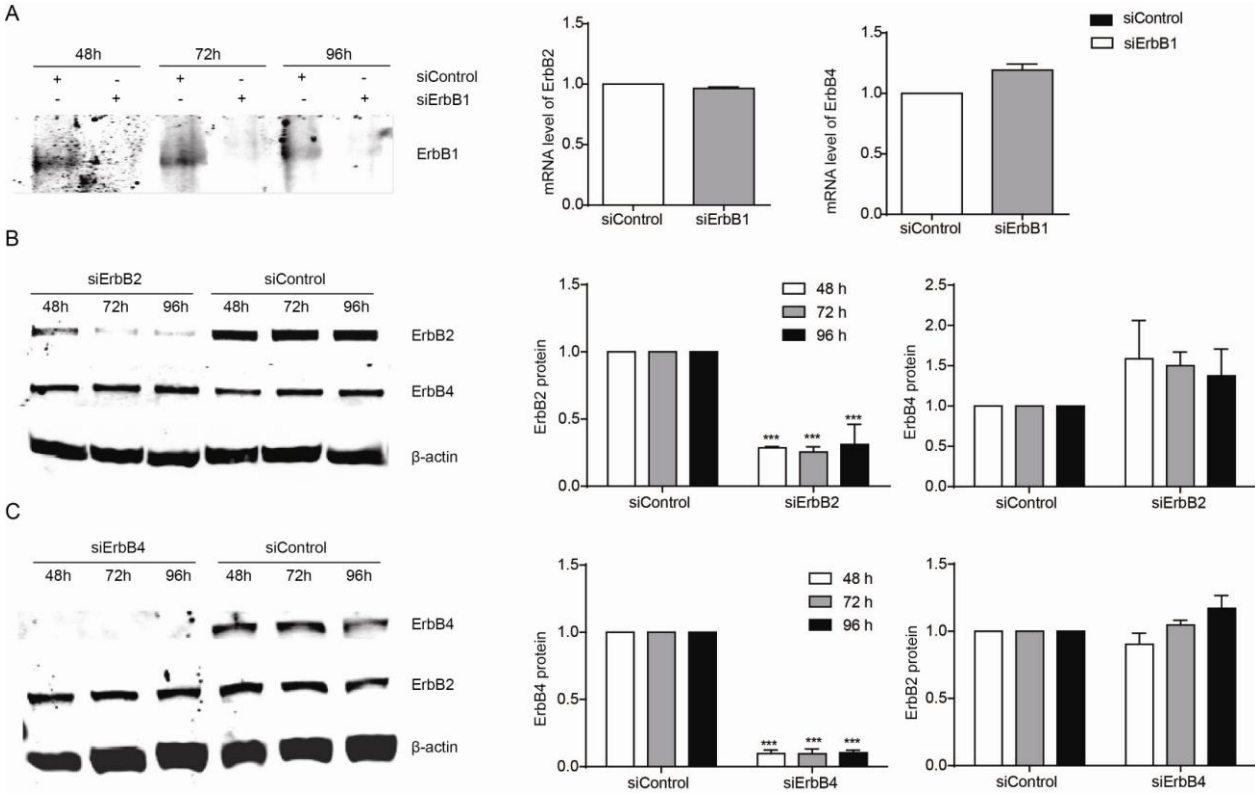

Figure 3.5 Selective knockdown of ErbB receptor expression with siRNA. CMs were transfected with 20 nM siRNA targeting individual ErbB receptors. Expression of ErbB receptors was determined via Western blotting or qPCR 48 - 96 h after transfection. A. Left panel shows a representative image of two independent Western blot experiments probing ErbB1. The right is quantification of the ErbB2 and ErbB4 expression by qPCR 48 h later after transfection (using 18S as internal control and expressed as a percentage of the siControl). Data shown as mean ± SEM (n=3) and analysed by Student's t-test. B and C. The left images are representative images of three independent Western blots probing for ErbB2 or ErbB4. The right shows quantification of ErbB2 and ErbB4 expression using Image Studio Lite software (version 3.1). Data shown as mean ± SEM (n=3-4) and analysed by two way ANOVA (***P <0.001 vs. siControl).

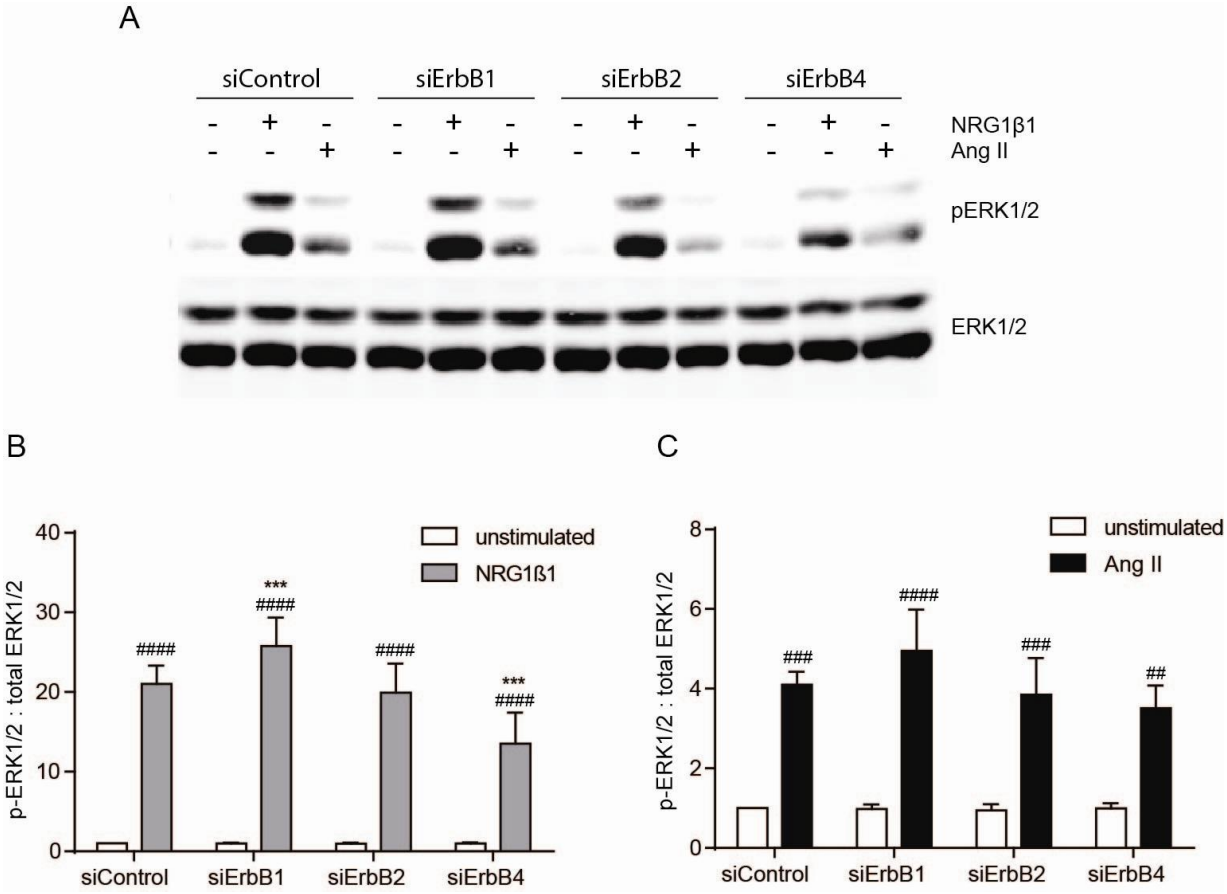

Figure 3.6 Selective knockdown of ErbB receptors differentially affects activation of ERK1/2 by NRG1β1 and Ang II. CMs were transfected with 20 nM of siErbB1, siErbB2, siErbB4 or siControl 24h prior to infection with AT_1R adenovirus. 48 h later, the cells were stimulated with either NRG1β1 (10 nM) or Ang II (100 nM) for 5 min. Activation of ERK1/2 was determined by Western blotting (A). The data were quantified and presented as mean ± SEM (n=4) for NRG1β1 (B) and Ang II (C). Data were analysed by Two-way ANOVA with Bonferroni post-test, ***P <0.001 vs siControl; ####P<0.0001, ###$P<0.001$, ##P<0.01 vs unstimulated in each siRNA treated group).

3.3.4 NRG1β1-induced hypertrophic growth requires ErbB4

Finally, we sought to confirm that NRG1β1 acts via the ErB4 receptor to cause hypertrophic growth as well as activation of hypertrophic signalling pathways. Stimulation with NRG1β1 increased the protein:DNA ratio by 18% in cardiomyocytes compared to unstimulated controls (Figure 3.7 A). This NRG1β1-induced hypertrophic growth was significantly reduced (~ 40 % reduction compared to siControl) by down-regulation of ErbB4. Knockdown of ErbB1 and ErbB2 caused a small reduction in NRG1β1-induced hypertrophy (16% and 14% increases in protein:DNA ratios respectively compared to unstimulated controls) however this was not statistically significant (Figure 3.7 A). Consistent with this, NRG1β1 induced sarcomere reorganization was affected by knockdown of ErbB4, but not ErbB1. The down regulation of ErbB2 seems to attenuate the NRG1β1-induced sarcomere reorganization but this effect is less pronounced compared to the siErbB4 treated cells (Figure 3.7 B).

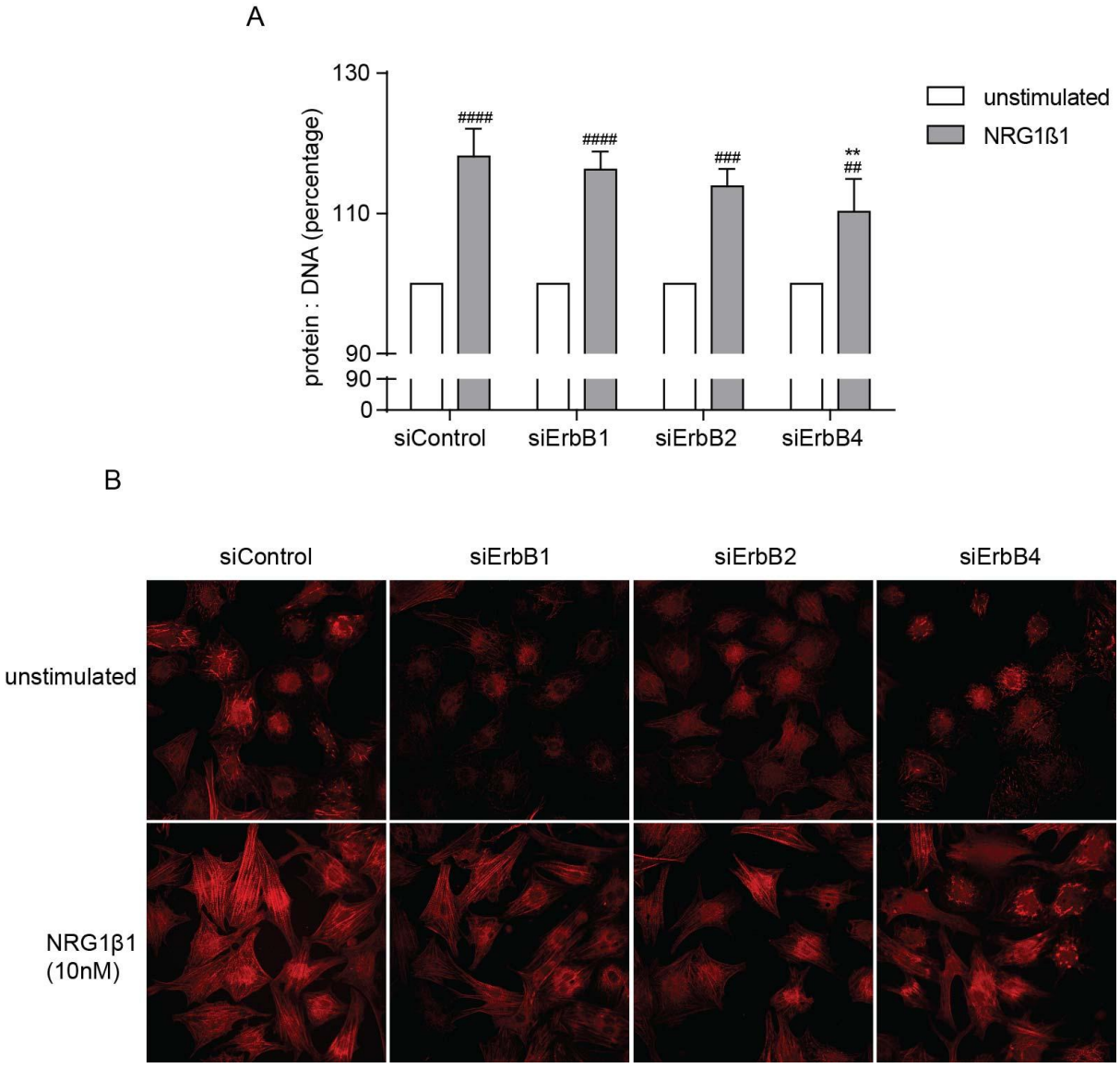

Figure 3.7 Effect of ErbB receptor knockdown on NRG1β1-induced hypertrophy. CMs were transfected with 20 nM of siErbB1, siErbB2, siErbB4 or siControl for 48 h prior to stimulation with NRG1β1 (10 nM) for an additional 48 h. A. Protein:DNA ratio was determined and data normalized to the unstimulated control. Data are presented as mean ± SEM (n=4) and analysed by two-way ANOVA with Bonferroni post-test, ***P*<0.01 vs siControl; ####*P*<0.0001, ###*P<0.001*, ##*P*<0.01 vs unstimulated in each siRNA treated group. B. Representative images of sarcomere reorganization measured by Phalloidin staining.

3.4 Discussion

The mechanism of AT_1R-EGFR transactivation has generated substantial interest due to the role of this pathway in cardiac hypertrophy (Kagiyama *et al.*, 2002; Thomas *et al.*, 2002), renal growth and dysfunction (Lautrette *et al.*, 2005) and vascular remodelling (Ohtsu *et al.*, 2006b). The central paradigm for transactivation has involved the AT_1R-mediated activation of metalloproteases that cleave cell surface EGF ligand precursors that then activate EGFR (ErbB1). The number and diversity of both metalloproteases (MMPs and ADAMs) (Edwards *et al.*, 2008; Hadler-Olsen *et al.*, 2011), EGF ligands and ErbB receptors means that it has been difficult to identify the specific players involved in any individual transactivation process. Based on the prevailing literature, we were surprised to discover in this study that ErbB1 appears to play little or no role in cardiomyocyte hypertrophy. In contrast, we have confirmed a significant role for ErbB4 in this process. Based on this, we then hypothesized that the pro-hypertrophic effects of Ang II may in fact be mediated by ErbB4; however, this was not the case. Using a variety of approaches (RNA interference, pharmacological blockade) we were unable to demonstrate any link between AT_1R activation and ErbB4. In total, our data raise questions concerning the role of individual ErbB receptors in Ang II-mediated cardiomyocyte hypertrophy.

However, a lack of involvement of ErbB receptors in Ang II-mediated cardiomyocyte growth does not discount these receptors from playing a major role in the heart. Indeed, a major finding of our study is that the ErbB4 receptor is critical for NRG1β1-induced cardiomyocyte hypertrophy. This supports previous studies which found that NRG1β1 induced hypertrophy in both neonatal and adult ventricular myocytes accompanied by up-regulation of hypertrophic genes (Zhao *et al.*, 1998). Indeed, NRG1β1-ErbB4 signalling is important in cardiac development: deletion of either gene causes embryonic lethality due to heart malformations (Gassmann *et al.*, 1995; Meyer *et al.*, 1995). NRG1β1-ErbB4 signalling also induces cardiomyocyte proliferation both *in vitro* and *in vivo* (Bersell *et al.*, 2009). We now show that ErbB4 activation by NRG1β1 can also stimulate ERK1/2 activity and hypertrophy in cardiomyocytes, further illustrating the important role of this mechanism in cardiac physiology.

We were surprised to observe that ErbB1 activation does not cause cardiomyocyte hypertrophy. In a variety of cells, we and others have previously demonstrated that AT_1R activation leads to phosphorylation of the ErbB1 receptor, downstream signalling and subsequent changes in cell physiology (Thomas *et al.*, 2002; Ohtsu *et al.*, 2006b). Moreover, deletion of ErbB1 in vascular

smooth muscle cells reduces GPCR-mediated signalling and has marked effects on vascular and cardiac remodelling (Schreier *et al.*, 2011; Schreier *et al.*, 2013).

One possible explanation for the discrepancy between this work and earlier studies relates to the method of inhibiting ErbB receptors. AG1478 is regarded as a selective inhibitor for ErbB1, however as an ATP-competitive antagonist it may also inhibit other receptor tyrosine kinases when used at higher concentrations (Levitzki *et al.*, 1995; Anastassiadis *et al.*, 2011). In this study, we used two different concentrations of AG1478 (0.5 and 5 μM), and found that the lower concentration selectively inhibited ErbB1, whereas the higher concentration inhibited both ErbB1 and ErbB4, consistent with previous reports (Anastassiadis *et al.*, 2011). Thus, it is possible that previous studies using AG1478 at 5 μM may have attributed actions to ErbB1 activation that are in fact being mediated by ErbB4 or other tyrosine kinases. Indeed, we have previously shown that 5 μM AG1478 is required to abolish Ang II-induced ERK1/2 activation and cardiomyocyte hypertrophy (Thomas *et al.*, 2002; Smith *et al.*, 2011), which suggests that multiple ErbB receptor subtypes may involved in this process.

We then sought to further validate these data using a third method of inhibiting ErbB receptors, siRNA. siRNAs to ErbB1, 2 and 4 all showed significant knockdown of their targeted receptor, and we found no evidence of compensatory up-regulation of the other receptor isoforms (Figure 3.5). Knockdown of individual ErbB receptors did not inhibit Ang II-induced ERK1/2 activation. Whilst it could be argued that perhaps the magnitude of ErbB receptor knockdown was insufficient to inhibit Ang II signalling, our results with NRG1β1 do not support this explanation. siRNA targeting of the ErbB4 receptor reduces both NRG1β1-induced ERK1/2 activation and cardiomyocyte hypertrophy, thus we would argue that siRNA-mediated down-regulation of ErbB4 was sufficient to cause a functional reduction in expression, but that Ang II does not appear to act via this receptor. Taken together, we have used three different methods to inhibit ErbB receptors (shRNA, siRNA and pharmacological inhibition) and found no evidence for the role of any individual ErbB receptor isoforms in Ang II-mediated hypertrophic signalling.

By raising questions about the mechanism of AT_1R-ErbB receptor transactivation in cardiomyocytes, this study highlights the potential for investigating signalling pathway networks using an unbiased, rather than candidate-driven, approach. Indeed, our group has recently used functional genomics to perform a siRNA screen of AT_1R-ErbB1 transactivation in a mammary epithelial cell line, and have identified a number of novel molecules involved in this process

(George *et al.*, 2013). It is also important to recognize the difficulties in characterizing systems that involve multiple molecular participants, and thus may have a high degree of redundancy. In the case of AT_1R-ErbB transactivation, this is typified by the number of potential MMP/EGF ligand/ErbB receptor combinations.

Transactivation of GPCRs and receptor tyrosine kinases is a broad phenomenon that is important in both normal physiology and numerous disease processes. We confirm an important role for NRG1β1-ErbB4 signalling in cardiomyocyte growth, yet our data calls into question the existence of a straightforward mechanism for the transactivation of ErbB receptors by the AT_1R. Accordingly, I will focus on further examining the role of ErbB4 in cardiomyocytes in the following studies described in this thesis.

CHAPTER 4

INVESTIGATION INTO THE ROLES OF ErbB4 ISOFORMS IN CARDIOMYOCYTE HYPERTROPHY

4. Investigation into the roles of ErbB4 isoforms in cardiomyocyte hypertrophy

4.1 Background

ErbB4 has four isoforms resulting from alternative splicing: JM-a CYT-1, JM-a CYT-2, JM-b CYT-1 and JM-b CYT-2 (as discussed in section 1.4). The four isoforms are structurally different in two domains: the extracellular juxtamembrane JM domain (JM-a and JM-b) and intracellular CYT domain (CYT-1 and CYT-2). Compared to the CYT-2 domain, the CYT-1 contains a 16 amino acid insertion that acts as a docking site for multiple factors including STAT5, Yap and PI3K (Elenius *et al.*, 1999; Omerovic *et al.*, 2004; Williams *et al.*, 2004). The JM-a isoform contains 23 amino acids in the JM domain that allow for ectodomain shedding (Junttila *et al.*, 2000). JM-b contains an alternative 13 amino acids that resistant to shedding (Junttila *et al.*, 2000). Cleavage of the JM-a isoform occurs in 2 steps, and produces an 80-kDa soluble fragment. First, the JM-a isoform can be subjected to ectodomain cleavage by the metalloprotease ADAM17 to produce a 120-kDa ectodomain fragment released into the extracellular medium and an 80-kDa fragment anchored in the membrane (Vecchi *et al.*, 1997; Rio *et al.*, 2000; Zhou *et al.*, 2000). The 80-kDa fragment can subsequently be subjected to further cleavage by γ-secretase within the lipid bilayer to release the intracellular domain (Chang-Yuan *et al.*, 2001). The cleavage can be induced by various stimulations such as PMA, NRG1-β1 or GPCR agonists, which potentially activate the ADAMs (Chang-Yuan *et al.*, 2001). The cleavage of JM-a isoform is cell type dependent. In breast cancer cells, ovarian cancer cells, lung cancer cells, and a glioma cell line (Vecchi *et al.*, 1996; Zhou *et al.*, 2000; Määttä *et al.*, 2006; Zeng *et al.*, 2009), the JM-a isoform of ErbB4 is cleaved to produce an 80 kDa intracellular domain (ICD). The ICD can enter the nucleus and interact with transcriptional factors to regulate transcriptional activity (Tidcombe *et al.*, 2003; Zhu *et al.*, 2006b; Gilmore-Hebert *et al.*, 2010). Depending on whether they can be cleaved to release the ICD, or possess the extra 16 amino acids in the intracellular domain, each ErbB4 isoform may therefore play a different role in regulating growth and differentiation (Muraoka-Cook *et al.*, 2009). For instance, the cleavable JM-a isoform is capable of regulating the astrogenesis timing by suppressing astrocyte differentiation, whereas the non-cleavable isoform JM-b cannot (Sardi *et al.*, 2006) (refer to the Chapter 1 section 1.4.3 for more detail); the CYT-2 ICD promotes mammary cell proliferation, whereas CYT-1 ICD promotes differentiation (more acinar structures in 3D culture) (Muraoka-Cook *et al.*, 2009). We have previously shown that all ErbB4 isoforms are detectable in rat neonatal

primary cardiomyocytes (Dr. Hsiu-wen Chan, PhD thesis). However, the regulation of these isoforms in cardiac development and pathological conditions has not been investigated. In addition, whether the JM-a-containing isoforms can be cleaved to release the ICD and enable trafficking of the ICD to the nucleus of cardiomyocytes is not known. Finally, the ability of each individual isoform to mediate cardiomyocyte hypertrophy has not been previously examined. The following studies aim to answer these questions.

4.2 Methods

4.2.1 Animals

To investigate the regulation of the ErbB4 isoforms in cardiac development and cardiac pathology models (ischaemia-reperfusion model and pathological cardiac hypertrophy model), we collaborated with other groups who have isolated RNA samples from these models. RNA isolated from embryonic CD-1 mouse hearts (E10.5, E13.5, E16.5, and E18.5) was a gift from Dr. David Pennisi (University of Queensland). The RNA from CD-1 mouse hearts at postnatal days 1, 6, 14 and 28 was kindly provided by Dr. Enzo Porrello (University of Queensland). The hearts from an ischaemia-reperfusion model and a pathological cardiac hypertrophy model were from Prof. Eric N. Olson's group (University of Texas) and RNA was extracted by Dr. Enzo Porrello. For the ischaemia model, 8-12-week old mice (under isoflurane anaesthesia) underwent 45 min of ischaemia induced by temporary ligation of the left anterior descending coronary artery (LAD) followed by reperfusion. Control animals underwent a sham operation without occlusion of the LAD. After 24 hours or 7 days recovery, cardiac tissues were collected from both groups (Aurora *et al.*, 2012) and RNA extracted. For pathological cardiac hypertrophy model, the calcium-dependent phosphatase calcineurin driven by cardiac-specific gene promoter αMHC was overexpressed in mice. The mutant mice develop cardiac hypertrophy soon after birth and reached maximal hypertrophy at 8 weeks of age. Then they progressed to dilated cardiomyopathy and heart failure (Molkentin *et al.*, 1998). RNA was extracted from hearts collected from transgenic and wild type animals at 8 weeks of age.

4.2.2 Relative quantitation real-time PCR with TaqMan probes

Real-time PCR quantification of ErbB4 isoforms was performed with specific primers and probes described previously in the literature (Junttila *et al.*, 2003; Veikkolainen *et al.*, 2012). Probes for JM-a, JM-b, CYT-1 and CYT-2 annealed to exons 16, 15, 26 or the junction between exons 25 and 27, respectively (Figure 4.1 A). The primers were synthesized based on the exon sequences flanking the site recognized by the probe. Amplification of ribosomal 18S was used as an internal control. PCR was performed in a solution containing 300 nM of each primer (Sigma), 200 nM of probe, 1×TaqMan advanced fast master mix (Applied Biosystems) and 5-10 ng cDNA template in a final volume of 10 µl. Thermal cycling was performed with StepOnePlus Real-Time PCR system (Applied Biosystems). Cycling was initiated 20 s at 95°C, followed by 40 cycles of 1 s at 95°C and 20 s at 60°C. Expression levels of all isoforms were normalized to 18S expression using the $2^{(-\Delta\Delta CT)}$ method as described (Livak *et al.*, 2001).

4.2.3 Absolute quantification real-time PCR

Absolute quantification uses serially diluted standards of known concentrations to generate a standard curve. The standard curve produces a linear relationship between the initial amounts of DNA template (N_0) and the threshold cycle (C_T) and thus can be used to quantify the unknown samples. This method assumes all standards and samples have equal amplification efficiency. Thus, standards and samples have to be amplified in the same plate under same PCR conditions (same probe, primers, reagents, etc). The relationship between the $\log(N_0)$ and $\log(C_T)$ is described in the linear function: $\text{Log}(N_0) = -\text{Log}(E+1)\cdot C_T + \text{Log}(N_T)$ as previously described (Rutledge *et al.*, 2003). E is amplification efficiency; N_T is the number of amplicon molecules at fluorescent threshold; N_T and E are constants (Rutledge *et al.*, 2003). In my study, serially diluted (1:5) standards for each ErbB4 isoform (see section 4.2.4 for standards generation) and the unknown samples were amplified in the same plates using the primers and probe described in section 4.2.2. Standard curves for each isoform of ErbB4 were generated by analyzing the initial amounts of standards and threshold cycle (Figure 4.2). The initial template amounts (N_0) of unknowns can be calculated by putting its C_T value into the corresponding function.

4.2.4 Generation of standards for absolute quantification real-time PCR

Standards should be made from a high quality template because any degradation will affect the results. PCR products can slightly degrade during storage and thus are not a suitable standards resource, whilst the cloned target sequence is more stable (Dhanasekaran *et al.*, 2010). To get a clean and consistent source for the standards, the PCR products in section 4.2.2 were cloned into TA vectors. Briefly, the PCR products were subjected to DNA purification (DNA extraction kit, Qiagen) following agarose gel electrophoresis. Then the purified PCR products were ligated into linearized T-overhang vectors using TOPO® TA Cloning® Kit (Invitrogen). The ligation was transformed into competent *E. coli* cells (New England Biolabs) and then subjected to kanamycin selection on LB agar plates. Positive clones were confirmed with plasmid extraction followed by sequencing. The positive clone was preserved at -80°C supplemented with 40 % glycerine.

The recombinant T vector cannot be used directly as a standard because it is circular DNA, whereas the samples to be tested are linear cDNAs. Circular DNA templates are amplified with a different efficiency from linear DNA templates even under the same PCR condition (Lin *et al.*, 2011). Thus, before performing the real-time PCR, the concentrated standard is released from the recombinant T vector by double enzyme digestion with Hind III and EcoV (New England Biolabs). These two

digestion sites were in the T-vector, and flanked the sequence of the inserted standards. The digest was purified via agarose gel electrophoresis and DNA extraction (Qiagen).

The concentration of the purified DNA fragment was measured in triplicate by Nano drop. The molar concentration was calculated as: molar concentration (mol/L) = mass concentration (g/L)/ molecular weight (g/mol). The molecular weight of each DNA fragment was determined by the online tool Oligo Calc (http://www.basic.northwestern.edu/biotools/oligocalc.html).

4.2.5 Generation of pEGFP-N1-ErbB4

The plasmid p-EGFP-N1-ErbB4, expressing full length rat ErbB4 individual isoform with a C-terminal EGFP fusion was generated by subcloning the ErbB4 isoform from the pIRESpuro2 vector into pEGFP-N1. Rat ErbB4 isoforms (JM-a CYT-1, JM-a CYT-2, JM-b CYT-1 and JM-b CYT-2) in the pIRESpuro2 vector were gifts from Dr Giovanna Gambarotta (University of Torino, Italy). For subcloning, stop codons were removed and NheI and AgeI sites were introduced into the N- and C-terminals of the ErbB4 sequence using PCR. The PCR product was ligated with NheI and AgeI digested p-EGFP-N1 vector before transformation in competent *E. coli* cells (New England Biolabs). Kanamycin resistance was used for colony selection. Positive clones were determined via NheI/HpaI double digestion followed by agarose gel electrophoresis and sequencing.

4.2.6 Live cell imaging using confocal microscopy

For confocal microscopy, cardiomyocytes were plated in glass-bottomed confocal dishes (MatTek) and maintained in DMEM CCT SS2 medium (refer to Appendix A for medium recipe). The recombinant vectors expressing individual ErbB4-GFP isoforms were delivered into myocytes via DNA transfection, as described earlier (section 2.5). At 48h after transfection, cell dishes were subject to live imaging with an Olympus FV1000 confocal microscope system. All observations were performed at 37°C with 60×10 magnification. To avoid interference with the observation, the intracellular fluorescence of ErbB4-GFP in the cytoplasm was bleached before stimulation with NRG1 or PMA. For this, the region of interest (ROI) (cytoplasm) was manually selected by drawing a circle around the ROI with the Olympus FV1000 software. The ROI was then subjected to photo-bleaching with 50% of the maximum power of the 405 laser in the SIM light bleaching mode for 800ms at 10.0 µs/pixel. The bleaching process was repeated 2-3 times until no fluorescence remained observable in the cytoplasm and nucleus. After photobleaching, cells were treated with PMA (100nM), NRG1 (10nM) or vehicle. Images were acquired immediately before

and 1 min, 5 min and 15 min after stimulation. The 405 and 473 lasers were sequentially used for fluorescence excitation with 5% of maximum laser power.

4.3 Results

4.3.1 Expression profiles of ErbB4 isoforms throughout development using relative quantification

The expression of ErbB4 isoforms (JM-a CYT-1, JM-a CYT-2, JM-b CYT-1 and JM-b CYT-2) exhibits distinct tissue specific patterns (Elenius *et al.*, 1997; Elenius *et al.*, 1999). Moreover, some studies showed that the expression of ErbB4 isoform is developmentally regulated by physiological stage: the JM-a isoform is reduced in neuronal precursor cells at late stages of embryonic development (Fox *et al.*, 2005; Sardi *et al.*, 2006). In the adult mouse and human heart, JM-b CYT-1 is predominant isoform (Elenius *et al.*, 1997; Elenius *et al.*, 1999), however there is limited information on how ErbB4 isoform expression is regulated during heart development. To address this, the developmental expression profile of each isoform was assessed. Mouse hearts at embryonic days (E) 13.5, 16.5, 18.5 and postnatal days (P) 1, 7, 14 and 28 were collected and RNA extracted. Quantitative PCR (TaqMan, relative expression) was used to detect each isoform with 18S as an internal control. Throughout development from E13.5 to P28 expression of all four isoforms decreased: JM-a isoform at P28 is approximately 300-fold lower than E13.5, JM-b is 17-fold lower, CYT-1 isoform is 73-fold lower, and CYT-2 is 40 fold lower (Figure 4.1 B). This pattern is similar for all four isoforms, suggesting that they are regulated in a similar manner during heart development.

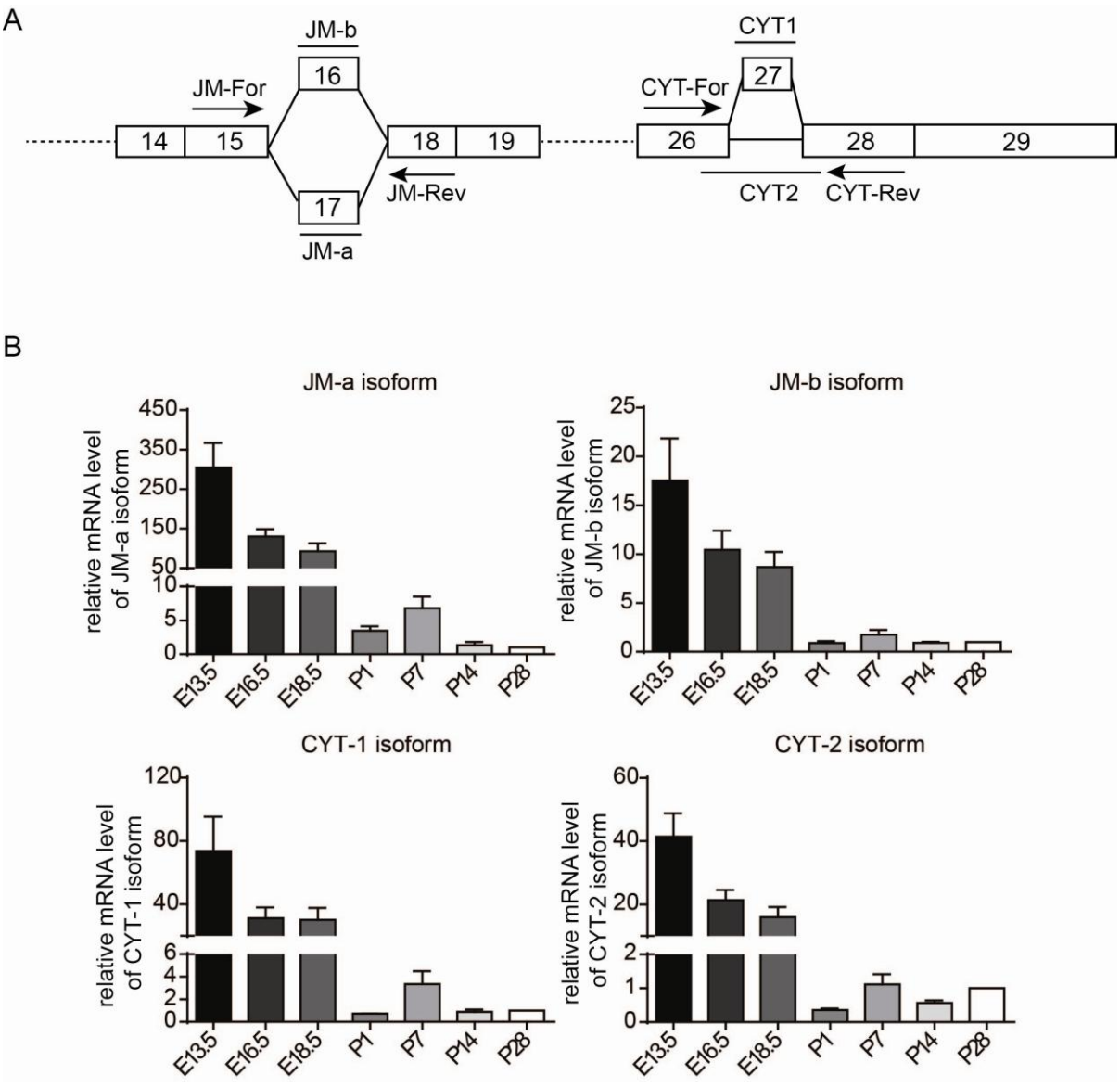

Figure 4.1 The developmental expression profile of ErbB4 isoforms. A. Design of primers and probes to specifically detect individual isoforms using qPCR. Probes for JM-a, JM-b, CYT-1 and CYT-2 were designed to anneal to exons 17, 16, 27 or the junction between exons 26 and 28, respectively. The primers were complementary to the exon sequences flanking the site recognized by the probe. The same pair of primer was used for detection of either JM-a and JM-b isoforms or CYT-1 and CYT-2 isoforms. B. Quantitative qPCR (TaqMan) was used to detect JM-a, JM-b, CYT-1 and CYT-2 isoforms at in mouse hearts embryonic days 13.5, 16.5, 18.5 and postnatal days 1, 7, 14 and 28. Ribosomal 18S was used as an internal control. Data was expressed as ratio of expression at P28 and presented as mean ± SEM, n=3.

4.3.2 Expression profiles of ErbB4 isoforms throughout development using absolute quantification

The results described above use different primer/probe sets to amplify the individual ErbB4 isoforms, and therefore the efficiency of PCR amplification may differ for each isoform. Thus, we cannot directly compare the expression levels of individual isoforms to each other from the relative quantification PCR data. Instead, we used absolute real-time PCR to identify the predominant isoforms expressed at different stages of cardiac development. Generation of the standard curves (Figure 4.2) is described in section 4.2.3 - 4.2.4. All four isoforms were detectable in mice heart throughout development (Figure 4.3). From the embryo stage (E10.5) into young adulthood (P28), the expression profile of all four isoforms was consistent with that identified using relative quantification (Figure 4.1). The JM-b:JM-a ratio ranged from 3:1 at E10.5 to 40:1 at P28, suggesting that during embryogenesis expression of the two isoforms is similar, but the JM-b isoform dominates as the heart matures. This is consistent with the literature (Elenius *et al.*, 1997; Elenius *et al.*, 1999) that JM-b is the primary isoform in the adult mice heart. In contrast, the CYT-2:CYT-1 ratio did not differ notably and only shifted from 1:1 at E10.5 to 1.7:1 at P28, suggesting that there are similar levels of CYT-1 and CYT-2 in the heart throughout development. The sum of the CYT-1 and CYT-2 copy numbers is approximately equal to the sum of the JM-a and JM-b copy numbers at each individual developmental stage, indicating this absolute quantification is accurate. Together, these suggest that the non-cleavable JM-b isoforms predominate in the adult heart, and may therefore be the isoforms most relevant for function.

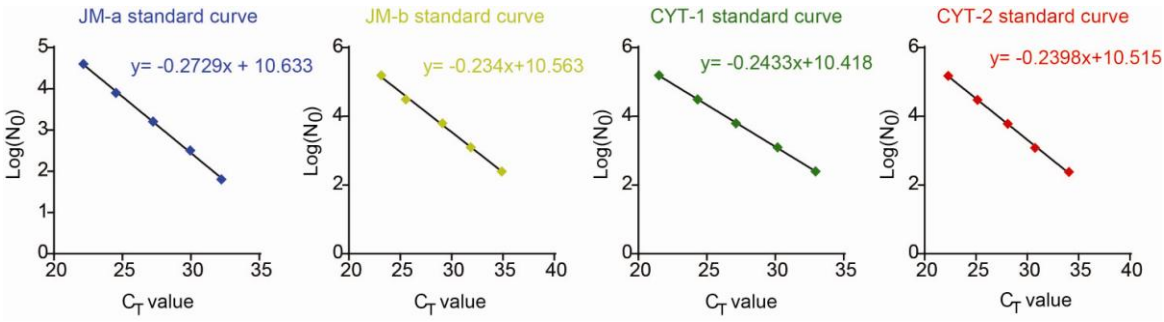

Figure 4.2 Standard curves for individual ErbB4 isoforms. DNA template dilution series (1:5) was used to generate standard curves by qPCR using the primers and probes specific for the JM-a, JM-b, CYT-1 or CYT-2 isoforms. The template for standard curve was generated by digestion of recombinant vectors containing JM or CYT domain of ErbB4 isoforms. N_0 is the copy number of templates for each dilution. C_T is the threshold cycle value.

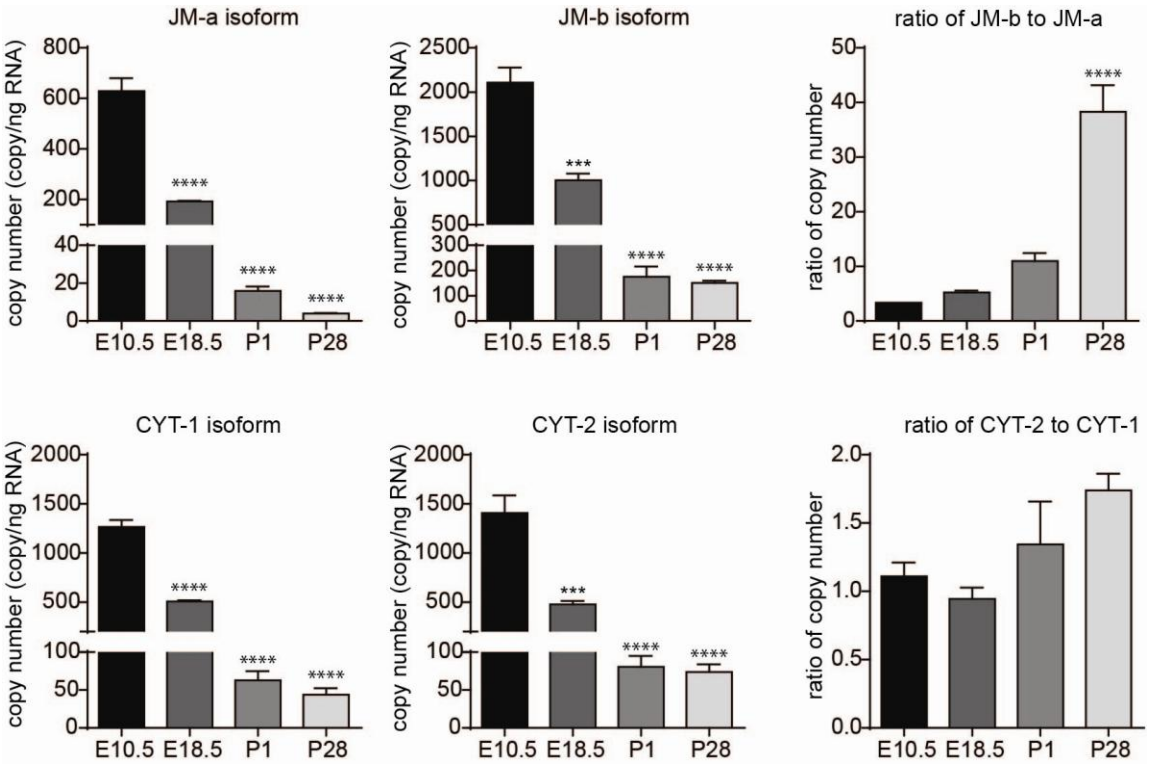

Figure 4.3 Absolute expression of ErbB4 isoforms in the heart at different developmental stages. Absolute quantitative qPCR (TaqMan) was used to measure expression of JM-a, JM-b, CYT-1 and CYT-2 ErbB4 isoforms at in mouse heart at E10.5, E18.5, P1 and P28. Ribosomal 18S was used as an internal control. Data was expressed as absolute copy number of each isoform per ng RNA, presented as mean ± SEM, n=3 for each time point. Data was analysed by one-way ANOVA with Bonferroni post-test, ****P<0.0001, ***$P<0.001$, vs E10.5.

4.3.3 Regulation of ErbB4 isoform expression in models of cardiac pathology

The regulation of ErbB4 isoform expression by cardiac stressors such as pathological cardiac hypertrophy or myocardial infarction was also assessed. First, we examined the regulation of the four isoforms in an ischaemia-reperfusion (IR) model (section 4.2.1). JM-a isoform expression was significantly increased at 24 h after reperfusion, whereas JM-b was not, suggesting that the cleavable JM-a isoform was up-regulated by the ischaemia-reperfusion injury (Figure 4.4). The mRNA level of the CYT-2 isoform was significantly reduced (by ~ 40 %) at 24 h after IR while CYT-1 was not changed (Figure 4.4). The JM-b:JM-a ratio is reduced by 50% at 24 h and 35% at 7 days after reperfusion compared to the sham-operated controls (Figure 4.4), suggesting that these two isoforms may play different roles in regulating cardiac biological activity after IR. In contrast, the ratio of CYT-2/CYT-1 was not changed indicating no potential functional differences related to the CYT-2 and CYT-1 isoforms in the heart after IR (Figure 4.4).

A transgenic model of cardiac hypertrophy caused by calcineurin overexpression was used to investigate the regulation of ErbB4 isoforms in pathological hypertrophy (section 4.2.1). Surprisingly, expression of all of four isoforms was significantly reduced in calcineurin-overexpressing animals compared to the controls (Figure 4.5). The JM-b:JM-a and CYT-2:CYT-1 ratios were not changed, suggesting that the reduction of all isoforms may be due to the inhibition of whole gene expression, but not specific regulation of an individual isoform. The down-regulation of ErbB4 expression in the pathologically hypertrophic heart suggests that ErbB4 may not mediate this pathological hypertrophy, and that calcineurin-induced signalling may negatively regulate ErbB4 signalling.

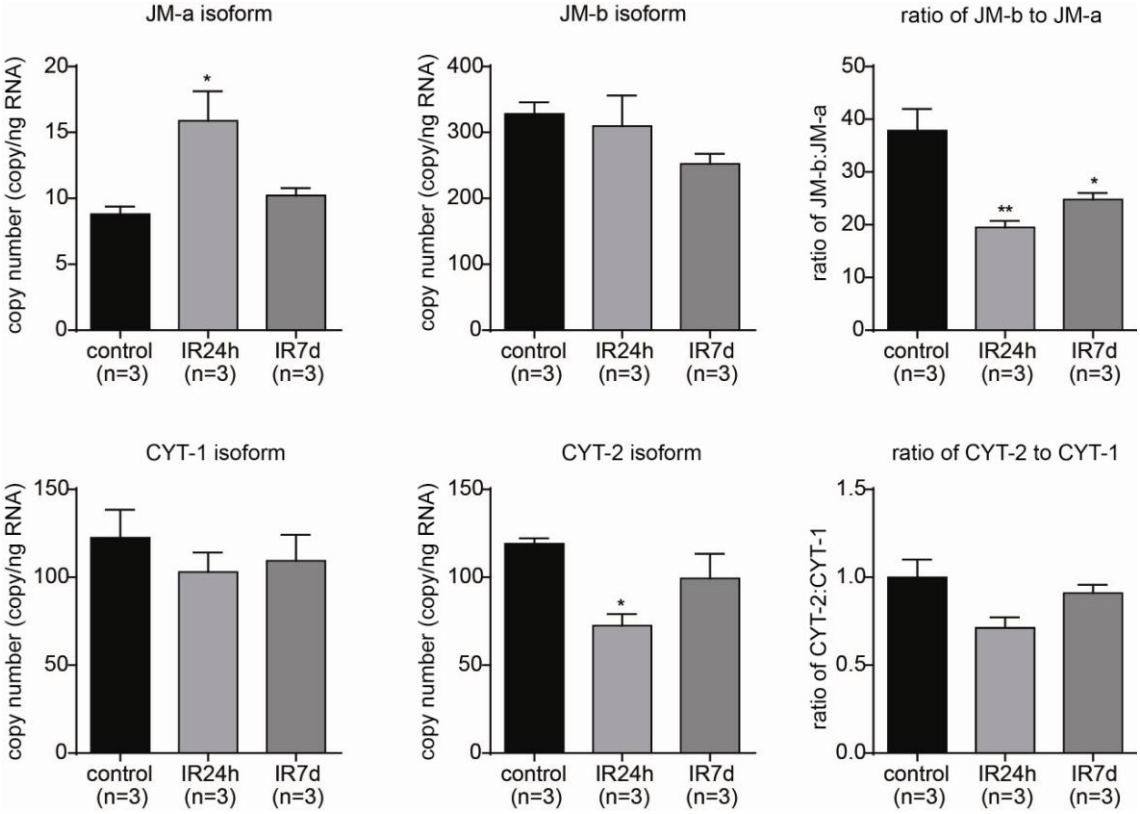

Figure 4.4 Regulation of ErbB4 isoform expression in an ischaemia-reperfusion model. Mouse hearts were collected following 24h (IR24h) or 7 days (IR7d) of reperfusion after 45 min of ischaemia, or from non-ischemic sham controls. Absolute quantitation qPCR (TaqMan) was used to measure the copy number of JM-a, JM-b, CYT-1 and CYT-2 isoforms per ng of total RNA. The right hand panels show the ratios (JM-b:JM-a and CYT-2:CYT-1) of the copy numbers. Data is presented as mean ± SEM and analysed with One-way ANOVA with Bonferroni's multiple comparisons; n=3 for each treatment, *P<0.05, **P<0.01 vs. control.

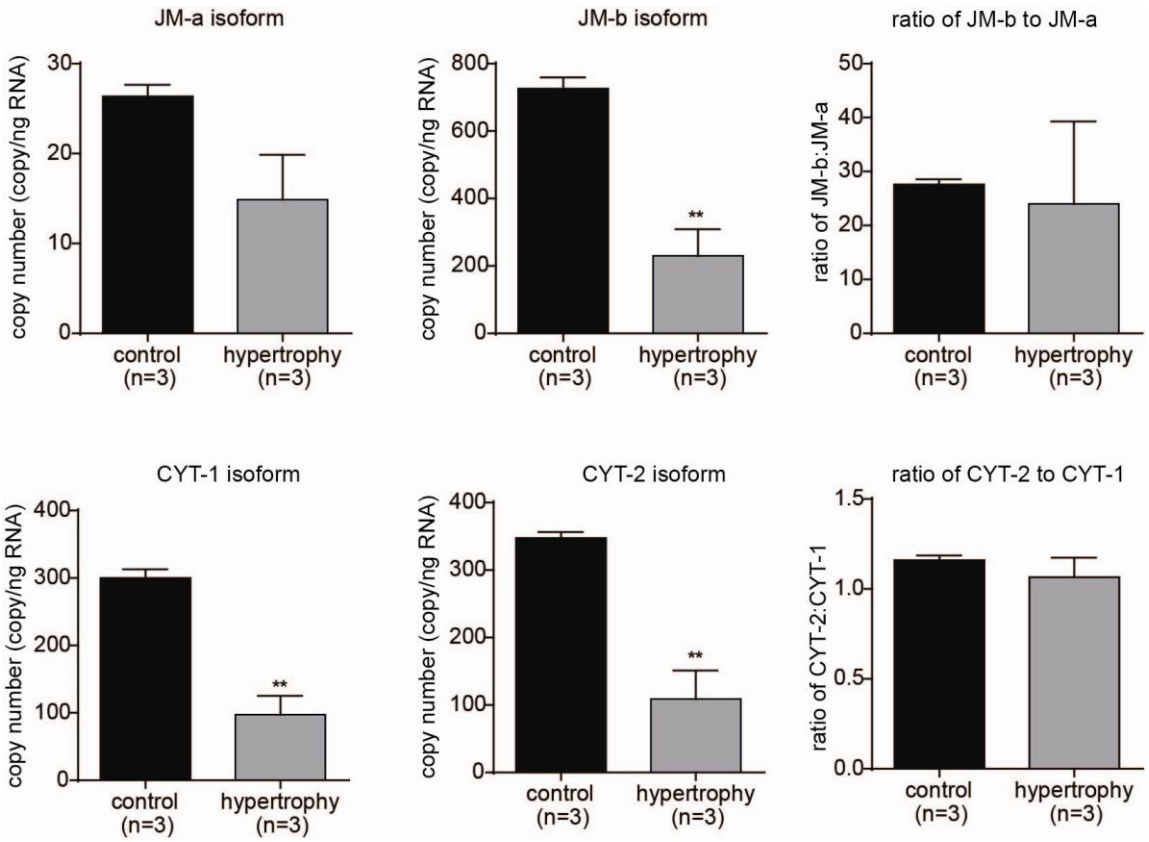

Figure 4.5 Regulation of ErbB4 isoform expression in a transgenic model of cardiac hypertrophy. Hearts were collected from calcineurin-overexpressing and wild type mice 8 weeks after birth and absolute quantitiation qPCR (TaqMan) used to measure the copy number of JM-a, JM-b, CYT-1 and CYT-2 isoforms per ng of total RNA. The right hand panels show the ratios (JM-b:JM-a and CYT-2:CYT-1) of the copy numbers. Data is presented as mean ± SEM and analysed with Student's unpaired t-test; n=3, $^{**}P<0.01$ vs. control.

4.3.4 The cleavage of ErbB4 isoforms in isolated cardiomyocytes

As discussed in section 4.3.3, the JM-a isoform is significantly up-regulated and the JM-b:JM-a ratio reduced after ischaemia-reperfusion injury. It can be inferred that the JM-a isoform has a unique role in heart after IR. There are many biological processes occurring after IR, such as cardiomyocytes apoptosis, fibroblast proliferation, and activation of immune system. In addition, a few studies showed that a small proportion of cardiomyocytes can proliferate as part of regeneration after IR (Beltrami *et al.*, 2001; Malliaras *et al.*, 2013). Given the ErbB4 receptors are mainly expressed in cardiomyocytes and primarily function as growth regulators, I proposed that the up-regulated JM-a isoform might play a role in cardiomyocyte regeneration, and this function might be contributed by the JM-a domain. The JM-a isoform has a protease cleavage site in the juxtamembrane domain, which allows the receptor to be cleaved, releasing an intracellular domain (ICD) that can enter into cytoplasm or nucleus (Vecchi *et al.*, 1997; Rio *et al.*, 2000; Zhou *et al.*, 2000). It has been suggested that the ICD plays a role in regulating cell apoptosis and proliferation in many cell types (Zhu *et al.*, 2006b; Gilmore-Hebert *et al.*, 2010). However, shedding of the ICD has not yet been demonstrated in primary cardiomyocytes. Thus, to investigate the function of the ICD in cardiomyocytes, we studied whether the JM-a isoform is cleaved after agonist stimulation. Phorbol 12-myristate 13-acetate (PMA) causes cleavage of the JM-a isoform and release of the ICD in many cell lines (Vecchi *et al.*, 1996; Zhou *et al.*, 2000; Määttä *et al.*, 2006; Zeng *et al.*, 2009). NRG1 also induces the cleavage of JM-a isoforms in fibroblast and ovarian carcinoma cell lines (Vecchi *et al.*, 1996; Zhou *et al.*, 2000). Thus, we stimulated isolated rat cardiomyocytes with PMA (10 nM - 5 µM) for 30 min and probed for the ICD and full-length intact ErbB4 using Western blotting. As shown in Figure 4.6 A, we detected no ICD in cardiomyocytes treated with increasing concentrations of PMA for 30 min. We then examined different time points for PMA (100 nM) stimulation. As shown in Figure 4.6 B treatment with PMA for 5 to 60 min did not produce any detectable ICD in cardiomyocytes. However, it should be noted that the endogenous JM-a isoform has very limited expression in primary cardiomyocytes, where expression of the ErbB4 JM-b isoforms is predominant (Figure 4.3). In addition, PMA only cleaves a portion of JM-a isoforms to generate the ICD in other cell types (Vecchi *et al.*, 1996), which could make it difficult to detect.

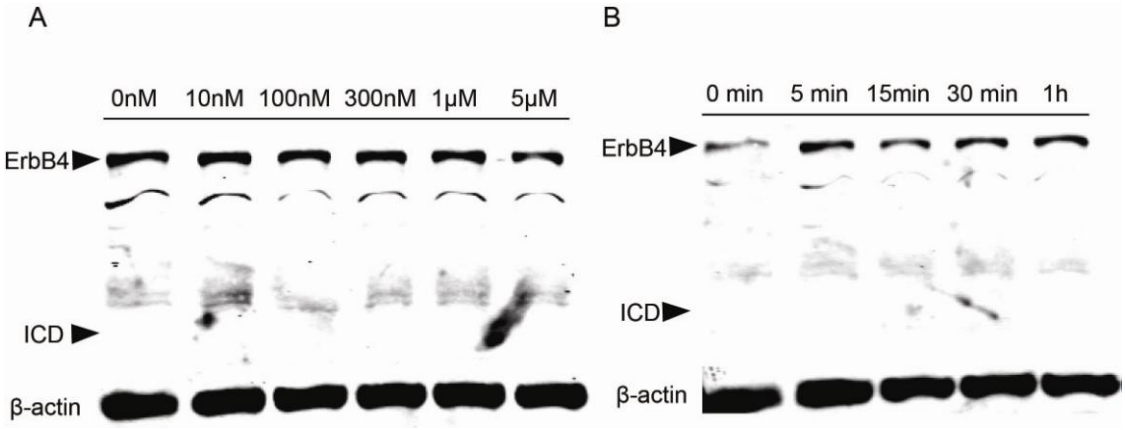

Figure 4.6 No evidence for cleavage of endogenous ErbB4 in primary cardiomyocytes following PMA stimulation. A. Cardiomyocytes were treated with increasing concentrations (10 nM – 5 μM) PMA or a vehicle control for 30 min, harvested with lysis buffer and subjected to Western blotting. B. Cardiomyocytes were treated with 100 nM PMA for 0 – 60 min before harvesting and Western blotting. A primary antibody (sc-283, Santa Cruz) recognizing the C-terminal of ErbB4 was used to probe for both the ICD and intact ErbB4, and β-actin was used as a loading control.

To further examine the cleavage of ErbB4 isoforms in cardiomyocytes, we generated four vectors expressing the individual isoforms tagged with GFP at the C-terminus. The vectors were delivered into cardiomyocytes via transfection, and the cleavage and trafficking of the ICD following stimulation with PMA or NRG1 was observed by live-cell imaging using confocal microscopy. To confirm that the GFP-tagged ErbB4 isoforms can be successfully expressed, the recombinant expressing vector was delivered into HEK-293 cells and Western blot used to detect the exogenously expressed ErbB4-GFP. We also confirmed that the GFP-tag did not affect the response of ErbB4 to PMA and the ability of cleavable isoform to release the ICD by stimulating the HEK-293 cells with PMA (100 nM) after transfection. Full-length ErbB4 and the ICD were detected by Western blot using an antibody to the C-terminus of ErbB4. As shown in Figure 4.7 A, a 210 kDa band was detected in all samples, representing the intact GFP-tagged JM-a CYT-1 isoform. An 110 kDa band representing the ICD-GFP was detected after 3 min of stimulation with PMA. The intensity of this 110 kDa band increased with prolonged PMA treatment, suggesting that cleavage of JM-a CYT-1-GFP (a1-GFP) and release of the ICD-GFP is PMA dependent and that the minimum time required for cleavage is 3 min. Cells transfected with JM-a CYT-2-GFP (a2-GFP) showed low levels of ICD-GFP in the absence of stimulation (Figure 4.7 B), suggesting some auto-cleavage of JM-a CYT-2 under basal conditions. The ICD-GFP band generated from JM-a CYT-2-GFP has more intensity than the band from JM-a CYT-1-GFP under the same conditions, suggesting that the intracellular CYT-2 domain promotes cleavage of the JM-a isoform. This is consistent with previous work showing that cleavage of the JM-a isoform and generation of the ICD is kinase dependent, and the CYT-2 isoform possesses stronger kinase activity (Sundvall *et al.*, 2007). There were no ICD-GFP bands detected in HEK-293 cells transfected with the non-cleavable isoforms JM-b CYT-1-GFP (b1-GFP, Figure 4.7 C) and JM-b CYT-2-GFP (b2-GFP, Figure 4.7 D).

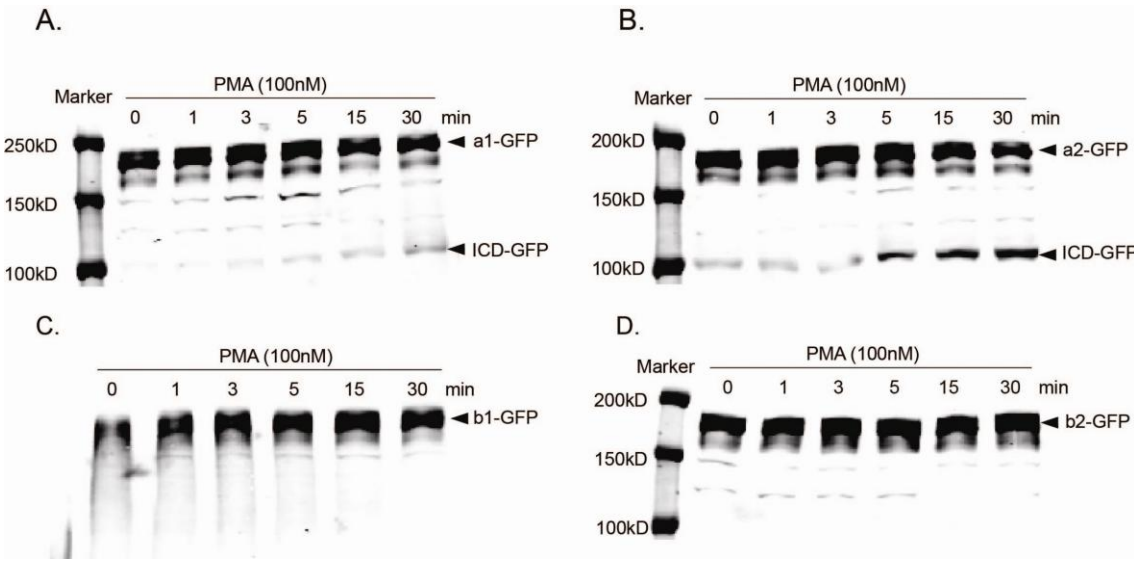

Figure 4.7 Cleavage of exogenous ErbB4-GFP in PMA-stimulated HEK-293 cells. HEK-293 cells were transfected with 600 ng of either JM-a CYT-1-GFP (a1-GFP, A), JM-a CYT-2-GFP (a2-GFP, B), JM-b CYT-1-GFP (b1-GFP, C) or JM-b CYT-2-GFP (b2-GFP, D). Following transfection, cells were cultured in serum-free DMEM for 24 h before stimulation with 100 nM PMA for 1 to 30 min. Cells were then harvested for Western blot analysis. The primary antibody (sc-283, Santa Cruz) recognizing the C-terminal of ErbB4 was used to detect both the ICD and the full-length ErbB4.

After confirming that the GFP tag did not affect the cleavage of ErbB4, we introduced these recombinant vectors to cardiomyocytes via transfection. Confocal microscopy was used to record the trafficking of ErbB4-GFP in primary cardiomyocytes following stimulation with PMA or NRG1 (section 4.2.6). Before stimulation, the majority of fluorescence representing the ErbB4-GFP was located on the cell membrane, as expected (Figure 4.8). However, a small amount of intracellular fluorescence was observed, potentially due to activities such as ErbB4 protein synthesis, recycling and trafficking. The intracellular fluorescence might interfere with observing the location of the ICD-GFP stimulation. To avoid this, I photo-bleached the intracellular area without affecting membrane before stimulation (section 4.2.6). As shown in Figure 4.8, after bleaching the fluorescence was only located in the cell membrane. After PMA and NRG1 stimulation, a small amount of fluorescence in a1-GFP transfected cells accumulated in the cytosol (Figure 4.8 A). However, little fluorescence was observed in the nucleus after stimulation. Vehicle (PBS) treatment did not induce trafficking of the green fluorescence from the membrane into the cytosol. Similarly, a2-GFP transfected live cardiomyocytes displayed PMA- and NRG1- but not vehicle- induced accumulation of the green fluorescence in cytosol (Figure 4.8 B). However, unexpectedly, the non-cleavable isoforms b1-GFP and b2-GFP also displayed intracellular fluorescence accumulation in cardiomyocytes (Figure 4.8 C and D). Thus, the fluorescence observed in the cytoplasm may represent the trafficking of intact receptor and not the released ICD. The mechanism by which the intact ErbB4 receptor trafficks into the cytosol is unclear. It is maybe due to receptor endocytosis, or movement of the receptor in cytoplasm following stimulation. When taken together with the Western blot data described above, this suggests that PMA or NRG1 do not cleave the JM-a isoform to release the ICD in cardiomyocytes.

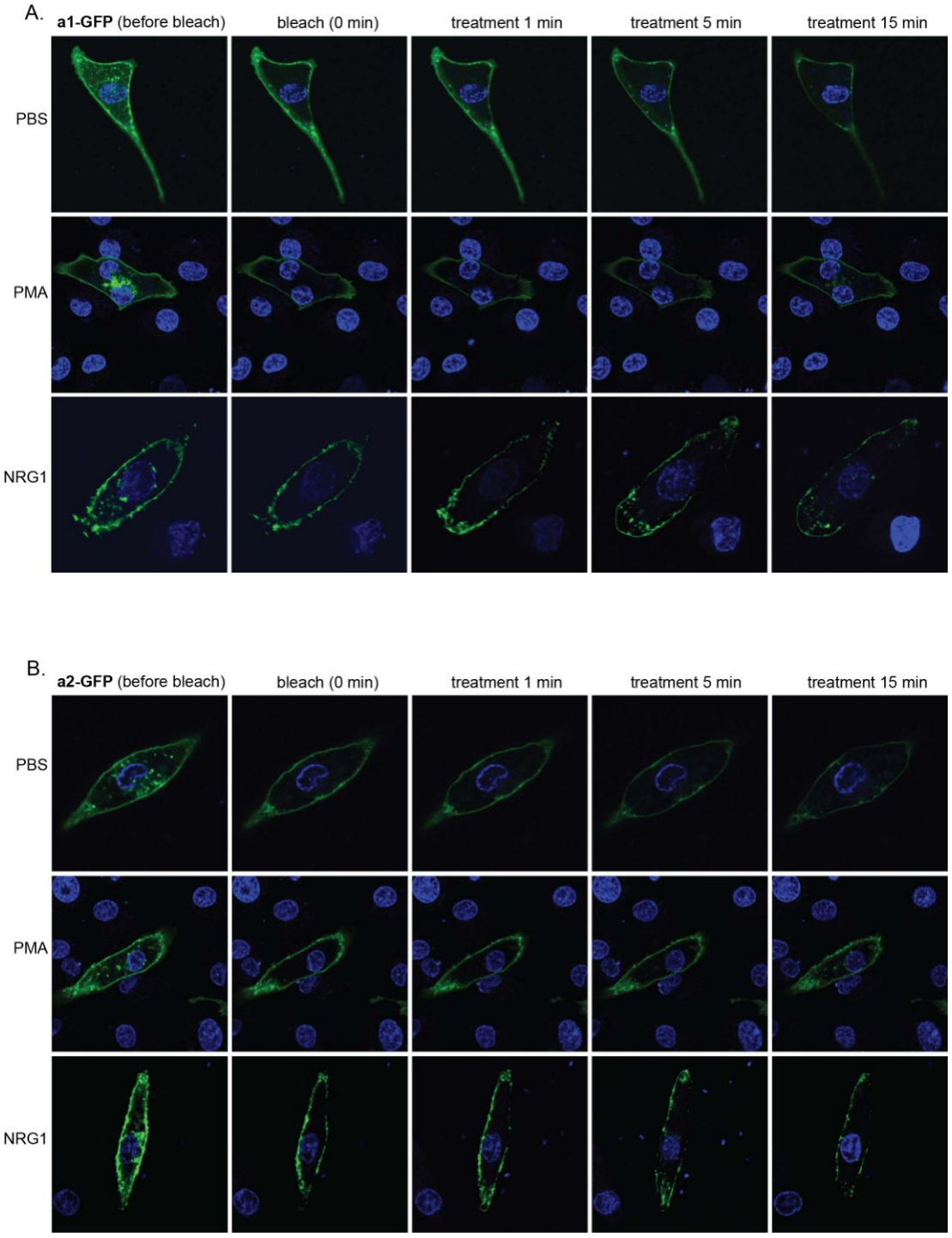
A.
a1-GFP (before bleach)
bleach (0 min)
treatment 1 min
treatment 5 min
treatment 15 min
PBS
PMA
NRG1
B.
a2-GFP (before bleach)
bleach (0 min)
treatment 1 min
treatment 5 min
treatment 15 min
PBS
PMA
NRG1

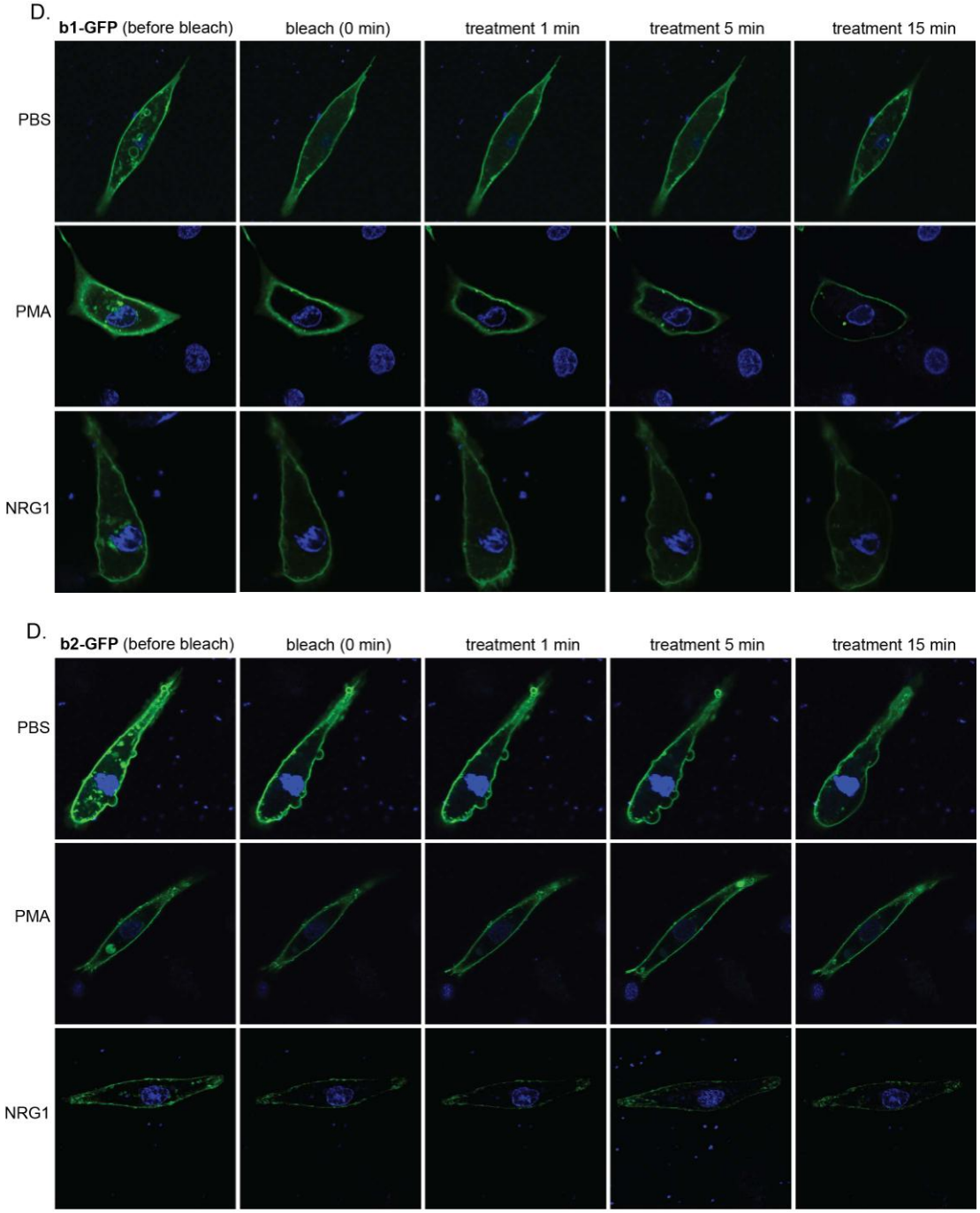

Figure 4.8 T**rafficking of ErbB4-GFP in cardiomyocytes following stimulation with PMA or NRG1.** Cardiomyocytes were maintained in serum-free DMEM CCT SS2 and transfected with 500ng pEGFP-N1-JM-a CYT-1 (A), pEGFP-N1-JM-a CYT-2 (B), pEGFP-N1-JM-b CYT-1 (C) or pEGFP-N1-JM-b CYT-2 (D). 48h after transfection cell nuclei were stained with 10 µg/ml Hoechst 333258 for 30 min before commencing live cell imaging. Cellular fluorescence was bleached as described in section 4.2.6. PMA (100 nM) or NRG1 (10 nM) were added immediately after bleaching and images taken at 1, 5 and 15 min after stimulation. All images were taken at 60×10 magnification.

4.3.5 The role of individual ErbB4 isoforms in mediating NRG1-induced cardiomyocyte hypertrophy

The results in section 4.3.4 suggest that the JM-a isoform cannot be cleaved in isolated cardiomyocytes *in vitro,* although it is endogenously expressed in neonatal cardiomyocytes (Dr. Hsiu-wen Chan, PhD thesis). This leads to the question of whether there is a functional difference between the JM-a and JM-b isoforms if the JM-a isoform cannot be cleaved in cardiomyocytes. In addition, whether there are any functional differences between the CYT-1 and CYT-2 isoforms in cardiomyocytes is unknown. The results in chapter 3 of this thesis show that NRG1-induced cardiomyocyte hypertrophy requires ErbB4. To investigate which isoform of ErbB4 contributes to this hypertrophic signalling, we designed a rescue system to generate cardiomyocytes in which only one ErbB4 isoform is expressed. In this system, the shRNA used to knockdown endogenous ErbB4 was co-transfected with a vector expressing a knockdown resistant variant of one ErbB4 isoform. NRG1 was used to induce hypertrophic signalling, and activation of ANP, CyclinD and MLC-2V measured with promoter-reporter assays as previously described (section 2.6). Knockdown of ErbB4 reduced the NRG1-induced MLC-2V (Figure 4.9 A) ANP (Figure 4.9 B), and Cyclin D (Figure 4.9 C) promoter activity. Interestingly, all isoforms of ErbB4 could rescue the hypertrophic response, suggesting that they can all mediate hypertrophic signalling. This may indicate that ErbB4-mediated activation of hypertrophic gene expression is dependent on a function common to all four isoforms - i.e. the tyrosine kinase activity. The hypertrophic signalling mediated by the individual isoforms follows a similar pattern for all hypertrophic genes: the CYT-2 isoform seems to have a greater ability to promote the signalling than CYT-1 isoform, although this difference is not statistically significant. In contrast, the JM-a and JM-b isoforms both promote hypertrophic signalling to a similar extent. Promoter activity for each hypertrophic gene was elevated in cells expressing individual ErbB4 isoforms (compared to the knockdown group) even without stimulation, indicating a low level of auto-activation of ErbB4. This activation is probably caused by the over-expression of the delivered isoform(s) of ErbB4.

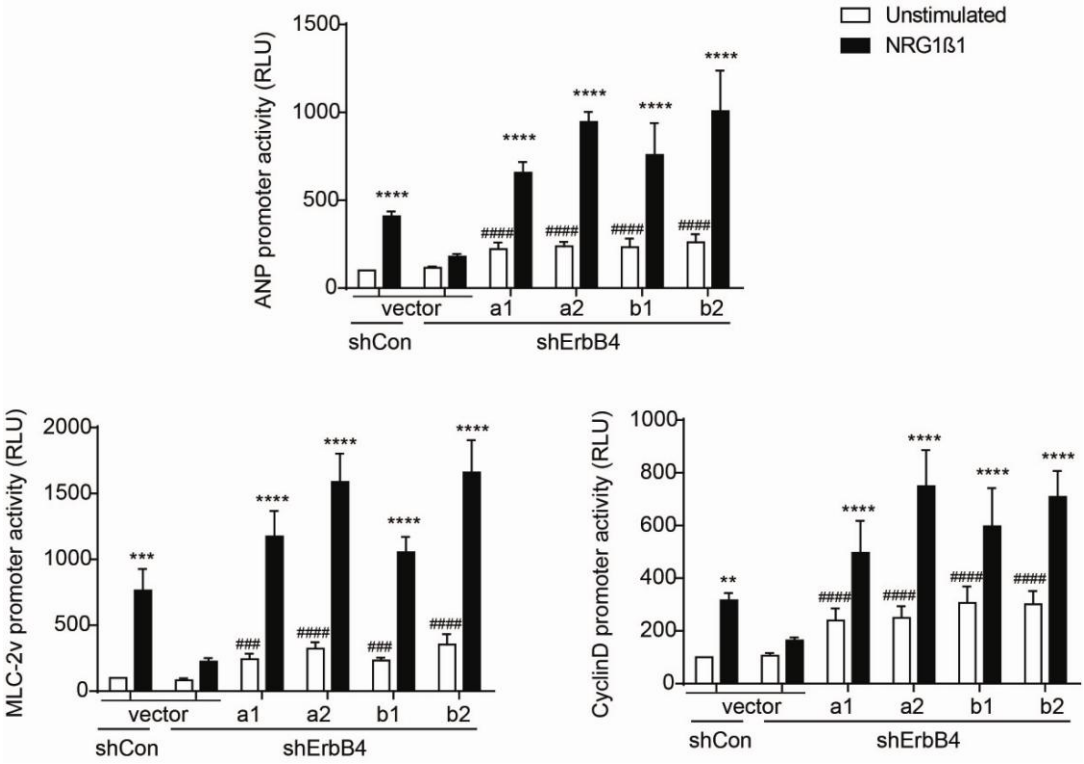

Figure 4.9: Hypertrophic gene promoter activity in NRG1-stimulated cardiomyocytes expressing only a single isoform of ErbB4. All cardiomyocytes were transfected with three separate constructs. The first construct (100 ng) encoded a knockdown resistant (kdr) isoform of ErbB4 (kdr-JM-a CYT1, a1; kdr-JM-a CYT2, a2; kdr-JM-b CYT1, b1; kdr-JM-b CYT2, b2) or an empty vector control. The second construct (100 ng) encoded either shErbB4 or shControl (shCon), whilst the third was a hypertrophic gene promoter driven luciferase reporter construct (300 ng) using the promoter sequence of either ANP (A), MLC-2V (B) or CyclinD (C). Cells were then stimulated with NRG1β1 for 48 h or left unstimulated. The promoter activity of each hypertrophic gene was measured using luciferase assays. Data are normalized to the unstimulated shControl group and presented as mean ± SEM. For statistical analysis, the original data was normalized by log transformation to achieve equal variance distribution for each group. Normalised data was then analysed by Two-way ANOVA with Dunnett's multiple comparison tests. ****P<0.0001, ***P<0.001 and **P<0.01 vs. NRG1-stimulated knockdown (vector); ###P<0.001 and ####P<0.0001 vs. unstimulated knockdown (ANP, n=5; MLC-2V, n=4; CyclinD, n=5).

4.4 Discussion

In this chapter, I investigated the expression and cleavage of ErbB4 isoforms, and their ability to promote hypertrophy in cardiomyocytes. The main discoveries of these studies are: (1) cardiac ErbB4 expression is highest in the embryonic state and declines postnatally. The expression of all four isoforms of ErbB4 gradually decreased from embryogenesis to the adult stage. The predominant isoform in the adult heart is the JM-b isoform. There is no obvious isoform alteration in IR injury or pathological models of cardiac hypertrophy. (2) JM-a cleavage cannot be observed in purified cultures of primary cardiomyocytes following stimulation with NRG1 or PMA. However, cleavage of the JM-a isoform could be demonstrated in HEK-293 cells. (3) All four ErbB4 isoforms could mediate NRG1-induced cardiomyocyte hypertrophy.

In the literature, the JM-b isoform is proposed to be the only isoform in the adult mice heart (Elenius *et al.*, 1997; Elenius *et al.*, 1999). My study showed that, whilst the JM-b isoform is predominant, both the JM-a and JM-b isoforms are detectable in the adult mice heart. The reason these previous studies did not detect JM-a may be because they used traditional end-point PCR and agar gel electrophoresis, which is less sensitive than the TaqMan method used in my study. Despite this disagreement on the expression of JM-a in postnatal heart, my finding that the JM-b isoform is the major isoform in adult heart is in agreement with previous work.

One interesting result in my study is that ErbB4 is expressed at a much higher level in the embryonic heart than in the adult. ErbB4 is essential for cardiac growth: deletion of ErbB4 inhibited normal cardiac growth in both the embryonic (Gassmann *et al.*, 1995) and postnatal stages (Garcia-Rivello *et al.*, 2005). The high level of ErbB4 in embryonic heart is consistent with the strong requirement for cardiac growth during development. However, determining which isoforms of ErbB4 are predominant in embryonic heart has not been investigated previously. Our results showed that in the earlier embryonic stage (E10.5) the JM-b:JM-a ratio is 3:1, whilst in the adult this increases to 40:1. We were unable to detect the expression of four isoforms any earlier than E9 due to the tiny size of the heart tube and inefficient RNA extraction from the heart tube at this stage. While alternative methods to detect RNA expression (i.e., *in situ* hybridisation) were not performed, based on the expression pattern throughout the cardiac development (Figure 4.1), it may be inferred that at earlier embryo stage E9, the JM-b and JM-a might be expressed at a similar level. Because ErbB4 is primarily expressed in cardiomyocytes (which comprise two thirds of the volume of the whole heart), and not detectable in fibroblasts (which comprise one third of the volume) (Zhao *et*

al., 1998), I would propose that my study reflects the developmental regulation of ErbB4 expression in cardiomyocytes instead of other cells, although further experiments can be employed to confirm this. The decrease in the JM-a:JM-b ratio is coincident with loss of the ability of cardiomyocytes to proliferate. In the embryonic heart, cardiomyocytes can both proliferate and enlarge to contribute to the cardiac growth. However, shortly after birth, the cardiomyocytes exit the cell cycle and heart growth becomes dependent on cardiomyocyte enlargement (cardiomyocyte hypertrophy) (Markwald *et al.*, 2010).Whilst the ability of ErbB4 to promote cardiac development is well-established in literature (section 1.6.7), it is not yet known whether the different isoforms of ErbB4 can mediate different functional effects. In many cell lines, ErbB4 isoforms have different growth promoting abilities. These differences are primarily related to the JM and CYT domains. By overexpressing full-length JM-a and JM-b in mouse embryonic astrocytes in an ErbB4-null background, Sardi *et al.* found only the cleavable JM-a isoform is capable of suppressing astrocyte precursor differentiation and maintaining their neurogenic potential (Sardi *et al.*, 2006). In human breast cancer cells, the JM-a CYT-2 isoform was found to promote the phosphorylation of itself and proliferation of the cancer cells, which was proposed to be related to cleavage of the receptor (Määttä *et al.*, 2006; Zhu *et al.*, 2006b). Mammary cell lines expressing exogenous CYT-2 ICD grow more rapidly than the same cell line expressing CYT-1 ICD (Muraoka-Cook *et al.*, 2009). In a mouse fibroblast cell line, the ICD of JM-a CYT-2 was found to interact with AP-2 to positively regulate the platelet-derived growth factor receptor-alpha (PDGFA) promoter leading to cell proliferation (Sundvall *et al.*, 2010). Taken together with these observations, our data suggests that cardiomyocytes require different isoforms to proliferate or hypertrophy. Embryonic cardiomyocytes, for example, might require the JM-a isoform, but not the JM-b isoform, to proliferate.

Although it has been confirmed in the literature (Elenius *et al.*, 1997; Elenius *et al.*, 1999) as well as in our laboratory that primary isoforms of ErbB4 in the adult heart are JM-b isoforms, there was the possibility that this could be altered in pathological conditions. We therefore characterized the cardiac expression of ErbB4 isoforms using *in vivo* models of ischaemia-reperfusion injury and pathological hypertrophy. Only the JM-a and CYT-2 isoforms are regulated after ischaemia while the expression levels of the JM-b and CYT-1 isoforms were not significantly altered. Although the increase of JM-a isoforms at 24h after ischaemia reperfusion is up to 2 fold, the absolute amount of JM-a is still diminutive compared to the JM-b isoforms (approximately 1:20). This suggests there is no alteration in the primary isoform of ErbB4 expressed in cardiac tissue, and that expression of the JM-b isoforms dominates in the heart, even in pathological conditions. If JM-a does relate to the

proliferation of the cardiomyocytes as discussed above, the low expression levels of JM-a in IR model described here is consistent with the limited regenerative capacity of the injured heart (Laflamme *et al.*, 2011). It is believed that shortly after birth the majority of cardiomyocytes in heart exit the cell cycle and lose the ability to proliferate. Thus, the injured adult heart cannot be repaired via generation of new cardiomyocytes.

In the pathological hypertrophy model, expression of all four isoforms was significantly reduced. However, since this affects all isoforms equally this change may reflect reduced transcription of the entire gene and not isoform specific regulation. In this model, the pathological hypertrophy is induced by genetically overexpressed calcineurin, a calcium-dependent phosphatase. It causes cardiac hypertrophy via dephosphorylating the transcription factor NF-AT3 and enabling its translocation to the nucleus where NF-AT3 can interact with GATA4 to activate cardiac transcription and hypertrophic growth (Molkentin *et al.*, 1998). The decrease of ErbB4 in pathological hypertrophy suggests that ErbB4 is not required by the calcineurin signalling to mediate cardiac hypertrophy. NRG1 induces cardiomyocyte hypertrophy via activation of ERK (Baliga *et al.*, 1999), which can also activate the GATA4 to contribute to the hypertrophic growth (Yanazume *et al.*, 2002; Akazawa *et al.*, 2003). However, the activation of calcineurin signalling and NRG1-ErbB4 signalling *in vivo* leads to different results in the heart. The former eventually leads to heart failure following cardiac hypertrophy (Molkentin *et al.*, 1998) whereas the latter enhances cardiac function via regulating contractile and sarcomere proteins in cardiomyocytes (Jiang *et al.*, 2010) and reducing the cardiomyocyte death even in the presence of pathological stress, such as infarction, cardiomyopathy and myocarditis (Liu *et al.*, 2006).

In addition to investigating the regulation of ErbB4 isoform expression in various models, I also studied the cleavage of JM-a isoforms. While specific cleavage of JM-a ErbB4 isoforms was confirmed in transfected HEK294 cells, no cleavage was observed in neonatal rat cardiomyocytes stimulated with either PMA or NRG1. This result was first demonstrated by Western blot and confirmed by observing the trafficking of ErbB4 with confocal microscopy live cell imaging. If the JM-a isoform cannot be cleaved in cardiomyocytes, there may be no functional differences between the JM-a and JM-b isoforms. Our lab has previously detected expression of both isoforms in purified cultures of primary neonatal rat cardiomyocytes (Dr. Hsiu-wen Chan, PhD thesis) and expression of the JM-b isoform is much higher than the JM-a isoform (Mr. Hengbo Shi, unpublished data). If there is no functional difference, the reasons underlying the marked difference in the expression levels of JM-a and JM-b isoforms in postnatal cardiomyocytes remain unclear.

The reason for the lack of cleavage of JM-a in cardiomyocytes has not been identified. One possibility is that cardiomyocytes lose some components required for the cleavage during the isolation and purification of the cells, and therefore cannot cleave ErbB4 *in vitro*. For instance, the functional loss of protein, such as the expression of AT_1R, during cardiomyocyte isolation has been proposed previously (Thomas *et al.*, 2002). Another possibility is that cardiomyocytes require the surrounding cells, such as fibroblasts or endothelial cells, in order to undertake cleavage. As discussed in section 1.4.2, the mechanism for JM-a isoform cleavage (in other cell types) involves the activation of ADAM17 or MMP to cleave the JM-a isoform in the juxtamembrane region and remove the ectodomian from the receptor (Rio *et al.*, 2000; Chang-Yuan *et al.*, 2001). The remaining intracellular part of the receptor anchored in the cell membrane is then subjected to additional cleavage by γ-secretase to generate the 80 kD ICD (Rio *et al.*, 2000; Chang-Yuan *et al.*, 2001). However, the mechanism is still not fully resolved and additional proteins may be involved in this process. Whether cardiomyocytes are subject to the full range of ErbB4 regulation observed in other cell types is unknown. Perhaps some unidentified components located on the membrane of neighbouring cells can cause cleavage of a substrate located on the membrane of adjacent cardiomyocytes - if so, this would explain why we did not observe JM-a cleavage in purified cardiomyocytes. Moreover, we only examined ErbB4 receptor trafficking after stimulation with factors that are known to induce cleavage of the JM-a isoform in other cell types. It is possible that there are additional factors that can induce cleavage of the JM-a isoform which have not yet been identified, and that these may initiate cleavage of the JM-a isoform in cardiomyocytes.

Finally, my study found that all four isoforms of ErbB4 can mediate NRG1-induced cardiomyocyte hypertrophy. This suggests that the pro-hypertrophic ability of the four isoforms depends on a common feature among them (e.g. the tyrosine kinase activity), but does not relate to possession of the cleavable domain or intracellular binding domain. However, the magnitude of hypertrophy seems to be influenced by the CYT domain although this was not statistically significant due to inherent variability in the data set. One reason why the CYT2 isoform can promote hypertrophic signalling more than CYT1 may be due to the intracellular kinase domain, which is more easily phosphorylated in CYT2 isoforms (Sundvall *et al.*, 2007). The mechanism for this is still not clear, however it is proposed that a “loop structure” exists in the intracellular domain possessing CYT1, and that this may inhibit tyrosine kinase activity (Sundvall *et al.*, 2007). Our data suggests that the JM-a and JM-b isoforms have comparable abilities to promote hypertrophic signalling. This is consistent with earlier studies in this chapter suggesting the JM-a isoform cannot be cleaved in purified cardiomyocytes. The only known difference between the JM-a and JM-b isoforms is that

the JM-a isoform can be cleaved while the JM-b cannot. If cardiomyocytes lack the JM-a cleavage mechanism, I would not predict any functional difference between the JM-a and JM-b isoforms. This could explain the absence of functional differences between JM-a and JM-b isoforms in our hypertrophic signalling experiments. It should be noted that the hypertrophic gene signal in all the 'rescued' groups is greater than that of the controls, suggesting that the expression level of the delivered ErbB4 isoforms is higher than endogenous expression levels. This high expression might mask the potential differences between the four isoforms in their ability to mediate hypertrophy. There is the possibility that when expressed at a lower level (closer to that of endogenous expression), the capacity of individual ErbB4 isoforms to differentially regulate hypertrophic gene expression may be exposed. Taken together, in my study, no cleavage of the JM-a isoforms has been found in cardiomyocytes, and the ability of ErbB4 to promote hypertrophic seems to be kinase activity dependent and independent of isoform cleavage.

CHAPTER 5

THE FUNCTION OF ErbB4 IN THE ADULT HEART

5. Function of ErbB4 in the adult heart

5.1 Background

ErbB4 is critical for heart development, anti-apoptosis and hypertrophy. Global deletion of ErbB4 is lethal by embryonic day 11 in mice due to defective development of the heart (Gassmann *et al.*, 1995). The heart defect in the ErbB4 null mice could be rescued by expressing ErbB4 under a heart specific myosin promoter. These mice reached adulthood and are fertile (Tidcombe *et al.*, 2003), indicating that ErbB4 plays a significant role in heart development. In addition to cardiac development, ErbB4 signalling also prevents cardiac injury in adults. The ErbB4 agonist neuregulin1 (NRG1) rescues adult ventricular myocytes from hypoxia-reoxygenation-induced apoptosis**,** whereas the endothelium-selective deletion of NRG1 decreases the ability of the myocytes to tolerate an ischemic insult (Hedhli *et al.*, 2011). Exogenous NRG1 also decreased the number of apoptotic cells and improved heart function in a rat model of diabetic cardiomyopathy with systolic and diastolic dysfunction (Li *et al.*, 2011), and in cultured myocytes NRG1 inhibits the apoptosis induced by serum starvation (Zhao *et al.*, 1998). Taken together, these studies indicate that NRG-ErbB4 signalling is important in cardiac protection. Finally, ErbB4 also mediates cardiac hypertrophy. NRG1 promotes hypertrophy in both adult and neonatal rat primary cardiomyocytes, which is accompanied by enhanced expression of the hypertrophic genes ANP and skeletal α-actin (Zhao *et al.*, 1998), indicating that ErbB4 might play an important role in adult cardiac function and structure maintenance. To date, few studies have examined the role of ErbB4 in the adult heart. A study using a targeted knockout model demonstrated that cardiac specific deletion of ErbB4 led to severe dilated cardiomyopathy in adult mice, characterized by thinner ventricular walls with reduced contractility and conduction delays (Garcia-Rivello *et al.*, 2005). However, in this study deletion of the ErbB4 occurred before birth making it hard to exclude the possibility that the cardiomyopathy observed in the adult stage was due to a defect during cardiac development. To overcome the requirement of ErbB4 for cardiac development and investigate the function of ErbB4 in the adult heart, we used a conditional knockout model, the αMHC-MerCreMer/loxP system (Sohal *et al.*, 2001), to specifically delete ErbB4 from adult cardiomyocytes.

The Cre-loxP system is a commonly used tool to provide targeted gene deletion. Cre recombinase is found in P1 bacteriophage and is a 38kD site-specific recombinase that catalyzes the recombination between two DNA recognition sites, termed loxP (Hamilton and Abremski, 1984). The loxP site is a 34 bp consensus sequence, consisting of a core spacer sequence of 8bp and two 13bp palindromic

flanking sequences. The asymmetric core sequence defines the orientation of the loxP site. The Cre recombinase can excise a DNA segment from the genome when the segment is flanked by loxP sites in the same orientation (Nagy, 2000). To delete genes in a tissue specific manner, Cre recombinase can be driven by a tissue specific gene promoter. To give temporal control of gene deletion, Cre recombinase can be fused to a mutated estrogen receptor ligand binding domain (ER-LBD) (MerCreMer) (Nagy, 2000; Chien, 2001). This mutant ER selectively binds the synthetic ER antagonist tamoxifen (rather than endogenous estrogen), and upon tamoxifen treatment, the activated ER-LBD causes translocation of Cre recombinase to the nucleus, where it causes recombination of the gene flanked by loxP (Sohal *et al.*, 2001). Thus, in this system, the targeted gene deletion is not only tissue specific but also temporally controlled by tamoxifen injection. The first application of this system to gene deletion from cardiomyocytes was achieved by Sohal *et al.* in 2001 (Sohal *et al.*, 2001). They linked the cardiac-specific α-MHC (alpha-myosin heavy chain) promoter to the Cre/ER-LBD gene (αMHC-MerCreMer transgene). Transgenic mice with Cre-dependent, loxP-inactivated lacZ were crossed with transgenic mice containing the αMHC-MerCreMer gene to generate the αMHC-MerCreMer/lacZ mice. Using lacZ as a reporter, they demonstrated that tamoxifen-induced Cre activity caused 80% recombination of targeted gene in the embryonic, neonatal, or adult heart, but not other tissues. Taking advantage of this model, we will delete ErbB4 from adult mice heart to investigate its function in this stage.

5.2 Methods

5.2.1 Animals

The homozygous ErbB4$^{fl/fl}$ mouse line (with exon2 of ErbB4 gene flanked by loxP sites) was crossed with the homozygous αMHC-MerCreMer mouse line (Cre$^{+/+}$) to generate double heterozygous αMHC-MerCreMer and ErbB4-floxed mice (Cre$^{+/-}$/ErbB4$^{fl/wt}$). These mice were then backcrossed with the ErbB4$^{fl/fl}$ line to generate heterozygous αMHC-MerCreMer and homozygous ErbB4-floxed animals (Cre$^{+/-}$/ErbB4$^{fl/fl}$), and homozygous Cre$^{-/-}$ErbB4$^{fl/fl}$ mice in the offspring (Figure 5.1). To generate the Cre$^{+/-}$/ErbB4$^{wt/wt}$ animals, Cre$^{+/-}$/ErbB4$^{fl/wt}$ mice were backcrossed with Cre$^{+/+}$ mice (Figure 5.4). The original homozygous ErbB4$^{fl/fl}$ and homozygous α-MHC-MerCreMer mice lines (Cre$^{+/+}$) were obtained from Dr Kent Lloyd, University of California (Mutant Mouse Regional Resource Centres) and Jackson Laboratories, respectively. Both of the strains are on a B6/129 mixed background.

Animals were housed under standard conditions at 22°C with a 12-h light/12-h dark cycle and free access to water and commercial mouse chow. All experiments were conducted in accordance with the Australian Code of Practise for Care and Use of Animals for Scientific Purposes and approved by the institutional ethics committees of The University of Queensland.

5.2.2 Genotyping

Mice were toe-clipped at 7-10 days of age to provide tissue samples for genotyping. The toes were digested in DNA extraction buffer (100 mM Tris-HCl (pH8.5), 5 mM EDTA (pH8.0), 200 mM NaCl, 0.2% SDS and 0.48mg/ml proteinase K) at 55°C overnight. The genomic DNA was precipitated with ammonium acetate and ethanol before PCR amplification using primers specific for Cre, or ErbB4 wild type and ErbB4 floxed DNA sequences (Figure 5.2 A). The former reaction will yield a 440bp band (Cre), and the latter will yield 350bp and 400bp products for ErbB4 wild type and ErbB4 floxed alleles respectively. The primer sequences are listed in Appendix B. PCR reactions (20µl total volume) contained 20 ng genomic DNA, 0.5 µM of each primer, 0.2 mM each of dNTPs, 5% DMSO, 0.375 U of Phire Hot Start II DNA Polymerase (Finnzymes) and 1× Phire reaction buffer (final concentration). The PCR cycling conditions started with an initial denaturation at 98°C for 30s, followed by 35 cycles of denaturing at 98°C for 5 s, annealing at 58°C for 5 s (for ErbB4 floxed and wild type) or 55°C for 5 s (for Cre), extension at 72°C for 10s, and a final incubation at 72°C for 1 min. PCR products were separated using 1.5-2% agarose gel electrophoresis and images were captured with the Quantity One system. To detect the Cre copy number, qPCR (SYBR) was employed to quantify the genomic Cre level and genomic 18S level was used as an internal control. The qPCR condition followed the standard amplification protocol (refer to section 2.8). The sequence of primers used is listed in Appendix B.

5.2.3 Tamoxifen injection

To induce Cre-mediated recombination, all animals (9-10 week of age) were treated with tamoxifen (Sigma) by intraperitoneal injection for 10 consecutive days at a dosage of 20 mg/kg/day. Tamoxifen was dissolved in peanut oil at a concentration of 4 mg/ml at 37°C for 2 hours and made up fresh each day. The success of deletion of ErbB4 in the $Cre^{+/-}ErbB4^{fl/fl}$ mouse heart was determined by qPCR in an initial cohort of animals at 10 days after tamoxifen injection. Separate cohorts of animals were then phenotypically examined at 3-4 months or 7-8 months after tamoxifen injection.

5.2.4 Echocardiography

Echocardiography was conducted on all animals using a Philips HD15 ultrasound system equipped with a 15-MHz transducer. Mice were anesthetized with 2% isoflurane in O_2 by inhalation and normal body temperature was maintained using an external heat source. Two-dimensional mid-papillary level short axis views of the ventricle were captured. M-mode images were obtained by positioning a cursor in the 2-dimensional view from the anterior to the posterior wall of the left ventricle and adjacent to the two papillary muscles. M-mode images were used to obtain the following measurements during both systole and diastole: interventricular septal thickness (IVS), left ventricular posterior wall thickness (LVPW), left ventricular internal diameter (LVID). The fractional shortening (FS) was calculated using the equation (FS= (LVID (diastolic)-LVID (systolic))/LVID (diastolic)). The measurements were repeated 5 times over 5 cardiac cycles for each parameter and the average of these used for statistical analysis. Heart rate was monitored by electrocardiography during the procedure. The experimenter was blinded to the genotype of the animals for all echocardiographic assessments and decoded post-analysis.

5.2.5 Measurement of heart/kidney/body weight and tibial length

Animals were euthansed and the heart and kidneys was carefully removed and weighed. Tibial length was measured after the skeletal muscle was completely removed from the bone. The left and right tibias were measured three times each with a digital calliper, and the average of these 6 measurements was used as the final tibial length for each mouse.

5.2.6 Histology

Mid-ventricular sections were fixed in 4% PFA for 48 hours and then embedded in paraffin. Sections (5 μm thick) cut from paraffin-embedded specimens was deparaffinised in xylene followed by hydration through an ethanol gradient to PBS or distilled water before being used for wheat germ agglutinin (WGA) staining, Masson's trichrome staining, TUNEL staining or immunofluoresence.

5.2.7 WGA staining

Sections were incubated with 50 μg/ml WGA conjugated with Alexa Fluor®594 (Invitrogen) for 60 min, washed 3 times with PBS and mounted for fluorescence microscopy. 5 images were taken for each section under 400 × magnification. The images were taken randomly from two fields next to the endocardium, two fields next to the epicardium and one field in the papillary muscle area. In each field, the cross sectional area of 40 - 130 cells was measured. For the cell size quantification,

images were opened with Image J. To perform an unbiased measurement, a grid with 3×4 (horizontal × vertical) test lines was generated with Image J and applied to every image. Only cells intersected with the grid lines were measured and the experimenter was blinded for all measurements.

5.2.8 Masson's trichrome staining

Masson's trichrome staining was performed according to the manufacturer's protocol (Polysciences). Briefly, sections were merged in Bouin's solution at 60°C for 1 hour, washed in running tap water to for 5 minutes, followed by incubation in Weigert's iron hematoxylin working solution for 10 minutes. After washing in running tap water, sections were placed in Biebrich Scarlet-Acid Fuchsin Solution for 5 minutes and rinsed in distilled water. Sections were differentiated with phosphotungstic/phosphomolybdic acid for 10 minutes and transferred directly into Aniline blue for 5 minutes for counterstaining. Sections were rinsed in distilled water before differentiating in 1% Acetic acid for 1 minute and performing a final rinse in distilled water. This stains collagen fibres in blue, nuclei in black and the cytoplasm in red. Five images were captured for each section and the area of cardiac fibrosis (excluding the perivascular area) was measured using Image J.

5.2.9 Immunofluorescence

For phospho-histone3 (pH3) staining and Troponin-T co-staining, the slides were pretreated with antigen retrieval buffer (refer to Appendix A for composition) at 110°C for 20 min in a Decloaker apparatus before gradually cooling to room temperature by addition of PBS. Following this, the slides were permeabilized in 0.3% Triton for 5 min before being washed with PBS and blocked with 10% goat serum at room temperature for 20 min. Sections were then incubated with anti-phosphohistone H3 (rabbit, Millipore) and anti-Troponin-T (mouse, Thermoscientific) primary antibodies (1:100 dilution with 2% goat serum in PBS) at 4°C overnight. After washing 3 times with PBS, the sections were incubated with Alexa Fluor 488-conjugated (goat anti-rabbit, Invitrogen) and Alexa Fluor 555-conjugated secondary antibodies (goat anti-mouse, Invitrogen) at RT for 1h. Hoechst (10µg/ml, Sigma) stain was used to visualize nuclei before slides were washed 3 times in PBS and mounted with Fluoromount G mounting medium (Southern Biotech).

5.2.10 Statistical analysis

Values are expressed as mean ± SEM, unless indicated otherwise. Comparisons between wild-type and ErbB4 conditional knockout animals were analysed by unpaired Student's t-test using Graphpad Prism 6. *P* values ≤ 0.05 were considered significant.

5.3 Result

5.3.1 Generation of $Cre^{+/-}ErbB4^{fl/fl}$ mice

To investigate the function of ErbB4 in adult mice heart, I adopted the αMHC-MerCreMer/loxP system, which allowed me to delete the ErbB4 receptor from cardiomyocytes in adult mice. Two original breeding lines of mice (homozygous αMHC-MerCreMer mice ($Cre^{+/+}$) and homozygous $ErbB4^{fl/fl}$) were used to generate $Cre^{+/-}/ErbB4^{fl/fl}$, and $Cre^{-/-}/ErbB4^{fl/fl}$ mice (section 5.2.1 and Figure 5.1). Following tamoxifen injection, the ErbB4 can be deleted from cardiomyocytes in $Cre^{+/-}/ErbB4^{fl/fl}$ animals since they contain both Cre and loxP flanked-ErbB4 genes, but not in the $Cre^{-/-}/ErbB4^{fl/fl}$ animals, which lack the Cre gene. Thus $Cre^{+/-}/ErbB4^{fl/fl}$ animals were used as the knockout group and $ErbB4^{fl/fl}$ animals were used as the control group. In total, 9 breeding pairs of $Cre^{+/-}/ErbB4^{fl/wt}$ and $ErbB4^{fl/fl}$ produced 75 offspring.

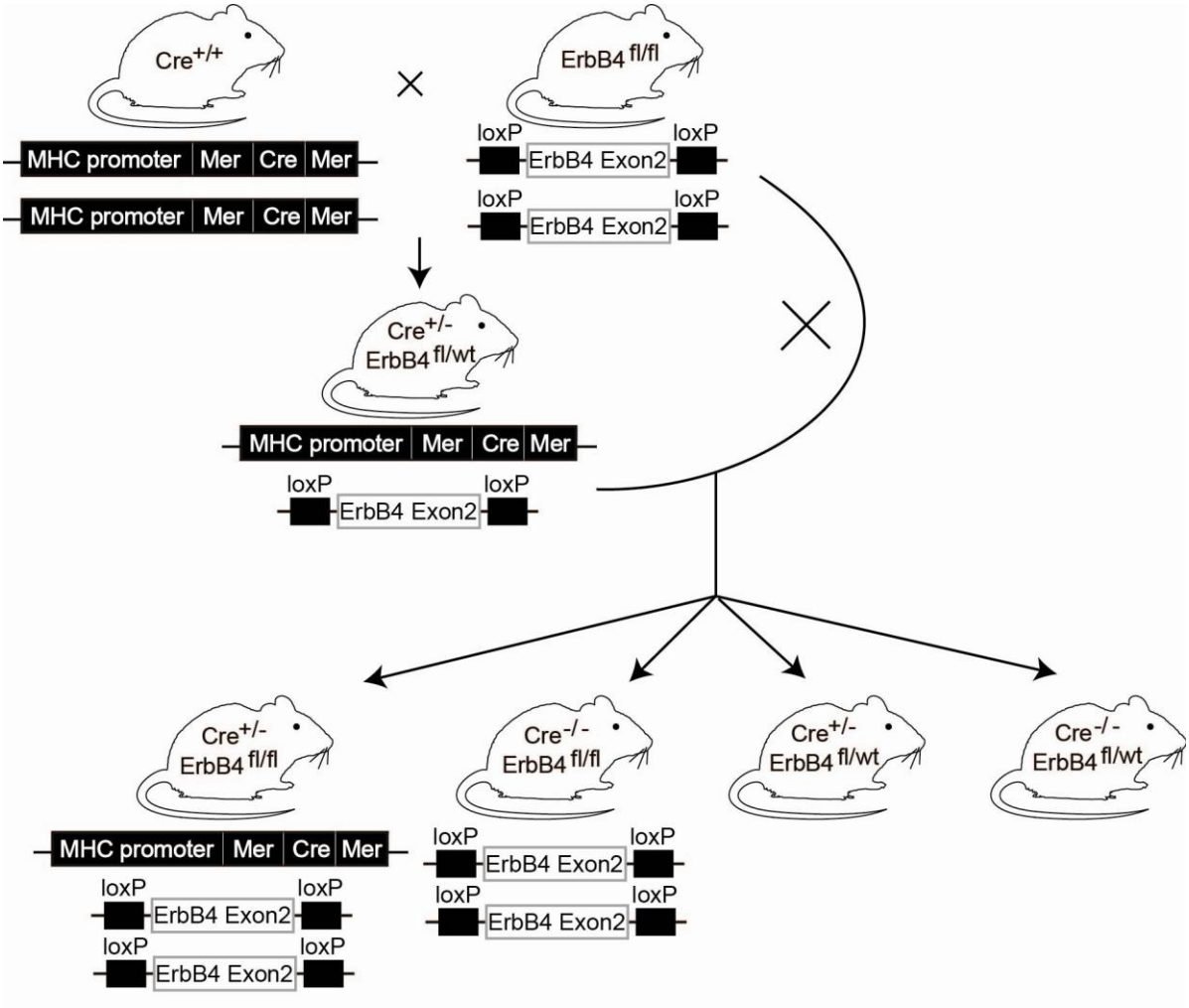

Figure 5.1 Breeding scheme for transgenic animal generation. The original homozygous ErbB4$^{fl/fl}$ breeders were bred with homozygous Cre$^{+/+}$ breeders to generate double heterozygous Cre$^{+/-}$/ErbB4$^{fl/wt}$ mice. These were then backcrossed with the ErbB4$^{fl/fl}$ mice to generate Cre$^{+/-}$/ErbB4$^{fl/fl}$ mice (conditional knockout group) and the Cre$^{-/-}$ErbB4$^{fl/fl}$ mice (control group).

5.3.2 Genotyping

All offspring were genotyped using separate PCR reactions for the Cre and Floxed ErbB4 transgenes. To detect the inserted Cre gene, PCR was used to amplify a 440 bp Cre gene fragment from whole DNA genome (Figure 5.2 A). A single band in 440bp in electrophoresis indicates the Cre positive genotype and otherwise indicates the Cre negative genotype (Figure 5.2 B). To differentiate the $ErbB4^{fl/fl}$ animals from the $ErbB4^{fl/wt}$ animals, PCR was used to amplify the wild type ErbB4 gene fragment and the mutated fragment (flanked by loxP site) with three primer sets in one reaction. One is a common sense primer annealing the 5' sequence in exon2 of ErbB4, and the others are two reverse primers annealing to the 3' sequence in exon2 and the sequence in the loxP site, separately (Figure 5.2 A). A single band in 400 bp in electrophoresis indicates the $ErbB4^{fl/fl}$ genotype, and two bands in a 350 bp and 400 bp, separately indicated the $ErbB4^{fl/wt}$ genotype (Figure 5.2 B) (Jackson-Fisher *et al*., 2006). Among the 75 offspring produced, 20 mice were the $Cre^{+/-}/ErbB4^{fl/fl}$ genotype and 20 mice were the $Cre^{-/-}ErbB4^{fl/fl}$.

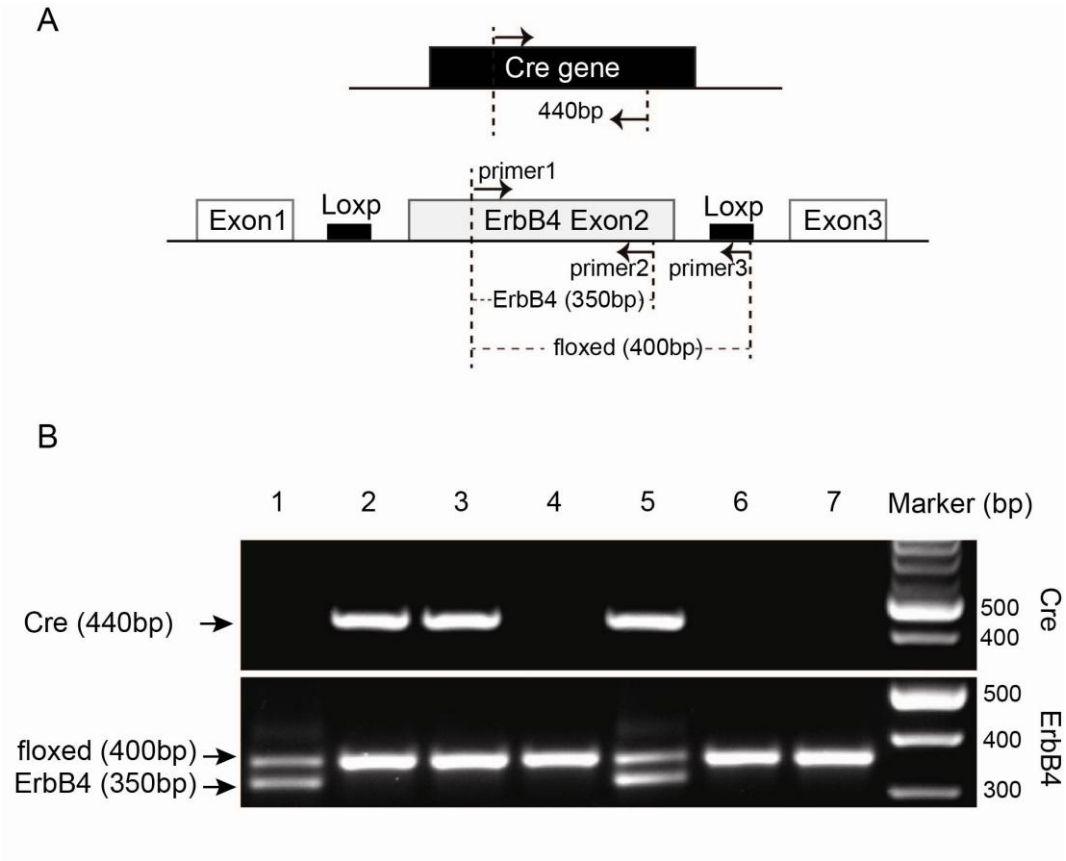

Figure 5.2 Genotyping of the Cre recombinase and floxed ErbB4 transgenes. A. The presence or absence of the Cre recombinase gene was determined by amplifying a 440 bp region of the Cre gene. In separate PCR reactions, we used a common sense primer binding within exon 2 of ErbB4, and two anti-sense primers which bound either the downstream region of exon2 or within the loxP site. This led to amplification of both the wild type (350 bp PCR product) and floxed ErbB4 (400 bp product) genes, respectively. Reaction products were separated by agarose gel electrophoresis (1.5% and 2% for Cre recombinase and ErbB4 respectively) B. Representative image of agarose gel electrophoresis for genotyping. Lane 1 represents the $Cre^{-/-}ErbB4^{fl/wt}$ genotype, lane 2 and 3 represent $Cre^{+/-}/ErbB4^{fl/fl}$, lane 4, 6, and 7 represent $Cre^{-/-}ErbB4^{fl/fl}$ and lane 5 represents the $Cre^{+/-}ErbB4^{fl/wt}$ genotype.

5.3.3 Optimization of tamoxifen administration

In this conditional knockout animal model, the deletion of ErbB4 is triggered by administration of tamoxifen. An insufficient dose of tamoxifen may cause failure of the deletion, but too high a dose of tamoxifen is toxic and may lead to the death of the mouse. Previous work in our lab used 3 different doses of tamoxifen: 20, 30 and 40 mg/kg/day for four days of consecutive ip injection. At the highest dose (40 mg/kg/day), tamoxifen induced an efficient deletion of ErbB4, but with a high mortality rate. The intermediate dose of tamoxifen (30 mg/kg/day) induced less deletion of ErbB4, and greatly reduced the mortality rate. The lowest dose of tamoxifen (20 mg/kg/day) failed to induce the deletion of ErbB4 (Schlegel *et al.*, unpublished data). To avoid the toxicity associated with high dose tamoxifen yet still achieve significant deletion of ErbB4, we tested the low dose of tamoxifen over an extended injection period (Hsieh *et al.*, 2007). We injected $Cre^{+/-}/ErbB4^{fl/fl}$ and $Cre^{-/-}/ErbB4^{fl/fl}$ animals with 20 mg/kg/day tamoxifen for 10 consecutive days**.** Animals were allowed 10 days recovery after the end of the tamoxifen treatment before being euthanased and tissues examined for ErbB4 expression by qPCR. This treatment regime had no obvious adverse effects on the health of the animals. The RT-qPCR revealed that the mRNA level of ErbB4 in heart was reduced by ~ 90% compared to the control, but the mRNA level of ErbB4 in skeletal muscle was not changed (Figure 5.3), thus confirming specific deletion of ErbB4 in the heart.

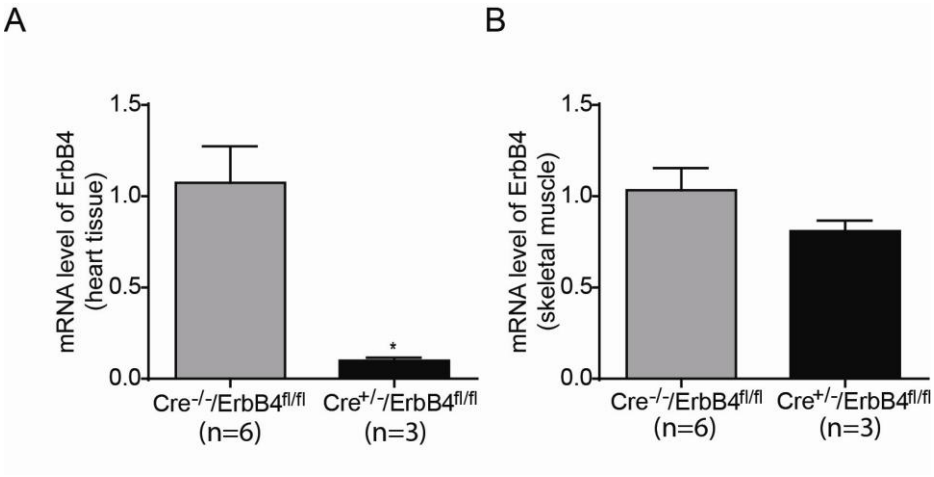

Figure 5.3 Heart-specific deletion of ErbB4 in knockout animals. Mice in both groups were injected with tamoxifen (20 mg/kg/d ip) for 10 days. After 10 days of recovery, animals were euthansed and RNA was extracted from heart (A) and skeletal muscle (B) tissue. The expression level of ErbB4 was determined using RT-qPCR, and normalized to 18S (endogenous control). Data was expressed relative to the $Cre^{-/-}ErbB4^{fl/fl}$ group. Data was analysed by unpaired Student's t-test and presented as mean ± SEM. * $P<0.05$ compared with $Cre^{-/-}ErbB4^{fl/fl}$ group; $Cre^{-/-}ErbB4^{fl/fl}$ group, n=6; $Cre^{+/-}ErbB4^{fl/fl}$ group, n=3.

5.3.4 Generation of the $Cre^{+/-}/ErbB4^{wt/wt}$ animals

In the study above, $Cre^{+/-}/ErbB4^{fl/fl}$ animals were used as the ErbB4 conditional knockout group (ErbB4-cKO) and $Cre^{-/-}/ErbB4^{fl/fl}$ animals as the control group. Because all animals received tamoxifen treatment, the effect of the drug itself potentially affecting the result can be excluded in this model. Another advantage of this model is that ErbB4-cKO and control animals can be generated from the same breeding and thus the cost for breeding was reduced and the workload for genotyping was minimized. Using these animals, we answered the question whether the ErbB4 can be deleted from the heart with tamoxifen injection and screened the optimal dose and treatment period of tamoxifen. However, the obvious possible confounder in this model is that the ErbB4-cKO group has increased Cre activity whereas the control group did not. Thus, enhanced Cre activity is another factor induced in the ErbB4-cKO group, besides the ErbB4 deletion. Accumulated studies have proposed that the Cre recombinase itself might be cardiotoxic (Koitabashi *et al.*, 2009; Hall *et al.*, 2011). Accordingly, whether any phenotype of the cardiac ErbB4 deleted mice ($Cre^{+/-}/ErbB4^{fl/fl}$) is due to the loss of ErbB4, or due to the induction of Cre activity might be hard to determine. To evaluate the effect of Cre recombinase activity, I compared cardiac parameters in Cre positive animals ($Cre^{+/-}/ErbB4^{wt/wt}$) and Cre negative animals ($Cre^{-/-}/ErbB4^{fl/fl}$) at 3-4 and 7-8 months after tamoxifen injection. The generation of the $Cre^{+/-}/ErbB4^{wt/wt}$ animals was described in 5.2.1. There are four potential genotypes in the offspring (Figure 5.4). To distinguish between offspring that were homozygous or heterozygous for Cre recombinase, we used qPCR to determine the Cre recombinase copy number. Two pairs of primers, pair Cre1 (pcre1) and pair Cre2 (pcre2) (refer to Appendix B for sequence), were designed to amplify two different region of Cre gene (Figure 5.5 A). Animals of a known genotype were used to show that we could successfully identify animals with any pair of primers that were heterozygous, homozygous or lacking the Cre gene (Figure 5.5 B). This method was then applied to detect the copy number of Cre in animals with unknown genotype (Figure 5.5 C). Among 107 offspring generated, 22 mice were $Cre^{+/-}ErbB4^{wt/wt}$ animals.

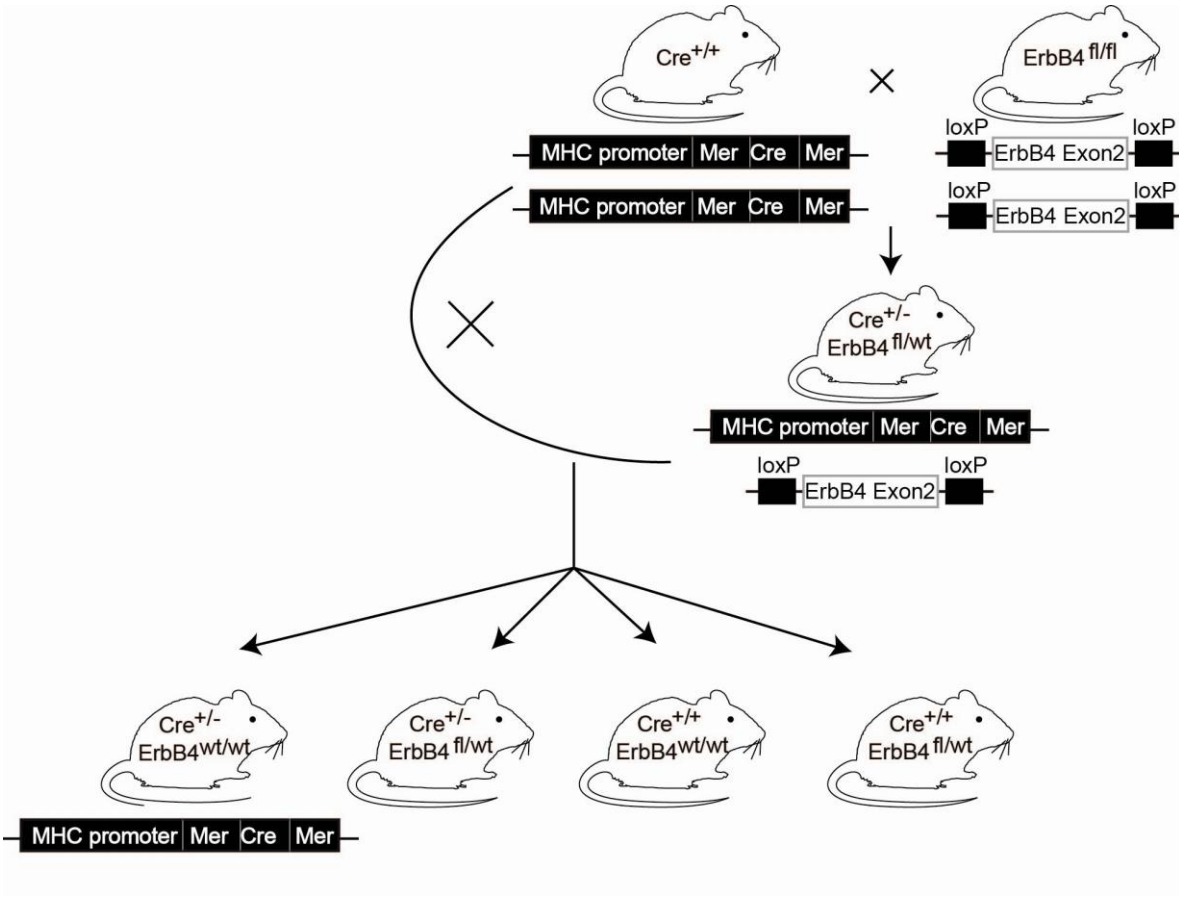

Figure 5.4 Breeding scheme for control animal generation. Homozygous ErbB4$^{fl/fl}$ mice were bred with homozygous Cre$^{+/+}$ mice to generate double heterozygous Cre$^{+/-}$/ErbB4$^{fl/wt}$ mice. These were then backcrossed with the Cre$^{+/+}$ mice to generate Cre$^{+/-}$/ErbB4$^{wt/wt}$ mice.

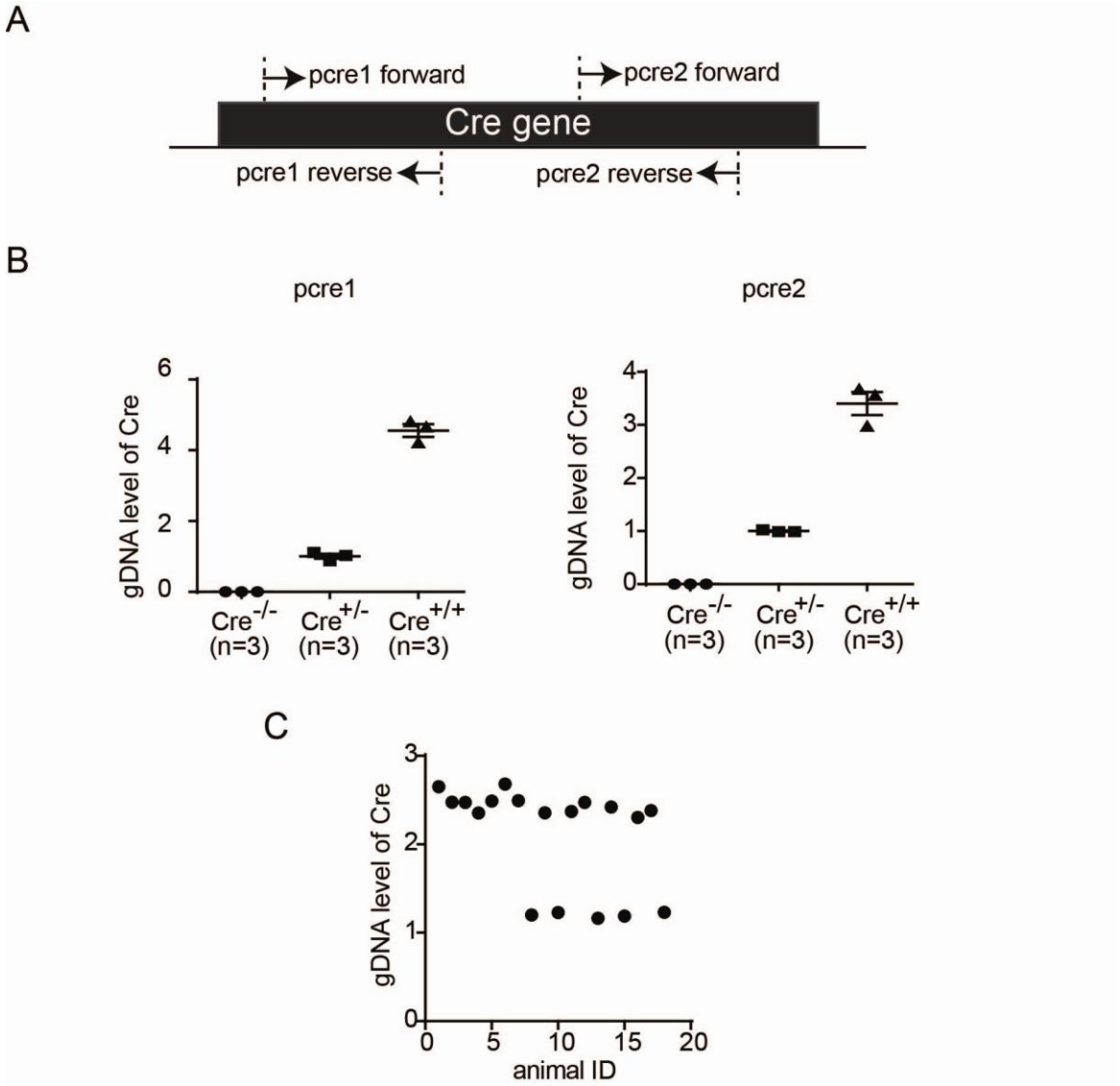

Figure 5.5 Cre copy number detected with qPCR. A. Two pairs of primers (termed as pcre1 and pcre2, refer to the Appendix B for the primer sequence) were designed to amplify the different regions of the Cre gene. B. Homozygous, heterozygous and wild type Cre animals can be differentiated by qPCR with both pairs of primers (validation using animals of known genotype). C. Representative graph for detection of Cre copy number in animals with unknown genotypes.

5.3.5 Determining the effects of Cre recombinase on the heart

To detect whether Cre activity itself induces a cardiac phenotype in adult mice without deletion of the floxed gene, we examined cardiac functional parameters on $Cre^{+/-}/ErbB4^{wt/wt}$ (Cre positive) and $Cre^{-/-}/ErbB4^{fl/fl}$ (Cre negative) animals at 3-4 or 7-8 months after the tamoxifen treatment. Echocardiography revealed that the left ventricular internal dimensions diastole (LVIDd) and systole (LVIDs) and fractional shortening (FS) (calculated as (LVIDd-LVIDs/LVIDd) was not significantly different between the two groups at 3-4 months post-tamoxifen, suggesting that the contractile ability of the heart was not affected by the induction of Cre (Figure 5.6 A and B). Similarly, the left ventricular wall thickness (reflected by the intraventricular septal wall thickness (IVS) and left ventricle posterior wall thickness (LVPW)) was not changed at 3-4 months post-tamoxifen (Figure 5.6 C). There was a modest decrease in fractional shortening in Cre positive animals at 7-8 months after tamoxifen injection, but this was not statistically significant (Figure 5.7 A). However, at 7-8 months post-tamoxifen both the IVS (systolic) and LVPW (both systolic and diastolic) were significantly decreased in Cre positive animals (Figure 5.7 B and C). This data suggests that that even short-term increases in Cre activity can have long-term effects on cardiac structure. This result was confirmed by the data from post-mortem studies, which showed that the heart weight:tibia length ratio of the Cre positive animals was significantly decreased at both 3-4 and 7-8 months post-tamoxifen (Figures 5.8 and 5.9). This was specific to the heart, as kidney weight was not changed during this period. This indicates that the cardiac-specific induction of Cre activity might cause the loss of cardiac mass. Then we investigated the expression of hypertrophic (α-MHC,β-MHC and BNP) and fibrosis genes (COL1A1 and PAI-1) in Cre positive and negative animals. RT-qPCR revealed that the hypertrophic genes and fibrosis genes are expressed at similar levels in both groups (Figure 5.10 A and B). In addition, expression of the ErbB receptors (ErbB1 and ErbB4) was also not affected by Cre activity (Figure 5.11). Together, these data indicate that induction of Cre activity can have a long term effect on the heart, although the mechanism of this is not clear. However, this does suggest that the $Cre^{-/-}/ErbB4^{fl/fl}$ genotype is not an appropriate control for our study. To circumvent the negative effect of Cre activity on cardiac tissues, I used the Cre-only transgenic mice ($Cre^{+/-}/ErbB4^{wt/wt}$) as the control in our following study examining the effects of cardiac ErbB4 deletion (Molkentin *et al.*, 2009). Both $Cre^{+/-}/ErbB4^{fl/fl}$ (ErbB4 conditional knockout group, ErbB4-cKO) and $Cre^{+/-}/ErbB4^{wt/wt}$ (control group) animals received tamoxifen treatment. Around 3-4 months or 7-8 months later, the cardiac phenotype of ErbB4 deletion was determined.

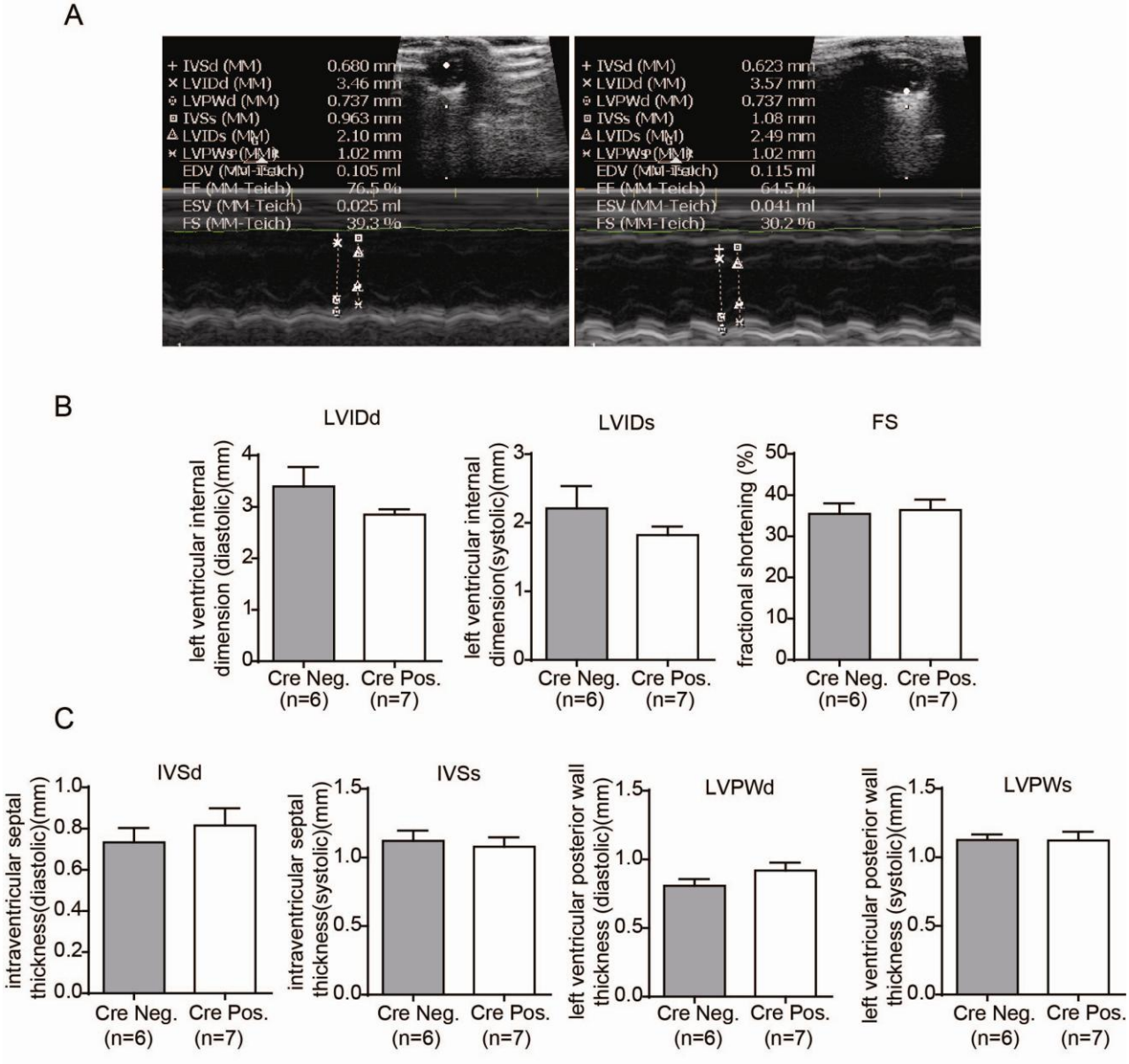

Figure 5.6 Effect of Cre recombinase induction on cardiac function at 3-4 months post-tamoxifen. A. Example of a typical echocardiogram in 2D (top) and M-mode (bottom) obtained in short axis view for the Cre negative ($Cre^{-/-}$/$ErbB4^{fl/fl}$, left) and Cre positive ($Cre^{+/-}$/$ErbB4^{wt/wt}$, right) animals. B. Left ventricular internal dimensions during diastole (left) and systole (middle) and fractional shortening (right) in Cre negative (Cre Neg.) and Cre positive (Cre Pos.) animals. C. Intraventricular septal wall thickness of diastolic (IVSd) and systolic (IVSs) dimension and left ventricle posterior wall thickness of diastolic (LVPWd) and systolic (IVPWs) dimension in Cre negative and Cre positive animals. Data was analysed by unpaired Student's t-test and presented as mean ± SEM.

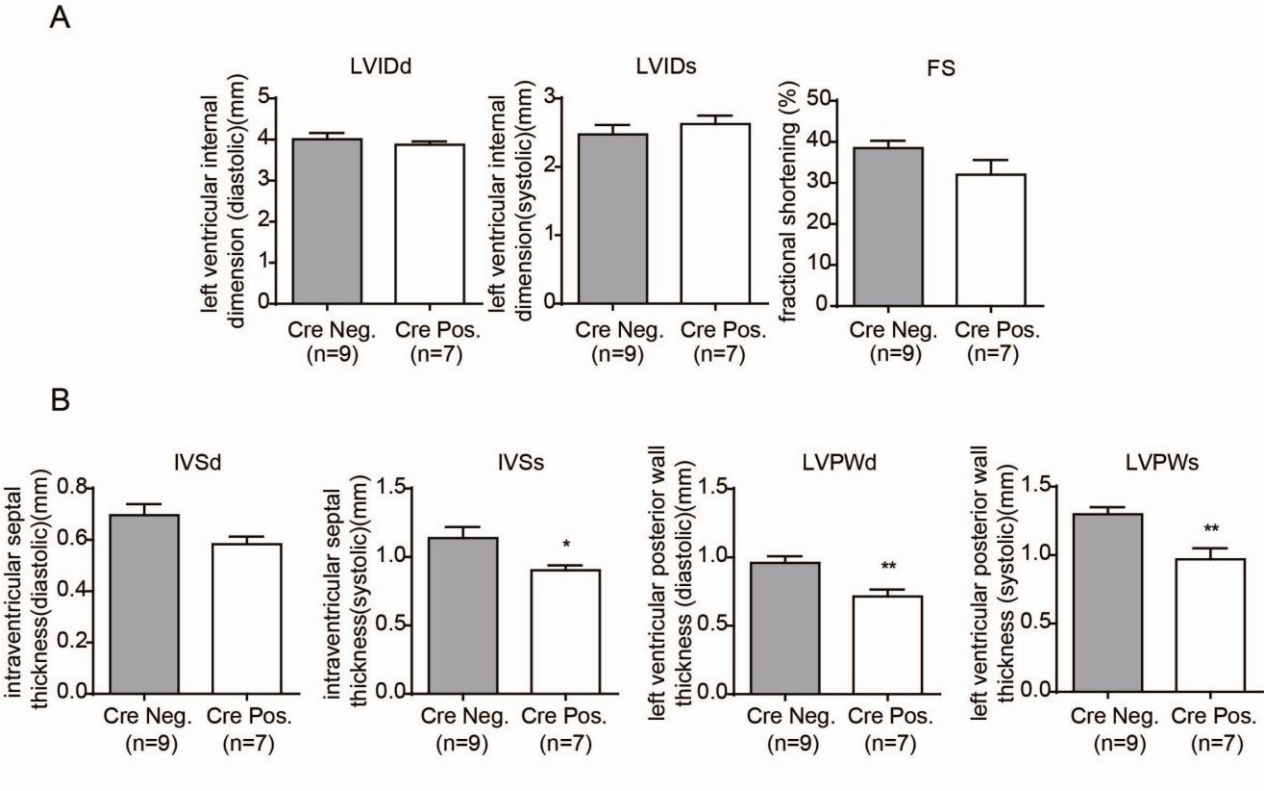

Figure 5.7 Effect of Cre recombinase induction on cardiac function at 7-8 months post-tamoxifen. A. Left ventricular dimensions during diastole (left) and systole (middle) and fractional shortening (right) in Cre negative ($Cre^{-/-}/ErbB4^{fl/fl}$, Cre Neg.) and Cre positive ($Cre^{+/-}/ErbB4^{wt/wt}$, Cre Pos.) animals. B. Intraventricular septal wall thickness of diastolic (IVSd) and systolic (IVSs) dimension and left ventricle posterior wall thickness of diastolic (LVPWd) and systolic (LVPWs) dimension in Cre negative and Cre positive animals. Data was analysed by unpaired Student's t-test and presented as mean ± SEM. * $P<0.05$ compared with Cre Neg.; ** $P<0.01$ compared with Cre Neg.; Cre Neg., n=9; Cre Pos., n=7.

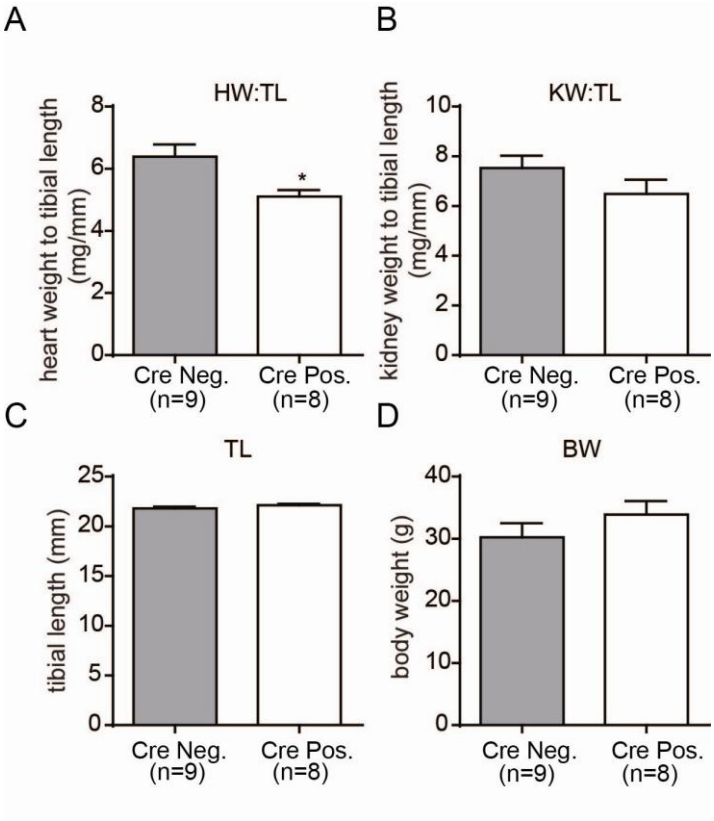

Figure 5.8 Effect of Cre recombinase induction on heart weight at 3-4 months post-tamoxifen. The heart weight normalized to tibial length (HW:TL) (A), kidney weight to tibial length (KW:TL) (B), the tibial length (TL) (C) and body weight (BW) (D) was measured in Cre positive and Cre negative animals at 3-4 months after induction of Cre activity. Data was analysed using unpaired Student's t-test and presented as mean ± SEM. * $P<0.05$ compared with Cre Neg.; Cre Neg., n=9; Cre Pos., n=8.

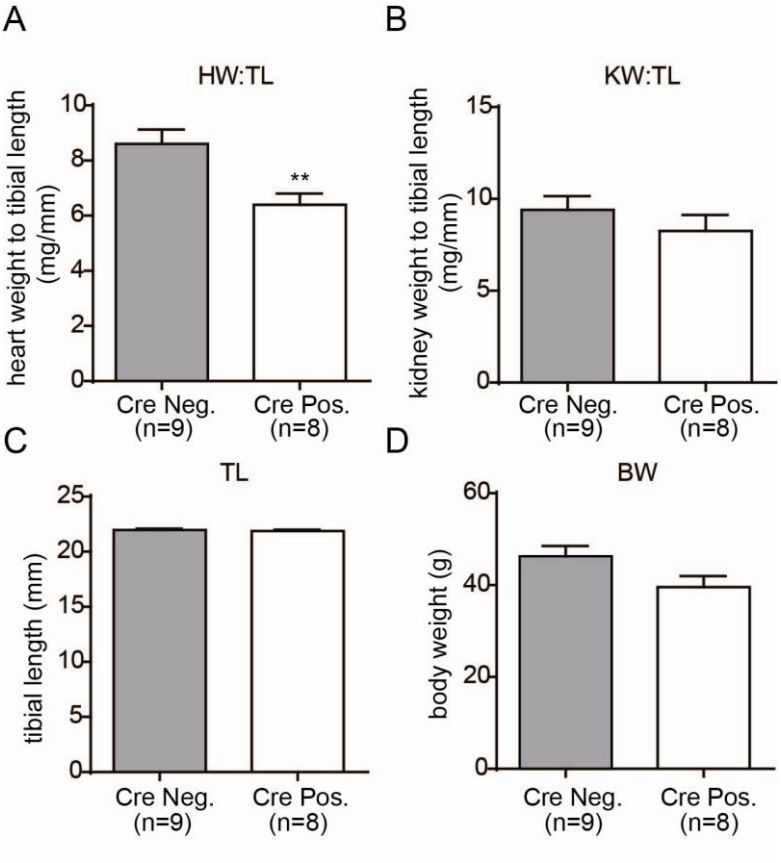

Figure 5.9 Effect of Cre recombinase induction on heart weight at 7-8 months post-tamoxifen. The heart weight (normalized to tibial length) (A), kidney weight to tibial length (B), the tibial length (C) and body weight (D) was measured in Cre positive and Cre negative animals at 7 months after induction of Cre activity. Data was analysed using unpaired Student's t-test and presented as mean ± SEM. ** $P<0.01$ compared with Cre Neg.; Cre Neg., n=9; Cre Pos., n=8.

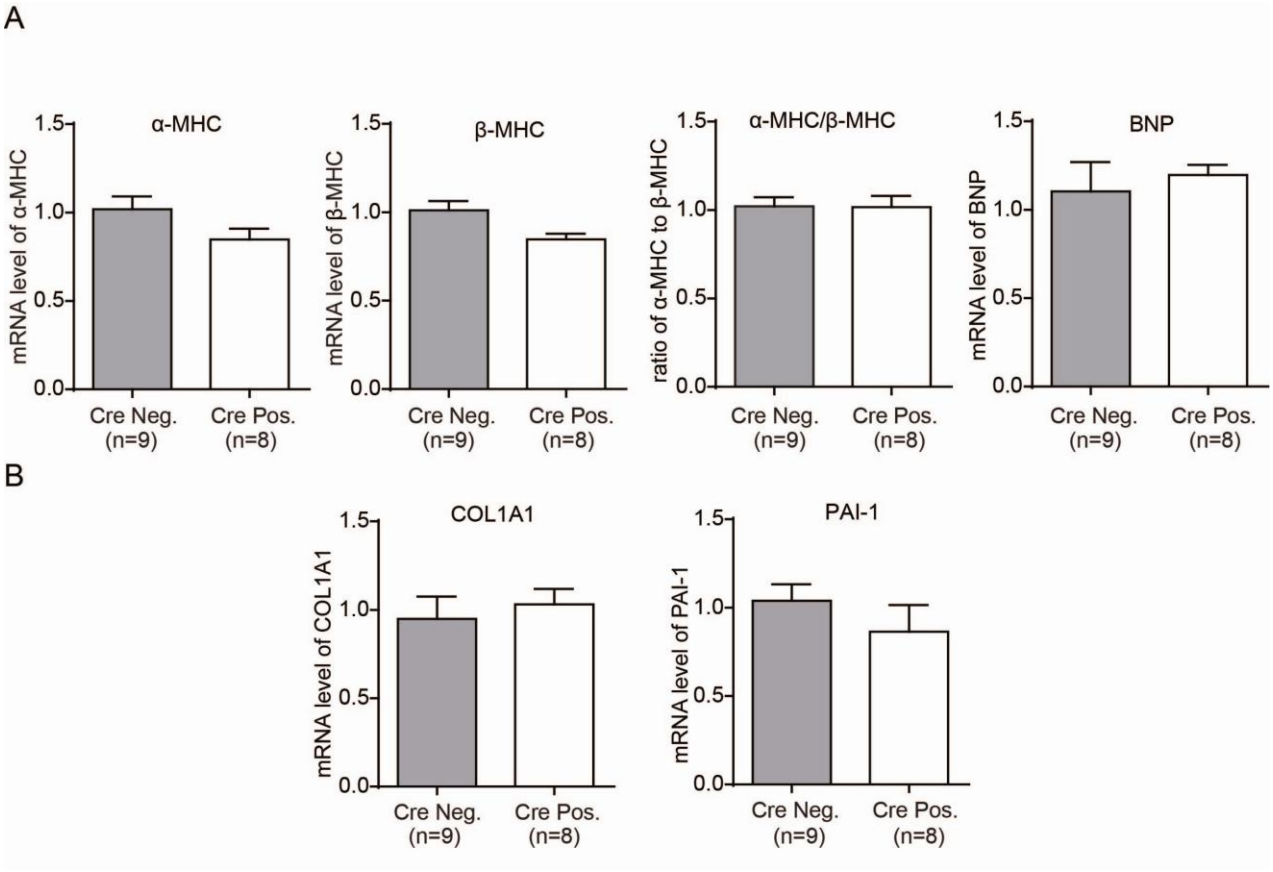

Figure 5.10 The regulation of hypertrophic genes and fibrosis genes at 8 months following Cre induction. Expression of the hypertrophic genes BNP, α-MHC, β-MHC and fibrosis genes COL1A1 and PAI-1 were detected by RT-qPCR, normalized to 18S (endogenous control) and expressed relative to the Cre negative group. Data was analysed using unpaired Student's t-test and presented as mean ± SEM. Cre Neg., n=9; Cre Pos., n=8.

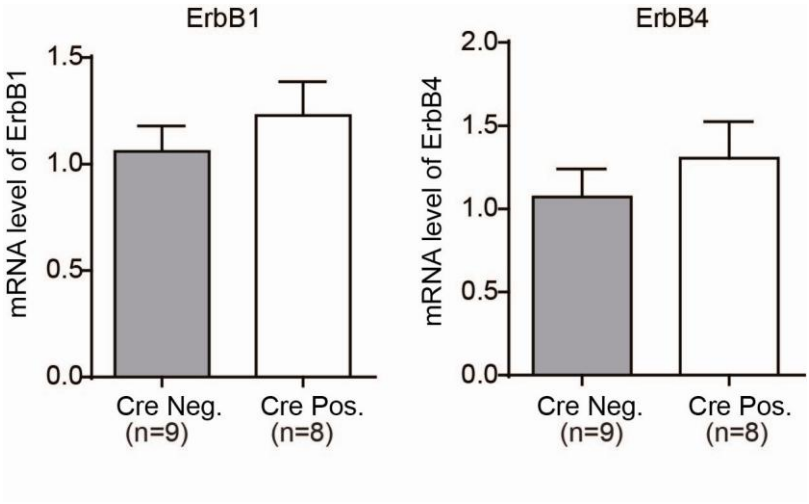

Figure 5.11 The expression of ErbBs was not affected by the induction of Cre activity. Expression of ErbB1 and ErbB4 was detected with RT-qPCR, normalized to18S (endogenous control) and expressed relative to the Cre negative group. Data was analysed using unpaired Student's t-test and presented as mean ± SEM. Cre Neg., n=9; Cre Pos., n=8.

5.3.6 Effect of cardiac-specific deletion of ErbB4 on cardiac function

As shown in Figure 5.3, tamoxifen treatment of ErbB4-cKO ($Cre^{+/-}ErbB4^{fl/fl}$) mice deleted approximate 90% of cardiac ErbB4 at 10 days after the tamoxifen treatment (measured by RT-qPCR). At 3-4 months after the tamoxifen injection, we performed echocardiography on the mice to examine their cardiac function. Key echocardiography parameters were measured in both systolic and diastolic phase, including left ventricular internal dimension (LVID), intraventricular septum thickness (IVS) and left ventricle posterior wall thickness (LVPW). Statistical analysis revealed a marked increase in the diastolic LVID, suggesting the ErbB4-cKO animals might undergo heart enlargement. No significant difference in systolic LVID was observed between the ErbB4-cKO and control ($Cre^{-/-}ErbB4^{fl/fl}$) animals (Figure 5.12 A). In addition, there was no significant change in the fractional shortening in ErbB4-cKO animals, indicating that the contractile ability of the heart was not affected after 3-4 months of ErbB4 deletion. The systolic IVS in ErbB4-cKO animals was significantly increased and the diastolic IVS tended to increase, but was not statistically significant (Figure 5.12 B).

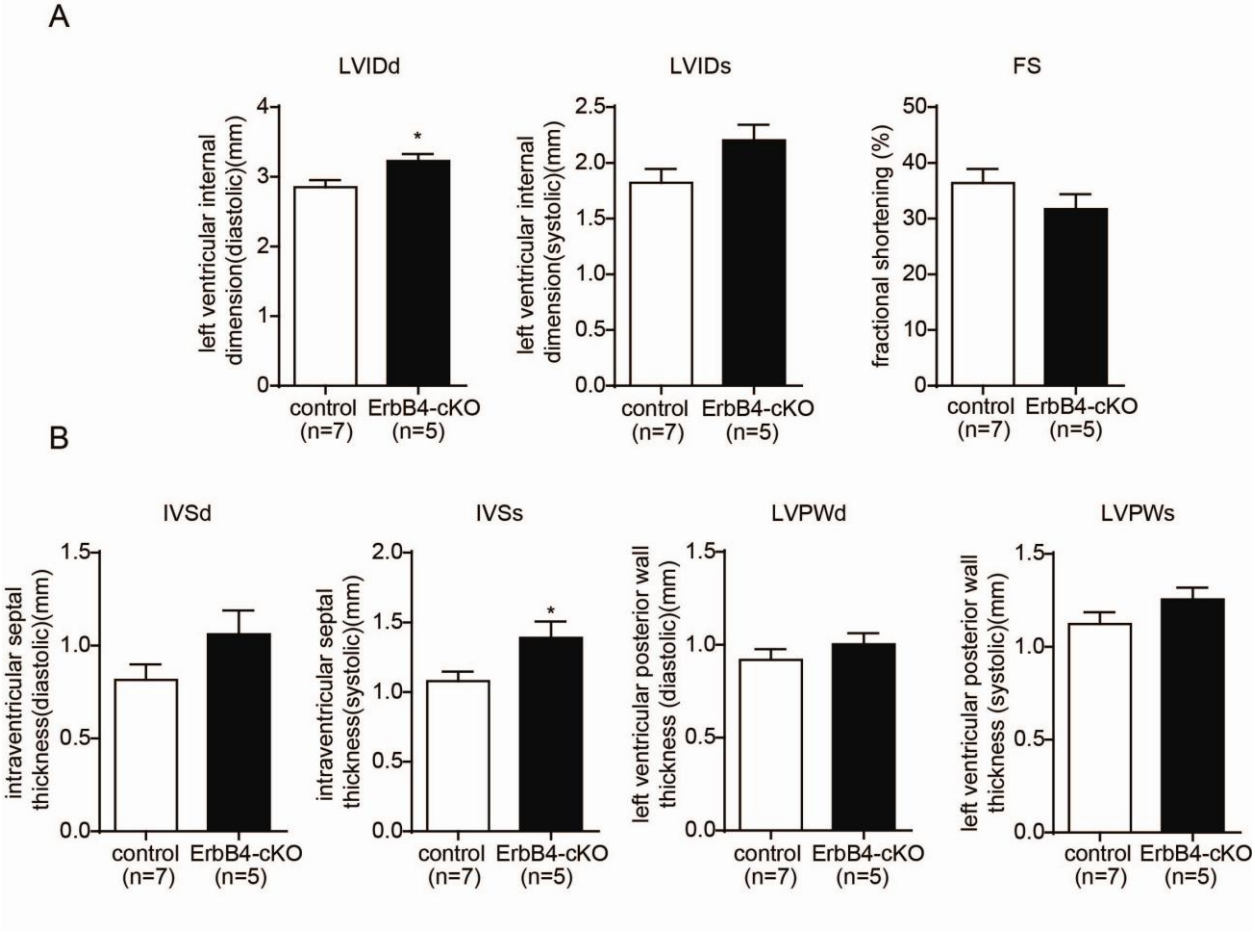

Figure 5.12 Echocardiographic assessment of cardiac function at 3-4 months after ErbB4 deletion. A. The diastolic (left) and systolic (middle) left ventricular internal dimension and fractional shortening (right) were measured in ErbB4-cKO and control animals. B. The diastolic and systolic IVS and left ventricle posterior wall thickness in diastolic and systolic dimension were measured in ErbB4-cKO (n=5) and control animals (n=7). Data was analysed using unpaired Student's t-test and presented as mean ± SEM. * $P<0.05$ compared with control; control, n=7; ErbB4-cKO, n=5.

5.3.7 Effect of cardiac-specific deletion of ErbB4 on heart weight

After the echocardiography measurement, both ErbB4-cKO animals and control animals were euthanased and the heart weight:tibia length ratio was determined. The ratio of heart weight to tibia length in ErbB4-cKO animals was significantly increased compared to the controls (Figure 5.13 A). In contrast, the kidney weight:tibia length was not changed (Figure 5.13 A). This suggested that the knockout of ErbB4 in cardiomyocytes leads to cardiac hypertrophy. RT-qPCR was used to examine whether this increase in heart weight was associated with altered expression of pathological hypertrophy marker genes. We found that the mRNA levels of α-MHC, β-MHC and BNP in ErbB4-cKO animals were not changed relative to the controls (Figure 5.13 B). Together, this suggested that the ErbB4-cKO animals undergo physiological, not pathological, hypertrophy.

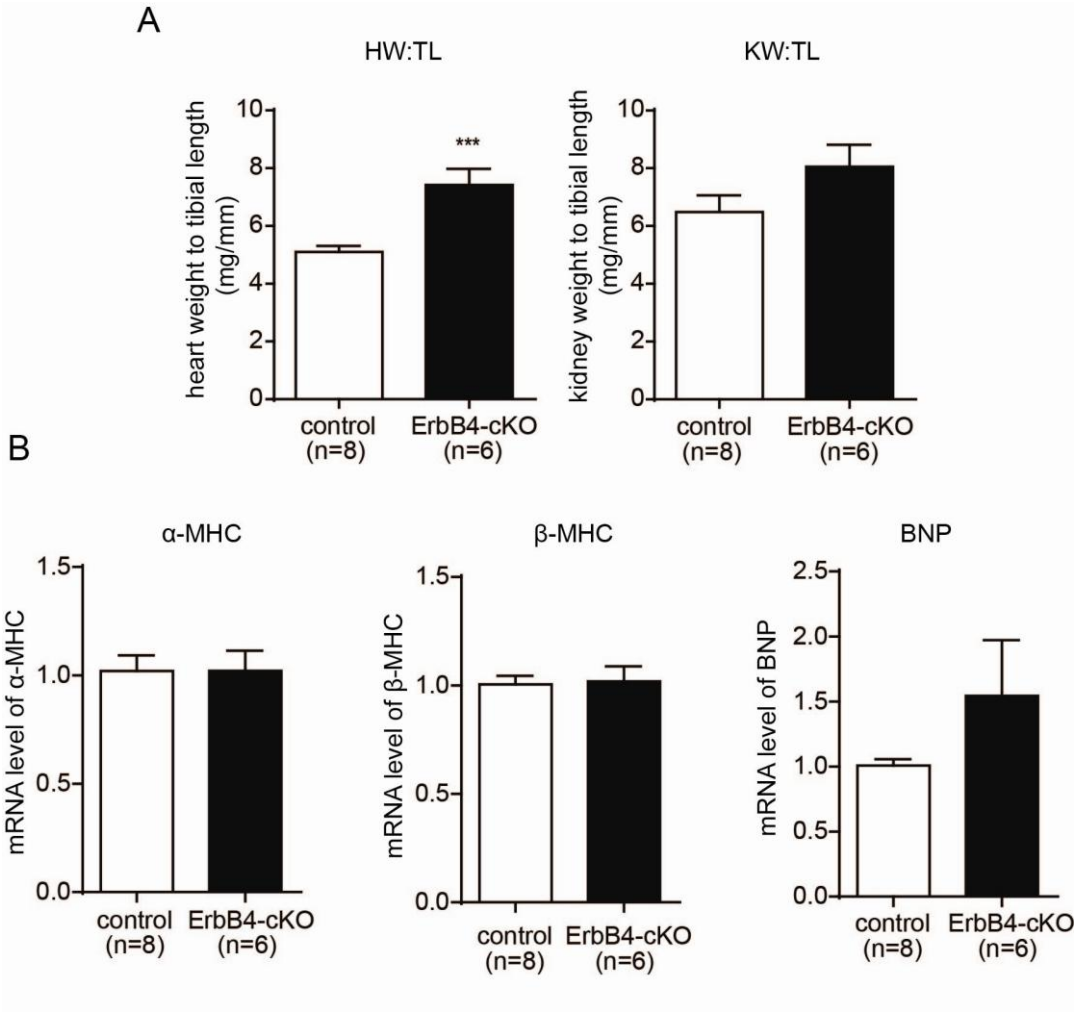

Figure 5.13 Effect of ErbB4 deletion on heart weight. A. Heart (left) and kidney (right) weight was measured and normalized to tibia length in control (n=8) and ErbB4-cKO (n=6) animals. B. The expression of BNP, α-MHC, β-MHC as detected by qPCR were normalized to the 18S (endogenous control) and expressed relative to the control group. Data was analysed using unpaired Student's t-test and presented as mean ± SEM. *** $P<0.001$ compared with control; control, n=8; ErbB4-cKO, n=6.

Following the study above, we investigated the mechanisms underlying the cardiac hypertrophy observed in ErbB4-cKO animals. We first investigated whether the cardiomyocytes undergo hypertrophy, which is defined as an increase in cell mass without proliferation. As we have not established a system in our lab to accurately determine the mass of individual cardiomyocytes, we used the measurement of cross sectional area to reflect cardiomyocyte hypertrophy. Statistical analysis showed that there was no significant change in the cross sectional area of cardiomyocytes in the ErbB4-cKO group compared to the control (Figure 5.14 A and B). To further confirm this result, the frequency distribution of cardiomyocyte area was analysed for both ErbB4-cKO and control groups. If cardiomyocytes undergo hypertrophic growth, the frequency of cardiomyocytes with a larger cell area will increase, thus shifting the frequency distribution curve to the right and increasing the area range in the X axis. However, our data showed no shift, and the frequency distribution curves for ErbB4-cKO and control groups were similar (Figure 5.14 C). Together, these studies suggested that the cardiac hypertrophy caused by cardiac ErbB4 deletion *in vivo* is not via hypertrophic growth of the cardiomyocytes, but occurs by some other mechanism.

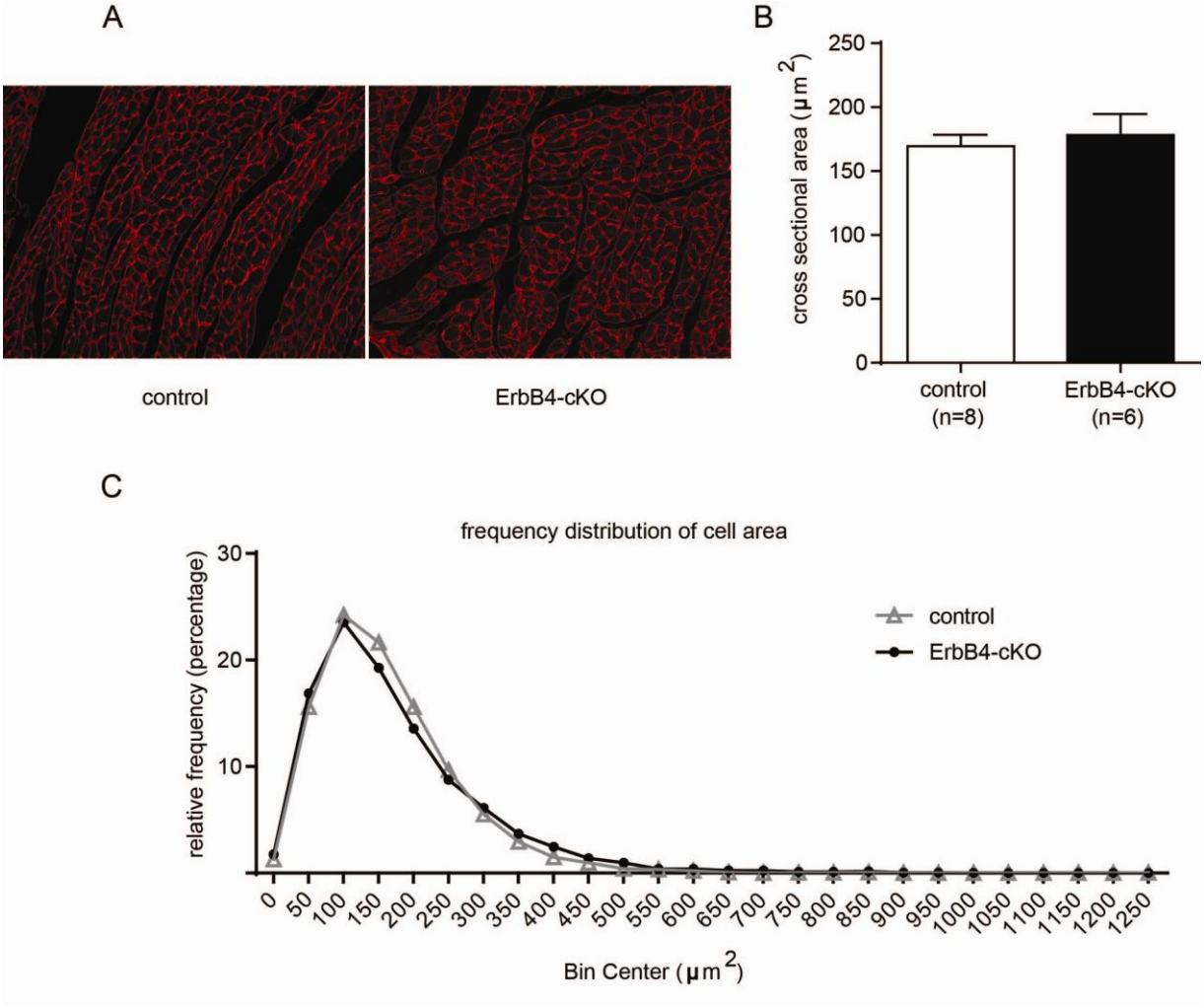

Figure 5.14 Effect of ErbB4 deletion on cardiomyocyte cross sectional area. A. Representative images of WGA stained sections of hearts from control (top) and ErbB4-cKO (bottom) animals (200×). B. The grouped data for cardiomyocyte cross sectional area. Data was analysed using unpaired Student's t-test and presented as mean ± SEM; control, n=8; knockout, n=6. C. The frequency distribution of cardiomyocyte cross sectional area for control and ErbB4-cKO animals. Bin width is set as 50 μm^2.

5.3.8 Effect of cardiac-specific deletion of ErbB4 on cardiac fibrosis.

Fibroblasts are the second major component of heart tissue besides cardiomyocytes (Brown *et al.*, 2005). Cardiac fibrosis (where lost cardiomyocytes are replaced by proliferating fibroblasts and the secreted collagen) can be observed in the late stages of pathological cardiac hypertrophy (Manabe *et al.*, 2002). Cardiac fibrosis can be measured by histological staining for collagen or by qPCR for the expression of fibrosis molecular marker genes such as alpha-1 type I collagen (COL1A1), alpha-1 type III collagen (COL3A1) and plasminogen activator inhibitor type 1 (PAI-1). In our study, RT-qPCR revealed that the mRNA levels of COL1A1, COL3A1 and PAI-1 didn't change in the ErbB4-cKO animals compared to the controls (Figure 5.15 A). To further confirm these results, we examined collagen deposition in heart sections using Masson's Trichrome. Masson's Trichrome stains the collagen in blue, the cytoplasm in red and the nucleus in black. The normal heart should have little collagen accumulated around cardiomyocytes, but some should be present in the perivascular area. Here, we observed blue collagen staining around the vascular area in heart sections from both the ErbB4-cKO and control animals. However, the myocardial area of both groups showed minimal collagen staining (Figure 5.15 B), suggesting that knockout of ErbB4 did not lead to cardiac fibrosis

.

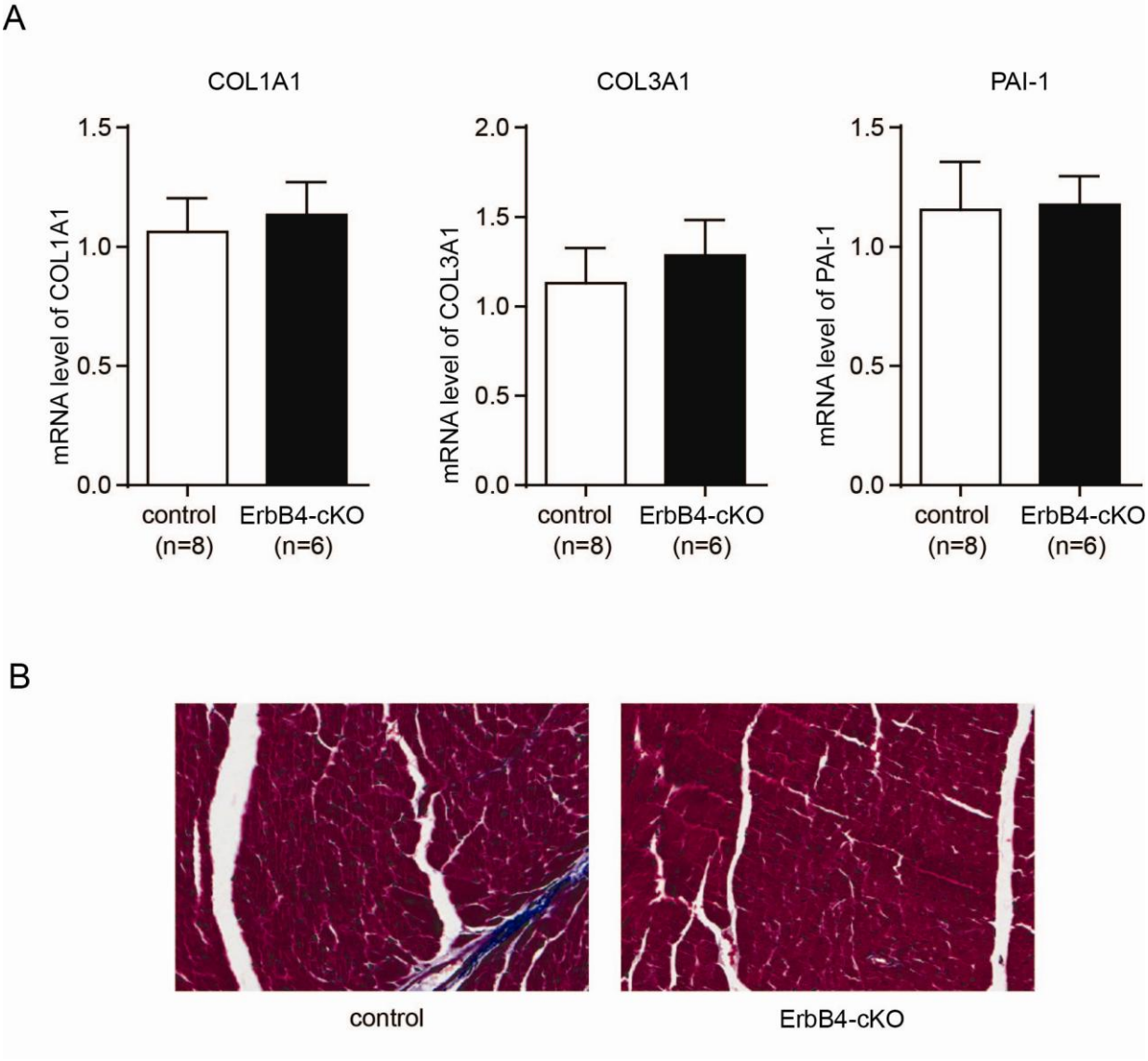

Figure 5.15 Effect of ErbB4 deletion on cardiac fibrosis. A. The expression levels of the fibrosis marker genes, COL1A1, COL3A1, and PAI-1 were detected by RT-qPCR and normalized to 18S. Data was expressed relative to the control group. Data was analysed using unpaired Student's t-test and presented as mean ± SEM; control, n=8; ErbB4-cKO, n=6. B. Representative sections of Masson's Trichrome staining on heart tissues from control (left) and ErbB4-cKO animals (right).

5.3.9 Expression of the ErbB receptor family following ErbB4 deletion

Only a mild phenotype was observed in the ErbB4-cKO animals, which were characterized by physiological cardiac hypertrophy. No severe cardiac dysfunction or other structural abnormalities were found. This result was surprising because accumulated evidence in literature indicates that ErbB4 is critical for cardiac function and structural maintenance (Gassmann *et al.*, 1995; Tidcombe *et al.*, 2003; Garcia-Rivello *et al.*, 2005). Thus in the following study, we investigated whether the deletion of ErbB4 was compensated for by other ErbB receptor systems. There are four subtypes of ErbB receptor (ErbB1, ErbB2, ErbB3, and ErbB4) detectable in the heart. We examined whether the deletion of ErbB4 may trigger a compensatory up-regulation of other ErbB receptors. At 3-4 months after ErbB4 deletion, there was a small increase in ErbB3 mRNA levels and a small decrease in both ErbB1 and ErbB2, however these effects did not reach statistical significance (Figure 5.16). Together, this suggests that the other members of the ErbB family were not significantly up-regulated to compensate for the deletion of the ErbB4.

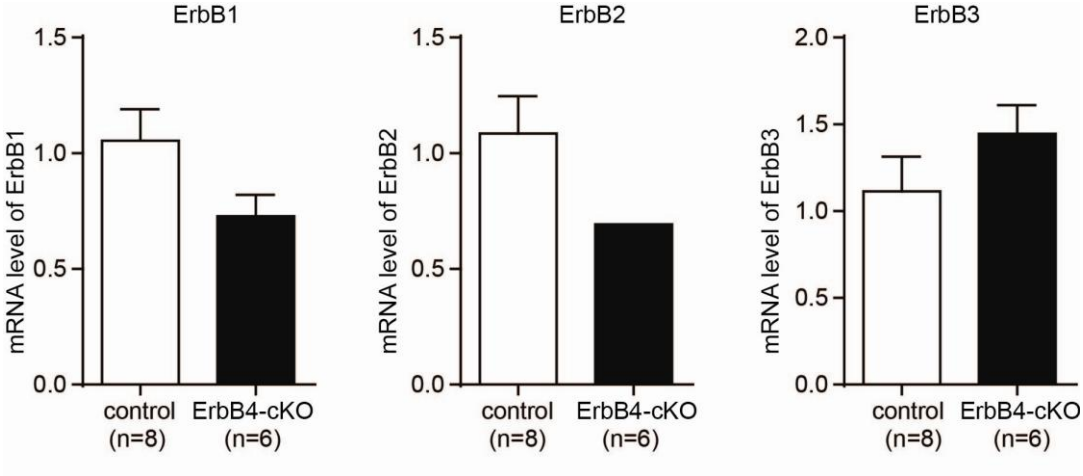

Figure 5.16 Expression of ErbB1, ErbB2 and ErbB3 following ErbB4 deletion. The expression level of ErbB1, ErbB2 and ErbB3 was detected by RT-qPCR and normalized to the 18S. Data was expressed relative to the control group. Data was analysed using unpaired Student's t-test and presented as mean ± SEM; control, n=8; ErbB4-cKO, n=6.

5.3.10 Expression of the EGF family following ErbB4 deletion.

Although expression of other ErbB receptors does not change after ErbB4 deletion, the activity of ErbBs can also be influenced by up-regulation of endogenous agonists, and this may serve as compensation for the lost ErbB4. There are multiple agonists (EGF-like factors) for each ErbB receptor, and thus we investigated whether the expression of these agonists was altered by cardiac ErbB4 deletion. We first studied the ErbB4 selective agonists, the NRG family (NRG1, NRG2, NRG3 and NRG4). NRG1 has two isoforms, NRG1α and NRG1β that are generated by alternative splicing. Using RT-qPCR, the expression of both NRG1α and NRG1β is dramatically up-regulated in ErbB4-cKO animals compared to controls (Figure 5.17 A). In contrast, the expression of NRG2, NRG3 and NRG4 (Figure 5.17 B) didn't change, suggesting that the up-regulation of NRG1 is a specific response to the lost ErbB4. We also examined the regulation of the endogenous agonists for other ErbB receptors. TGFα and amphiregulin (AREG) are selective agonists for ErbB1. HB-EGF, epiregulin (EREG) and betacellulin (BTC) are agonists for both ErbB1 and ErbB4. ErbB2 has no identified ligands. However, none of these factors were regulated at the mRNA level in ErbB4-cKO animals (Figure 5.18). Together, this suggests that NRG1 is the only member of the EGF family that is specifically up-regulated after deletion of ErbB4. NRG1 is a cardioprotective factor (see section 1.6.3) thus the up-regulation of NRG1 might serve as compensatory mechanism to for the deletion of ErbB4, and may explain why we did not see any cardiac dysfunction at 3-4 months after ErbB4 deletion.

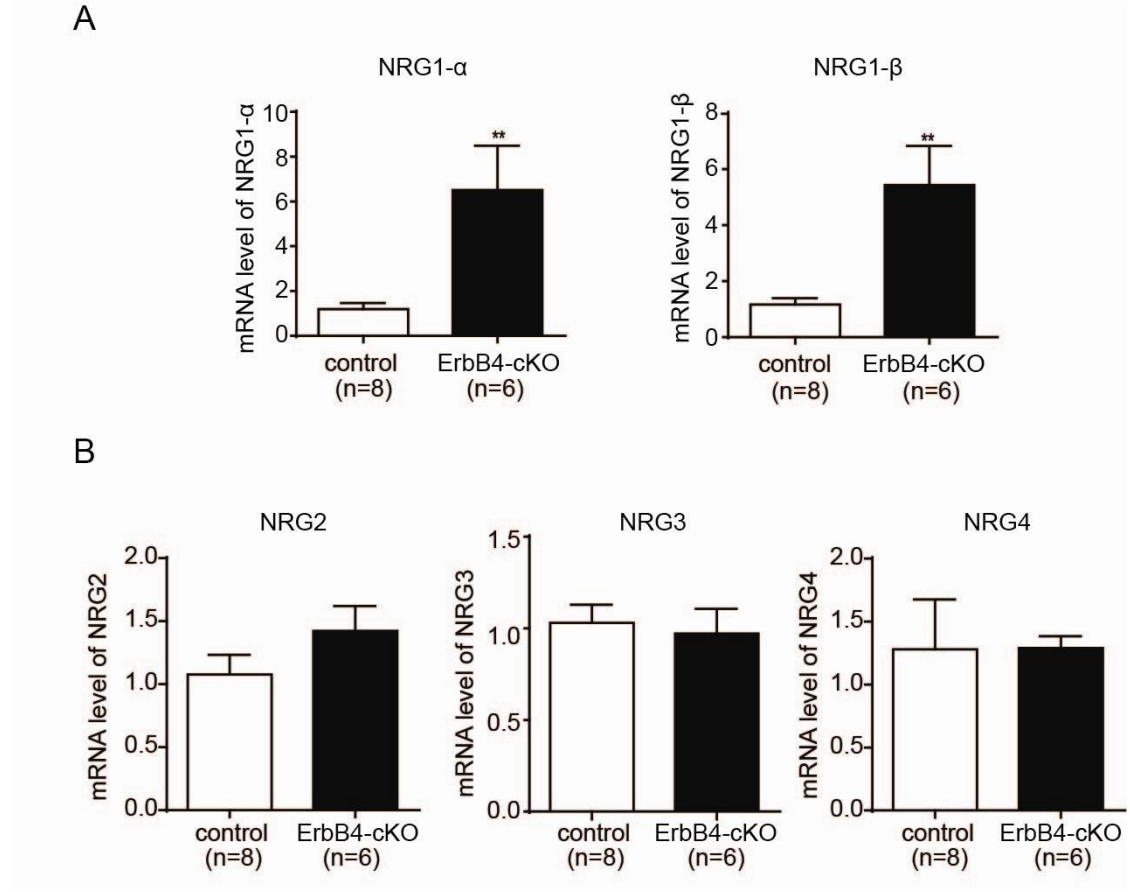

Figure 5.17 Expression of NRG family following ErbB4 deletion. The expression levels of NRG1α, NRG1β, NRG2, NRG3 and NRG4 was detected by RT-qPCR and normalized to 18S. Data was expressed relative to the control group. Data was analysed using unpaired Student's t-test and presented as mean ± SEM. ** $P<0.01$ compared with control; control, n=8; ErbB4-cKO, n=6.

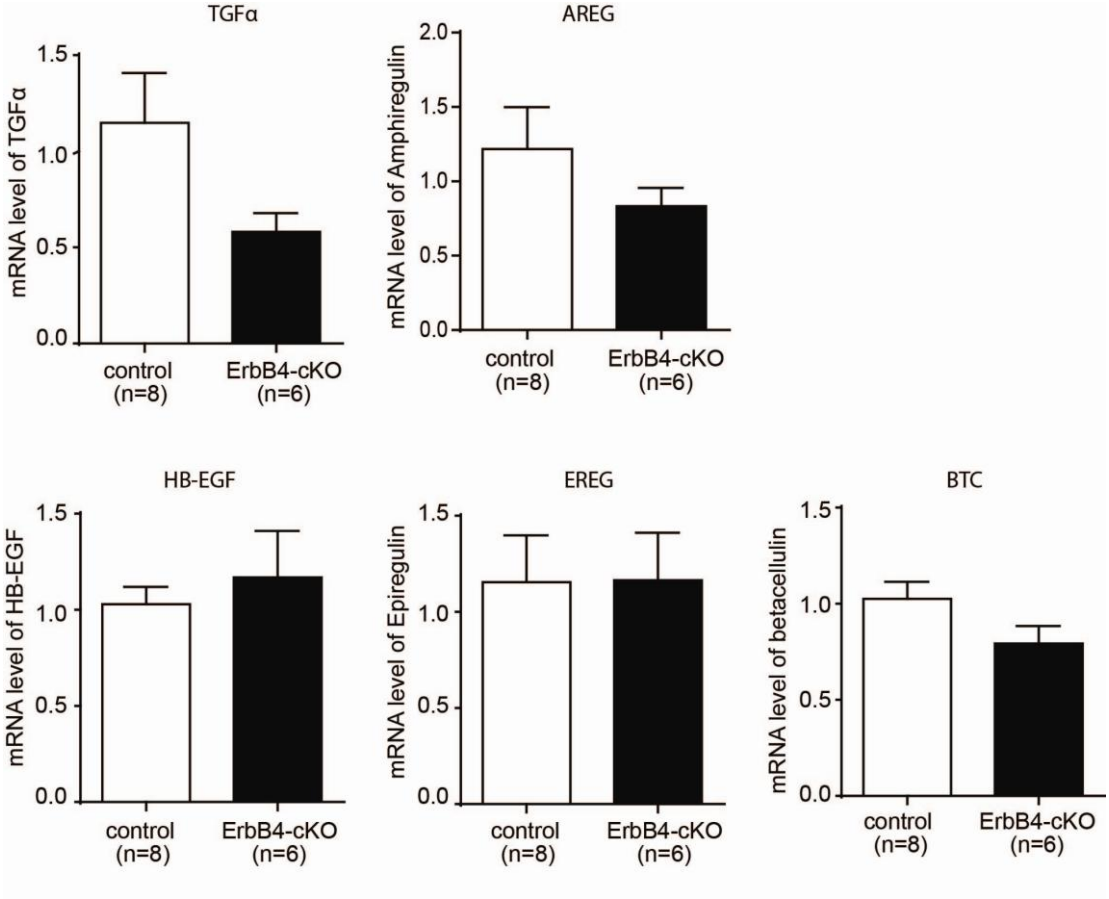

Figure 5.18 Expression of other EGF-like factors following deletion of ErbB4. The expression level of TGF-alpha, amphiregulin (AREG), HB-EGF, epiregulin (EREG) and betacelulin (BTC) was detected by the RT-qPCR and normalized to 18S. Data was expressed relative to the control group. Data was analysed using unpaired Student's t-test and presented as mean ± SEM; control, n=8; ErbB4-cKO, n=6.

5.3.11 The proliferation of cardiomyocytes following ErbB4 deletion

One question raised from the experiments described in 5.3.7 is how the ErbB4-cKO mice developed cardiac hypertrophy when there was no evidence of cardiomyocyte hypertrophy or fibrosis. The classic theory considers that in adult mammals the majority of cardiomyocytes are fully differentiated, and therefore have a very low rate of proliferation. However, a recent study suggested that NRG1 might promote the proliferation of adult cardiomyocytes (Bersell *et al.*, 2009). To investigate whether the up-regulation of NRG1 in ErbB4-cKO animals causes cardiomyocyte proliferation, we used immunofluorescence to examine expression of the proliferation marker phosphorylated histone H3 (pH3) in heart sections (Figure 5.19). Statistical analysis shows that the total number of pH3 positive cells in ErbB4-cKO animals was significantly increased, although the absolute number of proliferating cells remains low.

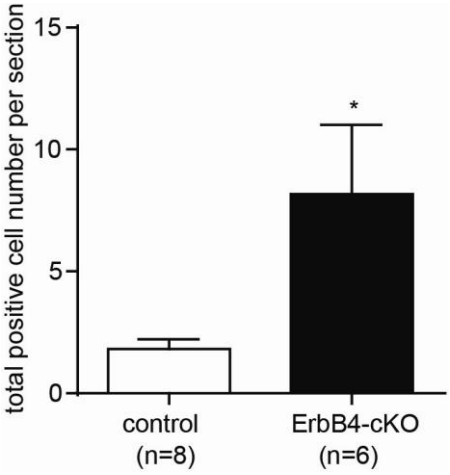

Figure 5.19 The proliferation of cardiac cells at 3-4 months following ErbB4 deletion. Heart sections in control and ErbB4-cKO animals were stained for pH3 by immunofluorescence. Data was analysed using unpaired Student's t-test and presented as mean ± SEM. * $P<0.05$ compared with control; control, n=8; ErbB4-cKO, n=6.

5.3.12 Expression of ErbB4 at 3-4 months after tamoxifen treatment

Following the investigation into the phenotype of ErbB4-cKO animals, we confirmed that the ErbB4 deletion is still valid 3-4 months after the tamoxifen injection. The RT-qPCR data revealed that the mRNA level of ErbB4 in the ErbB4-cKO group was reduced by ~67% compared to the control group (Figure 5.20).

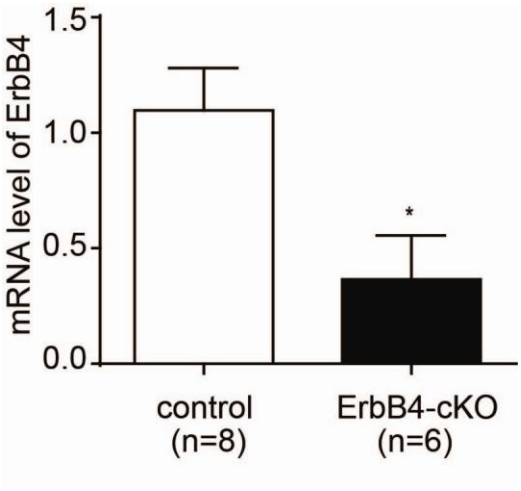

Figure 5.20 Expression of ErbB4 at 3-4 months after tamoxifen injection. At 3-4 months after tamoxifen treatment, the expression level of the ErbB4 was measured by RT-qPCR and normalized to the 18S. Data was expressed relative to the control group. Data was analysed using unpaired Student's t-test and presented as mean ± SEM. * $P<0.05$ compared with control; control, n=8; ErbB4-cKO, n=6.

5.3.13 Cardiac function at 7-8 months after ErbB4 deletion

All of the phenotypic experiments described above were conducted at 3-4 months after cardiac ErbB4 deletion was induced with tamoxifen. However, 3-4 months may be not long enough for the conditional ErbB4-cKO mice to develop a severe phenotype. To determine whether in the longer term the heart will develop dysfunction, we performed similar measurements on a separate cohort of ErbB4-cKO and control animals at 7-8 months after the deletion of ErbB4.

At 7-8 months after tamoxifen injection, we measured left ventricular internal dimension (LVID), interventricular septum thickness (IVS) and left ventricle posterior wall thickness (LVPW) in both the systolic and diastolic phase using echocardiography. Remarkably, in contrast to 3-4 months, statistical analysis revealed there were no marked differences between ErbB4-cKO and control animals at 7-8 months. The LVPW in ErbB4-cKO animals tended to increase but was not statistically significant compared to the controls (Figure 5.21).

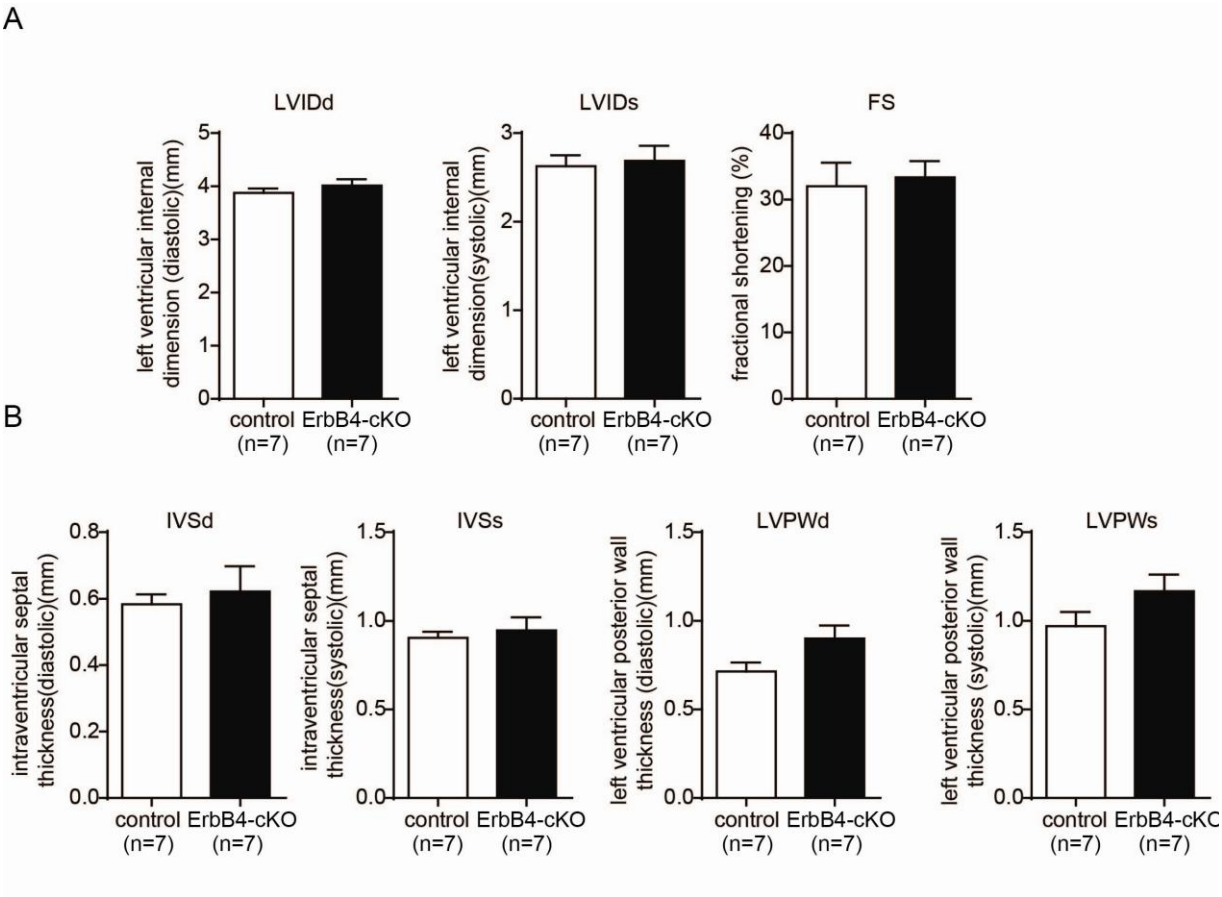

Figure 5.21 Echocardiographic assessment of cardiac function at 7-8 months following ErbB4 deletion. A. The diastolic (left) and systolic (middle) left ventricular internal dimension and fractional shortening (right) were measured in control and knockout animals. B. The diastolic and systolic IVS and LVPW dimension were measured in control and ErbB4-cKO animals. Data was analysed using unpaired Student's t-test and presented as mean ± SEM. * $P<0.05$ compared with control; control, n=7; knockout, n=7.

5.3.14 Cardiac hypertrophy at 7-8 months after ErbB4 deletion

Animals were euthanased following echocardiography, and indices of cardiac hypertrophy measured. The heart weight:tibia length ratio (HW:TL) of the ErbB4-cKO group was significantly increased (~ 19 %) compared to the control group (Figure 5.22). This suggests that ErbB4-cKO animals undergo mild hypertrophy. However, the magnitude of this increase is lower than in previous experiments when HW:TL was measured at 3-4 months after tamoxifen injection (Figure 5.13). We tested the expression of hypertrophic marker genes with RT-qPCR and found no significant changes in expression of the MHC isoforms or BNP (Figure 5.23 A). However, the ratio of α-MHC to β-MHC expression was reduced in the ErbB4-cKO, which may indicate a switch from α-MHC (which is predominant in adult heart) to β-MHC isoform (which is predominant in fetal heart) (Figure 5.23 A). This aligns with our data from the earlier set of experiments, which suggests that there may be increased generation of new cardiomyocytes. The fibrosis genes in both groups were expressed at similar levels (Figure 5.23 B), indicating there is no overt cardiac fibrosis in the ErbB4-cKO animals. Together, this suggests that the cardiac phenotype is milder at 7-8 months post-ErbB4 deletion compared to at 3-4 months after deletion, and that the phenotype observed at 3-4 months seems to undergo recovery by 7-8 months.

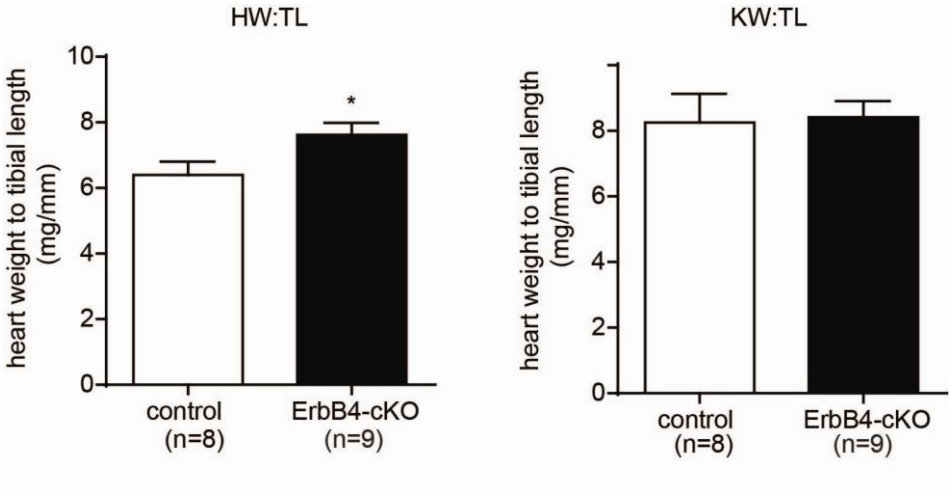

Figure 5.22 Effect of ErbB4 deletion on heart weight at 7-8 months after deletion. Heart (left) and kidney (right) weight was measured and normalized to tibia length in control (n=8) and knockout (n=9) animals. Data was analysed using unpaired Student's t-test and presented as mean ± SEM. * $P<0.05$ compared with control; control, n=8; ErbB4-cKO, n=9.

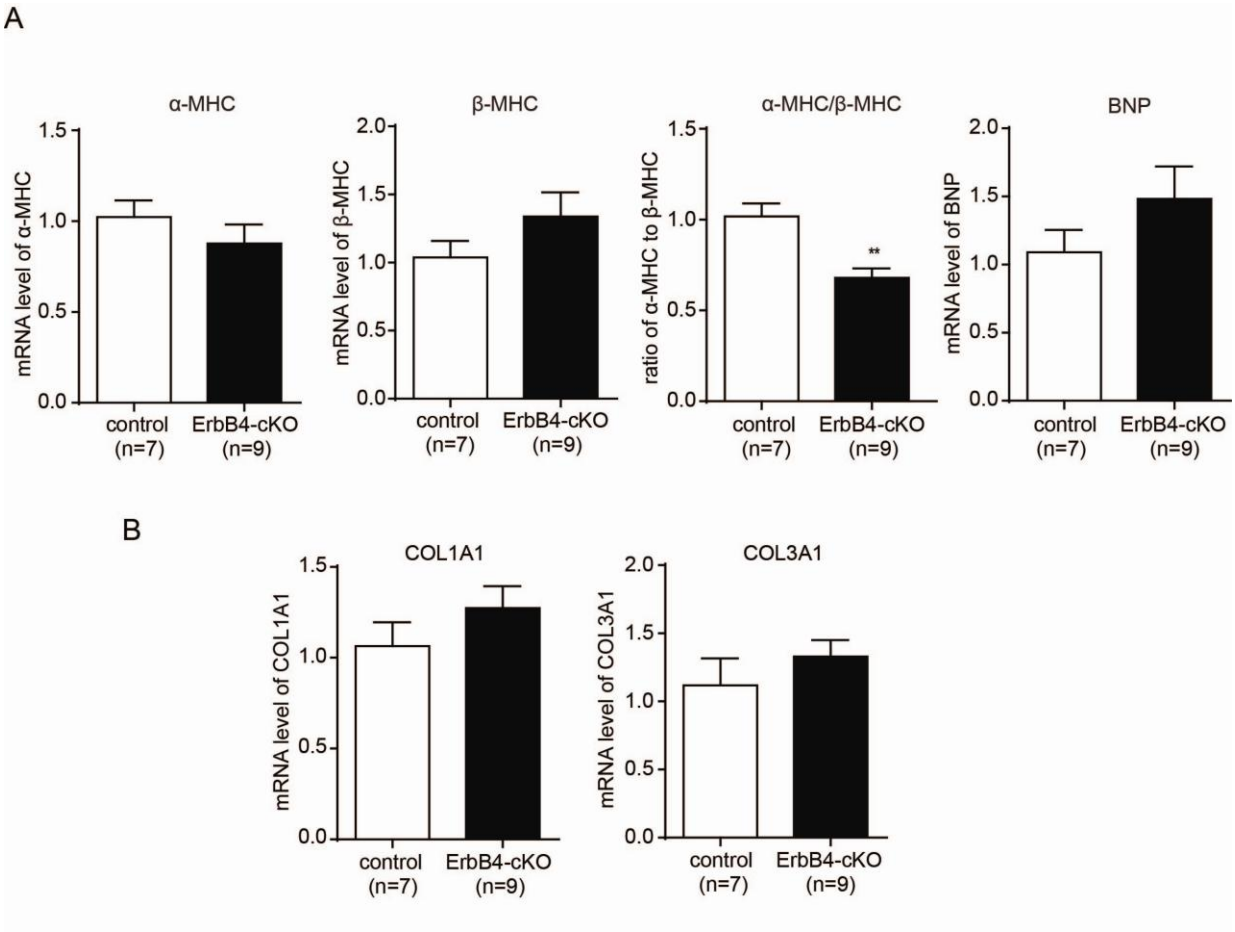

Figure 5.23 Effect of ErbB4 deletion on expression of hypertrophic and fibrosis genes at 7-8 months after deletion. The expression of hypertrophic genes BNP, α-MHC, β-MHC (A) and fibrosis genes COL1A1 and COL3A1 (B) detected by qPCR was normalized to 18S (endogenous control) and expressed relative to the control group. Data was analysed using unpaired Student's t-test and presented as mean ± SEM. ** $P<0.01$ compared with control; control, n=7; ErbB4-cKO, n=9.

5.3.15 Expression of ErbB4 at 7-8 months after tamoxifen treatment

After investigating the function of the heart after long-term deletion of ErbB4, we wanted to confirm that the ErbB4 is still absent in ErbB4-cKO animals at 7-8 months after ErbB4 gene deletion. We tested the expression of ErbB4 in heart tissues with RT-qPCR after 7-8 months of tamoxifen injection. Surprisingly, the ErbB4 expression in ErbB4-cKO animals was not significantly reduced compared to the controls (Figure 5.24). This indicated that either the gene was not initially deleted (unlikely), or that ErbB4 gene expression had somehow recovered by 7-8 months following tamoxifen treatment.

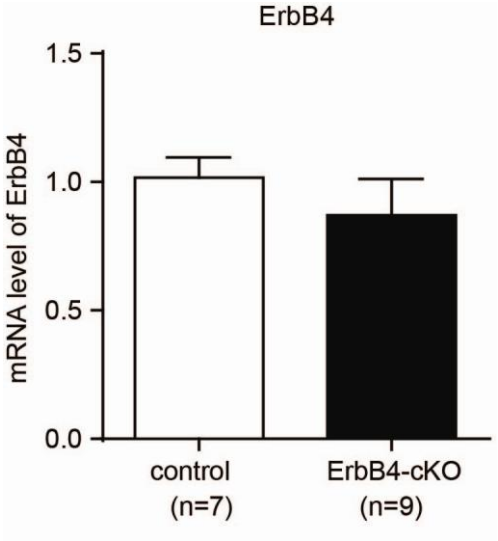

Figure 5.24 Expression of ErbB4 at 7-8 months after tamoxifen injection. At 7-8 months after tamoxifen treatment, the expression level of ErbB4 was measured by RT-qPCR, normalized to 18S and expressed relative to the control group. Data was analysed using unpaired Student's t-test and presented as mean ± SEM; control, n=7; ErbB4-cKO, n=9.

5.4 Discussion

The importance of NRG1 signalling in the cardiovascular system and its protective effect on the postnatal heart have been previously established (Zhao *et al.*, 1998; Kuramochi *et al.*, 2004; Liu *et al.*, 2006). As NRG1's primary receptor, ErbB4 is essential in heart (Gassmann *et al.*, 1995; Tidcombe *et al.*, 2003; Garcia-Rivello *et al.*, 2005). Based on these studies, we hypothesised that ErbB4 would be essential for adult heart maintenance, and predicted that ErbB4 deletion from the adult heart would lead to severe cardiomyopathy or heart failure. In this chapter, I used the αMHC-MerCreMer/loxP system to specifically delete ErbB4 from the adult heart, and investigated the cardiac phenotype for up to 7-8 months following deletion. The main findings in this study are: 1) An optimised tamoxifen treatment can specifically reduce ErbB4 mRNA levels by greater than 90% in the heart using the αMHC-MerCreMer/loxP system; 2) Transient Cre activity has long term effects on cardiac physiology; 3) Surprisingly, cardiac-specific deletion of ErbB4 did not lead to any obvious cardiac dysfunction or structural abnormalities except for a mild physiological hypertrophy; 4) Unique among EGF-like ligands, NRG1 was found to be selectively unregulated after ErbB4 deletion; and 5) There is increased proliferation of cardiac cells after ErbB4 deletion.

Tamoxifen is a drug has been used to treat breast cancer due to its anti-estrogen effects, and it is also used in the laboratory to induce gene deletion in MerCreMer/loxP conditional knockout mouse models. The described treatment regimes (dose, method of administration, duration of treatment) for tamoxifen induced gene deletion are highly variable. However, a high dose of tamoxifen can be toxic. In a previous study in our lab, tamoxifen treatment at 40mg/kg/day ip for 4 consecutive days led to a high mortality rate in adult mice. However, lower doses are sometimes not sufficient to cause efficient deletion of the target gene. To conquer this, we adopted the low dose but long term treatment method (Hsieh *et al.*, 2007). This idea is based on the fact that as long as the gene is deleted from genome, it cannot be recovered in the same cell. Although the efficiency of gene deletion is very low with a single tamoxifen injection at low dose, a prolonged accumulating treatment can achieve an excellent outcome. With this method, we achieved a more than 90 percentage deletion of the ErbB4 gene in adult mouse heart with minimal toxicity. There is no obvious or marked difference in the physiology or behaviour between the tamoxifen treated and untreated animals.

Although we were using the optimised dose tamoxifen which is not lethal, the potential side effect of this drug is hard to be excluded. To minimize the potential interference by tamoxifen itself, we

decided to treat both experimental and control groups with tamoxifen. The genotype of the conditional knockout animals is $Cre^{+/-}$/ $ErbB4^{fl/fl}$. Thus, the control animals have to lack either Cre ($Cre^{-/-}$/ $ErbB4^{fl/fl}$) or loxP sites ($Cre^{+/-}$/ $ErbB4^{wt/wt}$) to avoid deletion of ErbB4 when they received tamoxifen. If $Cre^{-/-}$/ $ErbB4^{fl/fl}$ animals are used as controls, tamoxifen injection will induce Cre activity in the ErbB4-cKO animals ($Cre^{+/-}$/ $ErbB4^{fl/fl}$) but not the controls ($Cre^{-/-}$/ $ErbB4^{fl/fl}$). Thus, Cre activity is another possible confounding factor induced in the ErbB4-cKO group besides the ErbB4 deletion. When Sohal *et al*. established the MHC-MerCreMer-loxP system in 2001, it was claimed that expression of the MerCreMer fusion protein in adult heart did not affect cardiac performance or cellular architecture. However, subsequent studies have indicated that the Cre recombinase is cardiotoxic. Hall *et al*. showed that the induction of Cre recombinase activity leads to decreased systolic function (SF) and alterations in proteins associated with cardiac oxidative phosphorylation. The decreased SF returned to baseline 10 days after tamoxifen injection (Hall *et al.*, 2011). Another study showed that cardiac Cre activity induced a transient dilated cardiomyopathy marked by cardiac dysfunction and reduction in the expression of genes related to metabolism and calcium handling. Some of these defects had disappeared by 1 month after the Cre activity was induced (Koitabashi *et al.*, 2009). Given these studies, supporting the idea that Cre activity might be cardiotoxic, it was important for me to evaluate the effect of Cre in our animals. To determine the Cre effect, we compared the cardiac function and structure of Cre positive animals to Cre negative animals. We found that the transient Cre activity decreased the heart weight (up to 8 months), while the cardiac function is not altered at either 3-4 months or 7-8 months after tamoxifen treatment. To circumvent the negative effect of Cre activity on cardiac tissues, I decided to use the Cre-only transgenic mice ($Cre^{+/-}$/$ErbB4^{wt/wt}$) as the control for my studies.

Against our expectations, we observed that the deletion of ErbB4 in adult mice did not lead to cardiac dysfunction. The important role of ErbB4 in cardiac development is well established (Gassmann *et al.*, 1995; Tidcombe *et al.*, 2003; Garcia-Rivello *et al.*, 2005), and the essentiality of ErbB4 in postnatal heart was confirmed by Garcia-Rivello *et al.* using a MLC-2V-Cre/loxP system to demonstrate that specific deletion of ErbB4 in cardiomyocytes leads to severe dilated cardiomyopathy in adulthood. Interestingly, no obvious cardiac abnormality (ventricle wall thickness, cardiac cell number) was observed at birth, and the phenotype they observed in adulthood primarily resulted from lack of ErbB4 in the postnatal stage (juvenile or adult) (Garcia-Rivello *et al.*, 2005). The results of my experiments in this chapter indicate that ErbB4 is not critical for maintenance and function of the adult heart, and remarkably its deletion did not result in cardiomyopathy. One interpretation could be that ErbB4 might be essential for the cardiac

development in the juvenile, but not in the older adult. Supporting this, Bersell *et al.* (Bersell *et al.*, 2009) showed that genetic deletion of ErbB4 at postnatal days 16-18 blocked the DNA synthesis of cardiomyocytes at baseline (measured by BrdU incorporation). Taken together, these studies and ours might suggest the ErbB4 is required for the cardiac development both in embryonic and early postnatal stages. However, once the cardiac development is completed, the subsequent loss of ErbB4 does not lead to severe cardiac dysfunction or structural abnormalities.

One clinical study has indirectly indicated that ErbB4 might be important for adult heart maintenance: trastuzumab (an ErbB2 blocking antibody) has been used for breast cancer therapy and when combined together with other chemotherapy agents the rate of heart failure was significantly increased (27% incidence) (Seidman *et al.*, 2002). Based on this observation, it has been proposed that ErbB2 is important in the adult heart. ErbB2 lacks any identified agonists, and preferentially dimerizes with other ErbB receptors to trigger downstream signalling (Timolati *et al.*, 2006). The inhibition of ErbB2 might affect the signalling of other ErbB receptors, especially its preferential partner ErbB4. Our study suggested ErbB4 deletion did not caused cardiac dysfunction. Thus, the cardiac dysfunction induced by trastuzumab treatment probably reflects effects on the signalling of other ErbB receptors. As mentioned earlier (section 1.2.1), the ErbB2 receptor can adopt an active formation without binding any agonists (Garrett *et al.*, 2003). It is therefore possible that the active ErbB2 signalling itself is essential for the maintenance of heart function.

ErbB4 has been suggested to play a role in the transition from hypertrophy to heart failure. In patients with heart failure, the cardiac expression of ErbB2 and ErbB4 are depressed (Rohrbach *et al.*, 2005). A study in rats also showed that ErbB2 and ErbB4 are significantly reduced in the heart failure period, but not the preceding hypertrophic period in an aortic stenosis model (Rohrbach *et al.*, 1999). However, in our study, the ErbB4-cKO mice developed significant hypertrophy but did not develop into heart failure in the longer term. This suggested that the loss of ErbB4 in the earlier studies might be the result of heart failure but not the reason.

Another interesting result in my study is that ErbB4 deletion caused (somewhat paradoxically) cardiac hypertrophy. Cardiomyocyte hypertrophy and cardiac fibrosis were absent in the ErbB4-cKO animals, and so we proposed that there might be more cardiomyocytes generated. Two potential sources could possibly regenerate new cardiomyocytes: one is stem cells or progenitor cells and another is existing cardiomyocytes. Detecting cardiac stem cells is currently not available in our lab, so I attempted to test whether cardiomyocytes were proliferating in our ErbB4-cKO

animals via co-staining of proliferation maker pH3 (located in nucleus) and the cardiomyocyte marker Troponin by immunofluorescence. However, the cell boundary could not be clearly resolved and there were many very small cells, such as endothelial cells, fibroblast or potential cardiac stem cells located among the cardiomyocytes. Thus, it was difficult to tell whether the positively stained nucleus for pH3 with positive Troponin staining around it was in a cardiomyocyte, or in a small cell among cardiomyocytes. This difficulty has also been described in the literature (Ang *et al.*, 2010). Thus, the positively stained cell number was presented as total cardiac cell number instead of "cardiomyocyte number". Although we cannot tell exactly the contribution of each cell type in this cardiac cell proliferation, we believe that new cardiomyocytes were generated by cardiomyocytes or stem cells, and contribute to the cardiac hypertrophy. It is important to note that pH3 only indicates cells undergoing the mitogenic phase, which is known to be transient in the whole cell cycle. The heart is one of the least regenerative organs in the body, so even if there is a regenerative response, it usually happens in a very small proportion of cells. Thus, the pH3 stained only a few cells in each section. It is still hard to predict how much of the heart can be regenerated with these proliferated cells. However, we believe with the accumulation effect over time, many new cardiomyocytes were generated in our ErbB4-cKO model and these might have contributed to the cardiac hypertrophy.

Another important discovery of our study is that we observed the up-regulation of NRG1 in our animals after ErbB4 deletion. To our knowledge, this is a new observation in ErbB4 deletion studies, but is concordant with the observation made by Robrbach *et al*. in heart failure where the ErbB4 expression was decreased and NRG1 increased (Rohrbach *et al.*, 1999; Rohrbach *et al.*, 2005). The link between the loss of ErbB4 and the compensatory up-regulation of its agonist NRG1 is indicative, but the mechanism is unknown. However, given that NRG1 is predominantly released by microvascular endothelial cells (Kuramochi *et al.*, 2004; Lemmens *et al.*, 2006) and targets the cardiomyocytes, we predict that there is a crosstalk between the cardiomyocytes and endothelial cells to regulate the expression of NRG1 after the ErbB4 deletion. The up-regulated NRG1 may function to compensate for the ErbB4 loss. NRG1 is a cardioprotective factor that enhances cardiac contraction and reduces the cardiomyocyte apoptosis caused by stress (Liu *et al.*, 2006; Bian *et al.*, 2009). I therefore propose that this NRG1 up-regulation explains why we haven't observed a severe phenotype following ErbB4 deletion. If this assumption is true, the prevailing question will be how NRG1 can mediate a cardioprotective effect in the absence of its cognate receptor ErbB4. One possibility is that NRG1 is acting via a different receptor, possibly ErbB3.

Currently, it is unclear whether cardiac stem cells can respond to NRG1 stimulation to proliferate. However, NRG1 can promote cardiomyocyte proliferation in the adult heart (Zhao *et al.*, 1998; Bersell *et al.*, 2009). Another question from the present study is how NRG1 induced cardiac cell proliferation in the absence of its receptor ErbB4. One possibility is that ErbB4 was not completely deleted from 100% of cardiomyocytes, and that the proliferation happened in ErbB4-replete cells. They would then pass their intact genome to their progeny cells, which thus possess the unaffected ErbB4 gene and could in turn respond to NRG1. When the newly generated cardiac cells accumulate, the proliferation process is accelerated. However, NRG1 only induces a small proportion of cardiomyocytes to proliferate in wild type animals (Bersell *et al.*, 2009). Accordingly, it can be inferred that in ErbB4 deleted animals, this cell population is even smaller and so it is very hard to imagine how a few cells proliferating at the initial stage (after deleting ErbB4 from the majority of cardiomyocytes) could promote such a robust increase in heart size in 3 months given the poor regenerative capacity of the adult heart. It is possible that the deletion of ErbB4 happens in cells expressing MHC but not in progenitor cells that do not express MHC. In this case, the proliferation rate of cardiac cells induced by NRG1 will be similar for wild type and ErbB4 deleted animals. Hence, when the NRG1 is up-regulated in ErbB4-cKO animals (but not wild type animals), the ErbB4-cKO animals will have more cardiomyocytes generated. A final possibility is that ErbB3 also plays a role in adult heart function and structural maintenance. ErbB3 is a receptor for NRG1 with a similar structure to ErbB4 but possessing additional PI3K binding domains, which contribute to cardiomyocyte survival. However, this possibility does not explain the recovery of the ErbB4 expression in the long-term after deletion. Whatever the merit of these speculations, we need to perform additional studies such as lineage tracing with immunofluorescence markers to tell if the proliferating cells are stem cells, cardiomyocytes with ErbB3 or ErbB4, or other cell types.

A final surprising discovery from this work was that the expression of ErbB4 in the ErbB4-cKO group gradually recovered to the level of the control group at 7 months after ErbB4 deletion. One trivial possibility is we didn't inject the tamoxifen properly. We cannot fully exclude this possibility because each set of animals was injected with tamoxifen independently, and the successful deletion of ErbB4 in one cohort does not mean the definite success of deletion in a later set of animals. However, the injections of tamoxifen were performed by the same person following the same procedures, and for ten consecutive days, so we consider that the possibility of technical failure is low. The only reasonable explanation is that ErbB4 was successfully deleted from the genome immediately after tamoxifen treatment, but that the expression of ErbB4 gradually recovered over 7-8 months via a process that likely involves the generation of new cardiomyocytes to replace the

cardiomyocytes with genomic deletion of ErbB4. The replacement of cardiomyocytes would presumably require apoptosis of the old cells in addition to new cell generation. We tried to detect cardiomyocyte apoptosis with TUNEL at 3 months after ErbB4 deletion, however, the results was not definitive due to the high levels of background staining in all groups. In summary, the cardiac specific deletion of ErbB4 in adult mice did not result in physiological hypertrophy without obvious cardiac dysfunction. The compensatory up-regulation of NRG1 in ErbB4-cKO mice heart might contribute to the cardiac function preservation and lead to cardiac hypertrophy via causing cardiomyocyte proliferation.

CHAPTER 6

GENERAL DISCUSSION

6. General Discussion

This thesis has explored the role of the epidermal growth factor receptors (particularly ErbB4) in mediating cardiomyocyte hypertrophy, the potential signalling differences among the ErbB4 isoforms, and the physiological function of ErbB4 in the adult mouse heart. While ErbB4 did not contribute to a classic model of cardiomyocyte hypertrophy (Ang II-induced hypertrophic signalling), this receptor was clearly involved in the hypertrophy caused by NRG1. ErbB4 has four isoforms due to alternative splicing, and the non-cleavable isoform JM-b was found to be predominant under both physiological and pathophysiological conditions. Interestingly, there was no significant difference in the ability of the four isoforms to mediate NRG1-induced hypertrophy. When ErbB4 was specifically deleted from the adult mouse heart using Cre-loxP technology, the mice developed physiological cardiac hypertrophy with up-regulation of NRG1 and no alterations in cardiac function and structure. Surprisingly, an increased proliferation of cardiac cells was observed following cardiac ErbB4 deletion, and I propose that the NRG1 up-regulation contributes to this cell proliferation, although the mechanisms remain unclear.

Crosstalk between ErbB receptors and GPCRs in cardiomyocyte hypertrophy

Cardiomyocytes are continuously exposed to diverse stimuli, such as soluble endocrine and paracrine factors from blood or neighboring cells. It is important that these signals are integrated to achieve an appropriate cellular response. Tyrosine kinase receptors (for factors including the EGF ligands, insulin-like growth factor-1, insulin, etc.) and GPCRs (for ligands such as angiotensin II, endothelin 1, adrenaline, etc.) play pivotal roles in interpreting such signals (Sugden *et al.*, 1998; Clerk *et al.*, 1999; Heineke *et al.*, 2006). These receptor systems do not work in isolation and there is irrefutable evidence for crosstalk between GPCRs and the growth factor receptors. An accumulating literature supports the idea that the type 1 angiotensin receptor (AT_1R) is able to transactivate the ErbB receptors (principally ErbB1) and thereby mediate cellular growth in a variety of tissues and organs (Eguchi *et al.*, 1998; Shah *et al.*, 2003b; Chen *et al.*, 2006). In this setting, and based on previous work from my host laboratory that showed the ErbB4 selective agonist NRG1 was a more potent inducer of cardiomyocyte hypertrophy than ErbB1 ligands, my first aim was to investigate whether the classic AT_1R-ErbB1 transactivation by extended to other ErbB receptors, explicitly ErbB4. To accomplish this aim, I used an approach that involved

knockdown of ErbB receptors using RNAi as well as pharmacological inhibition with the small molecule EGFR kinase antagonist, AG1478, which has been widely used in the field to discern EGFR function (Eguchi *et al.*, 1998; Asakura *et al.*, 2002; Thomas *et al.*, 2002; Shah *et al.*, 2003b; Chen *et al.*, 2006). I was able to unambiguously demonstrate knockdown of each ErbB receptor, and tested the effect of this knockdown on the capacity of Ang II (and NRG1) to promote cardiomyocyte hypertrophic signalling. As expected, knockdown of ErbB4, but not ErbB1 or ErbB2, was able to prevent NRG1 mediated cardiomyocyte hypertrophy. However, despite careful experimentation, I found no evidence that Ang II-mediated cardiomyocyte hypertrophic signalling was dependent on ErbB4. Much to my initial disappointment, I was also unable to prevent AT_1R-mediated cardiomyocyte hypertrophy with RNAi targeting ErbB1 or ErbB2. Based on extensive, compelling, previous literature in the heart, but also in many other cellular systems (Shah *et al.*, 2003a; Mendez *et al.*, 2005; Liebmann, 2011), our observation was unsettling but repeatable.

Given the importance (and potential controversy) of my data questioning the role of ErbB receptors in AT_1R hypertrophy, I undertook with my supervisors a systemic review of my approach and observations. We retested the specificity of my RNAi constructs - they were shown to be effective and specific - notably, the knockdown of individual ErbB receptors was confirmed by Western blotting and qPCR, showing there is up to 90% reduction of ErbB1or ErbB4 by RNAi. In addition to my initial data, using luciferase-based hypertrophic gene promoter reporter assays, I went on to confirm that there was also minimal effect of ErbB knockdown on the activation of AT_1R-mediated MAPK signalling and hypertrophic growth (measured as protein:DNA ratios and sacromeric reorganisation). We performed power calculations for luciferase assay data and determined that my experimental repeats (n = 7-8) were more than sufficient to allow valid conclusions. My grouped data for all experiments clearly showed no differences between knockdown and control groups with Ang II treatment. In contrast, under parallel experimental conditions (i.e., same cells, same days, same experimenter, same analyses), I was able to consistently and unequivocally observe that ErbB4 RNAi (but not ErbB1/2 RNAi) reduced cardiomyocyte hypertrophic signalling in response to the ErbB4 selective agonist, NRG1. The only interpretation for these results is that NRG1 requires the ErbB4 to mediate hypertrophy, whereas ErbB1, ErbB2 and ErbB4 are not individually required for AT_1R mediated cardiomyocyte hypertrophy.

So, how do I explain these results? It is difficult to answer this, as the experiments included appropriate controls, yet yielded different results from previous studies, where the majority of the literature indicates that GPCRs, like the AT_1R, use EGFRs to mediate growth signalling (Porcile *et*

al., 2005; Ohtsu *et al.*, 2006a; Ohtsu *et al.*, 2006b; Luppi *et al.*, 2007; Schlange *et al.*, 2007). A number of possibilities might be considered: **1)** the most trivial of explanations could be that despite overt knockdown of the ErbB mRNA/protein, the residual receptors were sufficient to mediate growth pathway signalling. This idea is consistent with the pharmacological concept of "spare receptors" (where in many cases only a portion of cell surface receptors are required for full efficacy) (Strickland *et al.*, 1981). Obviously, my control experiment, detailing the loss of NRG1 efficacy with ErbB4 RNAi knockdown, refutes such reasoning; **2)** Primary cultures of neonatal cardiomyocytes vary tremendously in terms of cellular composition (i.e., % contamination by fibroblasts, endothelial cells etc) and sensitivity to hypertrophic stimuli, between laboratories and even within laboratories over time. This might reflect subtle changes in protocols and purity (or otherwise) of the cultures; **3)** Many laboratories have evoked the contribution of EGFR transactivation based, almost exclusively, on experiments using pharmacological blockade with the small molecule inhibitor, AG1478. Certainly, the use of AG1478 alone (without confirmation with another technique like RNAi) can be problematic and is open to misinterpretation (detailed below); and **4)** My RNAi experiments tested the hypothesis that individual ErbB receptors were involved in cardiomyocyte hypertrophy and it remains possible that some redundancy exists between the ErbB receptors (given that multiple receptors can bind multiple ligands) such that knockdown of a single receptor might be compensated by another. So, whatever the merits of these possibilities, it certainly raises some uncertainties and potentially some reevaluation of the some of the literature in this broad field.

Indeed, as mentioned above, the reliance on data using AG1478 needs careful reexamination. There is no doubt that in controlled assays, under ideal conditions, AG1478 at nanomolar concentrations is a selective and specific inhibitor of the EGFR kinase (Anastassiadis *et al.*, 2011). However, in cell-based assays, where often conditions can widely vary and concentrations of the inhibitor range up to tens of micromolar, that specificity/selectivity is not assured. In regard to the EGFRs, the current consensus is that AG1478 is reasonably selective for ErbB1 (the EGFR) at concentrations <0.5 μM, but can inhibit the other ErbBs (and probably other tyrosine kinases) at higher concentrations (>5 μM). My data on MAPK signalling in cardiomyocytes (where EGF activation of ErbB1 was blocked by 0.5 μM, but where NRG1 mediated MAPK via ErbB4 was only inhibited by 5 μM AG1478) are entirely consistent with this consensus view. Previous studies, including some from my own laboratory, have used high μM levels of AG1478 and therefore cannot exclude the contribution of tyrosine kinases other than EGFR kinase. Indeed, other receptor tyrosine kinases, as well as soluble tyrosine kinases, have been associated with Ang II/AT_1R signalling and growth (Yin

et al., 2003), including, as an example, the platelet-derived growth factor receptors (Linseman *et al.*, 1995; Kelly *et al.*, 2004). Finally, I am certainly not criticizing all previous studies using AG1478 - some have used this inhibitor in the appropriate range (100-250 nM) - in, for example, hepatic C9 cells (Shah *et al.*, 2002), renal epithelial cells (Chen *et al.*, 2006), and vascular smooth muscles cells (Eguchi *et al.*, 1998). Some have also combined this with RNAi, and my experience would concur that it is important for future studies to use a combination of RNAi and pharmacological approaches together with well considered controls.

Another limitation of the EGFR transactivation field has been the strong focus on the entire triple membrane-passing signalling (TMPS) pathway occurring in a single cell - whereby the GPCR, ADAM, shed EGF ligand, and EGFR are all co-expressed and activated as a single unit. Of course, the possibility exists that shed ligands could work in a paracrine manner, perhaps even between different cell types as might occur in the heart. Indeed, the primary source of neuregulin in the heart is presumed to be the endothelial cells of the vasculature (Kuramochi *et al.*, 2004; Lemmens *et al.*, 2006) but the primary target in terms of hypertrophy is ErbB4 on the cardiomyocytes. So, while there can be no argument that all the components (i.e., AT_1R, ADAM12/15/17, ErbB receptors (ErbB1, ErbB2 and ErbB4) and multiple EGF-like factors) are present in cardiac tissue whether they necessarily need to occur in an individual cell type could be questioned, especially as I did not observe EGFR transactivation in the highly purified cardiomyocyte cultures. So when considering these mechanisms in an intact organism (or tissue), I would argue we need to consider that the ErbB receptor system does not have to be completed via transactivation in one cell type, like the cardiomyocyte, but it may happen via interaction of the many types of cells in response to neurohumoral factors/stimuli.

The functional relevance of ErbB4 isoforms in cardiomyocytes

In the initial stages of my candidature, we were strongly considering that the experiments detailed above would likely show, not only transactivation of ErbB1, but as I hypothesized, an additional ability to transactivate ErbB4. While ultimately this did not occur, in parallel I was initially interested in considering the possibility that this putative ErbB4 transactivation might result from one or more of the ErbB4 isoforms. As introduced earlier, ErbB4 has four isoforms due to alternative splicing, and these can be differentially processed in cells (Junttila *et al.*, 2000). Moreover, there is evidence in the literature that GPCR activation (Higa‐Nakamine *et al.*, 2012) and stimulation with NRG1 (Zhou *et al.*, 2000) induce cleavage of the JM-a isoform, releasing a

functional intracellular domain (ICD) into the nucleus to regulate cell activity as first shown by Graham Carpenter's group (Vecchi *et al.*, 1996). So, even though I did not observe transactivation of ErbB4 by Ang II in purified cardiomyocytes, I was still interested in investigating whether the specific ErbB4 isoforms could be cleaved to release the ICD in cardiomyocytes and whether this might contribute to the NRG1-induced cardiomyocyte hypertrophic signalling. Because previous, unpublished work in our laboratory had detected all of the four ErbB4 isoforms in primary neonatal rat cardiomyocytes, my prediction was that the cleavable JM-a isoform would be present and that I would be able to demonstrate that it could be processed to release the intracellular domain (80 kD ICD), which might interact with transcriptional factors to regulate cellular activity. Secondly, based on a study in the brain, where a specific ErbB4 isoform was cleaved and shown to regulate the time of astrogenesis in the mouse (Sardi *et al.*, 2006), I was intrigued by the idea that the four isoforms might make differing contributions to cardiomyocyte hypertrophy.

As part of investigating the cleavage of ErbB4 and any isoform-specific differences, I first sought to establish whether these isoforms are indeed expressed in whole mouse heart. In addition, I wondered whether the isoforms were expressed differently in various stages of cardiac development, or during pathology. There is strong evidence that ErbB4 is required for normal mouse cardiac development (Gassmann *et al.*, 1995; Tidcombe *et al.*, 2003) but the relevance of a specific ErbB4 isoform in normal growth or disease has not been reported. I performed an expression profile in the heart of all four isoforms from embryonic day 10.5 to postnatal day 28. All isoforms declined throughout cardiac development - the expression of total ErbB4 at the earlier embryonic stage (E10.5) is 250 times higher than at postnatal day 28. Interestingly, the expression levels of JM-a and JM-b isoforms are similar in the earlier embryonic stages. However, by the postnatal stage in mice, JM-b is the overwhelmingly predominant isoform. Why this might be is currently unclear, but it could relate to the proliferative (i.e., embryonic) or hypertrophic (i.e., post-natal) growth that occurs in the heart. It is tempting to speculate that perhaps JM-a is required for cardiac proliferation in the embryo and JM-b is required for hypertrophy in the adult. It would be interesting to isolate the embryonic cardiomyocytes and investigate whether the JM-a isoform mediates proliferation, especially given that JM-a is capable of regulating the timing of astrogenesis by suppressing astrocyte progenitor cell differentiation (Sardi *et al.*, 2006). Moreover, the release of the ICD (from JM-a) allows interaction with YAP to facilitate the translocation of the ICD into the nucleus (Komuro, Nagai *et al.* 2003; Omerovic, Puggioni *et al.* 2004). Given that YAP activation is sufficient to stimulate both embronic and postnatal cardiomyocyte proliferation (von Gise *et al.*,

2012), it would seem reasonable to hypothesise that release of the ICD from JM-a could associate with YAP to promote cardiomyocyte proliferation.

Experiments aimed at examining whether the JM-a isoform can be cleaved in cardiomyocytes were critical in attempting to make this link between ErbB4 isoform expression and cardiac cell growth. It is important to note two things: 1) that I performed these experiments prior to the isoform characterisation mentioned above (which showed predominance of JM-b in postnatal mouse heart) and 2) that a previous student has some preliminary PCR data to suggest that JM-a was expressed in rat neonatal cardiomyocytes (Hsiu-wen Chan, PhD thesis). Based on previous studies showing that cleavage of JM-a to yield the ICD is sensitive to cell activation with the phorbol ester PMA, and also to NRG1 (Vecchi *et al.*, 1996; Zhou *et al.*, 2000), I initially attempted to demonstrate shedding of the 85KDa ICD using Western blotting as previously described (Vecchi *et al.*, 1996; Zhou *et al.*, 2000). Disappointingly (but with hindsight not unexpectedly), no band corresponding to the ICD could be detected either basally or following stimulation of rat neonatal cardiomyocytes with PMA or NRG1. We went on to confirm that the primary isoform of ErbB4 in the rat heart is the JM-b isoform (Hengbo Shi, visiting scholar, unpublished data), as it is in mouse. So, the inability to detect generation of the ICD likely reflects the low expression level of the endogenous JM-a isoform in these cells.

To examine the potential for JM-a cleavage in these cells (which, while difficult to examine on the endogenous lowly-expressed receptor, might be functionally important), I developed a series of C-terminal GFP-tagged ErbB4 isoform constructs. These vectors were transfected into postnatal cardiomyocytes, allowing us to observe the potential cleavage and translocation of the ICD-GFP into the nucleus using confocal microscopy. If the cellular machinery for this process was present, I hypothesised that the ICD would be generated after stimulation and enter into nucleus. No obvious evidence for this was seen and no nuclear translocation of green fluorescence was observed following stimulation with PMA or NRG1 for up to 15 min. The lack of ICD generation is consistent with the low expression of JM-a, and indicates the shedding processes involved may also be postnatally down-regulated. Finally, I did not observe remarkable changes in ErbB4 isoform expression with cardiac disease (i.e., a model of myocardial infarction) and I therefore surmise that isoform-specific ErbB4 cleavage is unlikely to be a major driver of the effects of ErbB4 in heart.

This then leads to the important question as to why the cardiomyocytes might express multiple isoforms of the ErbB4, and are there any functional differences among these isoforms in

cardiomyocytes? An initial focus of my thesis was the role of ErbB4 in NRG1-mediated cardiomyocyte hypertrophy, so I examined whether the four ErbB4 isoforms could all equally mediate this effect. For this purpose, I knocked down the endogenous ErbB4 receptor and then replaced it with individual knockdown-resistant version of the ErbB4 isoforms. Hypertrophy was induced with the ErbB4 agonist NRG1 and hypertrophic signalling measured with luciferase reporter assays. I observed that all four isoforms can rescue NRG1-induced hypertrophy, indicating that the most likely scenario is that the hypertrophic signalling is reliant on the common tyrosine kinase activity of the ErbB4 receptor isoforms, and does not seem to involve either shedding to release ICD or a particular docking event mediated by CYT1/2.

The function of ErbB4 in the adult mice heart

My thesis then moved away from the focus on transactivation to a broader investigation of the role of ErbB4 in adult heart *in vivo*. For this purpose, I adopted the tamoxifen inducible MHC-MerCreMer/loxP system (Garcia-Rivello *et al.*, 2005) to specifically delete the ErbB4 from cardiomyocytes in adult mice. As described in Chapter 5, tamoxifen treatment specifically decreased ErbB4 expression in the adult heart by ~ 90%. My prediction was that the mice would develop cardiac dysfunction or structural abnormalities in the weeks/months following ErbB4 deletion. To my surprise, the knockout mice were active and healthy following ErbB4 deletion and no obvious pathology was observed, which suggested a potential lack of a cardiac phenotype in these mice. At 3 months after ErbB4 deletion, I measured cardiac contractility and heart weight, and analysed cardiac structure, including the cardiomyocyte size and cardiac fibrosis. Surprisingly, the cardiac function was not affected in the ErbB4 deleted mice. There were no structural changes (cardiomyocyte hypertrophy or cardiac fibrosis) observed in knockout animals, although these mice did develop cardiac hypertrophy (increased heart weight:tibia length ratio). This result is opposite to my original hypothesis that ErbB4 is essential in adult heart. This suggests a few possibilities. Firstly, there might be up-regulation of the EGFR family or their ligands to compensate for the reduced ErbB4 function. Secondly, maybe 3-4 months is not long enough to observe a phenotype. In addition to these questions, the mechanism by which the knockout mice developed cardiac hypertrophy without cardiomyocyte hypertrophy needs to be elucidated.

To answer the first question, I investigated the expression of the other members of the ErbB family (ErbB1, ErbB2 and ErbB3) and their selective agonists (the EGF-like factors) after ErbB4 deletion, and found that only the ErbB4 selective agonist NRG1 was significantly up-regulated (4-5 fold

increase). Accumulated evidence suggests that NRG1 is a beneficial factor that can preserve cardiac function in various cardiac pathological models (Liu *et al.*, 2006). NRG1 could protect the cardiomyocytes from apoptosis (Zhao *et al.*, 1998) and regulate the contraction of the cardiomyocytes by regulating the sarcomere reorganization (Muraoka-Cook *et al.*, 2006a; Bian *et al.*, 2009) and Ca^{2+} intake (Mery *et al.*, 1991; Brero *et al.*, 2010). In our model, it is possible that ErbB4 deletion causes a cardiac phenotype, but this is concealed by the protective effect of NRG1. How NRG1 functions in the absence of ErbB4 remains a question. It has been accepted in the field in the past 15 years that ErbB4 is the only receptor for NRG1 in cardiomyocytes, as the other NRG1 receptor, ErbB3, is not expressed. However, a recent publication found that the ErbB3 is also detected in cardiomyocytes, where it can be activated by NRG1 (Campreciós *et al.*, 2011). Whether the ErbB3 is activated by up-regulated NRG1 in our ErbB4-cKO mice to compensate for the lost ErbB4 function is unknown and needs further investigation.

There is evidence in the literature that NRG1 induces cardiomyocyte proliferation in adult mice (Bersell *et al.*, 2009). Thus, I investigated whether there is proliferation of cardiac cells in our ErbB4-cKO mice. For this purpose, I used the mitosis marker pH3 to label the proliferating cells by immunofluorescence, and found the number of pH3 positive cardiac cells was significantly increased in ErbB4-cKO heart. Whilst we did not perform lineage-tracing studies in this thesis, I hypothesize that these new cells were generated from existing cardiomyocytes or a subpopulation of stem/progenitor cells, which contributes to the cardiac hypertrophy in ErbB4-cKO mice in the absence of cardiomyocyte hypertrophy.

If the existing cardiomyocytes do proliferate in ErbB4-cKO mice to contribute to cardiac hypertrophy, the results will be very interesting. In chapter 3, I have shown that NRG1 induced cardiomyocyte hypertrophy *in vitro*. However, in chapter 5 the up-regulation of NRG did not result in cardiomyocyte hypertrophy *in vivo* but may have caused myocyte proliferation. Since 1998, the ability of NRG1 to promote the hypertrophic growth and proliferation of isolated cardiomyocytes has been documented (Zhao *et al.*, 1998). However, few studies have reported NRG1 induced cardiomyocyte hypertrophy *in vivo*. One recent study showed that NRG1 infusion in adult mice induced the proliferation, but not hypertrophy of cardiomyocytes (Bersell *et al.*, 2009). The reasons underlying the different observations *in vitro* and *in vivo* are unknown. However, differences in the local cardiomyocyte environment may provide one explanation. *In vitro*, the cardiomyocytes are purified and maintained at a subconfluent density. In contrast, *in vivo* cardiomyocytes are connected

with each other via junctions, and surrounded by many other cells (e.g. fibroblasts, endothelial cells) that may potentially influence cardiomyocyte function.

In addition to the proliferation of existing cardiomyocytes, another potential resource for new cardiomyocytes is cardiac progenitor cells or stem cells. This has been discussed in Chapter 5. If this does happen in our ErbB4-cKO mice, it remains to be seen whether these new cells have the same predominant isoforms of ErbB4 as the mature cardiomyocytes. In chapter 4, I found that expression of the JM-a isoform is much higher in embryonic hearts than adult hearts. It is possible that the JM-a expressing cells are the stem cells or cardiac progenitor cells. Currently, there have been no reports on the ErbB4 isoform expression in these cells. If the cardiac stem cells express the JM-a isoforms, it will be very important to know whether the JM-a isoforms can be cleaved in these cells to release the ICD. It is known that the coactivator of the ErbB4 ICD (Komuro *et al.*, 2003), YAP, is essential for the proliferation of stem cells (Zhao *et al.*, 2011). It will be interesting to know whether the cleavage of the JM-a isoform and release of the ICD are involved in the YAP controlled proliferation.

To investigate whether ErbB4 deletion leads to cardiac dysfunction or structural changes in the longer term, I measured the cardiac phenotype at 7-8 months post deletion in a separate cohort of animals. Again, cardiac function was preserved in knockout animals. Interestingly, these animals have milder cardiac hypertrophy than that seen at 3 months after ErbB4 deletion. Similar to the results from the study at 3 months, we observed neither cardiomyocyte hypertrophy nor cardiac fibrosis. Astonishingly, at 8 months the expression of ErbB4 in knockout animals was no longer different from the control animals, whereas it was reduced by ~67% at 3-4 months post-tamoxifen and ~90% at 10 days after tamoxifen treatment. To my knowledge, there have been no reports of this type of deleted gene recovery. Cardiomyocytes (consisting of the two thirds volume of the whole heart) are the main source of ErbB4 in cardiac tissues whilst other cells either don't express the ErbB4 (fibroblasts, taking one third volume of the heart), or express smaller amounts (endothelial cells). The only explanation I could propose is that new cardiomyocytes with an intact ErbB4 gene (that are thus able to express ErbB4) have been generated and replaced the cardiomyocytes lacking ErbB4. If this hypothesis is true, two processes would be required. First, new cardiomyocytes with an intact ErbB4 gene need to be generated. Second, the death of cardiomyocytes lacking ErbB4 would be needed for ErbB4 regeneration. I tried to detect cardiomyocyte apoptosis using TUNEL staining 3 months after ErbB4 deletion. However, we observed extensive positive staining in sections from both knockout and control animals. We

suspect that this staining may be an artifact of the fixation procedure (immersion in 4% PFA for 48 hours). To conquer this, in a future set of experiments we will perfusion fix the hearts using a Langendorff setup to immediately fix the cardiomyocytes after heart collection.

When taking my *in vivo* study along with those in the literature, it seems that the phenotype observed is closely related to the developmental stage where ErbB4 is deleted. Deletion of ErbB4 in the germline leads to embryonic death due to impaired cardiac development (Gassmann *et al.*, 1995). Targeted knockout of ErbB4 from cardiomyocytes using the MLC-2V promoter does not cause embryonic lethality, but does lead to dilated cardiomyopathy in the adult (Garcia-Rivello *et al.*, 2005). The deletion of ErbB4 from the adult mouse heart in my study led to the development of physiological cardiac hypertrophy without cardiac dysfunction or structure abnormalities. This might indicate the primary function of ErbB4 under physiological conditions is to promote cardiomyocyte growth. As long as the cardiac development has been completed, the reduction in ErbB4 does not affect the heart function. This hypothesis is consistent with data in Chapter 4 showing the relatively higher expression of ErbB4 in the embryonic stage (which probably reflects high demand for cardiomyocyte growth) compared to the adult (where there is a low requirement for cardiac growth in physiological conditions). However, it has been suggested that NRG1 is a beneficial cardiac factor that may protect the cardiomyocytes in various pathological conditions. Given that ErbB4 is the primary receptor for NRG1 in cardiomyocytes, these observations might suggest that ErbB4 may also be cardioprotective in pathological conditions. Thus, in a future study we plan to use our cardiac ErbB4 deletion model to investigate the function of ErbB4 in a model of pathological cardiac hypertrophy.

Limitations and future directions

In this thesis, the transactivation of ErbB receptors has been carefully studied with RNAi. Down-regulation of individual ErbB receptors did not affect the Ang II signalling in cardiomyocytes, and we have excluded the possibility that other ErbB subtypes were up-regulation after knockdown. However, although the expression level was not changed, these ErbBs may have been activated via alternative mechanisms to compensate for the deleted subtypes. To exclude this possibility, in the future down regulation of all of the ErbB receptors should be employed. In addition, all of the transactivation studies in my thesis were performed in purified cardiomyocytes. However, the transactivation might require the involvement of multiple cardiac cell types such as fibroblasts, endothelial cells and cardiomyocytes. It is important to know how these cells interact in any

potential transactivation process (for instance, the "triple membrane signalling pathway" mechanism as discussed earlier), and the role of each cell type in this mechanism. Regarding the ErbB4 isoforms, the JM-a was abundantly expressed in the embryonic heart. Whilst cardiac ErbB4 is predominantly localized to cardiomyocytes in the adult (Zhao *et al.*, 1999), this has not been shown in the embryo. I propose that in the embryo ErbB4 is also mainly expressed in cardiomyocytes or cardiomyocyte precursor cells, however this will require experimental confirmation. Furthermore, the exact cell types (mature cardiomyocytes, progenitor cells, or others) that express the JM-a have yet to be identified. An intriguing possibility is that the JM-a expressing cells are mainly cardiac stem cells or progenitor cells. It will be interesting to investigate whether the JM-a isoform can be cleaved in these cells to regulate cardiomyocyte generation.

In vivo, the physiological role of ErbB4 in the adult heart has been investigated using a conditional knockout model. The obtained data suggests that ErbB4 deletion leads to cardiac hypertrophy without affecting the cardiac function or structure, whereas the up-regulation of NRG1 in ErbB4-cKO mice might promote cardiac cell proliferation. It is important to confirm these results with further studies. Whilst this study showed no change in cardiomyocyte size, the cross sectional area measured in my study only reflects the cardiomyocyte size in the short axis, yet cardiomyocyte enlargement during hypertrophy can occur in both the longitudinal and short axis. To measure longitudinal changes, we plan to isolate single cell cardiomyocytes and use microscopy to quantify cell size. To further confirm the proliferation results, alternative proliferation markers such as Ki67 or measurement methods such as BrdU incorporation should be used to detect proliferation. It is critical to identify which cells are proliferating, which will require co-staining using cell-type specific and proliferation markers. In addition to these experiments, we are eager to explore the mechanism behind the observed phenomenon. The ErbB4 deficiency occurs in cardiomyocytes in our models, whist NRG1 is abundant in endothelial cells (Kuramochi *et al.*, 2004; Lemmens *et al.*, 2006). It will be interesting to examine how the ErbB4 deficiency caused the up-regulation of NRG1, and to then determine whether the cardiac cell proliferation in knockout animals was driven by the up-regulated NRG1. More importantly, we plan to elucidate the mechanism by which ErbB4 expression recovers in the months following recombination of the floxed gene. There is the possibility that the ErbB4 deficient cells are undergoing apoptosis and are being replaced by newly generated cardiomyocytes, however, this needs to be experimentally confirmed. One potential, but very important proposal, from my study is that another ErbB receptor (ErbB3) might be activated by the up-regulated NRG1 in cardiac tissues to compensate for the ErbB4 deficiency, and thus preserve cardiac function (as discussed in Chapter 5). The cardioprotective effect of NRG1 has been

demonstrated in various pathological animal models whilst phase II clinical trials demonstrated that NRG1 could improve the cardiac function of patients with chronic heart failure (Gao *et al.*, 2010) . Currently, ErbB4 is considered to be the only receptor for NRG1 in cardiomyocytes. If ErbB3 can be activated by NRG1 in the heart, the proposed molecular mechanism (where NRG1's beneficial effect occurs via ErbB4) needs to be re-evaluated and this new potential pathway via ErbB3 requires further exploration. Indeed, whether ErbB4 deficiency will affect the ability of NRG1 to protect the heart is yet to be determined. More fundamentally, the phenotype of the ErbB4-cKO mice under pathological conditions has not been elucidated. For this purpose, as a next step we are going to investigate how cardiac deletion of ErbB4 affects the response of the heart to a hypertrophic stimulus using an Ang II infusion model of hypertension and hypertrophy. This work will provide important information regarding the role of ErbB4 in cardiac function and structure under pathological conditions.

Conclusion

During my candidature, I have fully investigated the transactivation of ErbB family by Ang II in cardiomyocytes and provided evidence that the Ang II signalling in cardiomyocyte hypertrophy is independent of ErbB receptors. This is very important for elucidating the molecular pathway of the pathological cardiac hypertrophy related to the activation of local RAS system. My studies confirmed the requirement for ErbB4 in NRG1 induced hypertrophic signalling. The discovery that all four ErbB4 isoforms could mediate NRG1 signalling in postnatal cardiomyocytes suggested that NRG1 induced hypertrophic signalling is dependent on a fundamental common feature of the four isoforms. The decline in expression of the cleavable isoforms (JM-a) throughout development, and the lack of a cleavage mechanism in postnatal cardiomyocytes suggests that the postnatal heart does not require the ICD function. In contrast, the relative higher level of JM-a in embryonic stages suggests that the ICD might be released and required by the embryonic heart. This study indicates that further investigation on the biological function of JM-a isoform in the embryonic heart is required, particularly with respect to cardiomyocyte generation. The *in vivo* study established a new conditional knockout model in our lab, where the gene deletion is both tissue specific and temporally controlled. Using this model, we investigated the function of ErbB4 in adult mice heart. The cardiac specific deletion of ErbB4 in adult mice did not result in a severe cardiac phenotype (cardiac dysfunction and structural abnormality) but a series of compensatory responses (up-regulation of NRG1 and physiological cardiac hypertrophy). This proposes that, in contrast to the embryonic heart, the intact adult heart adopts alternative mechanisms to satisfy cardiac physiological requirements when ErbB4 is absent. More importantly, the lack of an obvious

phenotype may indicate that the primary function of the ErbB4 in the adult heart is different from the embryonic heart. The former might be mediating the NRG1 signalling to preserve cardiac function and structure under pathological conditions, whereas the latter promotes growth. Thus, deletion of ErbB4 in embryonic heart leads to pre-birth death due to the cessation of cardiac growth. In contrast, the phenotype of ErbB4 deletion in adult heart may only be observed under pathological conditions. In a future study we plan to use our conditional knockout model to investigate the function of ErbB4 in a model of pathological cardiac hypertrophy.

REFERENCES

Adabag AS, Luepker RV, Roger VL, Gersh BJ (2010). Sudden cardiac death: epidemiology and risk factors. *Nature Reviews Cardiology* 7**:** 216-225.

Adams Jr, Bodor GS, Davila-Roman VG, Delmez J, Apple F, Ladenson J, *et al.* (1993). Cardiac troponin I. A marker with high specificity for cardiac injury. *Circulation* 88**:** 101-106.

Adams JW, Sakata Y, Davis MG, Sah VP, Wang Y, Liggett SB, *et al.* (1998). Enhanced Gαq signaling: a common pathway mediates cardiac hypertrophy and apoptotic heart failure. *Proceedings of the National Academy of Sciences* 95**:** 10140-10145.

Adler C, Ringlage W, Böhm N (1981). DNA content and cell number in heart and liver of children. Comparable biochemical, cytophotometric and histological investigations (author's transl). *Pathology, research and practice* 172**:** 25.

Advani A, Kelly DJ, Cox AJ, White KE, Advani SL, Thai K, *et al.* (2009). The (Pro) Renin Receptor Site-Specific and Functional Linkage to the Vacuolar H+-ATPase in the Kidney. *Hypertension* 54**:** 261-269.

Akazawa H, Komuro I (2003). Roles of Cardiac Transcription Factors in Cardiac Hypertrophy. *Circulation Research* 92**:** 1079-1088.

An T, Zhang Y, Huang Y, Zhang R, Yin S, Guo X, *et al.* (2013). Neuregulin-1 protects against doxorubicin-induced apoptosis in cardiomyocytes through an Akt-dependent pathway. *Physiol Res Acad Sci Bohemoslov* 62**:** 379-385.

Anastassiadis T, Deacon SW, Devarajan K, Ma H, Peterson JR (2011). Comprehensive assay of kinase catalytic activity reveals features of kinase inhibitor selectivity. *Nature biotechnology* 29**:** 1039-1045.

Ang K-L, Shenje LT, Reuter S, Soonpaa MH, Rubart M, Field LJ, *et al.* (2010). Limitations of conventional approaches to identify myocyte nuclei in histologic sections of the heart. *American Journal of Physiology-Cell Physiology* 298**:** C1603-C1609.

Aoki H, Izumo S, Sadoshima J (1998). Angiotensin II Activates RhoA in Cardiac Myocytes: A Critical Role of RhoA in Angiotensin II–Induced Premyofibril Formation. *Circulation Research* 82**:** 666-676.

Aqeilan RI, Donati V, Palamarchuk A, Trapasso F, Kaou M, Pekarsky Y, *et al.* (2005). WW Domain–Containing Proteins, WWOX and YAP, Compete for Interaction with ErbB-4 and Modulate Its Transcriptional Function. *Cancer Research* 65**:** 6764-6772.

Artham SM, Lavie CJ, Milani RV, Patel DA, Verma A, Ventura HO (2009). Clinical Impact of Left Ventricular Hypertrophy and Implications for Regression. *Progress in Cardiovascular Diseases* 52**:** 153-167.

Asakura M, Kitakaze M, Liao Y, Ishikura F, Yoshinaka T, Ohmoto H, *et al.* (2002). Cardiac hypertrophy is inhibited by antagonism of ADAM12 processing of HB-EGF: Metalloproteinase inhibitors as a new therapy. *Nature Medicine* 8**:** 35-40.

Aurora AB, Mahmoud AI, Luo X, Johnson BA, van Rooij E, Matsuzaki S, *et al.* (2012). MicroRNA-214 protects the mouse heart from ischemic injury by controlling Ca2+ overload and cell death. *The Journal of clinical investigation* 122**:** 1222-1232.

Baliga RR, Pimental DR, Zhao Y-Y, Simmons WW, Marchionni MA, Sawyer DB, *et al.* (1999). *NRG-1-induced cardiomyocyte hypertrophy. Role of PI-3-kinase, p70S6K, and MEK-MAPK-RSK*. edn, vol. 277.

Barry SP, Davidson SM, Townsend PA (2008). Molecular regulation of cardiac hypertrophy. *The international journal of biochemistry & cell biology* 40**:** 2023-2039.

Beltrami AP, Urbanek K, Kajstura J, Yan S-M, Finato N, Bussani R, *et al.* (2001). Evidence that human cardiac myocytes divide after myocardial infarction. *New England Journal of Medicine* 344**:** 1750-1757.

Bergmann O, Bhardwaj RD, Bernard S, Zdunek S, Barnabé-Heider F, Walsh S, *et al.* (2009). Evidence for cardiomyocyte renewal in humans. *Science* 324**:** 98-102.

Bersell K, Arab S, Haring B, Kühn B (2009). Neuregulin1/ErbB4 signaling induces cardiomyocyte proliferation and repair of heart injury. *Cell* 138**:** 257-270.

Bian Y, Sun M, Silver M, Ho KKL, Marchionni MA, Caggiano AO, *et al.* (2009). *Neuregulin-1 attenuated doxorubicin-induced decrease in cardiac troponins*. edn, vol. 297.

Blumenthal DK, Stull JT, Gill GN (1978). Phosphorylation of cardiac troponin by guanosine 3': 5'-monophosphate-dependent protein kinase. *Journal of Biological Chemistry* 253**:** 334-336.

Bokemeyer D, Schmitz U, Kramer HJ (2000). Angiotensin II-induced growth of vascular smooth muscle cells requires an Src-dependent activation of the epidermal growth factor receptor. *Kidney international* 58**:** 549-558.

Bombelli M, Facchetti R, Carugo S, Madotto F, Arenare F, Quarti-Trevano F, *et al.* (2009). Left ventricular hypertrophy increases cardiovascular risk independently of in-office and out-of-office blood pressure values. *J Hypertens* 27**:** 2458-2464.

Braz JC, Bueno OF, De Windt LJ, Molkentin JD (2002). PKCα regulates the hypertrophic growth of cardiomyocytes through extracellular signal–regulated kinase1/2 (ERK1/2). *The Journal of cell biology* 156**:** 905-919.

Brero A, Ramella R, Fitou A, Dati C, Alloatti G, Gallo MP, *et al.* (2010). Neuregulin-1β1 rapidly modulates nitric oxide synthesis and calcium handling in rat cardiomyocytes. *Cardiovascular research* 88**:** 443-452.

Brown RD, Ambler SK, Mitchell MD, Long CS (2005). The cardiac fibroblast: therapeutic target in myocardial remodeling and failure. *Annu. Rev. Pharmacol. Toxicol.* 45**:** 657-687.

Bueno OF, De Windt LJ, Tymitz KM, Witt SA, Kimball TR, Klevitsky R, *et al.* (2000). The MEK1–ERK1/2 signaling pathway promotes compensated cardiac hypertrophy in transgenic mice. *The EMBO journal* 19**:** 6341-6350.

Buonanno A, Fischbach GD (2001). Neuregulin and ErbB receptor signaling pathways in the nervous system. *Current opinion in neurobiology* 11**:** 287-296.

Burgess AW (2008). EGFR family: structure physiology signalling and therapeutic targets. *Growth Factors* 26**:** 263-274.

Burgess AW, Cho H-S, Eigenbrot C, Ferguson KM, Garrett TPJ, Leahy DJ, *et al.* (2003). An Open-and-Shut Case? Recent Insights into the Activation of EGF/ErbB Receptors. *Molecular Cell* 12**:** 541-552.

Cabrera-Bueno F, García-Pinilla JM, Gómez-Doblas JJ, Montiel-Trujillo A, Rodríguez-Bailón I, de Teresa-Galván E (2007). Beta-blocker therapy for dynamic left ventricular outflow tract obstruction induced by exercise. *International journal of cardiology* 117**:** 222-226.

Campreciós G, Lorita J, Pardina E, Peinado-Onsurbe J, Soley M, Ramírez I (2011). Expression, localization, and regulation of the neuregulin receptor ErbB3 in mouse heart. *Journal of cellular physiology* 226**:** 450-455.

Carabatsos MJ, Combelles CM, Messinger SM, Albertini DF (2000). Sorting and reorganization of centrosomes during oocyte maturation in the mouse. *Microscopy research and technique* 49**:** 435-444.

Carabello BA (2002). Concentric versus eccentric remodeling. *Journal of cardiac failure* 8**:** S258-S263.

Casey P, Gilman A (1988). G protein involvement in receptor-effector coupling. *The Journal of biological chemistry* 263**:** 2577-2580.

Cassis LA, Gupte M, Thayer S, Zhang X, Charnigo R, Howatt DA, *et al.* (2009). ANG II infusion promotes abdominal aortic aneurysms independent of increased blood pressure in hypercholesterolemic mice. *Am J Physiol Heart Circ Physiol* 296**:** H1660-1665.

Ceylan-Isik AF, Dong M, Zhang Y, Dong F, Turdi S, Nair S, *et al.* (2013). Cardiomyocyte-specific deletion of endothelin receptor A rescues aging-associated cardiac hypertrophy and contractile dysfunction: role of autophagy. *Basic research in cardiology* 108**:** 1-19.

Chang-Yuan N, Murphy NP, Golde TE, Carpenter G (2001). Gamma-secretase cleavage and nuclear localization of ErbB-4 receptor tyrosine kinase. *Science* 294**:** 2179-2181.

Chen J, Chen J-K, Neilson EG, Harris RC (2006). Role of EGF receptor activation in angiotensin II-induced renal epithelial cell hypertrophy. *Journal of the American Society of Nephrology : JASN* 17**:** 1615-1623.

Chien KR (2001). To Cre or Not To Cre The Next Generation of Mouse Models of Human Cardiac Diseases. *Circulation research* 88**:** 546-549.

Clerk A, Sugden PH (1999). Activation of protein kinase cascades in the heart by hypertrophic G protein–coupled receptor agonists. *The American journal of cardiology* 83**:** 64-69.

Coleman ML, Marshall CJ, Olson MF (2004). RAS and RHO GTPases in G1-phase cell-cycle regulation. *Nature Reviews Molecular Cell Biology* 5**:** 355-366.

Cote GM, Miller TA, LeBrasseur NK, Kuramochi Y, Sawyer DB (2005). Neuregulin-1α and β isoform expression in cardiac microvascular endothelial cells and function in cardiac myocytes in vitro. *Experimental cell research* 311**:** 135-146.

Crowley SD, Gurley SB, Herrera MJ, Ruiz P, Griffiths R, Kumar AP, *et al.* (2006). Angiotensin II causes hypertension and cardiac hypertrophy through its receptors in the kidney. *Proceedings of the National Academy of Sciences* 103**:** 17985-17990.

Dahlöf B, Devereux RB, Kjeldsen SE, Julius S, Beevers G, de Faire U, *et al.* (2002). Cardiovascular morbidity and mortality in the Losartan Intervention For Endpoint reduction in hypertension study (LIFE): a randomised trial against atenolol. *The Lancet* 359**:** 995-1003.

Dahlöf B, Gosse P, Guéret P, Dubourg O, De Simone G, Schmieder R, *et al.* (2005). Perindopril/indapamide combination more effective than enalapril in reducing blood pressure and left ventricular mass: the PICXEL study. *Journal of hypertension* 23**:** 2063-2070.

Daub H, Weiss FU, Wallasch C, Ullrich A (1996). Role of transactivation of the EGF receptor in signalling by G-protein-coupled receptors. *Nature* 379**:** 557-560.

Devereux RB, Palmieri V, Sharpe N, De Quattro V, Bella JN, de Simone G, *et al.* (2001). Effects of Once-Daily Angiotensin-Converting Enzyme Inhibition and Calcium Channel Blockade-Based

Antihypertensive Treatment Regimens on Left Ventricular Hypertrophy and Diastolic Filling in Hypertension: The Prospective Randomized Enalapril Study Evaluating Regression of Ventricular Enlargement (PRESERVE) Trial. *Circulation* 104**:** 1248-1254.

Dhanasekaran S, Doherty TM, Kenneth J (2010). Comparison of different standards for real-time PCR-based absolute quantification. *Journal of immunological methods* 354**:** 34-39.

Dikic I, Tokiwa G, Lev S, Courtneidge SA, Schlessinger J (1996). A role for Pyk2 and Src in linking G-protein-coupled receptors with MAP kinase activation.

Dorn GW (2007). The Fuzzy Logic of Physiological Cardiac Hypertrophy. *Hypertension* 49**:** 962-970.

Drazner MH (2005). The Transition From Hypertrophy to Failure. *Circulation* 112**:** 936-938.

Edwards DR, Handsley MM, Pennington CJ (2008). The ADAM metalloproteinases. *Molecular aspects of medicine* 29**:** 258-289.

Eghbali M, Deva R, Alioua A, Minosyan TY, Ruan H, Wang Y, *et al.* (2005). Molecular and functional signature of heart hypertrophy during pregnancy. *Circulation research* 96**:** 1208-1216.

Eguchi S, Iwasaki H, Ueno H, Frank GD, Motley ED, Eguchi K, *et al.* (1999). Intracellular signaling of angiotensin II-induced p70 S6 kinase phosphorylation at Ser(411) in vascular smooth muscle cells. Possible requirement of epidermal growth factor receptor, Ras, extracellular signal-regulated kinase, and Akt. *The Journal of biological chemistry* 274**:** 36843-36851.

Eguchi S, Numaguchi K, Iwasaki H, Matsumoto T, Yamakawa T, Utsunomiya H, *et al.* (1998). Calcium-dependent Epidermal Growth Factor Receptor Transactivation Mediates the Angiotensin II-induced Mitogen-activated Protein Kinase Activation in Vascular Smooth Muscle Cells. *Journal of Biological Chemistry* 273**:** 8890-8896.

Elenius K, Choi CJ, Paul S, Santiestevan E, Nishi E, Klagsbrun M (1999). Characterization of a naturally occurring ErbB4 isoform that does not bind or activate phosphatidyl inositol 3-kinase. *Oncogene* 18**:** 2607-2615.

Elenius K, Corfas G, Paul S, Choi CJ, Rio C, Plowman GD, *et al.* (1997). A Novel Juxtamembrane Domain Isoform of HER4/ErbB4 ISOFORM-SPECIFIC TISSUE DISTRIBUTION AND DIFFERENTIAL PROCESSING IN RESPONSE TO PHORBOL ESTER. *Journal of Biological Chemistry* 272**:** 26761-26768.

Ellison GM, Waring CD, Vicinanza C, Torella D (2011). Physiological cardiac remodelling in response to endurance exercise training: cellular and molecular mechanisms. *Heart***:** heartjnl-2011-300639.

Erickson SL, O'Shea KS, Ghaboosi N, Loverro L, Frantz G, Bauer M, *et al.* (1997). ErbB3 is required for normal cerebellar and cardiac development: a comparison with ErbB2-and heregulin-deficient mice. *Development* 124**:** 4999-5011.

Esposito G, Rapacciuolo A, Naga Prasad SV, Rockman HA (2002). Cardiac hypertrophy: role of G protein-coupled receptors. *Journal of cardiac failure* 8**:** S409-S414.

Falls DL (2003). Neuregulins: functions, forms, and signaling strategies. *Experimental cell research* 284**:** 14-30.

Fang S-j, Wu X-s, Han Z-h, Zhang X-x, Wang C-m, Li X-y, *et al.* (2010). Neuregulin-1 preconditioning protects the heart against ischemia/reperfusion injury through a PI3K/Akt-dependent mechanism. *Chinese Medical Journal (English Edition)* 123**:** 3597.

Feng S-M, Sartor CI, Hunter D, Zhou H, Yang X, Caskey LS, *et al.* (2007). The HER4 Cytoplasmic Domain, But Not Its C Terminus, Inhibits Mammary Cell Proliferation. *Molecular Endocrinology* 21**:** 1861-1876.

Ferrario CM (2011). ACE2: more of Ang-(1–7) or less Ang II? *Current Opinion in Nephrology and Hypertension* 20**:** 1-6 10.1097/MNH.1090b1013e3283406f3283457.

Fischer O, Hart S, Gschwind A, Ullrich A (2003). EGFR signal transactivation in cancer cells. *Biochemical Society Transactions* 31**:** 1203-1208.

Fox IJ, Kornblum HI (2005). Developmental profile of ErbB receptors in murine central nervous system: Implications for functional interactions. *Journal of Neuroscience Research* 79**:** 584-597.

Franco D, Markman MM, Wagenaar G, Ya J, Lamers WH, Moorman AF (1999). Myosin light chain 2a and 2v identifies the embryonic outflow tract myocardium in the developing rodent heart. *The Anatomical Record* 254**:** 135-146.

Frey N, Olson E (2003). Cardiac hypertrophy: the good, the bad, and the ugly. *Annual review of physiology* 65**:** 45-79.

Frey N, Katus HA, Olson EN, Hill JA (2004). Hypertrophy of the Heart. *Circulation* 109**:** 1580-1589.

Fukazawa R, Miller TA, Kuramochi Y, Frantz S, Kim YD, Marchionni MA, *et al.* (2003). Neuregulin-1 protects ventricular myocytes from anthracycline-induced apoptosis via erbB4-dependent activation of PI3-kinase/Akt. *J Mol Cell Cardiol* 35**:** 1473-1479.

Gaestel M (2006). MAPKAP kinases — MKs — two's company, three's a crowd. *Nature Reviews Molecular Cell Biology* 7**:** 120-130.

Gao R, Zhang J, Cheng L, Wu X, Dong W, Yang X, *et al.* (2010). A Phase II, Randomized, Double-Blind, Multicenter, Based on Standard Therapy, Placebo-Controlled Study of the Efficacy and Safety of Recombinant Human Neuregulin-1 in Patients With Chronic Heart Failure. *Journal of the American College of Cardiology* 55**:** 1907-1914.

Garcia-Rivello H, Taranda J, Said M, Cabeza-Meckert P, Vila-Petroff M, Scaglione J, *et al.* (2005). Dilated cardiomyopathy in Erb-b4-deficient ventricular muscle. *Am J Physiol Heart Circ Physiol* 289**:** H1153-1160.

Garrett TP, McKern NM, Lou M, Elleman TC, Adams TE, Lovrecz GO, *et al.* (2003). The crystal structure of a truncated ErbB2 ectodomain reveals an active conformation, poised to interact with other ErbB receptors. *Molecular cell* 11**:** 495-505.

Gassmann M, Casagranda F, Orioli D, Simon H, Lai C, Klein R, *et al.* (1995). Aberrant neural and cardiac development in mice lacking the ErbB4 neuregulin receptor.

George AJ, Purdue BW, Gould CM, Thomas DW, Handoko Y, Qian H, *et al.* (2013). A functional siRNA screen identifies genes modulating angiotensin II-mediated EGFR transactivation. *Journal of Cell Science* 126**:** 5377-5390.

Gilmore-Hebert M, Ramabhadran R, Stern DF (2010). Interactions of ErbB4 and Kap1 Connect the Growth Factor and DNA Damage Response Pathways. *Molecular Cancer Research* 8**:** 1388-1398.

Giraud M-N, Flück M, Zuppinger C, Suter TM (2005). Expressional reprogramming of survival pathways in rat cardiocytes by neuregulin-1β. *Journal of applied physiology* 99**:** 313-322.

Gough NR (2010). Live or Die with ErbB4. *Sci. Signal.* 3**:** ec373-.

Grossman W (1980). Cardiac hypertrophy: useful adaptation or pathologic process? *The American journal of medicine* 69**:** 576-584.

Grossman W, Paulus WJ (2013). Myocardial stress and hypertrophy: a complex interface between biophysics and cardiac remodeling. *The Journal of clinical investigation* 123**:** 3701-3703.

Grossman W, Jones D, McLaurin L (1975). Wall stress and patterns of hypertrophy in the human left ventricle. *Journal of Clinical Investigation* 56**:** 56.

Hadler-Olsen E, Fadnes B, Sylte I, Uhlin-Hansen L, Winberg JO (2011). Regulation of matrix metalloproteinase activity in health and disease. *The FEBS journal* 278**:** 28-45.

Hall ME, Smith G, Hall JE, Stec DE (2011). Systolic dysfunction in cardiac-specific ligand-inducible MerCreMer transgenic mice. *American Journal of Physiology-Heart and Circulatory Physiology* 301**:** H253-H260.

Hanson MA, Stevens RC (2009). Discovery of new GPCR biology: one receptor structure at a time. *Structure* 17**:** 8-14.

Hao L, Du M, Lopez-Campistrous A, Fernandez-Patron C (2004). Agonist-induced activation of matrix metalloproteinase-7 promotes vasoconstriction through the epidermal growth factor-receptor pathway. *Circulation Research* 94**:** 68-76.

Harris DM, Chen X, Pesant S, Cohn HI, MacDonnell SM, Boucher M, *et al.* (2009). Inhibition of angiotensin II Gq signaling augments beta-adrenergic receptor mediated effects in a renal artery stenosis model of high blood pressure. *J Mol Cell Cardiol* 46**:** 100-107.

Hasegawa K, Lee SJ, Jobe SM, Markham BE, Kitsis RN (1997). cis-Acting sequences that mediate induction of β-myosin heavy chain gene expression during left ventricular hypertrophy due to aortic constriction. *Circulation* 96**:** 3943-3953.

Hedhli N, Huang Q, Kalinowski A, Palmeri M, Hu X, Russell RR, *et al.* (2011). Endothelium-Derived Neuregulin Protects the Heart Against Ischemic Injury / Clinical Perspective. *Circulation* 123**:** 2254-2262.

Heineke J, Molkentin JD (2006). Regulation of cardiac hypertrophy by intracellular signalling pathways. *Nature Reviews Molecular Cell Biology* 7**:** 589-600.

Henderson SA, Spencer M, Sen A, Kumar C, Siddiqui MA, Chien KR (1989). Structure, organization, and expression of the rat cardiac myosin light chain-2 gene. Identification of a 250-base pair fragment which confers cardiac-specific expression. *Journal of Biological Chemistry* 264**:** 18142-18148.

Hepler JR, Kozasa T, Smrcka AV, Simon MI, Rhee SG, Sternweis PC, *et al.* (1993). Purification from Sf9 cells and characterization of recombinant Gq alpha and G11 alpha. Activation of purified phospholipase C isozymes by G alpha subunits. *The Journal of biological chemistry* 268**:** 14367-14375.

Higa-Nakamine S, Maeda N, Toku S, Yamamoto T, Yingyuenyong M, Kawahara M, *et al.* (2012). Selective cleavage of ErbB4 by G-protein-coupled Gonadotropin-Releasing Hormone Receptor in Cultured Hypothalamic Neurons. *Journal of cellular physiology* 227**:** 2492-2501.

Hill CS, Treisman R (1995). Transcriptional Regulation by Extracellular signals: Mechanisms and Specificity. *Cell* 80**:** 199-211.

Houston S, Plunkett T, Barnes D, Smith P, Rubens R, Miles D (1999). Overexpression of c-erbB2 is an independent marker of resistance to endocrine therapy in advanced breast cancer. *British journal of cancer* 79**:** 1220.

Hsieh PCH, Segers VFM, Davis ME, MacGillivray C, Gannon J, Molkentin JD, *et al.* (2007). Evidence from a genetic fate-mapping study that stem cells refresh adult mammalian cardiomyocytes after injury. *Nat Med* 13**:** 970-974.

Hubbard SR, Mohammadi M, Schlessinger J (1998). Autoregulatory mechanisms in protein-tyrosine kinases. *The Journal of biological chemistry* 273**:** 11987-11990.

Iemitsu M, Miyauchi T, Maeda S, Sakai S, Kobayashi T, Fujii N, *et al.* (2001). Physiological and pathological cardiac hypertrophy induce different molecular phenotypes in the rat. *American Journal of Physiology-Regulatory, Integrative and Comparative Physiology* 281**:** R2029-R2036.

Iwata H, Goto H, Tanaka H, Sakaguchi Y, Kimura K, Kuwayama T, *et al.* (2011). Effect of maternal age on mitochondrial DNA copy number, ATP content and IVF outcome of bovine oocytes. *Reproduction, fertility, and development* 23**:** 424-432.

Jiang Z, Zhou M (2010). Neuregulin signaling and heart failure. *Current heart failure reports* 7**:** 42-47.

Jie B, Zhang X, Wu X, Xin Y, Liu Y, Guo Y (2012). Neuregulin-1 suppresses cardiomyocyte apoptosis by activating PI3K/Akt and inhibiting mitochondrial permeability transition pore. *Molecular and cellular biochemistry* 370**:** 35-43.

Jopling C, Sleep E, Raya M, Martí M, Raya A, Belmonte JCI (2010). Zebrafish heart regeneration occurs by cardiomyocyte dedifferentiation and proliferation. *Nature* 464**:** 606-609.

Jorissen RN, Walker F, Pouliot N, Garrett TPJ, Ward CW, Burgess AW (2003). Epidermal growth factor receptor: mechanisms of activation and signalling. *Experimental Cell Research* 284**:** 31-53.

Junttila TT, Sundvall M, Määttä JA, Elenius K (2000). ErbB4 and Its Isoforms: Selective Regulation of Growth Factor Responses by Naturally Occurring Receptor Variants. *Trends in Cardiovascular Medicine* 10**:** 304-310.

Junttila TT, Laato M, Vahlberg T, Söderström K-O, Visakorpi T, Isola J, *et al.* (2003). Identification of patients with transitional cell carcinoma of the bladder overexpressing ErbB2,

ErbB3, or specific ErbB4 isoforms real-time reverse transcription-PCR analysis in estimation of ErbB receptor status from cancer patients. *Clinical cancer research* 9**:** 5346-5357.

Kagiyama S, Eguchi S, Frank GD, Inagami T, Zhang YC, Phillips MI (2002). Angiotensin II-induced cardiac hypertrophy and hypertension are attenuated by epidermal growth factor receptor antisense. *Circulation* 106**:** 909-912.

Kajstura J, Urbanek K, Perl S, Hosoda T, Zheng H, Ogórek B, *et al.* (2010). Cardiomyogenesis in the adult human heart. *Circulation research* 107**:** 305-315.

Katholi RE, Couri DM (2011). Left Ventricular Hypertrophy: Major Risk Factor in Patients with Hypertension: Update and Practical Clinical Applications. *International Journal of Hypertension* 2011.

Katus HA, Remppis A, Neumann FJ, Scheffold T, Diederich KW, Vinar G, *et al.* (1991). Diagnostic efficiency of troponin T measurements in acute myocardial infarction. *Circulation* 83**:** 902-912.

Keely SJ, Calandrella SO, Barrett KE (2000). Carbachol-stimulated transactivation of epidermal growth factor receptor and mitogen-activated protein kinase in T(84) cells is mediated by intracellular ca(2+), PYK-2, and p60(src). *The Journal of biological chemistry* 275**:** 12619-12625.

Kelly DJ, Cox AJ, Gow RM, Zhang Y, Kemp BE, Gilbert RE (2004). Platelet-derived growth factor receptor transactivation mediates the trophic effects of angiotensin II in vivo. *Hypertension* 44**:** 195-202.

Kikuchi K, Holdway JE, Werdich AA, Anderson RM, Fang Y, Egnaczyk GF, *et al.* (2010). Primary contribution to zebrafish heart regeneration by gata4+ cardiomyocytes. *Nature* 464**:** 601-605.

Kjeldsen SE, Dahlöf B, Devereux RB, Julius S, Aurup P, Edelman J, *et al.* (2002). Effects of losartan on cardiovascular morbidity and mortality in patients with isolated systolic hypertension and left ventricular hypertrophy: a Losartan Intervention for Endpoint Reduction (LIFE) substudy. *Jama* 288**:** 1491-1498.

Klein T, Bischoff R (2011). Active metalloproteases of the A Disintegrin and Metalloprotease (ADAM) family: biological function and structure. *J Proteome Res* 10**:** 17-33.

Klingbeil AU, Schneider M, Martus P, Messerli FH, Schmieder RE (2003). A meta-analysis of the effects of treatment on left ventricular mass in essential hypertension. *The American journal of medicine* 115**:** 41-46.

Klug MG, Soonpaa MH, Koh GY, Field LJ (1996). Genetically selected cardiomyocytes from differentiating embronic stem cells form stable intracardiac grafts. *Journal of Clinical Investigation* 98**:** 216.

Knowlton KU, Baracchini E, Ross R, Harris A, Henderson S, Evans S, *et al.* (1991). Co-regulation of the atrial natriuretic factor and cardiac myosin light chain-2 genes during alpha-adrenergic stimulation of neonatal rat ventricular cells. Identification of cis sequences within an embryonic and a constitutive contractile protein gene which mediate inducible expression. *Journal of Biological Chemistry* 266**:** 7759-7768.

Kodama H, Fukuda K, Takahashi T, Sano M, Kato T, Tahara S, *et al.* (2002). Role of EGF Receptor and Pyk2 in endothelin-1-induced ERK activation in rat cardiomyocytes. *Journal of molecular and cellular cardiology* 34**:** 139-150.

Koitabashi N, Bedja D, Zaiman AL, Pinto YM, Zhang M, Gabrielson KL, *et al.* (2009). Avoidance of transient cardiomyopathy in cardiomyocyte-targeted tamoxifen-induced MerCreMer gene deletion models. *Circulation research* 105**:** 12-15.

Komuro A, Nagai M, Navin NE, Sudol M (2003). WW domain-containing protein YAP associates with ErbB-4 and acts as a co-transcriptional activator for the carboxyl-terminal fragment of ErbB-4 that translocates to the nucleus. *Journal of Biological Chemistry* 278**:** 33334-33341.

Kühn B, del Monte F, Hajjar RJ, Chang Y-S, Lebeche D, Arab S, *et al.* (2007). Periostin induces proliferation of differentiated cardiomyocytes and promotes cardiac repair. *Nature medicine* 13**:** 962-969.

Kumar V, Zhang M-X, Swank MW, Kunz J, Wu G-Y (2005). Regulation of dendritic morphogenesis by Ras–PI3K–Akt–mTOR and Ras–MAPK signaling pathways. *The Journal of neuroscience* 25**:** 11288-11299.

Kuramochi Y, Cote GM, Guo X, Lebrasseur NK, Cui L, Liao R, *et al.* (2004). Cardiac endothelial cells regulate reactive oxygen species-induced cardiomyocyte apoptosis through neuregulin-1β/erbB4 signaling. *Journal of Biological Chemistry* 279**:** 51141-51147.

Laflamme MA, Murry CE (2011). Heart regeneration. *Nature* 473**:** 326-335.

Lautrette A, Li S, Alili R, Sunnarborg SW, Burtin M, Lee DC, *et al.* (2005). Angiotensin II and EGF receptor cross-talk in chronic kidney diseases: a new therapeutic approach. *Nature Medicine* 11**:** 867-874.

Law AJ, Kleinman JE, Weinberger DR, Weickert CS (2007). Disease-associated intronic variants in the ErbB4 gene are related to altered ErbB4 splice-variant expression in the brain in schizophrenia. *Human Molecular Genetics* 16**:** 129-141.

Lee E, Taussig R, Gilman AG (1992). The G226A mutant of Gs alpha highlights the requirement for dissociation of G protein subunits. *Journal of Biological Chemistry* 267**:** 1212-1218.

Lee K-F, Simon H, Chen H, Bates B, Hung M-C, Hauser C (1995). Requirement for neuregulin receptor erbB2 in neural and cardiac development.

Lemmens K, Segers VF, Demolder M, De Keulenaer GW (2006). Role of neuregulin-1/ErbB2 signaling in endothelium-cardiomyocyte cross-talk. *Journal of Biological Chemistry* 281**:** 19469-19477.

Lemmens K, Fransen P, Sys SU, Brutsaert DL, De Keulenaer GW (2004). Neuregulin-1 Induces a Negative Inotropic Effect in Cardiac Muscle Role of Nitric Oxide Synthase. *Circulation* 109**:** 324-326.

Lepilina A, Coon AN, Kikuchi K, Holdway JE, Roberts RW, Burns CG, *et al.* (2006). A dynamic epicardial injury response supports progenitor cell activity during zebrafish heart regeneration. *Cell* 127**:** 607-619.

Levitzki A, Gazit A (1995). Tyrosine kinase inhibition: an approach to drug development. *Science* 267**:** 1782-1788.

Li B, Zheng Z, Wei Y, Wang M, Peng J, Kang T, *et al.* (2011). Therapeutic effects of neuregulin-1 in diabetic cardiomyopathy rats. *Cardiovascular Diabetology* 10**:** 69.

Liang Q, Molkentin JD (2002). Divergent signaling pathways converge on GATA4 to regulate cardiac hypertrophic gene expression. *Journal of molecular and cellular cardiology* 34**:** 611-616.

Liang Q, Wiese RJ, Bueno OF, Dai Y-S, Markham BE, Molkentin JD (2001). The Transcription Factor GATA4 Is Activated by Extracellular Signal-Regulated Kinase 1- and 2-Mediated Phosphorylation of Serine 105 in Cardiomyocytes. *Molecular and Cellular Biology* 21**:** 7460-7469.

Liebmann C (2011). EGF receptor activation by GPCRs: an universal pathway reveals different versions. *Molecular and cellular endocrinology* 331**:** 222-231.

Lin C-H, Chen Y-C, Pan T-M (2011). Quantification bias caused by plasmid DNA conformation in quantitative real-time PCR assay. *PloS one* 6**:** e29101.

Linggi B, Carpenter G (2006). ErbB receptors: new insights on mechanisms and biology. *Trends in Cell Biology* 16**:** 649-656.

Linseman DA, Benjamin CW, Jones DA (1995). Convergence of Angiotensin II and Platelet-derived Growth Factor Receptor Signaling Cascades in Vascular Smooth Muscle Cells. *Journal of Biological Chemistry* 270**:** 12563-12568.

Linz W, Schölkens BA, Ganten D (1989). Converting Enzyme Inhibition Specifically Prevents the Development and Induces Regression of Cardiac Hypertrophy in Rats. *Clinical and Experimental Hypertension* a11**:** 1325-1350.

Liu X, Gu X, Li Z, Li X, Li H, Chang J, *et al.* (2006). Neuregulin-1/erbB-activation improves cardiac function and survival in models of ischemic, dilated, and viral cardiomyopathy. *Journal of the American College of Cardiology* 48**:** 1438-1447.

Livak KJ, Schmittgen TD (2001). Analysis of Relative Gene Expression Data Using Real-Time Quantitative PCR and the 2< sup>− ΔΔCT</sup> Method. *methods* 25**:** 402-408.

Long W, Wagner K-U, Lloyd KCK, Binart N, Shillingford JM, Hennighausen L, *et al.* (2003). Impaired differentiation and lactational failure of Erbb4-deficient mammary glands identify ERBB4 as an obligate mediator of STAT5. *Development* 130**:** 5257-5268.

Luo J, McMullen JR, Sobkiw CL, Zhang L, Dorfman AL, Sherwood MC, *et al.* (2005). Class IA phosphoinositide 3-kinase regulates heart size and physiological cardiac hypertrophy. *Molecular and cellular biology* 25**:** 9491-9502.

Luppi F, Longo A, De Boer W, Rabe K, Hiemstra P (2007). Interleukin-8 stimulates cell proliferation in non-small cell lung cancer through epidermal growth factor receptor transactivation. *Lung Cancer* 56**:** 25-33.

Määttä JA, Sundvall M, Junttila TT, Peri L, Laine VJO, Isola J, *et al.* (2006). Proteolytic Cleavage and Phosphorylation of a Tumor-associated ErbB4 Isoform Promote Ligand-independent Survival and Cancer Cell Growth. *Molecular Biology of the Cell* 17**:** 67-79.

Macdougall LK, JONES LR, COHEN P (1991). Identification of the major protein phosphatases in mammalian cardiac muscle which dephosphorylate phospholamban. *European journal of biochemistry* 196**:** 725-734.

Mackay K, Mochly-Rosen D (2001). Localization, anchoring, and functions of protein kinase C isozymes in the heart. *Journal of molecular and cellular cardiology* 33**:** 1301-1307.

Malliaras K, Zhang Y, Seinfeld J, Galang G, Tseliou E, Cheng K, *et al.* (2013). Cardiomyocyte proliferation and progenitor cell recruitment underlie therapeutic regeneration after myocardial infarction in the adult mouse heart. *EMBO molecular medicine* 5**:** 191-209.

Manabe I, Shindo T, Nagai R (2002). Gene expression in fibroblasts and fibrosis involvement in cardiac hypertrophy. *Circulation research* 91**:** 1103-1113.

Markwald RR, Norris RA, Moreno-Rodriguez R, Levine RA (2010). Developmental basis of adult cardiovascular diseases. *Annals of the New York Academy of Sciences* 1188**:** 177-183.

McMullen JR, Jennings GL (2007). Differences between pathological and physiological cardiac hypertrophy: novel therapeutic strategies to treat heart failure. *Clinical and Experimental Pharmacology and Physiology* 34**:** 255-262.

McMullen JR, Shioi T, Zhang L, Tarnavski O, Sherwood MC, Kang PM, *et al.* (2003). Phosphoinositide 3-kinase (p110α) plays a critical role for the induction of physiological, but not pathological, cardiac hypertrophy. *Proceedings of the National Academy of Sciences* 100**:** 12355-12360.

Mehta PK, Griendling KK (2007). Angiotensin II cell signaling: physiological and pathological effects in the cardiovascular system. *Am J Physiol Cell Physiol* 292**:** C82-97.

Mendelsohn J, Baselga J (2003). Status of epidermal growth factor receptor antagonists in the biology and treatment of cancer. *Journal of clinical oncology : official journal of the American Society of Clinical Oncology* 21**:** 2787-2799.

Mendez M, LaPointe MC (2005). PGE2-induced hypertrophy of cardiac myocytes involves EP4 receptor-dependent activation of p42/44 MAPK and EGFR transactivation. *American Journal of Physiology-Heart and Circulatory Physiology* 288**:** H2111-H2117.

Mery P-F, Lohmann SM, Walter U, Fischmeister R (1991). Ca2+ current is regulated by cyclic GMP-dependent protein kinase in mammalian cardiac myocytes. *Proceedings of the National Academy of Sciences* 88**:** 1197-1201.

Meyer D, Birchmeier C (1995). Multiple essential functions of neuregulin in development.

Miettinen PJ, Berger JE, Meneses J, Phung Y, Pedersen RA, Werb Z, *et al.* (1995). Epithelial immaturity and multiorgan failure in mice lacking epidermal growth factor receptor. *Nature* 376**:** 337-341.

Mifune M, Ohtsu H, Suzuki H, Nakashima H, Brailoiu E, Dun NJ, *et al.* (2005). G Protein Coupling and Second Messenger Generation Are Indispensable for Metalloprotease-dependent, Heparin-binding Epidermal Growth Factor Shedding through Angiotensin II Type-1 Receptor. *Journal of Biological Chemistry* 280**:** 26592-26599.

Misfeldt AM Endocardial cells are a distinct endothelial lineage derived from multipotent cardiovascular progenitors, Vanderbilt University, 2008.

Mizobuchi S, Kanzaki H, Omiya H, Matsuoka Y, Obata N, Kaku R, *et al.* (2013). Spinal nerve injury causes upregulation of ErbB2 and ErbB3 receptors in rat dorsal root ganglia. *Journal of pain research* 6**:** 87-94.

Mochizuki S, Okada Y (2007). ADAMs in cancer cell proliferation and progression. *Cancer Science* 98**:** 621-628.

Molkentin JD (2000). The zinc finger-containing transcription factors GATA-4,-5, and-6 ubiquitously expressed regulators of tissue-specific gene expression. *Journal of Biological Chemistry* 275**:** 38949-38952.

Molkentin JD, Robbins J (2009). With great power comes great responsibility: using mouse genetics to study cardiac hypertrophy and failure. *Journal of molecular and cellular cardiology* 46**:** 130-136.

Molkentin JD, Lu J-R, Antos CL, Markham B, Richardson J, Robbins J, *et al.* (1998). A calcineurin-dependent transcriptional pathway for cardiac hypertrophy. *Cell* 93**:** 215-228.

Mone SM, Sanders SP, Colan SD (1996). Control mechanisms for physiological hypertrophy of pregnancy. *Circulation* 94**:** 667-672.

Morimoto T, Hasegawa K, Kaburagi S, Kakita T, Wada H, Yanazume T, *et al.* (2000). Phosphorylation of GATA-4 Is Involved in α1-Adrenergic Agonist-responsive Transcription of the Endothelin-1 Gene in Cardiac Myocytes. *Journal of Biological Chemistry* 275**:** 13721-13726.

Mukoyama M, Nakajima M, Horiuchi M, Sasamura H, Pratt RE, Dzau VJ (1993). Expression cloning of type 2 angiotensin II receptor reveals a unique class of seven-transmembrane receptors. *Journal of Biological Chemistry* 268**:** 24539-24542.

Müller P, Kazakov A, Semenov A, Jagoda P, Friedrich EB, Böhm M, *et al.* (2012). Ramipril and Telmisartan Exhibit Differential Effects in Cardiac Pressure Overload-Induced Hypertrophy

Without an Additional Benefit of the Combination of Both Drugs. *Journal of Cardiovascular Pharmacology and Therapeutics*.

Muraoka-Cook RS, Sandahl M, Husted C, Hunter D, Miraglia L, Feng S-m, *et al.* (2006a). The Intracellular Domain of ErbB4 Induces Differentiation of Mammary Epithelial Cells. *Molecular Biology of the Cell* 17**:** 4118-4129.

Muraoka-Cook RS, Sandahl MA, Strunk KE, Miraglia LC, Husted C, Hunter DM, *et al.* (2009). ErbB4 Splice Variants Cyt1 and Cyt2 Differ by 16 Amino Acids and Exert Opposing Effects on the Mammary Epithelium In Vivo. *Molecular and cellular biology* 29**:** 4935-4948.

Muraoka-Cook RS, Caskey LS, Sandahl MA, Hunter DM, Husted C, Strunk KE, *et al.* (2006b). Heregulin-Dependent Delay in Mitotic Progression Requires HER4 and BRCA1. *Molecular and cellular biology* 26**:** 6412-6424.

Muscella A, Greco S, Elia MG, Storelli C, Marsigliante S (2003). PKC-? is required for angiotensin II-induced activation of ERK and synthesis of C-FOS in MCF-7 cells. *Journal of cellular physiology* 197**:** 61-68.

Nagase H, Visse R, Murphy G (2006). Structure and function of matrix metalloproteinases and TIMPs. *Cardiovascular Research* 69**:** 562-573.

Nagendran J, Sutendra G, Paterson I, Champion HC, Webster L, Chiu B, *et al.* (2013). Endothelin Axis Is Upregulated in Human and Rat Right Ventricular Hypertrophy. *Circulation Research* 112**:** 347-354.

Nagy A (2000). Cre recombinase: the universal reagent for genome tailoring. *genesis* 26**:** 99-109.

Naresh A, Long W, Vidal GA, Wimley WC, Marrero L, Sartor CI, *et al.* (2006). The ERBB4/HER4 Intracellular Domain 4ICD Is a BH3-Only Protein Promoting Apoptosis of Breast Cancer Cells. *Cancer Research* 66**:** 6412-6420.

Nishimoto S, Nishida E (2006). MAPK signalling: ERK5 versus ERK1/2. *EMBO reports* 7**:** 782-786.

Ohtsu H, Dempsey PJ, Eguchi S (2006a). ADAMs as mediators of EGF receptor transactivation by G protein-coupled receptors. *American Journal of Physiology-Cell Physiology* 291**:** C1-C10.

Ohtsu H, Dempsey PJ, Frank GD, Brailoiu E, Higuchi S, Suzuki H, *et al.* (2006b). ADAM17 mediates epidermal growth factor receptor transactivation and vascular smooth muscle cell hypertrophy induced by angiotensin II. *Arteriosclerosis, thrombosis, and vascular biology* 26**:** e133-E137.

Ohtsu H, Higuchi S, Shirai H, Eguchi K, Suzuki H, Hinoki A, *et al.* (2008). Central Role of Gq in the Hypertrophic Signal Transduction of Angiotensin II in Vascular Smooth Muscle Cells. *Endocrinology* 149**:** 3569-3575.

Okin PM, Devereux RB, Jern S, Kjeldsen SE, Julius S, Nieminen MS, *et al.* (2003). Regression of Electrocardiographic Left Ventricular Hypertrophy by Losartan Versus Atenolol The Losartan Intervention For Endpoint Reduction in Hypertension (LIFE) Study. *Circulation* 108**:** 684-690.

Okoshi K, Nakayama M, Yan X, Okoshi MP, Schuldt AJ, Marchionni MA, *et al.* (2004). Neuregulins Regulate Cardiac Parasympathetic Activity Muscarinic Modulation of β-Adrenergic Activity in Myocytes From Mice With Neuregulin-1 Gene Deletion. *Circulation* 110**:** 713-717.

Olayioye MA, Neve RM, Lane HA, Hynes NE (2000). The ErbB signaling network: receptor heterodimerization in development and cancer. *The EMBO journal* 19**:** 3159-3167.

Omerovic J, Puggioni EMR, Napoletano S, Visco V, Fraioli R, Frati L, *et al.* (2004). Ligand-regulated association of ErbB-4 to the transcriptional co-activator YAP65 controls transcription at the nuclear level. *Experimental Cell Research* 294**:** 469-479.

Özcelik C, Erdmann B, Pilz B, Wettschureck N, Britsch S, Hübner N, *et al.* (2002). Conditional mutation of the ErbB2 (HER2) receptor in cardiomyocytes leads to dilated cardiomyopathy. *Proceedings of the National Academy of Sciences* 99**:** 8880-8885.

Page-McCaw A, Ewald AJ, Werb Z (2007). Matrix metalloproteinases and the regulation of tissue remodelling. *Nat Rev Mol Cell Biol* 8**:** 221-233.

Paradis P, Dali-Youcef N, Paradis FW, Thibault G, Nemer M (2000). Overexpression of angiotensin II type I receptor in cardiomyocytes induces cardiac hypertrophy and remodeling. *Proceedings of the National Academy of Sciences of the United States of America* 97**:** 931-936.

Parker TG, Packer SE, Schneider MD (1990). Peptide growth factors can provoke "fetal" contractile protein gene expression in rat cardiac myocytes. *The Journal of clinical investigation* 85**:** 507-514.

Pentassuglia L, Sawyer DB (2009a). The role of Neuregulin-1β/ErbB signaling in the heart. *Experimental cell research* 315**:** 627-637.

Pentassuglia L, Graf M, Lane H, Kuramochi Y, Cote G, Timolati F, *et al.* (2009b). Inhibition of ErbB2 by receptor tyrosine kinase inhibitors causes myofibrillar structural damage without cell death in adult rat cardiomyocytes. *Experimental cell research* 315**:** 1302-1312.

Pitt B, Reichek N, Willenbrock R, Zannad F, Phillips RA, Roniker B, *et al.* (2003). Effects of Eplerenone, Enalapril, and Eplerenone/Enalapril in Patients With Essential Hypertension and Left Ventricular Hypertrophy The 4E–Left Ventricular Hypertrophy Study. *Circulation* 108**:** 1831-1838.

Porcile C, Bajetto A, Barbieri F, Barbero S, Bonavia R, Biglieri M, *et al.* (2005). Stromal cell-derived factor-1α (SDF-1α/CXCL12) stimulates ovarian cancer cell growth through the EGF receptor transactivation. *Experimental cell research* 308**:** 241-253.

Porrello ER, Mahmoud AI, Simpson E, Hill JA, Richardson JA, Olson EN, *et al.* (2011). Transient regenerative potential of the neonatal mouse heart. *Science* 331**:** 1078-1080.

Proud CG (2004). Ras, PI3-kinase and mTOR signaling in cardiac hypertrophy. *Cardiovascular research* 63**:** 403-413.

Pucéat M, Hilal-Dandan R, Strulovici B, Brunton LL, Brown JH (1994). Differential regulation of protein kinase C isoforms in isolated neonatal and adult rat cardiomyocytes. *Journal of Biological Chemistry* 269**:** 16938-16944.

Rajagopalan V, Zucker IH, Jones JA, Carlson M, Ma YJ (2008). Cardiac ErbB-1/ErbB-2 mutant expression in young adult mice leads to cardiac dysfunction. *American Journal of Physiology-Heart and Circulatory Physiology* 295**:** H543-H554.

Razeghi P, Young ME, Alcorn JL, Moravec CS, Frazier OH, Taegtmeyer H (2001). Metabolic Gene Expression in Fetal and Failing Human Heart. *Circulation* 104**:** 2923-2931.

Reiss K, Saftig P (2009). The “A Disintegrin And Metalloprotease” (ADAM) family of sheddases: Physiological and cellular functions. *Seminars in Cell & Developmental Biology* 20**:** 126-137.

Riethmacher D, Sonnenberg-Riethmacher E, Brinkmann V, Yamaai T, Lewin GR, Birchmeier C (1997). Severe neuropathies in mice with targeted mutations in the ErbB3 receptor. *Nature* 389**:** 725-730.

Rio C, Buxbaum JD, Peschon JJ, Corfas G (2000). Tumor Necrosis Factor-α-converting Enzyme Is Required for Cleavage of erbB4/HER4. *Journal of Biological Chemistry* 275**:** 10379-10387.

Rohrbach S, Niemann B, Silber RE, Holtz J (2005). Neuregulin receptors erbB2 and erbB4 in failing human myocardium. *Basic Research in Cardiology* 100**:** 240-249.

Rohrbach S, Yan X, Weinberg EO, Hasan F, Bartunek J, Marchionni MA, *et al.* (1999). Neuregulin in Cardiac Hypertrophy in Rats With Aortic Stenosis : Differential Expression of erbB2 and erbB4 Receptors. *Circulation* 100**:** 407-412.

Roman MJ, Okin PM, Kizer JR, Lee ET, Howard BV, Devereux RB (2010). Relations of central and brachial blood pressure to left ventricular hypertrophy and geometry: the Strong Heart Study. *Journal of Hypertension* 28**:** 384-388 310.1097/HJH.1090b1013e328333d328228.

Ruilope LM, Schmieder RE (2008). Left ventricular hypertrophy and clinical outcomes in hypertensive patients. *American journal of hypertension* 21**:** 500-508.

Rutledge R, Cote C (2003). Mathematics of quantitative kinetic PCR and the application of standard curves. *Nucleic Acids Research* 31**:** e93-e93.

Sabri A, Steinberg SF (2003). Protein kinase C isoform-selective signals that lead to cardiac hypertrophy and the progression of heart failure. In. *Biochemistry of Hypertrophy and Heart Failure*, edn: Springer. p^pp 97-101.

Sadoshima J, Izumo S (1993). Molecular characterization of angiotensin II--induced hypertrophy of cardiac myocytes and hyperplasia of cardiac fibroblasts. Critical role of the AT1 receptor subtype. *Circulation Research* 73**:** 413-423.

Saito S, Frank GD, Motley ED, Dempsey PJ, Utsunomiya H, Inagami T, *et al.* (2002). Metalloprotease inhibitor blocks angiotensin II-induced migration through inhibition of epidermal growth factor receptor transactivation. *Biochemical and Biophysical Research Communications* 294**:** 1023-1029.

Sardi SP, Murtie J, Koirala S, Patten BA, Corfas G (2006). Presenilin-Dependent ErbB4 Nuclear Signaling Regulates the Timing of Astrogenesis in the Developing Brain. *Cell* 127**:** 185-197.

Sartor CI, Zhou H, Kozlowska E, Guttridge K, Kawata E, Caskey L, *et al.* (2001). HER4 Mediates Ligand-Dependent Antiproliferative and Differentiation Responses in Human Breast Cancer Cells. *Molecular and cellular biology* 21**:** 4265-4275.

Scaltriti M, Baselga J (2006). The Epidermal Growth Factor Receptor Pathway: A Model for Targeted Therapy. *Clinical Cancer Research* 12**:** 5268-5272.

Scheffzek K, Ahmadian MR, Kabsch W, Wiesmüller L, Lautwein A, Schmitz F, *et al.* (1997). The Ras-RasGAP complex: structural basis for GTPase activation and its loss in oncogenic Ras mutants. *Science* 277**:** 333-339.

Schlange T, Matsuda Y, Lienhard S, Huber A, Hynes NE (2007). Autocrine WNT signaling contributes to breast cancer cell proliferation via the canonical WNT pathway and EGFR transactivation. *Breast Cancer Res* 9**:** R63.

Schneider MR, Wolf E (2009). The epidermal growth factor receptor ligands at a glance. *Journal of cellular physiology* 218**:** 460-466.

Schneider MR, Dahlhoff M, Herbach N, Renner-Mueller I, Dalke C, Puk O, *et al.* (2005). Betacellulin overexpression in transgenic mice causes disproportionate growth, pulmonary hemorrhage syndrome, and complex eye pathology. *Endocrinology* 146**:** 5237-5246.

Schreier B, Dohler M, Rabe S, Schneider B, Schwerdt G, Ruhs S, *et al.* (2011). Consequences of epidermal growth factor receptor (ErbB1) loss for vascular smooth muscle cells from mice with targeted deletion of ErbB1. *Arterioscler Thromb Vasc Biol* 31**:** 1643-1652.

Schreier B, Rabe S, Schneider B, Bretschneider M, Rupp S, Ruhs S, *et al.* (2013). Loss of epidermal growth factor receptor in vascular smooth muscle cells and cardiomyocytes causes arterial hypotension and cardiac hypertrophy. *Hypertension* 61**:** 333-340.

Schultz JEJ, Witt SA, Glascock BJ, Nieman ML, Reiser PJ, Nix SL, *et al.* (2002). TGF-β1 mediates the hypertrophic cardiomyocyte growth induced by angiotensin II. *The Journal of clinical investigation* 109**:** 787-796.

Seidman A, Hudis C, Pierri MK, Shak S, Paton V, Ashby M, *et al.* (2002). Cardiac Dysfunction in the Trastuzumab Clinical Trials Experience. *Journal of Clinical Oncology* 20**:** 1215-1221.

Shah BH, Catt KJ (2002). Calcium-Independent Activation of Extracellularly Regulated Kinases 1 and 2 by Angiotensin II in Hepatic C9 Cells: Roles of Protein Kinase Cδ, Src/Proline-Rich Tyrosine Kinase 2, and Epidermal Growth Factor Receptor trans-Activation. *Molecular Pharmacology* 61**:** 343-351.

Shah BH, Catt KJ (2003a). A central role of EGF receptor transactivation in angiotensin II-induced cardiac hypertrophy. *Trends in pharmacological sciences* 24**:** 239-244.

Shah BH, Farshori MP, Jambusaria A, Catt KJ (2003b). Roles of Src and epidermal growth factor receptor transactivation in transient and sustained ERK1/2 responses to gonadotropin-releasing hormone receptor activation. *The Journal of biological chemistry* 278**:** 19118-19126.

Shah BH, Yesilkaya A, Olivares-Reyes JA, Chen H-D, Hunyady L, Catt KJ (2004). Differential pathways of angiotensin II-induced extracellularly regulated kinase 1/2 phosphorylation in specific cell types: role of heparin-binding epidermal growth factor. *Molecular endocrinology (Baltimore, Md.)* 18**:** 2035-2048.

Shioi T, Kang PM, Douglas PS, Hampe J, Yballe CM, Lawitts J, *et al.* (2000). The conserved phosphoinositide 3-kinase pathway determines heart size in mice. *The EMBO journal* 19**:** 2537-2548.

Shiojima I, Sato K, Izumiya Y, Schiekofer S, Ito M, Liao R, *et al.* (2005). Disruption of coordinated cardiac hypertrophy and angiogenesis contributes to the transition to heart failure. *The Journal of clinical investigation* 115**:** 2108-2118.

Sibilia M, Wagner EF (1995). Strain-dependent epithelial defects in mice lacking the EGF receptor. *Science* 269**:** 234-238.

Smith NJ, Chan HW, Qian H, Bourne AM, Hannan KM, Warner FJ, *et al.* (2011). Determination of the exact molecular requirements for type 1 angiotensin receptor epidermal growth factor receptor transactivation and cardiomyocyte hypertrophy. *Hypertension* 57**:** 973-980.

Smrcka AV, Sternweis PC (1993). Regulation of purified subtypes of phosphatidylinositol-specific phospholipase C beta by G protein alpha and beta gamma subunits. *The Journal of biological chemistry* 268**:** 9667.

Sohal DS, Nghiem M, Crackower MA, Witt SA, Kimball TR, Tymitz KM, *et al.* (2001). Temporally regulated and tissue-specific gene manipulations in the adult and embryonic heart using a tamoxifen-inducible Cre protein. *Circulation research* 89**:** 20-25.

Solomon SD, Appelbaum E, Manning WJ, Verma A, Berglund T, Lukashevich V, *et al.* (2009). Effect of the Direct Renin Inhibitor Aliskiren, the Angiotensin Receptor Blocker Losartan, or Both on Left Ventricular Mass in Patients With Hypertension and Left Ventricular Hypertrophy. *Circulation* 119**:** 530-537.

Solomon SD, Hee Shin S, Shah A, Skali H, Desai A, Kober L, *et al.* (2011). Effect of the direct renin inhibitor aliskiren on left ventricular remodelling following myocardial infarction with systolic dysfunction. *European Heart Journal* 32**:** 1227-1234.

Soltoff SP (1998). Related adhesion focal tyrosine kinase and the epidermal growth factor receptor mediate the stimulation of mitogen-activated protein kinase by the G-protein-coupled P2Y2 receptor. Phorbol ester or [Ca2+]i elevation can substitute for receptor activation. *The Journal of biological chemistry* 273**:** 23110-23117.

Søraas CL, Wachtell K, Okin PM, Dahlöf B, Devereux RB, Tønnessen T, *et al.* (2010). Lack of regression of left ventricular hypertrophy is associated with higher incidence of revascularization in hypertension: The LIFE Study. *Blood Pressure* 19**:** 145-151.

Sørlie T, Perou CM, Tibshirani R, Aas T, Geisler S, Johnsen H, *et al.* (2001). Gene expression patterns of breast carcinomas distinguish tumor subclasses with clinical implications. *Proceedings of the National Academy of Sciences* 98**:** 10869-10874.

Stefansson H, Sigurdsson E, Steinthorsdottir V, Bjornsdottir S, Sigmundsson T, Ghosh S, *et al.* (2002). Neuregulin 1 and susceptibility to schizophrenia. *American journal of human genetics* 71**:** 877-892.

Steinberg SF (2012). Cardiac actions of protein kinase C isoforms. *Physiology* 27**:** 130-139.

Strickland S, Loeb JN (1981). Obligatory separation of hormone binding and biological response curves in systems dependent upon secondary mediators of hormone action. *Proceedings of the National Academy of Sciences* 78**:** 1366-1370.

Strunk KE, Husted C, Miraglia LC, Sandahl M, Rearick WA, Hunter DM, *et al.* (2007). HER4 D-Box Sequences Regulate Mitotic Progression and Degradation of the Nuclear HER4 Cleavage Product s80HER4. *Cancer Research* 67**:** 6582-6590.

Sugden PH, Clerk A (1998). Cellular mechanisms of cardiac hypertrophy. *Journal of molecular medicine* 76**:** 725-746.

Sundvall M, Veikkolainen V, Kurppa K, Salah Z, Tvorogov D, van Zoelen EJ, *et al.* (2010). Cell Death or Survival Promoted by Alternative Isoforms of ErbB4. *Molecular Biology of the Cell* 21**:** 4275-4286.

Sundvall M, Peri L, Määttä JA, Tvorogov D, Paatero I, Savisalo M, *et al.* (2007). Differential nuclear localization and kinase activity of alternative ErbB4 intracellular domains. *Oncogene* 26**:** 6905-6914.

Suzuki-Yagawa Y, Guermah M, Roeder RG (1997). The ts13 mutation in the TAF (II) 250 subunit (CCG1) of TFIID directly affects transcription of D-type cyclin genes in cells arrested in G1 at the nonpermissive temperature. *Molecular and cellular biology* 17**:** 3284-3294.

Sweeney C, Carraway 3rd K (2000). Ligand discrimination by ErbB receptors: differential signaling through differential phosphorylation site usage. *Oncogene* 19**:** 5568-5573.

Taegtmeyer H, Sen S, Vela D (2010). Return to the fetal gene program. *Annals of the New York Academy of Sciences* 1188**:** 191-198.

Telley I, Denoth J (2007). Sarcomere dynamics during muscular contraction and their implications to muscle function. *Journal of Muscle Research and Cell Motility* 28**:** 89-104.

Thomas WG, Brandenburger Y, Autelitano DJ, Pham T, Qian H, Hannan RD (2002). Adenoviral-directed expression of the type 1A angiotensin receptor promotes cardiomyocyte hypertrophy via transactivation of the epidermal growth factor receptor. *Circulation Research* 90**:** 135-142.

Threadgill DW, Dlugosz AA, Hansen LA, Tennenbaum T, Lichti U, Yee D, *et al.* (1995). Targeted disruption of mouse EGF receptor: effect of genetic background on mutant phenotype. *Science* 269**:** 230-234.

Tidcombe H, Jackson-Fisher A, Mathers K, Stern DF, Gassmann M, Golding JP (2003). Neural and mammary gland defects in ErbB4 knockout mice genetically rescued from embryonic lethality. *Proceedings of the National Academy of Sciences* 100**:** 8281-8286.

Timolati F, Ott D, Pentassuglia L, Giraud M-N, Perriard J-C, Suter TM, *et al.* (2006). Neuregulin-1 beta attenuates doxorubicin-induced alterations of excitation–contraction coupling and reduces oxidative stress in adult rat cardiomyocytes. *Journal of Molecular and Cellular Cardiology* 41**:** 845-854.

Vanhaesebroeck B, Guillermet-Guibert J, Graupera M, Bilanges B (2010). The emerging mechanisms of isoform-specific PI3K signalling. *Nature reviews Molecular cell biology* 11**:** 329-341.

Vecchi M, Carpenter G (1997). Constitutive Proteolysis of the ErbB-4 Receptor Tyrosine Kinase by a Unique, Sequential Mechanism. *The Journal of Cell Biology* 139**:** 995-1003.

Vecchi M, Baulida J, Carpenter G (1996). Selective Cleavage of the Heregulin Receptor ErbB-4 by Protein Kinase C Activation. *Journal of Biological Chemistry* 271**:** 18989-18995.

Veikkolainen V, Vaparanta K, Halkilahti K, Iljin K, Sundvall M, Elenius K (2011). Function of ERBB4 is determined by alternative splicing. *Cell Cycle* 10**:** 2647-2657.

Veikkolainen V, Naillat F, Railo A, Chi L, Manninen A, Hohenstein P, *et al.* (2012). ErbB4 modulates tubular cell polarity and lumen diameter during kidney development. *Journal of the American Society of Nephrology* 23**:** 112-122.

Verboomen H, Wuytack F, De Smedt H, Himpens B, Casteels R (1992). Functional difference between SERCA2a and SERCA2b Ca2+ pumps and their modulation by phospholamban. *Biochem. J* 286**:** 591-595.

Visnagri A, Kandhare AD, Ghosh P, Bodhankar SL (2013). Endothelin receptor blocker bosentan inhibits hypertensive cardiac fibrosis in pressure overload-induced cardiac hypertrophy in rats. *Cardiovascular Endocrinology* 2**:** 85-97 10.1097/XCE.0000000000000010.

Vliegen H, Van der Laarse A, Cornelisse C, Eulderink F (1991). Myocardial changes in pressure overload-induced left ventricular hypertrophy A study on tissue composition, polyploidization and multinucleation. *European heart journal* 12**:** 488-494.

von Gise A, Lin Z, Schlegelmilch K, Honor LB, Pan GM, Buck JN, *et al.* (2012). YAP1, the nuclear target of Hippo signaling, stimulates heart growth through cardiomyocyte proliferation but not hypertrophy. *Proceedings of the National Academy of Sciences* 109**:** 2394-2399.

Wachtell K, Okin PM, Olsen MH, Dahlöf B, Devereux RB, Ibsen H, *et al.* (2007). Regression of Electrocardiographic Left Ventricular Hypertrophy During Antihypertensive Therapy and Reduction in Sudden Cardiac Death. *Circulation* 116**:** 700-705.

Wadugu B, Kühn B (2012). The role of neuregulin/ErbB2/ErbB4 signaling in the heart with special focus on effects on cardiomyocyte proliferation. *American Journal of Physiology-Heart and Circulatory Physiology* 302**:** H2139-H2147.

Wall MA, Coleman DE, Lee E, Iñiguez-Lluhi JA, Posner BA, Gilman AG, *et al.* (1995). The structure of the G protein heterotrimer G< sub> iα1</sub>< i> β</i>< sub> 1</sub>< i> γ</i>< sub> 2</sub>. *Cell* 83**:** 1047-1058.

Wang L, Gout I, Proud CG (2001). Cross-talk between the ERK and p70 S6 Kinase (S6K) Signaling Pathways: MEK-DEPENDENT ACTIVATION OF S6K2 IN CARDIOMYOCYTES. *Journal of Biological Chemistry* 276**:** 32670-32677.

Weiss A, Schlessinger J (1998). Switching signals on or off by receptor dimerization. *Cell* 94**:** 277-280.

Williams CC, Allison JG, Vidal GA, Burow ME, Beckman BS, Marrero L, *et al.* (2004). The ERBB4/HER4 receptor tyrosine kinase regulates gene expression by functioning as a STAT5A nuclear chaperone. *The Journal of Cell Biology* 167**:** 469-478.

Yamazaki T, Komuro I, Kudoh S, Zou Y, Shiojima I, Hiroi Y, *et al.* (1996). Endothelin-1 is involved in mechanical stress-induced cardiomyocyte hypertrophy. *Journal of Biological Chemistry* 271**:** 3221-3228.

Yanazume T, Hasegawa K, Wada H, Morimoto T, Abe M, Kawamura T, *et al.* (2002). Rho/ROCK pathway contributes to the activation of extracellular signal-regulated kinase/GATA-4 during myocardial cell hypertrophy. *Journal of Biological Chemistry* 277**:** 8618-8625.

Yano N, Suzuki D, Endoh M, Zhao TC, Padbury JF, Tseng Y-T (2007). A novel phosphoinositide 3-kinase-dependent pathway for angiotensin II/AT-1 receptor-mediated induction of collagen synthesis in MES-13 mesangial cells. *Journal of Biological Chemistry* 282**:** 18819-18830.

Yarden Y, Sliwkowski MX (2001). Untangling the ErbB signalling network. *Nature reviews. Molecular cell biology* 2**:** 127-137.

Yasuda N, Miura S, Akazawa H, Tanaka T, Qin Y, Kiya Y, *et al.* (2008). Conformational switch of angiotensin II type 1 receptor underlying mechanical stress-induced activation. *EMBO Rep* 9**:** 179-186.

Yin G, Yan C, Berk BC (2003). Angiotensin II signaling pathways mediated by tyrosine kinases. *The International Journal of Biochemistry & Cell Biology* 35**:** 780-783.

Yoshioka J, Prince RN, Huang H, Perkins SB, Cruz FU, MacGillivray C, *et al.* (2005). Cardiomyocyte hypertrophy and degradation of connexin43 through spatially restricted autocrine/paracrine heparin-binding EGF. *Proceedings of the National Academy of Sciences of the United States of America* 102**:** 10622-10627.

Yu W-H, Woessner JJF, McNeish JD, Stamenkovic I (2002). CD44 anchors the assembly of matrilysin/MMP-7 with heparin-binding epidermal growth factor precursor and ErbB4 and regulates female reproductive organ remodeling. *Genes & development* 16**:** 307-323.

Zeng F, Xu J, Harris RC (2009). Nedd4 mediates ErbB4 JM-a/CYT-1 ICD ubiquitination and degradation in MDCK II cells. *The FASEB Journal* 23**:** 1935-1945.

Zhai P, Galeotti J, Liu J, Holle E, Yu X, Wagner T, *et al.* (2006). An angiotensin II type 1 receptor mutant lacking epidermal growth factor receptor transactivation does not induce angiotensin II-mediated cardiac hypertrophy. *Circulation Research* 99**:** 528-536.

Zhang X, Gureasko J, Shen K, Cole PA, Kuriyan J (2006). An Allosteric Mechanism for Activation of the Kinase Domain of Epidermal Growth Factor Receptor. *Cell* 125**:** 1137-1149.

Zhao B, Tumaneng K, Guan K-L (2011). The Hippo pathway in organ size control, tissue regeneration and stem cell self-renewal. *Nat Cell Biol* 13**:** 877-883.

Zhao Y-Y, Feron O, Dessy C, Han X, Marchionni MA, Kelly RA (1999). Neuregulin Signaling in the Heart Dynamic Targeting of erbB4 to Caveolar Microdomains in Cardiac Myocytes. *Circulation research* 84**:** 1380-1387.

Zhao Y-y, Sawyer DR, Baliga RR, Opel DJ, Han X, Marchionni MA, *et al.* (1998). Neuregulins Promote Survival and Growth of Cardiac Myocytes. *Journal of Biological Chemistry* 273**:** 10261-10269.

Zhou W, Carpenter G (2000). Heregulin-dependent Trafficking and Cleavage of ErbB-4. *Journal of Biological Chemistry* 275**:** 34737-34743.

Zhu M, Feng J, Lucchinetti E, Fischer G, Xu L, Pedrazzini T, *et al.* (2006a). Ischemic postconditioning protects remodeled myocardium via the PI3K–PKB/Akt reperfusion injury salvage kinase pathway. *Cardiovascular research* 72**:** 152-162.

Zhu Y, Sullivan LL, Nair SS, Williams CC, Pandey AK, Marrero L, *et al.* (2006b). Coregulation of Estrogen Receptor by ERBB4/HER4 Establishes a Growth-Promoting Autocrine Signal in Breast Tumor Cells. *Cancer Research* 66**:** 7991-7998.

Zou Y, Komuro I, Yamazaki T, Aikawa R, Kudoh S, Shiojima I, *et al.* (1996). Protein kinase C, but not tyrosine kinases or Ras, plays a critical role in angiotensin II-induced activation of Raf-1 kinase and extracellular signal-regulated protein kinases in cardiac myocytes. *Journal of Biological Chemistry* 271**:** 33592-33597.

Zwick E, Wallasch C, Daub H, Ullrich A (1999). Distinct calcium-dependent pathways of epidermal growth factor receptor transactivation and PYK2 tyrosine phosphorylation in PC12 cells. *Journal of Biological Chemistry* 274**:** 20989-20996.

APPENDICES

Appendix A: Solutions and buffers

DMEM + 10%FBS: DMEM powder (#12100-038, Invitrogen), NaHCO3 (3.75 g/L), penicillin (1×10^5 U/L), streptomycin (100 mg/L), FBS (10%, v/v), pH7.2.

DMEM CCTSS2: DMEM powder (#12100-038, Invitrogen), NaHCO3 (3.75g/L), 1×vitamins solution (#11120-052, Invitrogen), 1×essential amino acid solution (#11130-051, Invitrogen), 1×non-essential amino acids solution (#11140-050, Invitrogen), sodium pyruvate (1 mM), insulin (5 mg/L), BrdU(0.1 mM), antibiotic antimyocotic (#15240-062, Invitrogen), potassium chloride (50mM), pH7.2.

MEM + 10% NBCS: MEM powder (#11900-016, Invitrogen), NaHCO3 (3.75 g/L), 1×vitamins solution (#11120-052, Invitrogen), 1×essential amino acid solution (#11130-051, Invitrogen), 1×non-essential amino acids solution (#11140-050, Invitrogen), antibiotic antimyocotic (#15240-062, Invitrogen), NBCS (10%, v/v), pH7.2.

ADS buffer: NaCl (6.8 g/L), HEPES (4.76 g/L), NaH_2PO_4 (0.12 g/L), glucose (1 g/L), KCl (0.4 g/L), MgSO4 (0.1 g/L), pH7.3-7.4.

Myocyte enzyme solution: Collagenase II (1.15×10^5 U/L, Worthington Biochemical Corporation), Pancreatin (0.8 g/L, Gibco) in ADS buffer.

Cell line enzyme solution: 0.5% trypsin in PBS

PBS: NaCl (80 g/L), KCl (2 g/L), $Na_2HPO_4{\cdot}12H_2O$ (15.4 g/L), KH_2PO_4 (2 g/L), pH7.2.

LB agar: tryptone (10 mg/ml), yeast extract (5 mg/ml), agar (15 mg/ml), NaCl (10 mg/ml), pH7.3.

LB media: tryptone (10 mg/ml), yeast extract (5 mg/ml), NaCl (10 mg/ml), pH7.3.

RIPA lysis buffer: Tris (50 mM, pH 7.4), NaCl (100 mM), EDTA (2 mM), sodium fluoride (50 mM), TritonX-100 (1%, v/v), sodium deoxycholate (0.5%, w/v), sodium dodecyl sulfate (SDS) (0.1%, w/v), sodium pyrophosphate (10 mM), aprotinin (1 μg/ml), leupeptin (5 μg/ml), pepstatin (1μg/ml).

5× SDS loading buffer: Tris-HCl (250 mM, pH 6.8), SDS (10%, w/v), bromophenol blue (0.5%, w/v), β-mercaptoethanol (20%, v/v), and glycerol (50%, v/v).

Western blot running Buffer: Tris (25 mM), glycine (192 mM), SDS (0.1%, w/v).

Western blot wash Buffer: NaCl (80 g/L), KCl (2 g/L), $Na_2HPO_4 \cdot 12H_2O$ (15.4 g/L), KH_2PO_4 (2 g/L), Tween-20 (0.1%, v/v), pH7.3.

Western blot transfer Buffer: Tris (48 mM), glycine (39 mM), methanol (0.2%, v/v).

Appendix B: PCR primers

Normal PCR primers:

1. Genotyping

ErbB4

Primer1 CAAATGCTCTCTCTGTTCTTTGTGTCTG

Primer2 TATTGTGTTCATCTATCATTGCAACCCAG

Primer3 TTTTGCCAAGTTCTAATTCCATCAGAAGC

Cre

Forward AGGTGGACCTGATCATGGAG

Reverse ATACCGGAGATCATGCAAGC

2. Cloning

pEGFP-N1-ErbB4 vector

Forward CCACTGTGACTCCACTGCTTACTGGCTTATCG

Reverse CCTAACCGGTAACACCACAGTATTCCGGTGTC

Note: The Nhe I and Age l I restriction sites are underlined in the above forward and reverse primers, respectively.

Real-time PCR primers (SYBR)

α-MHC

forward CTTCATCCATGGCCAATTCT

reverse GCGCATTGAGTTCAAGAAGA

β-MHC

forward GTGAAGGGCATGAGGAAGAGT

reverse AGGCCTTCACCTTCAGCTGC

BNP

forward CTT TAT CTG TCA CCG CTG GGA G

reverse TTT GGG TGT TCT TTT GTG AGG C

Col1A1

forward GCTCCTCTTAGGGGCCACT

reverse CCACGTCTCACCATTGGGG

Col3A1

forward	CACCCTTCTTCATCCCACTC
reverse	TGGTTCTGGCTTCCAGACAT

PAL

forward	TTCAGCCCTTGCTTGCCTC
reverse	ACACTTTTACTCCGAAGTCGGT

ErbB1

Forward	CAGATGGATGTCAACCCTGAAG
Reverse	TGGAGAGTGTGTCTTTAAATTCACC

ErbB2

Forward	GCAAGCACTGTCTGCCATGC
Reverse	GGGCACAAGCCTCACACTGG

ErbB3

Forward	CGAGATGGGCAACTCTCAGGC
Reverse	AGGTTACCCATGACCACCTCACAC

HB-EGF

Forward	CGGGGAGTGCAGATACCTG
Reverse	TTCTCCACTGGTAGAGTCAGC

TGFα

Forward	GCCCAGATTCCCACACTCAG
Reverse	CACGGCACCACTCACAGTG

EREG

Forward	CTGCCTCTTGGGTCTTGACG
Reverse	GCGGTACAGTTATCCTCGGATTC

BTC

Forward	AATTCTCCACTGTGTGGTAGCA
Reverse	GGTTTTCACTTTCTGTCTAGGGG

NRG3

Forward	CCAGCCTATCAAGCACCACA

Reverse GGTGGTGCCCTTCTGAAAGT

NRG1α

Forward GTGCGGAGAAGGAGAAAACTTTC

Reverse TTGCTCCAGTGAATCCAGGTTG

NRG1β

Forward GTGCGGAGAAGGAGAAAACTTTC

Reverse AACGATCACCAGTAAACTCATTTGG

m18s

Forward TCGAGGCCCTGTAATTGGAA

Reverse CCCTCCAATGGATCCTCGTT

Cre1

Forward TTTCCCGCAGAACCTGAAGATG

Reverse ATCCGCCGCATAACCAGTG

Cre2

Forward AACATGCTTCATCGTCGGTCC

Reverse CCGCCGCATAACCAGTGAA

TaqMan probe and primers set

JM isoform:

JM-a probe [6FAM]ATGGACGGGCCATTCCACTTTACCA[BHQ1]

JM-b probe [6FAM]TTCAAGCATTGAAGACTGCATCGGCCT[BHQ1]

JM-a/JM-b forward TTGCCATCCAAACTGCACC

JM-a/JM-b reverse TCCAATGACTCCGGCTGC

CYT isoform

CYT-1 probe [6FAM]TGAAATTGGACACAGCCCTCCTCCTG[BHQ1]

CYT-2 probe [6FAM]AAGAATTGACTCCAATAGGAATCAGTTTGTGTACCA[BHQ1]

CYT-1/CYT-2 forward TCCTCCCATCTACACATCCAGAA

CYT-1/CYT-2 reverse GGCATTCCTTGTTGTGTAGCAA

18S

18S probe [6FAM]CAGCAGGCGCGCAAATTACCCA[BHQ1]

18S forward	CGGCTACCACATCCAAGGAA
18S reverse	GGGCCTCGAAAGAGTCCTGT

The TaqMan probe and primer set used for amplifying following genes are predesigned and premixed by company:

NRG2: Mm01158087_m1 (Applied Biosystem)

NRG4: Mm00446254_m1 (Applied Biosystem)

AGEG: Mm00437583_m1 (Applied Biosystem)

Appendix C: pEGFP-N1-ErbB4 vector cloning strategy

Individual isoforms of ErbB4 was PCR cloned from pIRESpuro-ErbB4 vector into pEGFP-N1vector Two restricition sites (NheI and AgeI) were incorporated into primers to facilitate the cloning.

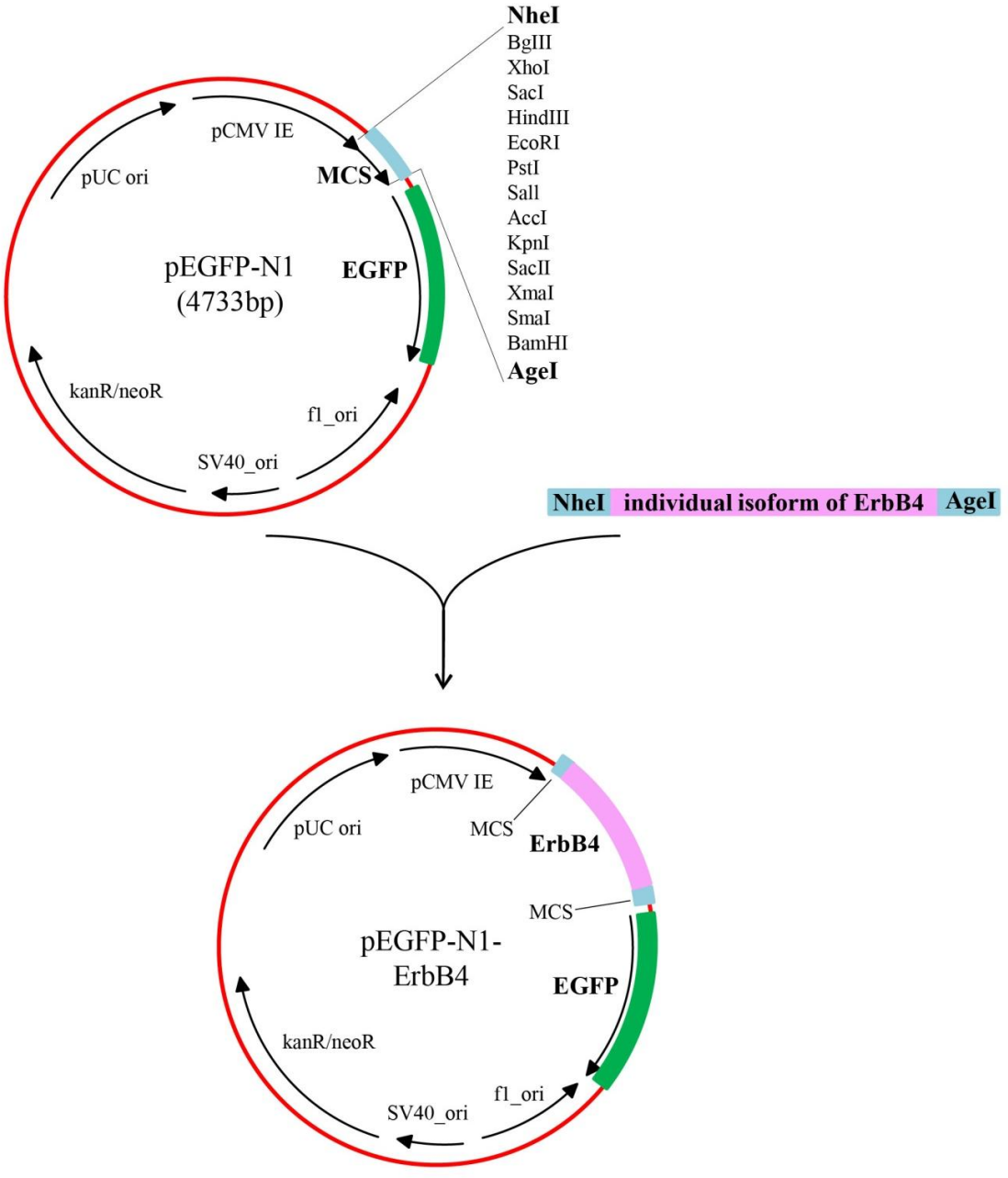

MCS sequence

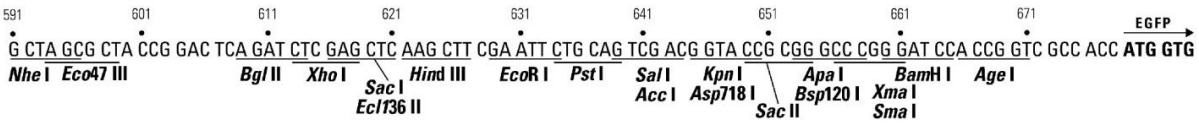

Appendix D: pCR®-TOPO-ErbB4-JM/CYT vector cloning strategy

JM or CYT domains of ErbB4 were PCR cloned from mouse cDNA into pCR®-TOPO vector using the overhanging T-A sites.